Charles University
Faculty of Science

Study programme: Immunology

Mgr. Julie Vacková

Checkpoint blockade in cancer immunotherapy

Blokování inhibičních receptorů při imunoterapii nádorů

Doctoral thesis

Supervisor: RNDr. Michal Šmahel, Ph.D.

Prague, 2021

Prohlášení:

Prohlašuji, že jsem závěrečnou práci vypracovala samostatně a uvedla jsem veškeré použité informační zdroje a literaturu. Tato práce ani žádná její část nebyla předložena k získání jiného nebo stejného akademického titulu.

V Praze, ……..

…….

Julie Vacková

ACKNOWLEDGEMENTS

I would like to thank to my supervisor Michal Šmahel for his patient guidance during my doctoral studies. Furthermore, I would like to acknowledge all members of the Laboratory of Immunotherapy and the Laboratory of Molecular and Tumour Virology for their help. Moreover, I wish to express deepest gratitude to my family and friends for their support.

CONTENTS

LIST OF ABBREVIATIONS

APCs	Antigen presenting cells
BTLA	B and T lymphocyte attenuator
B2m	Beta-2-microglobulin
CD	Cluster of differentiation
CDR3	Complementarity determining region 3
CRC	Colorectal cancer
CTC	Circulating tumour cells
CTLA-4	Cytotoxic T lymphocyte antigen 4
CXCL	Chemokine (C-X-C motif) ligand
DCB	Durable clinical benefit
DCs	Dendritic cells
DNA	Deoxyribonucleic acid
EBV	Epstein-Barr virus
GEJ	Gastro-oesophageal junction
GITR	Glucocorticoid-induced tumour necrosis factor receptor
GrzB	Granzyme B
HCC	Hepatocellular carcinoma
HL	Hodgkin's lymphoma
HNSCC	Head and neck squamous cell carcinoma
HPV	Human papillomavirus
ICIs	Immune checkpoint inhibitors
ICOS	Inducible T cell costimulatory
IDO	Indoleamine 2,3-dioxygenase
IFN	Interferon
IFNGR1	Interferon gamma receptor 1
IHC	Immunohistochemistry
ILC	Innate lymphoid cell
iNOS	Inducible nitric oxide synthase
ISGs	IFN stimulated genes
JAK	Janus kinase
KLRG-1	Killer cell lectin-like receptor subfamily G member 1
Lag-3	Lymphocyte-activation gene 3
MCC	Merkel cell carcinoma
MCPyV	Merkel cell polyomavirus
MDSCs	Myeloid-derived suppressor cells
mGC	Metastatic gastric cancer
MHC	Major histocompatibility complex
mRNA	Messenger ribonucleic acid
NK	Natural killer
NO	Nitric oxide
Nrp-1	Neuropilin 1
NSCLC	Non-small-cell lung carcinoma

ODN	Oligodeoxynucleotide
ORR	Overall response rate
OS	Overall survival
PD-1	Programmed death 1
PD-L1	Programmed death ligand 1
PD-L2	Programmed death ligand 2
PET	Positron-emission tomography
PFS	Progression free survival
PGE2	Prostaglandin E2
PMBCL	Primary mediastinal B-cell lymphoma
RCC	Renal cell carcinoma
RR	Response rate
SCC	Squamous cell carcinoma
SCLC	Small-cell lung cancer
SHP	Sarcoma homology 2 domain-containing protein tyrosine phosphatase
STAT	Signal transducer and activator of transcription proteins
TAMs	Tumour associated macrophages
TCR	T cell receptor
TGF-β	Transforming growth factor β
Th	T helper cell
TIGIT	T cell immunoreceptor with immunoglobulin and immunoreceptor tyrosine-based inhibition motif domains
Tim-3	T-cell immunoglobulin mucin-3
TMB	Tumour mutational burden
TNB	Triple-negative breast cancer
Treg	Regulatory T cell
UC	Urothelial cancer
α-GalCer	α-galactosylceramide

ABSTRACT

The immune checkpoint blockade is a novel approach of cancer therapy, which markedly enhanced treatment efficacy of several cancer types. However, the frequency of cancer patients non-responding to this treatment is high. Establishment of predictive markers to distinguish patients suitable for the immune checkpoint blockade would enhance the number of patients receiving benefit from the therapy. This dissertation thesis focuses on the enhancement of efficacy of immune checkpoint inhibitors (ICIs) and predictive markers in experimental models of mouse tumours induced by TC-1 and TC-1/A9 cell lines and its clones with deactivation of interferon (IFN)-γ signalling (TC-1/dIfngr1 and TC-1/A9/dIfngr1), or CD80 molecule (TC-1/dCD80-1). IFN-γ is presumed to be the main inducer of programmed death ligand 1 (PD-L1) and a major histocompatibility complex I (MHC-I). Moreover, PD-L1 expression may predict sensitivity to PD-1/PD-L1 blockade. Non-functional IFN-γ signalling or downregulated MHC-I expression has been associated with resistance to ICIs in some patients. We found that IFNs type I (IFN-α and IFN-β) induced the expression of PD-L1 and MHC-I on TC-1/A9/dIfngr1 tumour cells with reversible downregulation of both molecules. We also showed that deactivation of IFN-γ signalling in TC-1/A9 cells was not a contraindication to PD-1/PD-L1 blockade combined with DNA vaccination. As TC-1-induced tumours were not sensitive to PD-L1 blockade, we next investigated the impact of CD80 expressed in tumour cells on the efficacy of ICIs and the tumour microenvironment. Although the CD80 deactivation in tumour cells did not induce the efficacy of anti-PD-L1 antibody, it considerably promoted the efficacy of anti-CTLA-4 antibody. Moreover, TC-1/dCD80-1 cells were more immunogenic than the TC-1 cell line. Therefore, CD80 molecule should be assessed as a predictive marker for cancer treatment by CTLA-4 blockade and as a possible target for the development of tumour cell-specific cancer therapy. Besides the major projects, experimental combined therapy of tumours with reversible downregulation of MHC-I and development of mouse oncogenic cell line with irreversible downregulation of MHC-I by deactivation of beta-2-microglobulin (B2m) are included in the thesis. Altogether, we developed clinically relevant models of mouse tumours with deactivated IFNGR1, CD80, and B2m and used them for enhancement of cancer immunotherapy and for search of its predictive markers.

ABSTRAKT

Blokování kontrolních bodů imunitních reakcí je novým terapeutickým přístupem v léčbě nádorů, který značně zvýšil účinnost léčby různých typů nádorů. Avšak podíl pacientů s nádory neodpovídajících na tuto léčbu je vysoký. Zavedení predikčních znaků pro rozlišení pacientů vhodných pro léčbu blokováním kontrolních bodů by mohlo zvýšit počet pacientů, kteří by měli z této léčby užitek. Tato disertační práce je zaměřena na zvýšení účinnosti inhibitorů kontrolních bodů imunitních reakcí (ICIs) a na predikční znaky s využitím experimentálních modelů myších nádorů vyvolaných buněčnými liniemi TC-1 a TC-1/A9 a jejich klony s deaktivací signalizace interferonu (IFN)-γ (TC-1/dIfngr1 a TC-1/A9/dIfngr1) nebo molekuly CD80 (TC-1/dCD80-1). IFN-γ je považován za hlavní cytokin zvyšující expresi ligandu programované buněčné smrti 1 (PD-L1) a hlavního histokompatibilního komplexu I (MHC-I). Exprese PD-L1 může předpovídat citlivost k blokování PD-1/PD-L1. Nefunkční signalizace IFN-γ nebo snížená exprese MHC-I u některých pacientů souvisela s rezistencí k ICIs. Zjistili jsme, že IFN I. typu (IFN-α a IFN-β) zvyšují expresi PD-L1 a MHC-I na nádorových buňkách TC-1/A9/dIfngr1 s reverzibilně sníženou expresí obou molekul. Také jsme ukázali, že deaktivace signalizace IFN-γ v buňkách TC-1/A9 nebyla kontraindikací pro blokování PD-1/PD-L1 v kombinaci s DNA vakcinací. Protože nádory vyvolané buňkami TC-1 nebyly citlivé na blokování PD-L1, následně jsme vyšetřovali vliv molekuly CD80, produkované v nádorových buňkách, na účinnost ICIs a na nádorové mikroprostředí. Přesto, že deaktivace CD80 v nádorových buňkách nezvýšila účinnost protilátky anti-PD-L1, významně podpořila účinnost protilátky anti-CTLA-4. Buňky TC-1/dCD80-1 byly více imunogenní než buněčná linie TC-1. Proto by měl být posouzen význam molekuly CD80 jako predikčního znaku pro léčbu nádorů blokováním CTLA-4 a také jako možný cíl pro vývoj terapie proti nádorovým buňkám. Kromě hlavních projektů je v této práci zahrnuta experimentální kombinovaná terapie nádorů s reverzibilním snížením MHC-I a vývoj myší onkogenní buněčné linie s ireverzibilně sníženou expresí MHC-I prostřednictvím deaktivace beta-2-mikroglobulinu (B2m). Vyvinuli jsme klinicky významné myší modely nádorů s deaktivací IFNGR1, CD80 a B2m a využili je pro zvýšení účinnosti nádorové terapie a hledání jejich prediktivních znaků.

1. INTRODUCTION

1.1. Immune checkpoints

Co-stimulatory and co-inhibitory molecules, defined as immune checkpoints, tightly regulate immune reactions in order to maintain homeostasis of the host and to avoid immunopathology (*1*, *2*). The immune checkpoints were originally studied in T cells. Besides the 1st signal, which naïve T cells receive from the T cell receptor (TCR) after recognition of antigen presented on the major histocompatibility complex (MHC), co-stimulatory and co-inhibitory receptors provide the 2nd signal in antigen-independent manner (*3*, *4*). Co-stimulatory receptors (such as cluster of differentiation (CD)28, CD80, CD86, inducible T cell costimulatory (ICOS), glucocorticoid-induced tumour necrosis factor receptor (GITR) and many others) support T cell activation, effector functions and survival (*5*, *6*). On the contrary, co-inhibitory receptors and their corresponding ligands promote the state of unresponsiveness to antigenic stimulation. Overexpression of co-inhibitory molecules is one of the major characteristics of T cell exhaustion, which can be induced by persistent antigenic stimulation due to a chronic infection or cancer (*7*).

Expression of co-inhibitory receptors alternates during the T cell activation and differentiation (*8*). Naïve T cells express a high level of B and T lymphocyte attenuator (BTLA) and T cell immunoglobulin mucin-3 (Tim-3) is detectable during this early stage too (*9*). Additional co-inhibitory receptors, such as (cytotoxic T lymphocyte antigen 4 (CTLA-4), programmed death 1 (PD-1), lymphocyte-activation gene 3 (Lag-3), CD244, T cell immunoreceptor with immunoglobulin and immunoreceptor tyrosine-based inhibition motif domains (TIGIT) and killer cell lectin-like receptor subfamily G member 1 (KLRG-1)), are upregulated following antigenic stimulation (*10*, *11*). Majority of the terminally differentiated effector T cells undergo apoptosis after clearance of antigen, whereas long-lived memory T cells maintain the response after the secondary exposure to antigen (*12*, *13*). Immune checkpoint molecules are important regulators of T cell memory establishment. Expression of various immune checkpoints is specific for distinct types of memory T cells, such as relatively high expression of immune checkpoints on effector memory T cells in comparison with central memory T cells (*10*). Interestingly, some immune checkpoints, such as PD-1, inhibit $CD8^+$ T cell differentiation into memory phenotype (*14*).

The firstly discovered immune checkpoint was CTLA-4, a type I transmembrane receptor of the immunoglobulin family, expressed by T cells (*15*). CTLA-4 competes with CD28 for binding to the ligands CD80 and CD86 in order to inhibit activation of naïve T cells (*16–18*). The affinity of CTLA-4 for CD80 and CD86 binding is approx. ten times higher than that of CD28 (*18*). The study also shows that CD80 and CTLA-4 expression increases in activated antigen presenting cells (APCs) and T cells, respectively, whereas the expression of CD86 and CD28 is constitutive. CD80 is therefore considered to be the primary ligand of CTLA-4, while CD86 predominantly interacts with CD28 (*18*, *19*). Expression of CTLA-4 varies in different T cell subsets. CTLA-4 is expressed especially on activated $CD4^+$ T cells and to a lesser extent on $CD8^+$ T cells (*20*). CTLA-4 mediated immunosuppression is one of the major effector mechanisms of regulatory T (Treg) cells, which constitutively express high level of this molecule (*21*, *22*). The essential role of CTLA-4 in Treg mediated immunosuppression has been determined by Treg-specific CTLA-4 deactivation (*23*). In that study, CTLA-4^- Treg cells were unable to maintain self-tolerance and Treg specific CTLA-4 deactivation promoted anti-tumour immunity.

Furthermore, one of the most frequently studied immune checkpoints is PD-1, a type I transmembrane receptor and a member of the CD28/CTLA-4 family of immunoglobulin receptors (*24*). The *PD-1* gene was originally studied in apoptotic cell lines and in mouse thymocytes (*25*). Function of this molecule was determined in a PD-1 deficient mouse model (*26*). The animals developed severe lupus-like autoimmune disease, which indicated the immunosuppressive role of PD-1. The PD-1 protein structure consists of N-terminal Ig-like variable domain, a transmembrane region, and an intracellular tail (*27*). Binding of ligand to PD-1 through the variable domain triggers phosphorylation of immunoreceptor tyrosine-based inhibition motif and immunoreceptor tyrosine-based switch motif on the PD-1 intracellular domain and association with sarcoma homology 2 domain-containing protein (SHP) 1 and SHP2 tyrosine phosphatases (*27–29*). Subsequently, SHP1/2 interfere with TCR and CD28 signalling pathways, suppress T cell functions and promote apoptosis (*30–32*).

PD-1 is expressed especially on activated and effector memory T cells, Treg cells, and natural killer (NK) T cells, and to some extent on B cells and NK cells (*10*, *33–35*). MHC-I restricted cytotoxic $CD8^+$ T cells are presumably the main target of PD-1/programmed death ligand 1 (PD-L1) axis in tumours (*36*). The anti-tumour response in

some tumours with downregulated MHC-I expression is mediated by NK cells, independently of $CD8^+$ T cells, and such tumours may also be sensitive to the PD-1/PD-L1 blockade (*37*). However, the direct effect of PD-1 blockade on NK cell effector functions remains unclear (*38*). Moreover, recent study has revealed an essential role of myeloid cells in PD-1 mediated tumour protection (*39*). Specific deactivation of PD-1 in myeloid cells resulted in enhanced effector functions of monocytes, macrophages, and dendritic cells (DCs), reduced frequency of myeloid-derived suppressor cells (MDSCs), and elevated frequency of effector memory T cells with improved anti-tumour effector functions, although PD-1 expression on lymphoid cells was preserved.

PD-1 interacts with PD-L1 (Fig. 1) as well as PD-L2 (*24*, *40*). Tumour cells and several types of tumour infiltrating cells, such as T cells, B cells, NK cells, macrophages, and DCs, may express PD-L1 and inhibit anti-cancer immune response (*41–43*). PD-L2

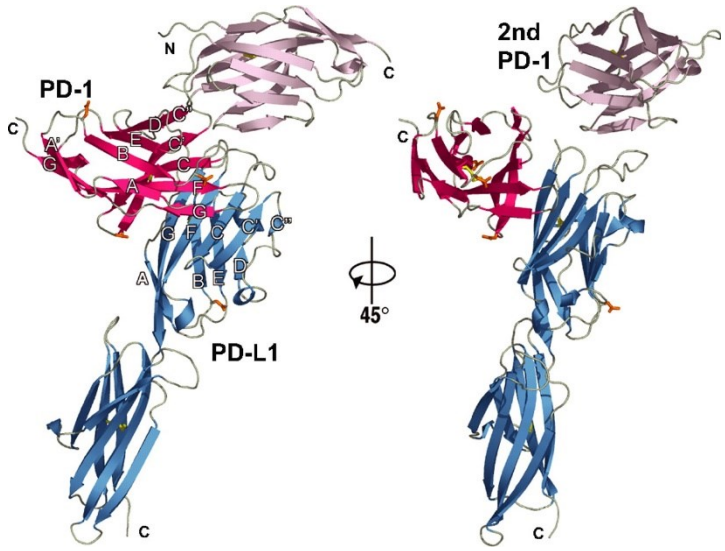

Figure 1: Molecular structure of PD-1/PD-L1 complex. The PD-1 domains are shown in red and violet, and PD-L1 is blue (28).

is expressed on stimulated macrophages and DCs, or B cells (*44–46*). Unlike PD-L1, the contribution of PD-L2 in the immune response is controversial. In some settings, PD-L2 acts as a co-stimulatory molecule, independent of PD-1, and inhibits tumour growth (*45*).

PD-L1 expression on tumour cells and/or host cells promotes tumour growth of some tumour types (*47–51*). Importance of PD-L1 expression on host cells in the inhibition of anti-tumour immunity was identified in B16 melanoma (*47*). Moreover, PD-L1 expression on myeloid cells was found to be essential for response to PD-1/PD-L1 blockade in MC38-, A20-, and E.G7-induced tumours (*51*). Another study showed that MC38 tumour cells as well as host cells inhibit T cell cytotoxicity and contribute to

tumour escape from immune surveillance (*49*, *50*). Therefore, PD-L1 expression on tumour cells and host cells may be predictive in the selection of patients suitable for PD-1/PD-L1 blockade.

PD-L1 overexpression is a frequently occurring immune escape mechanism in tumours. 9p24.1 amplification, enhancement of *PD-L1* transcription, or increased messenger ribonucleic acid (mRNA) stability due to disruption of the *PD-L1* mRNA three prime untranslated region upregulate PD-L1 expression (*52–54*). PD-L1 expression may also be enhanced by constitutive activation of some signalling pathways in tumours, such as mitogen-activated protein kinase kinase/extracellular signal-regulated kinase, phosphatidylinositol 3-kinase/protein kinase B, Janus kinase (JAK)/signal transducer and activator of transcription proteins (STAT), neurogenic locus notch homolog protein 3/mammalian target of rapamycin, or microRNA-200/zinc-finger E-box-binding homeobox 1 (*55–58*). Some transcription factors have been reported to induce PD-L1 expression, for example, hypoxia-inducible factor 2α or STAT3 (*59*, *60*). Furthermore, PD-L1 upregulation in cancer is associated with viruses, such as Epstein-Barr virus (EBV) and hepatitis B virus, and some bacteria, such as *Helicobacter pylori* (*61–64*). However, the relationship between PD-L1 and viruses is not uniform in various studies (*65–67*). Significantly upregulated PD-L1 expression was associated with lymphocyte infiltration in tumours and interferon (IFN)-γ expression in some human papillomavirus $(HPV)^+$ head and neck squamous cell carcinoma (HNSCC) patients (*66*). On the contrary, another study of HNSCC reported that HPV infection correlated with methylation of PD-L1 promotor and silenced transcription of the corresponding gene (*65*). In conjunctival squamous cell carcinoma (SCC), PD-L1 expression did not correlate with HPV status (*67*).

Several studies evaluated PD-L1 as a prognostic marker in various cancer types. For instance, upregulated PD-L1 implied reduced overall survival (OS) in breast cancer (*68*). The study showed that PD-L1 expression was associated with increased tumour size, metastasis into lymph nodes, and oestrogen receptor negativity. Moreover, genetic alteration of 9p24.1 and PD-L1 upregulation in hepatocellular carcinoma correlated with poor outcome of patients (*69*). On the contrary, PD-L1 in melanoma did not predict the prognosis, although upregulation of PD-L1 correlated with the absence of metastasis in lymph nodes (*70*).

1.2. Cytokines in the tumour microenvironment

Cytokines are indispensable regulators of immune reactions and modulate anti-cancer immune response. One of the most frequently studied cytokines in cancer is IFN-γ, a type II IFN occurring in the form of a homodimer, which was discovered in activated human leucocytes (*71*). This cytokine is produced in tumours mainly by stimulated T cells, innate lymphoid cells (ILC)1, NK cells, and NKT cells (*72–74*). IFN-γ receptor (IFNGR) comprises two IFNGR1 and two IFNGR2 subunits. The IFNGR recruits non-receptor tyrosine kinases JAK1 and JAK2 upon binding IFN-γ that activate transcription factors STAT1 or STAT3 (*75*, *76*). IFN-γ induces the expression of IFN stimulated genes (ISGs) in tumour cells as well as host cells and affects tumour growth (*77*). So far, 124 proteins of IFN-γ signalling pathway have been described (*78*, *79*).

IFN-γ is a pleiotropic cytokine that can regulate multiple mechanisms in tumours, for instance, antigen presentation, cell infiltration, cell cycle, metabolism, invasiveness, and immunosuppression (*78*). IFN-γ induces MHC-I expression and production of chemokines with anti-tumour functions such as chemokine (C-X-C motif) ligand (CXCL) 9, CXCL10 and CXCL11 (*80*, *81*). IFN-γ can downregulate PD-1 and act in a synergy with immune checkpoint blockade (*82*). Furthermore, IFN-γ contributes to the polarization of macrophages into anti-tumour M1 phenotype (*83*). This cytokine may also switch immunosuppressive tumour associated macrophages (TAMs) to M1 macrophages, which express inducible nitric oxide synthase (iNOS) and produce nitric oxide (NO) (*84*).

Besides the immunostimulatory function of IFN-γ, this cytokine promotes the expression of immunosuppressive molecules, such as PD-L1 or indolamine 2,3-dioxygenase (IDO). IFN-γ upregulates the PD-L1 on tumour cells and host cells and PD-L1 upregulation was also observed on exosomes derived from tumour cells (*85*, *86*). Efficiency of IFN-γ to stimulate PD-L1 was even enhanced in triple negative breast cancer (TNBC) by amplification of 9p24.1 chromosome (*87*). However, contradictory effect of IFN-γ signalling on anti-tumour immune response has been determined in tumour cells in comparison with immune cells (*77*). IFN-γ promoted PD-L1 expression on colorectal and melanoma cancer cells, while it simultaneously stimulated effector functions of immune cells in that study. Deactivation of IFN-γ signalling in tumour cells resulted in increased accumulation of T cells, maturation of NK/ILC1 cells, and elimination of cancer cells.

Even though IFN-γ is considered to be the major cytokine inducing MHC-I and PD-L1, other cytokines may have similar effect. A broad range of cytokines induce MHC-I expression, such as IFN-α, IFN-β, tumour necrosis factor (TNF)-α, interleukin (IL)-1α, or IL-27 (*80*, *88–90*). Furthermore, IFN-α, IFN-β, IL-1α, IL-1β, IL-27, CCL2, and granulocyte-macrophage colony stimulating factor (GM-CSF) can induce the PD-L1 expression (*80*, *86*, *91–95*). Some cytokines (for instance, TNF-α, epidermal growth factor (EGF), and IL-6) regulate post-translational modifications of PD-L1 and stabilize the molecule by inhibition of proteasomal degradation (*96–98*).

1.3. Immune checkpoint inhibitors

Recent discovery of the immune checkpoints and approval of immune checkpoint inhibitors (ICIs) was a real breakthrough in cancer therapy because it prolonged survival of many patients with different tumour types (*99*). In 2018, James Allison and Tasuku Honjo were awarded the Nobel Prize in Physiology and Medicine for their discovery of CTLA-4 and PD-1 and the development of ICIs (*100*). The first ICI, a monoclonal antibody blocking CTLA-4 (ipilimumab), was approved by FDA in 2011 for treatment of malignant melanoma (*101*). In 2014, first antibodies targeting PD-1 (pembrolizumab and nivolumab) were approved for the treatment of metastatic melanoma and approvals for additional types of cancer (such as non-small-cell lung carcinoma (NSCLC), renal cell carcinoma (RCC), and head and neck carcinoma) were approved later (*102–104*). Moreover, another anti-PD-1 antibody (cemiplimab) was approved in 2018 for treatment of cutaneous SCC (*105*). Furthermore, PD-L1 blockade has been found effective in anti-cancer therapy. In 2016, the first anti-PD-L1 monoclonal antibody (atezolizumab) was approved for the treatment of bladder cancer, NSCLC, and triple-negative breast cancer (*106–108*). Additional approvals of new anti-PD-L1 antibodies (avelumab and durvalumab) followed later (*109*, *110*).

1.4. Mechanisms of tumour resistance to immune checkpoint inhibitors

Successful immunotherapy promotes recognition of tumour cells by the immune system and tumour elimination (*111*). Although the immune checkpoint blockade was a breakthrough in cancer therapy, many cancer patients are resistant to ICIs (*112*, *113*). Patients with primary (innate) resistance are completely non-sensitive to the therapy and patients with secondary (acquired) resistance initially respond to the treatment and develop resistance during the treatment (*114*). The selective pressure of immune system

and the cancer therapy shape characteristics of tumours and may result in the tumour elimination, or evasion of the immune system and therapy (*115–117*).

The tumour microenvironment affects the therapeutic outcome of immune checkpoint blockade (*118*). Distinct types of tumours have been characterised as "cold" or "hot" based on the level of tumour infiltration by immune cells and anti-cancer immune response. The cold tumours are often resistant to immunotherapy and therefore the development of combined therapy to switch cold tumours into hot is a challenging issue (*119*). Cold tumours are deficient in activated immune cells owing to the absence of danger signals, insufficient tumour antigen presentation, or inability of immune cells to infiltrate the tumour. Immune cells accumulate in hot tumours, although persistent stimulation with tumour antigens leads to exhaustion of T cells and to strengthening of suppressive mechanisms in the tumour microenvironment. The hot tumours are especially sensitive to immune checkpoint blockade (*120*, *121*). ICIs may restore the activation of exhausted T cells accumulated in hot tumours and promote tumour regression.

Abrogation of tumour antigen presentation due to defects in the antigen-processing machinery or downregulation of MHC-I expression frequently occurs in patients resistant to ICIs (*122–125*). Moreover, primary as well as secondary resistance to ICIs were observed in patients with truncating mutations in JAK-1 or JAK-2 that inhibited the function of IFN-γ signalling in tumours (*122*, *126*). Low PD-L1 expression, downregulation of antigen presentation, the lack of anti-proliferative effect of IFN-γ, and inhibition of tumour infiltration by T cells might have caused the resistance to ICIs in tumours insensitive to IFN-γ (*122*, *126*, *127*). Expression of immunosuppressive molecules by tumour cells may bypass blockade of PD-1/PD-L1 and mediate resistance to ICIs (*128–130*). For example, IDO, prostaglandin E2, IL-10, or transforming growth factor β (TGF-β) may promote differentiation of immune cells into immunosuppressive phenotype, which enhance tumour growth, such as Treg cells, M2 macrophages, or MDSCs. PD-1/PD-L1 blockade may be compensated by upregulation of additional immune checkpoints, such as CTLA-4, Tim-3, TIGIT, or Lag-3 (*11*, *131*). Another study reported that CTLA-4, Tim-3, Lag-3, or BTLA blockade synergised with inhibition of PD-1/PD-L1 axis (*132*). Thus, single ICI may be less effective than simultaneous targeting of different pathways in cancer treatment. A single blockade of PD-1/PD-L1 axis may strengthen CTLA-4/CD80 signalling, as PD-L1 interaction with CD80 *in cis* (on the same cell) inhibits immunosuppressive effect of CTLA-4 in some cases (*133*).

Resistance to PD-1/PD-L1 blockade may also be mediated by PD-L1 on the surface of exosomes, which inhibits the effector functions of $CD8^+$ T cells and induce apoptosis of these cells (*134*, *135*). However, the mechanism of exosomal PD-L1 mediated resistance to the anti-PD-L1 is unclear.

Furthermore, extrinsic factors, such as gut microbiota, may influence immune reactions and sensitivity to ICIs (*136*). The impact of gut microbiota on the sensitivity to ICIs was tested in germ-free mice that received faecal transplantation from cancer patients (*137–139*). The efficacy of ICIs observed in cancer patients was preserved in mice, in that study. Moreover, it was determined that changed microbiota composition after treatment with antibiotics, tyrosine kinase inhibitors (TKIs), or corticosteroids may induce primary resistance to ICIs (*137*, *140*). For example, deficiency of *Akkermansia muciniphila* (Verrucomicrobiae order) in the gut of the NSCLC, and RCC patients and *Bacteroides salyersiae* (Bacteroidales order) in the RCC patients correlated with resistance to blockade of PD-1/PD-L1 axis (*137*, *139*). Moreover, Bacteroidales order was abundant in non-responders to anti-PD-1 in metastatic melanoma patients (*141*).

Besides resistance to ICIs, some individuals may develop hyper-progressive disease, a rapid increase of tumour growth after treatment with ICIs which is significantly faster than in non-responders (*142*). The hyper-progressive disease may be mediated by rapid proliferation and immunosuppressive functions of Treg cells, exhausted T cells, M2 macrophages, or MDSCs (*143*). However, mechanisms inducing the hyper-progressive disease are not completely understood.

1.5. Predictive markers of response to immune checkpoint inhibitors

1.5.1. The tumour microenvironment

The tumour microenvironment regulates the therapeutic outcome of ICIs. Accordingly, the characteristics of tumour microenvironment may predict efficacy of the therapy (*144*). Analysis of PD-L1 expression on tumour cells or tumour infiltrating cells was approved as the first predictive biomarker for response to PD-1/PD-L1 blockade in several tumour types (Fig. 2). However, PD-L1 expression as a single biomarker was predictive in only 28.9% of various cancer cases (*145*). Low sensitivity of immunohistochemistry (IHC), a standard technique of PD-L1 detection in the tumour microenvironment, may contribute to the limited predictive capacity of PD-L1.

Therefore, more sensitive methodologies are being developed, such as radiolabelled monoclonal antibodies imaging with positron-emission tomography (PET) (*146*). PD-L1 imaging with PET predicted the response of cancer patients to blockade of PD-1/PD-L1 more accurately than IHC. Standardisation of diagnostic assays in clinical use and biomarkers additional to PD-L1 expression in tumours should increase accuracy to predict the sensitivity of patients to ICIs (*147*). Thus, predictive value of various markers is investigated.

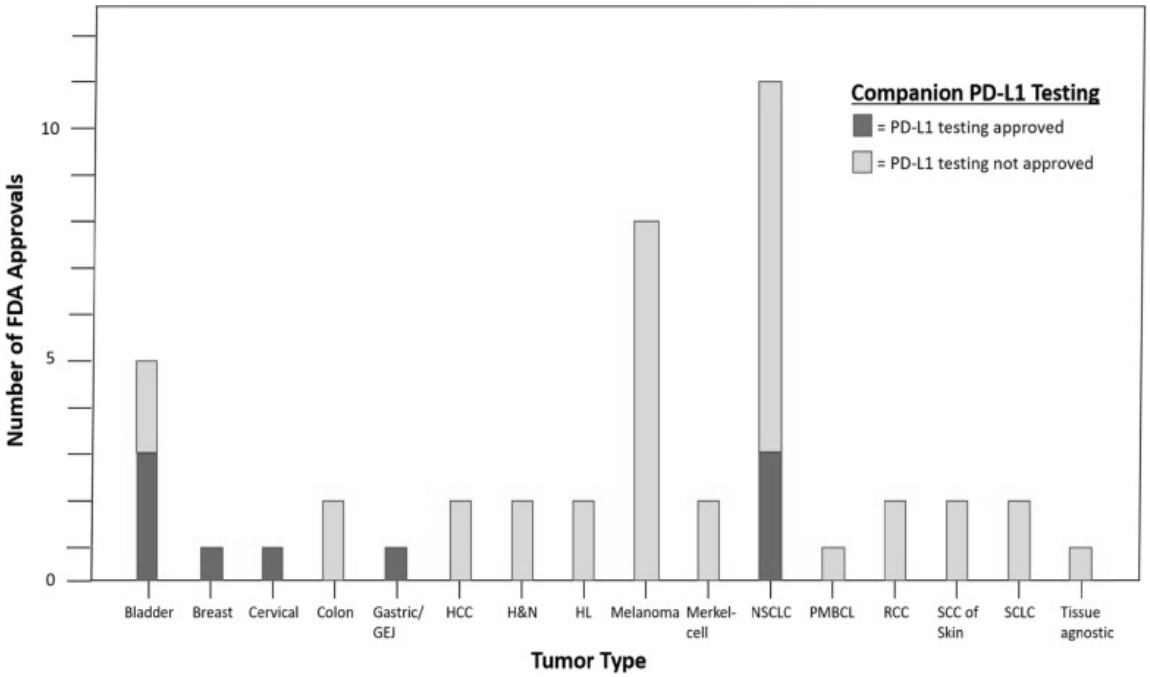

Figure 2: PD-L1 testing as a companion diagnostic for administration of immune checkpoint inhibitors. Bars represents the number of FDA approvals for immune checkpoint inhibitors (pembrolizumab (N = 18), nivolumab (N = 11), atezolizumab (N = 5), ipilimumab with nivolumab (N = 3), ipilimumab (N = 2), durvalumab (N = 2), cemiplimab (N = 2), and avelumab (N = 2). The dark-gray colour illustrates approved and the light-grey colour non-approved PD-L1 testing. Abbreviations: gastro-oesophageal junction (GEJ), hepatocellular carcinoma (HCC), Hodgkin's Lymphoma (HL), non-small-cell lung cancer (NSCLC), primary mediastinal B-cell lymphoma (PMBCL), renal cell carcinoma (RCC), squamous cell carcinoma (SCC), small-cell lung cancer (SCLC) (*145*).

The level of immune cell infiltration into tumour and a functional state of tumour infiltrating cells are fundamental factors in the therapeutic outcome of ICIs. The frequency of selected immune cells infiltrating tumours was described as an

„immunoscore" (*148*). As $CD8^+$ T cells play the major role in tumour rejection in response to ICIs, the accumulation of these cells in tumours is evaluated together with expression of PD-1 and PD-L1 (*149*). Enhanced abundance of $CD8^+$, $PD\text{-}1^+$, or $PD\text{-}L1^+$ cells in tumours, detected by IHC before treatment with ICIs, predicted the response in melanoma patients (*11*, *150*). These studies showed that blockade of PD-1/PD-L1 axis induced $CD8^+$ T cell proliferation, activation of effector functions, infiltration into tumour parenchyma, and control of tumour growth. On the contrary to these studies, the frequency of $CD8^+$ T cells and the ratio of $CD4^+/CD8^+$ cells was not associated with response to ICIs in metastatic melanoma patients receiving ipilimumab, pembrolizumab or nivolumab, although the level of tumour infiltration by lymphocytes correlated with OS (*148*). Furthermore, expression of immune checkpoints on $CD8^+$ T cells infiltrated into tumour has been reported as a predictive marker for ICIs in cancer (*151*). In that study, partially exhausted ($PD\text{-}1^+$ $CTLA\text{-}4^+$) $CD8^+$ T cells infiltrated into tumour predicted response to pembrolizumab or nivolumab in metastatic melanoma patients. The study indicated that the frequency of partially exhausted $CD8^+$ T cells exceeding 20% of all tumour infiltrating $CD8^+$ T cells detected before treatment was associated with significantly higher response rate (RR) and longer progression free survival (PFS) after PD-1 blockade. The treatment induced functional activation of $CD8^+$ T cells and infiltration into tumours, while infiltration of $CD4^+$ T cells declined and the ratio of $CD4^+/CD8^+$ cells was decreased. Accumulation of tumour-antigen-specific exhausted $CD8^+$ T cells within the tumours, especially tissue-resident memory cells ($CD103^+$ $CD69^+$ $CD49a^+$), was also a predictive factor of response to PD-1/PD-L1 blockade in patients with HNSCC (*152*). ICIs restored effector functions of exhausted cells, induced proliferation of memory T cells in the circulation, and initiated anti-tumour immune response. Moreover, effector memory ($EOMES^+$ $CD69^+$ $CD45RO^+$) T cells were associated with prolonged PFS in melanoma patients, and upregulated abundance of these cells was predictive of response to ICIs (*11*).

Besides T cell infiltration into tumours and immune checkpoint expression by these cells, diversity of TCR repertoire and clonal expansion was evaluated as a predictive marker of response to ICIs. Accumulation of T cells in tumours correlated with reduced diversity of TCR β-chain and upregulated clonality in melanoma patients subsequently responding to pembrolizumab (*150*). Proliferation was restricted to tumour-specific T cells and such clones expanded in responders after pembrolizumab administration.

Another study evaluated the predictive value of TCR diversity and clonality in peripheral blood T cells (*153*). The high clonality and the lack of TCR diversity predicted a favourable outcome of pembrolizumab, or nivolumab, but poor response to anti-CTLA-4 in melanoma patients.

1.5.2. Genetic alterations in tumours

Genetic instability enhances tumour immunogenicity and sensitivity to immunotherapy. The predictive capacity of tumour mutational burden (TMB) in the immune checkpoint blockade has been evaluated in cancer patients. The level of TMB predicted therapeutic outcome in a dataset of patients with various tumour types (melanoma, NSCLC, and 19 other types of tumours; N = 52, 36, and 63 patients, respectively) (*154*). In that study, the RR after PD-1/PD-L1 blockade was approx. three times higher in patients with high TMB than in patients with low to intermediate TMB across all tumour types. Interestingly, TMB was not predictive of the combined PD-1/PD-L1 and CTLA-4 blockade. Other studies evaluated TMB as a predictive marker for specific types of cancer, such as melanoma, NSCLC, or metastatic RCC (*77*, *155–157*). TMB correlated with the probability of response to PD-1 blockade in melanoma (*77*). Furthermore, nivolumab and ipilimumab were significantly more efficient than chemotherapy in stage IV or recurrent NSCLC patients with high TMB compared with low TMB tumours (*155*). However, TMB was not predictive in metastatic RCC patients treated with nivolumab and/or ipilimumab or pembrolizumab (*156*). Despite the correlation of TMB with response to ICIs in several studies, 54.5% of patients with high TMB in various tumour types did not respond to PD-1/PD-L1 blockade (*158*). Therefore, the combination of TMB with additional markers may improve prediction accuracy in cancer.

Besides TMB, mismatch repair (MMR) and microsatellite instability (MSI) have been evaluated as predictive markers of response to ICIs (*159*). The frequency of defects in deoxyribonucleic acid (DNA) repair, including MMR, did not correlate with RR to PD-1/PD-L1 blockade across 13 different cancer types (*112*). Moreover, proficient MMR, low status of MSI, and low to intermediate TMB were identified in a fraction of cancer patients who achieved objective response to ICIs (*154*, *160*). In contrast to those studies, MSI status contributed to the identification of metastatic gastric cancer (mGC) patients

suitable for the therapy with ICIs (*161*). In that study, MSI had stronger predictive capacity than PD-L1 expression.

Determination of the immunoscore alongside the MMR and MSI may improve the accuracy of prediction which patients may benefit from ICIs. In most cases, deficiency of MMR and high MSI correlated with upregulated expression of PD-L1 and PD-L2, infiltration of $CD4^+$ and $CD8^+$ cells and enhanced activation of IFN-γ signalling in majority of patients with colorectal cancer (CRC) (*160*). However, the study also showed increased PD-L1 expression and activated IFN-γ signalling in tumours with proficient MMR and low MSI. In that tumours, the level of $CD4^+$ and $CD8^+$ cells infiltration was comparable to high MSI tumours and therefore PD-1/PD-L1 blockade may be efficient in both tumour types.

Genetic instability may generate immunogenic neoantigens (*154*, *162*). Therefore, the occurrence of neoantigens is evaluated alongside markers of genetic instability in order to predict the efficacy of ICIs. For example, increased somatic non-synonymous TMB and neoantigens detected in NSCLC correlated with favourable prognosis in response to pembrolizumab (upregulated (ORR), durable clinical benefit (DCB), and PFS) (*163*). Another study was conducted on 12 different types of advanced cancer deficient in MMR and with high MSI status (*113*). In that study, expansion of neoantigen specific T cells was identified in responders to pembrolizumab, according to the sequencing analysis of CDR3 regions of TCR. Moreover, neoantigens suitable for presentation on MHC molecules have been shown to correlate with better clinical outcome of patients with high TMB in different types of solid tumours treated with ICIs (*158*). Genotype of HLA corresponds to the repertoire of epitopes presented on MHC molecules (*164*). Patients with heterozygosity at HLA-I, and especially HLA-B44 allele, had a significantly better outcome of ICIs compared to patients with loss of heterozygosity or HLA-B62.

Furthermore, copy number chromosomal aberrations in various types of cancer are associated with the efficacy of ICIs. Focal copy number gain of 9p24.1, which upregulates PD-L1, PD-L2, and JAK-2 expression, occurred in several malignancies, such as Hodgkin's lymphoma (HL), triple-negative breast cancer (TNB), diffuse large B cell lymphoma, hepatocellular carcinoma (HCC) or CRC (*69*, *166–169*). Predictive value of this genetic alteration and constitutive upregulation of PD-L1 was evaluated for the

efficacy of ICIs. *PD-L1* was amplified in 0.7% of various types of solid tumours and 66.7% of patients with the upregulation of this gene responded to ICIs independently of TMB or MSI (*52*). Furthermore, nivolumab was an effective treatment in relapsed or refractory HL and the majority of patients bearing this type of tumour responded to the therapy (*166*, *170*). All patients in the study had genetic alterations of the *PD-L1* and *PD-L2* loci, and upregulation of PD-L1 protein production was associated with increased efficacy of nivolumab (*170*). Upregulated PD-L1 was also detected in patients with rare types of large B-cell lymphoma (relapsed/refractory primary central nervous system and testicular lymphoma) sensitive to nivolumab (*171*). The portion of responders to pembrolizumab in relapsed or refractory classical HL was similar to nivolumab and the majority of tumours were PD-L1$^+$, presumably due to 9p24.1 genetic alteration (*172*). Moreover, enhanced efficacy of pembrolizumab in a patient with advanced CRC and 9p24.1 copy number gain in liver metastasis further supports the predictive value of this biomarker (*168*).

1.5.3. Viruses and microbiota

Some viruses associated with tumorigenesis may affect sensitivity to ICIs and serve as predictive markers. For instance, detection of EBV strongly correlated with enhanced ORR to pembrolizumab in mGC (*161*). On the contrary, Merkel cell polyomavirus (MCPyV) detected in patients did not correlate with the response to pembrolizumab in Merkel cell carcinoma (MCC) (*34*). Instead of the MCPyV status, the high abundance of PD-1$^+$ and PD-L1$^+$ cells in tumours and the interaction of these molecules were associated with clinical outcome. Another study also reported that MCPyV did not correlate with response to pembrolizumab in MCC (*173*). Furthermore, sensitivity to nivolumab was independent of HPV infection or PD-L1 expression in patients with HNSCC (*174*).

Treatment with antibiotics prior to administration of ICIs predicted reduced OS and PFS of cancer patients due to altered composition of microbiota (*175*). Several studies analysed the enrichment of particular bacterial species in the gut of melanoma patients before treatment and its impact on the efficacy of ICIs (*138*, *141*, *176*). For instance, *Bifidobacterium longum*, *Collinsella aerofaciens*, and *Enterococcus faecium* indicated response to the PD-1 blockade (*138*). Moreover, *Faecalibacterium* in melanoma patients was associated with response to ipilimumab or PD-1 blockade (*141*, *176*). Clostridiales

order and Ruminococcaceae family were enriched in the gut of responders to anti-PD-1 in metastatic melanoma patients (*141*). As the level of tumour infiltrating leucocytes is associated with the efficacy of ICIs, the impact of bacteria on immune cell infiltration into tumours has been assessed in some studies (*139*, *141*). For instance, *A. muciniphila* increased the accumulation of $CD4^+$ T cells in mouse tumours (*139*). Moreover, the occurrence of other bacteria, *Faecalibacterium* genus (Clostridiales order), in the gut of melanoma patients correlated with increased abundance of $CD4^+$ and $CD8^+$ T cells in the periphery and it enhanced the accumulation of $CD8^+$ T cells in the tumours (*141*). On the contrary, the high abundance of Bacteroidales supported the increased frequency of Treg cells and MDSCs in the circulation and promoted resistance to PD-1 blockade in that study.

1.5.4. Systemic factors

Liquid biopsy is advantageous in routine clinical practice thanks to its feasibility and non-invasiveness. Prognostic value of several systemic factors examined from the blood of cancer patients is studied in order to monitor the efficacy of ICIs and to predict the suitability of treatment. Circulating tumour cells (CTC) and expression of immunosuppressive molecules by CTC appeared to be prognostic in patients receiving PD-1/PD-L1 inhibitors (*177–179*). CTC in the peripheral blood and PD-L1 expression on these cells during the therapy correlated with inferior outcome of NSCLC and urothelial cancer (UC) patients (*177*, *178*, *180*). Expression of IDO in CTC indicated shorter PFS and OS, and increased risk of death in advanced NSCLC patients treated with anti-PD-1, while PD-L1 surface expression on CTC was not predictive (*179*). Moreover, the amount of circulating tumour DNA was associated with response to CTLA-4 and PD-1/PD-L1 blockade in various types of tumours (*161*, *181*, *182*).

The composition of immune cells in the peripheral blood was evaluated as a predictive marker of sensitivity to ICIs. The frequency of $CD14^+CD16^-HLA\text{-}DR^{hi}$ monocytes was described as a strong predictive marker of response to pembrolizumab or nivolumab in patients with stage IV melanoma (*183*). In that study, high frequency of monocytes and low frequency of T cells in the blood of responders indicated T cell accumulation in tumours before treatment. The frequency of activated T cells, central memory T cells, and NKT cells was enhanced in the circulation after PD-1 blockade in responders. Another study focused on the predictive capacity of cytokines in the

peripheral blood in patients with NSCLC receiving pembrolizumab or nivolumab (*184*). Cytokines (IFN-γ, TNF-α, IL-1β, IL-2, IL-4, IL-5, IL-6, IL-8, IL-10, and IL-12) detected before therapy did not predict therapeutic outcome of ICIs. However, increased concentration of these cytokines after treatment markedly correlated with favourable prognosis. Another study showed that increased concentration of IFN-γ in blood samples, which were stimulated with tuberculosis antigen *in vitro*, predicted response to PD-1/PD-L1 blockade in NSCLC patients treated with nivolumab, pembrolizumab, or atezolizumab (*185*).

1.5.5. IFN-γ signalling

Several studies tested the capacity of IFN-γ and IFN-γ-related genes to predict the therapeutic outcome of ICIs in various cancer types (*11*, *124*, *186*). Expression of IFN-γ and IFN-γ-related genes correlated with "hot"/"inflamed" tumour microenvironment and predicted response to ICIs in cancer patients (*186*, *187*). For instance, the expression of IFN-γ and IFN-γ-inducible genes were upregulated in melanoma before atezolizumab administration in responders (*187*). Furthermore, the set of IFN-γ-responsive genes, which represented activation of IFN-γ signalling, activation and effector functions of immune cells and recruitment of $CD8^+$ T cells into tumours, predicted the efficacy of pembrolizumab (*186*). The set of IFN-γ-responsive genes was initially defined in melanoma and HNSCC patients and subsequently validated on a large cohort of patients with nine different cancer types. Moreover, *IFNG* expression and markers of IFN-γ stimulation in tumours before treatment were predictive in melanoma patients responding to nivolumab (*124*). Another study determined the expression of genes associated with IFN-γ and its downstream signalling, such as *STAT1* and *IRF1* (*11*). Expression of these genes correlated with response to nivolumab or pembrolizumab in melanoma patients. Similarly, elevation of pSTAT1 and its spatial colocalization with $CD8^+$ cells at the invasive tumour margin indicated the response to pembrolizumab in metastatic melanoma (*150*). Moreover, IFN-γ expression signature in tumour microenvironment predicted the efficacy of ICIs in NSCLC patients (*77*). In that study, the response to anti-PD-1 and anti-CTLA-4 therapy surprisingly correlated with mutations in IFN type I and II pathways, on the contrary to the aforementioned studies. This observation further supports the dual role of IFNs in cancer.

1.6. Integration of immune checkpoint blockade predictive markers

High throughput techniques have been used to integrate various predictive markers to ICIs based on genomic and transcriptomic features (*188*, *189*). TMB did not predict sensitivity to ICIs in melanoma in these studies. However, mutations in the DNA repair gene BRCA2 were identified in tumours of responders, while innate anti-PD-1 resistance signature (IPRES) characterised by upregulated transcription of genes associated with angiogenesis, hypoxia, remodelling of extracellular matrix, and mesenchymal transition predicted primary resistance to the treatment (*188*). Model integrating clinical, genomic and transcriptomic characteristics of tumours showed that MHC-II expression, tumour purity (the proportion of tumour cells in the tumour tissue), heterogeneity (the occurrence of subclonal mutations), and ploidy predicted response to anti-PD-1 (*189*). Next, markers of resistance to PD-1/PD-L1 blockade were determined in the tumour microenvironment based on clinical-grade RNA sequencing assay (*190*). Expression of immune checkpoint molecules Tim3 and VISTA, and CD68 marker of macrophages predicted worst clinical outcome and markedly shorter PFS in patients with diverse types of tumours treated with PD-1/PD-L1 blockade.

In conclusion, cancer is a heterogeneous disease and multiple factors affect the therapeutic outcome of ICIs. Besides the integration of biomarkers, a personalized approach would improve the accuracy of patient selection for the therapy. A tool “cancer immunogram” designed to evaluate the probability of response to ICIs based on multiple parameters has been recently introduced (*191*). The cancer immunogram comprises markers that represent the level of immune cell infiltration, mutational status, occurrence of neoantigens, and the degree of immunosuppression in tumours. Subsequent studies introduced alternative cancer immunograms related to UC or NSCLC (*192*, *193*). Development of immunograms related to additional cancer types and extension of a set of predictive markers would contribute to the effective cancer treatment.

2. AIMS

During my doctoral studies, I focused on the development of clinically relevant experimental mouse tumour models with altered expression of molecules involved in anti-tumour immune response and regulation of sensitivity to cancer immunotherapy.

The main aims of the dissertation thesis were:

- To assess whether deactivation of IFN-γ signalling in tumour cells with reversibly downregulated PD-L1 and MHC-I may be a contraindication to PD-1/PD-L1 blockade and to evaluate the impact of cytokines on PD-L1 and/or MHC-I expression on tumour cells.
- To characterise the microenvironment of tumours with deactivation of CD80 costimulatory molecules and to test the sensitivity of these tumours to the ICIs.

Besides the main projects of this thesis, I participated in two projects focused on mouse tumour models characterized by downregulation of MHC-I molecules. The aim of the first project was to test experimental combined immunotherapy against tumours with reversible MHC-I downregulation. In the second project, the aim was to generate a mouse tumour model with irreversible downregulation of MHC-I molecules and to examine the combined immunotherapy in this model.

3. RESULTS AND DISCUSSION

3.1. Publication 1: Abrogation of IFN-γ signalling may not worsen sensitivity to PD-1/PD-L1 blockade

3.1.1. Main characteristics of cell lines used in the study

In order to assess whether the IFN-γ signalling regulates the efficacy of the PD-1/PD-L1 blockade, we used mouse oncogenic TC-1 cell line, which was prepared by transformation of primary C57BL/6 mouse lung cells with the HPV16 *E6/E7* oncogenes and human activated *H-ras*. This cell line was kindly provided by Dr. T.-C. Wu, John Hopkins University, Baltimore, MD, USA (*194*). These cells constitutively express PD-L1 and MHC-I. Next, TC-1/A9 cell line with reversible downregulation of PD-L1 and MHC-I was generated from the TC-1 cell line (*195*). The expression of both molecules can be induced by cytokines, such as IFN-γ. We used TC-1 and TC-1/A9 cell lines to generate cells insensitive to IFN-γ (TC-1/dIfngr1 and TC-1/A9/dIfngr1). We functionally deactivated the IFNGR1 subunit of the IFN-γ receptor with the CRISPR/Cas9 system (Publication 1, Fig. 1A). Oncogenicity of the TC-1/dIfngr1 or TC-1/A9/dIfngr1 cells was comparable to that of the TC-1 or TC-1/A9 cells, respectively (Publication 1 Fig. 1B). This finding is in line with a previous study that has also shown similar oncogenicity of melanoma cells with deactivated expression of IFNGR1 and parental cells (*196*).

As the enhancement of tumour growth by PD-L1, expressed on tumour cells and host cells, is dependent on tumour type (*47–51*), we evaluated the role of PD-L1 in the oncogenicity of TC-1 and TC-1/A9 cell lines. We deactivated PD-L1 molecule with the CRISPR/Cas9 system and produced TC-1/dPD-L1 and TC-1/A9/dPD-L1 cells (Publication 1, Fig. 1C). Mice injected with various doses (3×10^4, 3×10^5, and 3×10^6) of TC-1/dPD-L1 cells did not form any tumour and only the 1×10^5 dose induced tumour formation in two out of five mice (Publication 1, Fig. 1D). The TC-1/A9/dPD-L1 cells were more oncogenic than the TC-1/dPD-L1 cells. However, the growth of TC-1/A9/dPD-L1-induced tumours was significantly slower in comparison with TC-1/A9-induced tumours. The reduced oncogenicity of both cell lines suggests the involvement of PD-L1 expression on tumour cells in the suppression of anti-tumour immunity and implies the potential sensitivity of TC-1- and TC-1/A9-induced tumours to PD-L1 blockade.

3.1.2. The role of IFNGR1 in anti-tumour immunity

We next tested the impact of IFNGR1 deactivation in tumour cells on pro-/anti-oncogenic function of $CD4^+$, $CD8^+$, $NK1.1^+$ and macrophages in mouse tumours (Publication 1, Fig. 2). We depleted immune cells in tumour bearing mice with anti-CD4, anti-CD8, or anti-NK1.1 antibody and treated mice with carrageenan to achieve macrophage depletion. As IFN-γ signalling of host cells was functional in tumours with IFNGR1 deactivation, we also treated mice with anti-IFN-γ in order to evaluate the effect of IFN-γ on tumour growth. Deactivation of IFNGR1 in TC-1 cells eliminated the anti-oncogenic role of $CD8^+$ cells and pro-oncogenic role of macrophages, while anti-oncogenic function of $NK1.1^+$ cells and IFN-γ remained preserved in TC-1/dIfngr1-induced tumours. Only $NK1.1^+$ cells were anti-oncogenic in TC-1/A9-induced tumours, which was not preserved in TC-1/A9/dIfngr1-induced tumours. Interestingly, deactivation of IFNGR1 in TC-1/A9 promoted the pro-oncogenic function of IFN-γ. The mechanisms of the impact of IFNGR1 deactivation in tumour cells on alterations in pro-/anti-oncogenic immune cell functions are currently unclear.

3.1.3. PD-L1 and MHC-I expression in tumours in comparison with cell lines

Furthermore, we analysed PD-L1 and MHC-I expression on tumour cells obtained from tumours (Publication 1, Fig. 3). The expression of both molecules was slightly upregulated on TC-1/dIfngr1 and TC-1/A9/dIfngr1 cells isolated from tumours compared with parental cells. Moreover, the expression on TC-1/A9/dIfngr1 cells in tumours was comparable to the level of expression on TC-1/A9 cells stimulated with IFN-γ *in vitro*. These data suggest that besides IFN-γ, other factors induced PD-L1 and MHC-I expression on tumour cells in the tumour microenvironment.

3.1.4. Detection of cytokines in tumours and their secretion by cell lines

Multiple factors may induce PD-L1 or MHC-I expression, such as IFN-γ, IFN-α, IFN-β, IL-1α, IL-6, IL-27, TNF-α, chemokine CCL2, GM-CSF, and EGF (*80*, *86*, *88–95*, *97*, *98*). We therefore analysed the occurrence of these presumed inducers of PD-L1 and/or MHC-I expression in tumours and cell lines with a LEGENDplex assay (Publication 1, Fig. 4A). We found almost all cytokines in tumours. The exception was the absence of IFN-α in TC-1- and TC-1/dIfngr1-induced tumours. The cell lines produced IL-6 and CCL2. Downregulation of PD-L1 and MHC-I expression on TC-1/A9 cells indicated that IL-6 and CCL2 did not induce the expression of these molecules. We

therefore excluded these two cytokines from further analysis and tested the effect of remaining cytokines on PD-L1 and MHC-I expression *in vitro* (Publication 1, Fig. 4B). Among these cytokines, IFN-α and IFN-β significantly increased PD-L1 and MHC-I, especially on TC-1/A9 and TC-1/A9/dIfngr1 cells. Relative upregulation of both molecules on TC-1/A9/dIfngr1 cells by type I IFNs was comparable to the effect of IFN-γ on TC-1/A9 cells. TNF-α slightly induced MHC-I expression on TC-1/A9/dIfngr1 cells. According to previous studies, type I IFNs promote anti-tumour immune response and may enhance the efficacy of ICIs (*197*, *198*). Our data indicate that type I IFNs can be potent inducers of PD-L1 and MHC-I expression on tumour cells that are insensitive to IFN-γ signalling.

3.1.5. PD-L1 and MHC-I expression in tumours with blockade of IFN-α and IFN-β signalling

We next assessed the effect of type I IFNs on PD-L1 and MHC-I expression in mouse tumours (Publication 1, Fig. 5). We neutralized IFN-α and IFN-β function by antagonistic monoclonal antibody anti-IFNAR1, which targets a shared IFN-α and IFN-β receptor, in mice bearing TC-1/dIfngr1- and TC-1/A9/dIfngr1-induced tumours. The PD-L1 and MHC-I expression was markedly downregulated on TC-1/A9/dIfngr1 tumour cells isolated from mice treated with anti-IFNAR1, whereas the expression on TC-1/dIfngr1 was not significantly changed. As mentioned above, IFN-α was not detected in TC-1/dIfngr1-induced tumours, whereas this cytokine was present in TC-1/A9/dIfngr1-induced tumours. The expression of PD-L1 and MHC-I on TC-1/A9/dIfngr1 cells isolated from tumours was comparable to the expression of IFN-γ stimulated TC-1/A9 cells *in vitro*. It implies the predominant contribution of IFN-α in PD-L1 and MHC-I stimulation on tumour cells *in vivo*, although the concentration of IFN-β was higher than the concentration of IFN-α in all tumours. Type I IFNs are important inducers of anti-tumour immune response and IFN-α has been particularly shown to enhance the efficacy of PD-L1 blockade (*197*, *198*). In line with the previous studies, we hypothesised that type I IFNs might have enhanced the efficacy of PD-1/PD-L1 blockade in TC-1/A9/dIfngr1-induced tumours.

3.1.6. Sensitivity of tumours to combined therapy

Finally, we evaluated the sensitivity of TC-1/A9- and TC-1/A9/dIfngr1-induced tumours to anti-PD-L1 therapy (Publication 1, Fig. 6). We combined PD-L1 blockade

with DNA vaccination in order to stimulate the immune response against HPV16 E7 oncoprotein. TC-1/A9- as well as TC-1/A9/dIfngr1-induced tumours were sensitive to PD-L1 blockade in combination with the DNA vaccination. Sensitivity to immune checkpoint inhibition in tumours with deactivated IFN-γ signalling has been also studied in mouse tumours induced by CRC cell line (CT26) (*77*). Unlike the TC-1/A9 cell line with cytokine inducible MHC-I expression used in our study, the CT26 cells are highly immunogenic due to the constitutive expression of MHC-I. Deactivation of IFNGR and IFNAR promoted the efficacy of PD-1/PD-L1 blockade owing to the inhibition of resistance-associated IFN stimulated genes in CT26-induced tumours.

Recent evidence suggests that mutations in *Ifngr1*, *Ifngr2*, *JAK1*, and *JAK2*, involved in IFN-γ signalling, were detected in cancer patients regardless of response to PD-1/PD-L1 blockade (*123*, *157*, *188*, *199–201*). These studies further support the clinical relevance of our model of PD-1/PD-L1 blockade in mice bearing tumours with deactivated IFN-γ signalling. Therefore, reduced sensitivity of tumour cells to IFN-γ as a single predictive marker should not be a contraindication to PD-1/PD-L1 blockade. In conclusion, the predictive capacity of both, IFN-γ and type I IFNs signalling should be evaluated in PD-1/PD-L1 blockade.

3.2. Publication 2: CD80 expression on tumour cells alters tumour microenvironment and the efficacy of cancer immunotherapy by CTLA-4 blockade

CD80 is expressed by tumour cells as well as host cells and its pro-/anti-oncogenic nature depends on various factors (*202–206*). In this study, we aimed to determine whether CD80 expressed by tumour cells affects the tumour microenvironment and sensitivity to ICIs.

3.2.1. Characteristics of TC-1/dCD80-1 cancer cell line

Firstly, we deactivated CD80 molecule in the TC-1 oncogenic cell line with CRISPR/Cas9 system and generated TC-1/dCD80-1 cells (Publication 2, Fig. 1). These cells were more immunogenic than TC-1 cell line (Publication 2, Fig. 2A). Ten times higher dose of TC-1/dCD80-1 than TC-1 cells formed tumours of comparable growth (Publication 2, Fig. 2B). Our observation is in agreement with previously reported reduction of tumour formation and growth due to CD80 deactivation (*204*).

3.2.2. CD80 expression on tumour cells regulates immune reactions

Next, we analysed whether CD80 on tumour cells regulate anti-tumour immune response (Publication 2, Fig. 3). The deactivation of CD80 switched pro-oncogenic nature of macrophages to anti-oncogenic and abrogated the anti-oncogenic function of $NK1.1^+$ cells. Consistent with our findings, another study has shown that CD80 expression on tumour cells enhanced NK cell-mediated control of tumour growth (*207*). Furthermore, CD80 deactivation promoted the immunosuppressive activity of $CD4^+$ cells, while the anti-oncogenic function of $CD8^+$ cells remained preserved in the TC-1/dCD80-1-induced tumours in our study. $CD4^+$ T cells express CTLA-4 with higher intensity than $CD8^+$ T cells (*20*). As CD80 is still expressed by host cells in mice bearing TC-1/dCD80-1-induced tumours, enhancement of CTLA-4 expression by $CD4^+$ cells might contribute to immunosuppressive mechanisms.

3.2.3. CD80 expression on tumour cells affects sensitivity to CTLA-4 blockade

We next tested the effect of CTLA-4 blockade in TC-1- and TC-1/dCD80-1-induced tumours (Publication 2, Fig. 4). CD80 deactivation induced sensitivity of tumours to CTLA-4 blockade. However, PD-L1 blockade did not significantly reduce tumour growth and it did not support the effect of CTLA-4 blockade regardless of CD80 expression on tumour cells. Depletion of immune cells in mice bearing TC-1/dCD80-1-induced tumours showed that $CD8^+$ cells were essential for the efficacy of anti-CTLA-4 treatment, whereas depletion of $CD4^+$ cells supported the effect of the therapy. Similarly, direct killing of tumour cells by activated $CD8^+$ T cells in anti-CTLA-4 treated tumours has been previously reported (*208*, *209*).

3.2.4. CD80 expression on tumour cells regulates tumour microenvironment

We designed flow cytometry panels to compare microenvironment of TC-1- and TC-1/dCD80-1-induced tumours. CD80 deactivation enhanced the frequency of both lymphoid and myeloid cells in tumours (Publication 2, Fig. 5). Another studies have shown that CD80 blockade induced infiltration of mouse adenocarcinoma (*210*, *211*). Furthermore, the frequency of M1 macrophages increased and M2 decreased in the TC-1/dCD80-1- compared with the TC-1-induced tumours. Our data are in line with a previous study which has shown that blockade of CTLA-4/CD80 axis induced M1 polarization of macrophages in melanoma patients (*212*). Moreover, CD80 deactivation enhanced CTLA-4 expression on T helper (Th) 17 cells and upregulated the frequency of

APCs in tumours. Consistently, enhanced APCs co-stimulation of lymphocytes has been reported to induce CTLA-4 expression, particularly on Th17 cells (*213*).

Moreover, the CTLA-4 blockade downregulated frequencies of most immune cell types in the TC-1-induced tumours, whereas it promoted the frequency of lymphoid cells in the TC-1/dCD80-1-induced tumours (Publication 2, Fig. 6). Within the $CD4^+$ T cells, especially the frequency of Th1 subset was enhanced in TC-1/CD80-1-, unlike the TC-1-induced tumours. Increased infiltration of tumours by Th1 cells has been previously shown in mouse models as well as cancer patients treated with CTLA-4 blockade (*196*, *214*, *215*).

3.2.5. CD80 expression regulates immunosuppressive potential of Treg cells

The Treg cells were the most abundant $CD4^+$ T cell subset in untreated tumours. In order to analyse immunosuppressive potential of Treg cells, we measured expression of markers CTLA-4, GITR, ICOS, Lag3, CD73, granzyme B (GrzB), and neuropilin 1 (Nrp-1), which imply immunosuppressive potential of Treg cells (*216–220*), (Publication 2, Fig. 7). Furthermore, we performed unsupervised clustering by FlowSOM algorithm and generated four distinct Treg subpopulations (subpopulation 1 ($CTLA\text{-}4^{hi}$ $GITR^{hi}$ $ICOS^{hi}$ $Lag3^{lo}$ $CD73^-$ $GrzB^+$ $Nrp\text{-}1^{lo}$) and subpopulation 2 ($CTLA\text{-}4^{hi}$ $GITR^{hi}$ $ICOS^{hi}$ $Lag3^{lo}$ $CD73^+$ $GrzB^+$ $Nrp\text{-}1^{lo}$) with high immunosuppressive potential, and subpopulation 3 ($CTLA\text{-}4^-$ $GITR^{hi}$ $ICOS^{hi}$ $Lag3^+$ $CD73^+$ $GrzB^+$ $Nrp\text{-}1^{lo}$) and subpopulation 4 ($CTLA\text{-}4^{lo}$ $GITR^{lo}$ $ICOS^{lo}$ $Lag3^-$ $CD73^+$ $GrzB^+$ $Nrp\text{-}1^+$) with weak immunosuppressive potential). The anti-CTLA-4 treatment downregulated the frequency of subpopulation 3 Treg cells in the TC-1-induced tumours, while it supported these cells and reduced frequency of subpopulation 2 Treg cells in the TC-1/dCD80-1-induced tumours.

Collectively, our data indicate that CD80 deactivation in tumour cells promotes infiltration of immune cells into tumours, inhibits the immunosuppressive microenvironment and enhances tumour sensitivity to CTLA-4 blockade.

3.3. Publication 3: Experimental combined immunotherapy of tumours with major histocompatibility complex class I downregulation

We have previously shown that the immune response to DNA vaccination targeting tumour specific antigen E7 in TC-1/A9-induced tumours was weak in comparison with TC-1-induced tumours (*195*). Next, we have enhanced the efficacy of

DNA vaccination by combination with adjuvants in mice bearing tumours induced by parental TC-1 cells (*221*). Several other studies have also reported that combined cancer therapy targeting innate as well as adaptive immunity is more efficient than a single therapy (*222*, *223*). To achieve the immune response against the TC-1/A9-induced tumours, we tested combined therapy comprising DNA vaccination against the tumour specific antigen E7, an adjuvant (oligodeoxynucleotide (ODN) 1585, levamisole, ODN 1826, or α-galactosylceramide (α-GalCer) – the mechanisms of action of these compounds have been reviewed in the study (*224*), and the immune checkpoint blockade with anti-Tim-3 monoclonal antibody (Publication 3, Fig. 1). The adjuvants alone did not significantly influence tumour growth. Administration of ODN 1826 or α-GalCer combined with DNA vaccination markedly reduced tumour growth and some tumours completely regressed. This observation indicates indispensable cooperation of the innate immune system and tumour specific adaptive immunity in tumour regression. Moreover, anti-Tim-3 antibody enhanced the reduction of tumour growth in mice treated with combination of ODN 1826, α-GalCer and DNA vaccine. Next, we delayed the administration of adjuvants by one week after DNA vaccination and achieved enhanced efficacy of the therapy (Publication 3, Fig. 2). Tim-3 blockade unfortunately did not have a significant additional effect in the modified schedule.

Furthermore, we performed flow cytometry analysis of tumours during the period of tumour regression induced by combined therapy (Publication 3, Fig. 3). Administration of adjuvants in combination with DNA vaccine increased the frequency of $CD45^+$ immune cells in tumours (Publication 3, Fig. 3A), particularly $CD8^+$ T cells, cDCs, and neutrophils (Publication 3, Fig. 3B). Tim-3 blockade did not have additional effect to the combined therapy. Moreover, the frequency of Treg cells in $CD3^+$ population was reduced (Publication 3, Fig. 3A). We also analysed the frequency of Nrp-1^+ Treg cells, because Nrp-1 stabilise the phenotype of Treg cells and promote the survival and immunosuppressive function of these cells in the tumour microenvironment (*225*). Treatment of mice with adjuvants or anti-Tim-3 monoclonal antibody combined with DNA vaccination reduced the frequency of $Nrp1^+$ Treg cells. We also tested *in vivo* the anti-tumour mechanism of the therapy by the administration of anti-CD4, anti-CD8, or anti-NK1.1 antibody, carrageenan (depletion of macrophages), or anti-IFN-γ neutralising antibody (Publication 3, Fig. 3C). Particularly $CD8^+$ cells and IFN-γ, and to a lesser extent $NK1.1^+$ cells and macrophages contributed to anti-tumour response induced by ODN

1826 combined with DNA vaccine. Similarly, $CD8^+$, $NK1.1^+$ cells and IFN-γ played anti-tumour role in mice treated with α-GalCer combined with DNA vaccine, whereas macrophages did not significantly affect tumour growth.

Previous studies have also shown cooperation between cells of innate and adaptive immunity and important role of $CD8^+$ T cells and macrophages in killing of tumour cells (*226–228*). We therefore focused on $CD8^+$ T cell activation and macrophage polarization in TC-1/A9 tumours. In this respect, we measured IFN-γ production, a marker of T cell activation, with an ELISPOT assay (Publication 3, Fig. 4A). We isolated mononuclear splenocytes from mice treated with DNA vaccine alone, or combined with ODN 1826, α-GalCer and/or anti-Tim-3 monoclonal antibody and re-stimulated these mononuclear splenocytes with E7 (MHC-I restricted) or PADRE (MHC-II restricted) peptides. The treatment of mice with ODN 1826 enhanced IFN-γ production, especially in PADRE re-stimulated cells. α-GalCer, anti-Tim-3 or the combination of adjuvants with anti-Tim-3 did not improve the activation of splenocytes. Subsequently, we conducted flow cytometry analysis of T-cell markers of activation (IFN-γ and TNF-α) and exhaustion (PD-1 and Tim-3) (*7*) in tumour infiltrating $CD8^+$ T cells (Publication 3, Fig. 4B). Immunotherapy significantly induced IFN-γ production in a relatively small portion of $CD8^+$ T cells, and the frequency of PD-1^+ or $Tim3^+$ $CD8^+$ T cells in tumours was also significantly increased. The expression of the immune checkpoints was reduced after Tim-3 blockade.

According to the previous study, M2 macrophages are the major immunosuppressive cells in TC-1-induced tumours (*229*). Macrophages are prominent myeloid population also in TC-1/A9-induced tumours (Publication 3, Fig. 3B). Based on the intensity of MHC-II expression (*230*), we monitored macrophage polarization into M1 ($MHC\text{-}II^{hi}$) and M2 ($MHC\text{-}II^{neg}$) phenotype. M1 macrophages are also defined by other markers, such as iNOS and TNF-α and M2 macrophages by expression of arginase and urea production (*230–232*). $MHC\text{-}II^{hi}$ M1 macrophages were markedly enriched in tumours of mice receiving immunotherapy, while $MHC\text{-}II^{neg}$ M2 macrophages were abundant in tumours of non-treated mice (Publication 3, Fig. 5A). ODN 1826 combined with DNA vaccination significantly induced the expression of iNOS, while TNF-α intracellular expression was not enhanced with combined therapy (Publication 3, Fig. 5B). TAMs were partially $Tim\text{-}3^+$ and the immunotherapy upregulated the expression. However, anti-Tim-3 monoclonal antibody did not support the shift of TAMs to the M1

phenotype. In order to further test the role of ODN 1826 and Tim-3 blockade in the polarization and activity of macrophages, we stimulated TAMs *in vitro* and used peritoneal macrophages as a reference. We measured production of NO (a marker of iNOS activity) (Publication 5, Fig. 5D) and TNF-α (Publication 5, Fig. 5E). NO and TNF-α were significantly induced by ODN 1826 in the IFN-γ dependent manner in peritoneal macrophages. The NO production by TAMs corresponded to the production by peritoneal macrophages but ODN 1826 induced TNF-α independently of IFN-γ treatment. Interestingly, Tim-3 blockade did not have any effect on NO or TNF-α production. To assess the ability of TC-1/A9 cells to directly influence the polarization of TAMs, we co-cultivated TAMs and TC-1/A9 cells *in vitro* (Publication 3, Fig. 6). We measured the production of NO (Publication 3, Fig. 6A) and urea (a marker of arginase activity; Publication 3, Fig. 6B) as markers of M1 and M2 polarization, respectively. TC-1/A9 cells induced NO production in TAMs stimulated by ODN 1826, whereas urea production was independent of the stimulation. Tim-3 blockade did not have the effect neither on NO nor urea production. Altogether, these data indicate that TAMs in TC-1/A9-induced tumours can be polarized to M1 phenotype by immunotherapy.

As the reduction of tumour growth after combined therapy was temporary, we assessed the immunosuppressive mechanisms of acquired resistance to combined therapy. With RT-qPCR, we measured expression of genes (*Ifng*, *Ido1*, *Il10*, *Foxp3*, *Ncf1*, *Tgfb1*, and *Arg1*) potentially associated with immunosuppression within the tumour microenvironment (Publication 3, Fig. 7). *Ifng* and *Ido1* expression was enhanced with combined therapy and both markers correlated with each other, which implies the induction of *Ido1* expression by IFN-γ in TC-1/A9-induced tumours. This observation further supports the dual role of IFN-γ in the tumour microenvironment (*233*).

3.4. Publication 4: Establishment and characterization of mouse tumour cell line with irreversible downregulation of MHC class I molecules

Heterogeneity of MHC-I expression on tumour cells regulates their oncogenicity and invasiveness and efficacy of immunotherapy (*234*). Downregulation of MHC-I expression is one of the most frequent mechanisms of tumour escape from immune surveillance and is associated with primary and acquired resistance to cancer therapy (*122*, *235*). In our study, we developed a model of TC-1-derived mouse tumours with irreversibly downregulated MHC-I expression.

Firstly, we deactivated beta-2-microglobulin (B2m) in TC-1 cells with CRISPR/Cas9 system and established TC-1/dB2m cells with irreversible downregulation of MHC-I. Next, we compared *in vitro* characteristics of TC-1, TC-1/A9, and TC-1/dB2m cell lines (Publication 4, Fig. 1). Surface expression of H-2K^b, H-2D^b, and B2m molecules was considerable on unstimulated TC-1 cells and IFN-γ even slightly upregulated the expression (Publication 4, Fig. 1A). Expression of these molecules on unstimulated TC-1/A9 cells was downregulated but inducible by IFN-γ. We confirmed the abrogation of B2m and downregulated the surface expression of MHC-I heavy chains H-2K^b and H-2D^b on TC-1/dB2m. Although B2m is also associated with CD1d molecule (*236*), the deactivation of B2m did not affect the surface expression of CD1d. Furthermore, the proliferation rate of TC-1/dB2m cells was significantly reduced compared to TC-1 and TC-1/A9 cell lines and IFN-γ did not affect this parameter in any cell line (Publication 4, Fig. 1B). This observation is consistent with previous reports that showed B2m as a factor promoting proliferation and invasiveness of tumour cells (*237*, *238*).

Oncogenicity of TC-1/dB2m cells was markedly decreased in comparison with TC-1- and TC-1/A9-induced tumours (Publication 4, Fig. 2A). Furthermore, MHC-I downregulation was associated with abrogation of anti-oncogenic role of CD8$^+$ cells, whereas NK1.1$^+$ cells significantly reduced the growth of all three types of tumours (Publication 4, Fig. 2B). Consistently, a previous study has also shown enhanced growth of mouse tumours with deactivated B2m after depletion of NK1.1$^+$ cells (*239*). Moreover, MHC-I downregulation markedly decreased sensitivity to DNA vaccination (Publication 4, Fig. 2C). TC-1/dB2m-induced tumours did not respond to the DNA vaccine, although the preventive DNA vaccination completely abrogated the growth of TC-1-induced tumours and significantly reduced the growth of TC-1/A9-induced tumours. These data indicate the importance of MHC-I expression on tumour cells in the efficacy of DNA vaccine. In order to induce anti-cancer immune response in TC-1/dB2m-induced tumours, we combined DNA vaccination with adjuvants (ODN 1826 or α-GalCer; Publication 4, Fig. 3) successfully tested in TC-1/A9-induced tumours in the previous study (*224*). Combined therapy significantly reduced the growth of TC-1/dB2m-induced tumours, but this effect was weak.

We next analysed the tumour microenvironment in TC-1/dB2m-induced tumours in non-treated mice and mice receiving immunotherapy (ODN 1826 alone or combined with DNA vaccination; Publication 4, Fig. 4). The frequency of some lymphoid (CD4$^+$ T

cells, Treg cells, and γδT cells) and myeloid (cDCs and pDCs) cells was significantly increased, while the frequency of NK cells and TAMs was downregulated in TC-1/dB2m-induced tumours in comparison with TC-1- and TC-1/A9-induced tumours. The ratio of MHC-II^{hi} M1 to MHC-II^{neg} M2 macrophages was higher in TC-1/dB2m- than in TC-1- and TC-1/A9-induced tumours. Immunotherapy did not significantly alter the proportion of M1 and M2 macrophages in TC-1/dB2m-induced tumours, whereas we observed a considerable increase of M1 macrophages in TC-1/A9-induced tumours after immunotherapy in our previous study (*224*). In addition, immunotherapy increased the frequency of TAMs, PD-1^{+} TAMs, and activated PD-1^{+} NK and NKT cells in TC-1/dB2m-induced tumours to the level comparable with TC-1- and TC-1/A9-induced tumours.

To further examine anti-tumour effect of immunotherapy, we depleted CD4^{+}, CD8^{+}, and NK1.1^{+} cells, and macrophages and we neutralised IFN-γ in mice bearing TC-1/dB2m tumours treated with DNA vaccine and ODN 1826 (Publication 4, Fig. 4D). Combined therapy of TC-1/dB2m-induced tumours was associated exclusively with anti-oncogenic function of NK1.1^{+} cells and IFN-γ. We observed activated phenotype of both subpopulations of NK1.1^{+} cells, i.e., NK and NKT cells, with flow cytometry. However, α-GalCer, which can be presented on CD1d molecule and stimulate NKT cells (*240*), was less efficient than ODN 1826 in combined immunotherapy and we therefore hypothesise that NK cells are dominant in reactions against TC-1/dB2m-induced tumours. These data support the conclusion that irreversible downregulation of MHC-I inhibited the adaptive anti-tumour response in TC-1/dB2m tumours and thus reduced the efficacy of cancer therapy.

4. CONCLUSIONS

Despite the recent success of ICIs in cancer therapy, many patients suffer from primary or acquired resistance. Personalised approach in the selection of patients suitable for a specific type of cancer immunotherapy would prolong patients' life expectancy, minimise side effects, and reduce treatment expenses. Therefore, predictive markers are necessary to distinguish which patients will benefit from the therapy. The objective of this thesis was to establish clinically relevant mouse experimental tumour models in order to study predictive markers for ICIs and anti-tumour immune response.

The main project of this dissertation thesis focused on the sensitivity of tumours with abrogated IFN-γ signalling to PD-1/PD-L1 blockade. IFN-γ is considered to be the major inducer of PD-L1 and MHC-I expression (*81*). PD-L1 expression in tumours predicts sensitivity to PD-1/PD-L1 axis blockade in most cases (*145*). Defects in IFN-γ signalling or MHC-I expression have been found in some cancer patients with primary and acquired resistance to ICIs (*122*, *126*). We showed that IFN-α and IFN-β induced PD-L1 and MHC-I expression on tumour cells with abrogated IFNGR1 receptor *in vitro* and we confirmed this effect with antibody neutralizing IFN-α/IFN-β receptor in mouse tumours. As both the TC-1/A9- and TC-1/A9/dIfngr1-induced tumours were sensitive to the PD-L1 blockade combined with DNA vaccination, abrogation of IFN-γ signalling may not be a contraindication for PD-1/PD-L1 axis blockade. Sensitivity of tumour cells to type I IFNs as well as IFN-γ should be therefore evaluated as a predictive marker of PD-1/PD-L1 blockade.

Efficacy of the anti-PD-L1 antibody was low in TC-1-induced tumours. Previous study has shown that PD-L1 blockade may promote CTLA-4/CD80 axis (*133*). Thus, we tested whether CD80 expression on tumour cells inhibits sensitivity to PD-L1 blockade in mice bearing TC-1-induced tumours. Although CD80 deactivation in TC-1 cells did not enhance the efficacy of anti-PD-L1 treatment, TC-1/dCD80-1-induced tumours were more immunogenic and more sensitive to anti-CTLA-4 antibody than TC-1-induced tumours. Analysis of the tumour microenvironment revealed that CD80 deactivation increased the frequency of lymphoid as well as myeloid cells infiltrating tumours. It also promoted M1 phenotype of macrophages and enhanced CTLA-4 expression on Th17 cells. Therefore, CD80 expression on tumour cells should be assessed as a predictive

marker of CTLA-4 blockade. Development of tumour cell targeted CD80 blockade should be considered as a novel tumour treatment.

Next, we tested the combined therapy of tumours with reversible MHC-I downregulation and evaluated the efficacy of another ICI, an anti-Tim-3 antibody. In this study, activation of innate immune response with adjuvants (ODN 1826 and/or α-GalCer) promoted the efficacy of DNA vaccination, which elicited adaptive immune response and resulted in markedly reduced TC-1/A9-induced tumour growth. Although Tim-3 was expressed in the tumour microenvironment, Tim-3 blockade had a weak effect on tumour growth and anti-tumour immune response. The combined therapy enhanced the frequency of immune cells (mainly $CD8^+$ T cells) in the tumours and induced macrophage polarization into M1 phenotype. We showed that activation of innate and adaptive immune response with combined therapy was beneficial in cancer treatment.

Finally, we introduced a tumour model with irreversible downregulation of MHC-I. Expression of this molecule regulated sensitivity to DNA vaccination. While TC-1-induced tumours were sensitive to DNA vaccination, the TC-1/A9-induced tumours were less affected and TC-1/dB2m-induced tumours were resistant to DNA vaccination. Combination of DNA vaccination with the adjuvant ODN 1826 only slightly reduced TC-1/dB2m-induced tumour growth. The combined therapy did not increase the number of cells infiltrating TC-1/dB2m-induced tumours. As the irreversible MHC-I downregulation impaired the anti-tumour effect of $CD8^+$ T cells, $NK1.1^+$ cells controlled the growth of TC-1/dB2m-induced tumours and were associated with the efficacy of the combined therapy.

Taken together, this thesis contributed to the development of clinically relevant mouse experimental models of tumours with abrogated IFN-γ signalling or CD80 expression, or reversible and irreversible MHC-I downregulation. We used these models to test the efficacy of ICIs and to study predictive biomarkers for this cancer treatment. Research into single predictive markers should be implemented into the "cancer immunograms" to select cancer patients suitable for the treatment with ICIs and to choose the appropriate type of this treatment. Moreover, we developed experimental combined therapy of tumours with reversible MHC-I downregulation, one of the most frequently occurring mechanism of tumour escape from immune surveillance. Our experimental model of reversible and irreversible MHC-I downregulation resembles the heterogeneity

of MHC-I expression in human tumours and may contribute to the further clinical research into cancer therapy.

5. CONTRIBUTION TO PROJECTS/PUBLICATIONS

5.1. Abrogation of IFN-γ signalling may not worsen sensitivity to PD-1/PD-L1 blockade

During my doctoral studies, I focused mainly on the sensitivity to PD-1/PD-L1 blockade in tumours with abrogation of IFN-γ signalling. I had joined the lab when the cell lines with IFNGR1 deactivation have already been prepared and the oncogenicity of respective cell lines was evaluated. From then on, with the kind support of my supervisor, I acquired funding for the continuation of this project (GAUK 988218), designed and conducted most experiments (Publication 1, Fig. 1A, C, and D, Fig. 2-6), analysed the data, and wrote the original draft of the publication where I am the first author.

5.2. CD80 expression on tumour cells alters tumour microenvironment and the efficacy of cancer immunotherapy by CTLA-4 blockade

This study was the second project, where I was the first author of the respective publication. I designed and conducted most experiments (data presented in all figures of Publication 2), analysed the data, and wrote the manuscript of the publication, with the kind support of my supervisor and colleagues.

5.3. Experimental combined immunotherapy of tumours with major histocompatibility complex class I downregulation

In this study, I contributed to the analysis of tumour infiltrating leucocytes. I had the opportunity to be involved in multicolour flow cytometry experiments and the data analysis of lymphoid cells with FlowJo software (Publication 3, Fig. 3A, B and Fig. 4B). I also helped with editing of the manuscript.

5.4. Establishment and characterization of mouse tumour cell line with irreversible downregulation of MHC class I molecules

In this project, I assisted with in vitro proliferation assay (Publication 4, Fig. 1B), was involved in *in vivo* depletion experiments (Publication 4, Fig. 2B, 4D) and participated in the combined therapy (Publication 4, Fig. 3). Next, I was involved in multicolour flow cytometry (Publication 4, Fig. 4) and helped with the design of

multicolour panels of antibodies, the setup of flow cytometer, the experimental procedure, and data analysis with FlowJo software. I was also involved in editing of the manuscript.

Prohlášení školitele o podílu studenta na výsledcích

I agree with the author's contribution statement.

Prague, ……..

…….

RNDr. Michal Šmahel, Ph.D.

6. REFERENCES

1. C. Huang, H.-X. Zhu, Y. Yao, Z.-H. Bian, Y.-J. Zheng, L. Li, H. M. Moutsopoulos, M. E. Gershwin, Z.-X. Lian, Immune checkpoint molecules. Possible future therapeutic implications in autoimmune diseases. *J. Autoimmun.* **104**, 102333 (2019).

2. F. Xu, T. Jin, Y. Zhu, C. Dai, Immune checkpoint therapy in liver cancer. *J. Exp. Clin. Cancer Res.* **37**, 110 (2018).

3. D. L. Mueller, M. K. Jenkins, R. H. Schwartz, Clonal Expansion Versus Functional Clonal Inactivation: A Costimulatory Signalling Pathway Determines the Outcome of T Cell Antigen Receptor Occupancy. *Annu. Rev. Immunol.* **7**, 445–480 (1989).

4. A. H. Sharpe, Mechanisms of costimulation. *Immunol. Rev.* **229**, 5–11 (2009).

5. L. Chen, D. B. Flies, Molecular mechanisms of T cell co-stimulation and co-inhibition. *Nat. Rev. Immunol.* **13**, 227–242 (2013).

6. N. Peyravian, E. Gharib, A. Moradi, M. Mobahat, P. Tarban, P. Azimzadeh, E. Nazemalhosseini-Mojarad, H. Asadzadeh Aghdaei, Evaluating the expression level of co-stimulatory molecules CD 80 and CD 86 in different types of colon polyps. *Curr. Res. Transl. Med.* **66**, 19–25 (2018).

7. M. Y. Balkhi, Receptor signaling, transcriptional, and metabolic regulation of T cell exhaustion. *Oncoimmunology*. **9**, 1747349 (2020).

8. S. A. Fuertes Marraco, N. J. Neubert, G. Verdeil, D. E. Speiser, Inhibitory Receptors Beyond T Cell Exhaustion. *Front. Immunol.* **26**, 310 (2015).

9. L. Derré, J.-P. Rivals, C. Jandus, S. Pastor, D. Rimoldi, P. Romero, O. Michielin, D. Olive, D. E. Speiser, BTLA mediates inhibition of human tumor-specific $CD8^+$ T cells that can be partially reversed by vaccination. *J. Clin. Invest.* **120**, 157–167 (2010).

10. L. Baitsch, A. Legat, L. Barba, S. A. F. Marraco, J.-P. Rivals, P. Baumgaertner, C. Christiansen-Jucht, H. Bouzourene, D. Rimoldi, H. Pircher, N. Rufer, M. Matter, O. Michielin, D. E. Speiser, Extended Co-Expression of Inhibitory Receptors by Human CD8 T-Cells Depending on Differentiation, Antigen-Specificity and Anatomical Localization. *PLOS ONE*. **7**, e30852 (2012).

11. T. N. Gide, C. Quek, A. M. Menzies, A. T. Tasker, P. Shang, J. Holst, J. Madore, S. Y. Lim, R. Velickovic, M. Wongchenko, Y. Yan, S. Lo, M. S. Carlino, A. Guminski, R. P. M. Saw, A. Pang, H. M. McGuire, U. Palendira, J. F. Thompson, H. Rizos, I. P. da Silva, M. Batten, R. A. Scolyer, G. V. Long, J. S. Wilmott, Distinct Immune Cell Populations Define Response to Anti-PD-1 Monotherapy and Anti-PD-1/Anti-CTLA-4 Combined Therapy. *Cancer Cell*. **35**, 238-255.e6 (2019).

12. J. Sprent, C. D. Surh, T Cell Memory. *Annu. Rev. Immunol.* **20**, 551–579 (2002).

13. M. S. Soon, J. A. Engel, H. J. Lee, A. Haque, Development of circulating CD4+ T-cell memory. *Immunol. Cell Biol.* **97**, 617–624 (2019).

14. T. Takahashi, H. Hsiao, S. Tanaka, W. Li, R. Higashikubo, D. Scozzi, A. Bharat, J. Ritter, A. Krupnick, A. Gelman, D. Kreisel, PD-1 expression on CD8+ T cells regulates their differentiation within lung allografts and is critical for tolerance induction. *Am. J. Transplant.* **18**, 216–225 (2018).

15. J. F. Brunet, F. Denizot, M. F. Luciani, M. Roux-Dosseto, M. Suzan, M. G. Mattei, P. Golstein, A new member of the immunoglobulin superfamily--CTLA-4. *Nature*. **328**, 267–270 (1987).

16. A. Ganesan, T. C. Moon, K. H. Barakat, Revealing the atomistic details behind the binding of B7–1 to CD28 and CTLA-4: A comprehensive protein-protein modelling study. *Biochim. Biophys. Acta BBA* **1862**, 2764–2778 (2018).

17. D. J. Lenschow, G. H. Su, L. A. Zuckerman, N. Nabavi, C. L. Jellis, G. S. Gray, J. Miller, J. A. Bluestone, Expression and functional significance of an additional ligand for CTLA-4. *Proc. Natl. Acad. Sci. U. S. A.* **90**, 11054–11058 (1993).

18. D. M. Sansom, CD28, CTLA-4 and their ligands: who does what and to whom? *Immunology*. **101**, 169–177 (2000).

19. T. Pentcheva-Hoang, J. G. Egen, K. Wojnoonski, J. P. Allison, B7-1 and B7-2 Selectively Recruit CTLA-4 and CD28 to the Immunological Synapse. *Immunity*. **21**, 401–413 (2004).

20. D. V. Chan, H. M. Gibson, B. M. Aufiero, A. J. Wilson, M. S. Hafner, Q.-S. Mi, H. K. Wong, Differential CTLA-4 expression in human CD4+ versus CD8+ T cells is associated with increased NFAT1 and inhibition of CD4+ proliferation. *Genes Immun.* **15**, 25–32 (2014).

21. T. Lindsten, K. P. Lee, E. S. Harris, B. Petryniak, N. Craighead, P. J. Reynolds, D. B. Lombard, G. J. Freeman, L. M. Nadler, G. S. Gray, Characterization of CTLA-4 structure and expression on human T cells. *J. Immunol.* **151**, 3489–3499 (1993).

22. S. Sakaguchi, N. Mikami, J. B. Wing, A. Tanaka, K. Ichiyama, N. Ohkura, Regulatory T Cells and Human Disease. *Annu. Rev. Immunol.* **38**, 541–566 (2020).

23. K. Wing, Y. Onishi, P. Prieto-Martin, T. Yamaguchi, M. Miyara, Z. Fehervari, T. Nomura, S. Sakaguchi, CTLA-4 Control over Foxp3+ Regulatory T Cell Function. *Science*. **322**, 271–275 (2008).

24. G. J. Freeman, A. J. Long, Y. Iwai, K. Bourque, T. Chernova, H. Nishimura, L. J. Fitz, N. Malenkovich, T. Okazaki, M. C. Byrne, H. F. Horton, L. Fouser, L. Carter, V. Ling, M. R. Bowman, B. M. Carreno, M. Collins, C. R. Wood, T. Honjo, Engagement of the Pd-1 Immunoinhibitory Receptor by a Novel B7 Family Member Leads to Negative Regulation of Lymphocyte Activation. *J. Exp. Med.* **192**, 1027–1034 (2000).

25. Y. Ishida, Y. Agata, K. Shibahara, T. Honjo, Induced expression of PD-1, a novel member of the immunoglobulin gene superfamily, upon programmed cell death. *EMBO J.* **11**, 3887–3895 (1992).

26. H. Nishimura, M. Nose, H. Hiai, N. Minato, T. Honjo, Development of lupus-like autoimmune diseases by disruption of the PD-1 gene encoding an ITIM motif-carrying immunoreceptor. *Immunity*. **11**, 141–151 (1999).

27. M. Marasco, A. Berteotti, J. Weyershaeuser, N. Thorausch, J. Sikorska, J. Krausze, H. J. Brandt, J. Kirkpatrick, P. Rios, W. W. Schamel, M. Köhn, T. Carlomagno, Molecular mechanism of SHP2 activation by PD-1 stimulation. *Sci. Adv.* **6**, eaay4458 (2020).

28. D. Y. -w. Lin, Y. Tanaka, M. Iwasaki, A. G. Gittis, H.-P. Su, B. Mikami, T. Okazaki, T. Honjo, N. Minato, D. N. Garboczi, The PD-1/PD-L1 complex resembles the antigen-binding Fv domains of antibodies and T cell receptors. *Proc. Natl. Acad. Sci.* **105**, 3011–3016 (2008).

29. T. Yokosuka, M. Takamatsu, W. Kobayashi-Imanishi, A. Hashimoto-Tane, M. Azuma, T. Saito, Programmed cell death 1 forms negative costimulatory microclusters that directly inhibit T cell receptor signaling by recruiting phosphatase SHP2. *J. Exp. Med.* **209**, 1201–1217 (2012).

30. H. Dong, S. E. Strome, D. R. Salomao, H. Tamura, F. Hirano, D. B. Flies, P. C. Roche, J. Lu, G. Zhu, K. Tamada, V. A. Lennon, E. Celis, L. Chen, Tumor-associated B7-H1 promotes T-cell apoptosis: a potential mechanism of immune evasion. *Nat. Med.* **8**, 793–800 (2002).

31. E. Hui, J. Cheung, J. Zhu, X. Su, M. J. Taylor, H. A. Wallweber, D. K. Sasmal, J. Huang, J. M. Kim, I. Mellman, R. D. Vale, T cell costimulatory receptor CD28 is a primary target for PD-1–mediated inhibition. *Science*. **355**, 1428–1433 (2017).

32. K.-A. Sheppard, L. J. Fitz, J. M. Lee, C. Benander, J. A. George, J. Wooters, Y. Qiu, J. M. Jussif, L. L. Carter, C. R. Wood, D. Chaudhary, PD-1 inhibits T-cell receptor induced phosphorylation of the ZAP70/CD3ζ signalosome and downstream signaling to PKCθ. *FEBS Lett.* **574**, 37–41 (2004).

33. Y. Agata, A. Kawasaki, H. Nishimura, Y. Ishida, T. Tsubat, H. Yagita, T. Honjo, Expression of the PD-1 antigen on the surface of stimulated mouse T and B lymphocytes. *Int. Immunol.* **8**, 765–772 (1996).

34. N. A. Giraldo, P. Nguyen, E. L. Engle, G. J. Kaunitz, T. R. Cottrell, S. Berry, et al., Multidimensional, quantitative assessment of PD-1/PD-L1 expression in patients with Merkel cell carcinoma and association with response to pembrolizumab. *J. Immunother. Cancer*. **6**, 99 (2018).

35. I. Datar, M. F. Sanmamed, J. Wang, B. S. Henick, J. Choi, T. Badri, W. Dong, N. Mani, M. Toki, L. D. Mejías, M. D. Lozano, J. L. Perez-Gracia, V. Velcheti, M. D. Hellmann, J. F. Gainor, K. McEachern, D. Jenkins, K. Syrigos, K. Politi, S. Gettinger, D. L. Rimm, R. S. Herbst, I. Melero, L. Chen, K. A. Schalper, Expression Analysis and Significance of PD-1, LAG-3, and TIM-3 in Human

Non–Small Cell Lung Cancer Using Spatially Resolved and Multiparametric Single-Cell Analysis. *Clin. Cancer Res.* **25**, 4663–4673 (2019).

36. V. A. Boussiotis, Molecular and Biochemical Aspects of the PD-1 Checkpoint Pathway. *N. Engl. J. Med.* **375**, 1767–1778 (2016).

37. J. Hsu, J. J. Hodgins, M. Marathe, C. J. Nicolai, M.-C. Bourgeois-Daigneault, T. N. Trevino, C. S. Azimi, A. K. Scheer, H. E. Randolph, T. W. Thompson, L. Zhang, A. Iannello, N. Mathur, K. E. Jardine, G. A. Kirn, J. C. Bell, M. W. McBurney, D. H. Raulet, M. Ardolino, Contribution of NK cells to immunotherapy mediated by PD-1/PD-L1 blockade. *J. Clin. Invest.* **128**, 4654–4668 (2018).

38. S. J. Judge, C. Dunai, E. G. Aguilar, S. C. Vick, I. R. Sturgill, L. T. Khuat, K. M. Stoffel, J. Van Dyke, D. L. Longo, M. A. Darrow, S. K. Anderson, B. R. Blazar, A. M. Monjazeb, J. S. Serody, R. J. Canter, W. J. Murphy, Minimal PD-1 expression in mouse and human NK cells under diverse conditions. *J. Clin. Invest.* **130**, 3051–3068 (2020).

39. L. Strauss, M. A. A. Mahmoud, J. D. Weaver, N. M. Tijaro-Ovalle, A. Christofides, Q. Wang, R. Pal, M. Yuan, J. Asara, N. Patsoukis, V. A. Boussiotis, Targeted deletion of PD-1 in myeloid cells induces antitumor immunity. *Sci. Immunol.* **5**, eaay1863 (2020).

40. Y. Latchman, C. R. Wood, T. Chernova, D. Chaudhary, M. Borde, I. Chernova, Y. Iwai, A. J. Long, J. A. Brown, R. Nunes, E. A. Greenfield, K. Bourque, V. A. Boussiotis, L. L. Carter, B. M. Carreno, N. Malenkovich, H. Nishimura, T. Okazaki, T. Honjo, A. H. Sharpe, G. J. Freeman, PD-L2 is a second ligand for PD-1 and inhibits T cell activation. *Nat. Immunol.* **2**, 261–268 (2001).

41. W. Dong, X. Wu, S. Ma, Y. Wang, A. P. Nalin, Z. Zhu, J. Zhang, D. M. Benson, K. He, M. A. Caligiuri, J. Yu, The mechanism of anti-PD-L1 antibody efficacy against PD-L1 negative tumors identifies NK cells expressing PD-L1 as a cytolytic effector. *Cancer Discov.* **9**, 1422–1437 (2019).

42. D.-N. Tong, J. Guan, J.-H. Sun, C.-Y. Zhao, S.-G. Chen, Z.-Y. Zhang, Z.-Q. Zhou, Characterization of B cell-mediated PD-1/PD-L1 interaction in pancreatic cancer patients. *Clin. Exp. Pharmacol. Physiol.* **47**, 1342–1349 (2020).

43. T. Yamazaki, H. Akiba, H. Iwai, H. Matsuda, M. Aoki, Y. Tanno, T. Shin, H. Tsuchiya, D. M. Pardoll, K. Okumura, M. Azuma, H. Yagita, Expression of Programmed Death 1 Ligands by Murine T Cells and APC. *J. Immunol.* **169**, 5538–5545 (2002).

44. E. Furusawa, T. Ohno, S. Nagai, T. Noda, T. Komiyama, K. Kobayashi, H. Hamamoto, M. Miyashin, H. Yokozeki, M. Azuma, Silencing of PD-L2/B7-DC by Topical Application of Small Interfering RNA Inhibits Elicitation of Contact Hypersensitivity. *J. Invest. Dermatol.* **139**, 2164-2173.e1 (2019).

45. K. Tomihara, T. Shin, V. J. Hurez, H. Yagita, D. M. Pardoll, B. Zhang, T. J. Curiel, T. Shin, Aging-associated B7-DC+ B cells enhance anti-tumor immunity via Th1 and Th17 induction. *Aging Cell*. **11**, 128–138 (2012).

46. S. Wang, J. Bajorath, D. B. Flies, H. Dong, T. Honjo, L. Chen, Molecular Modeling and Functional Mapping of B7-H1 and B7-DC Uncouple Costimulatory Function from PD-1 Interaction. *J. Exp. Med.* **197**, 1083–1091 (2003).

47. V. R. Juneja, K. A. McGuire, R. T. Manguso, M. W. LaFleur, N. Collins, W. N. Haining, G. J. Freeman, A. H. Sharpe, PD-L1 on tumor cells is sufficient for immune evasion in immunogenic tumors and inhibits CD8 T cell cytotoxicity. *J. Exp. Med.* **214**, 895–904 (2017).

48. J. W. Kleinovink, K. A. Marijt, M. J. A. Schoonderwoerd, T. van Hall, F. Ossendorp, M. F. Fransen, PD-L1 expression on malignant cells is no prerequisite for checkpoint therapy. *OncoImmunology*. **6**, e1294299 (2017).

49. J. Lau, J. Cheung, A. Navarro, S. Lianoglou, B. Haley, K. Totpal, L. Sanders, H. Koeppen, P. Caplazi, J. McBride, H. Chiu, R. Hong, J. Grogan, V. Javinal, R. Yauch, B. Irving, M. Belvin, I. Mellman, J. M. Kim, M. Schmidt, Tumour and host cell PD-L1 is required to mediate suppression of anti-tumour immunity in mice. *Nat. Commun.* **8**, 14572 (2017).

50. T. Noguchi, J. P. Ward, M. M. Gubin, C. D. Arthur, S. H. Lee, J. Hundal, M. J. Selby, R. F. Graziano, E. R. Mardis, A. J. Korman, R. D. Schreiber, Temporally Distinct PD-L1 Expression by Tumor and Host Cells Contributes to Immune Escape. *Cancer Immunol. Res.* **5**, 106–117 (2017).

51. H. Tang, Y. Liang, R. A. Anders, J. M. Taube, X. Qiu, A. Mulgaonkar, X. Liu, S. M. Harrington, J. Guo, Y. Xin, Y. Xiong, K. Nham, W. Silvers, G. Hao, X. Sun, M. Chen, R. Hannan, J. Qiao, H. Dong, H. Peng, Y.-X. Fu, PD-L1 on host cells is essential for PD-L1 blockade-mediated tumor regression. *J. Clin. Invest.* **128**, 580–588 (2018).

52. A. M. Goodman, D. Piccioni, S. Kato, A. Boichard, H.-Y. Wang, G. Frampton, S. M. Lippman, C. Connelly, D. Fabrizio, V. Miller, J. K. Sicklick, R. Kurzrock, Prevalence of PDL1 Amplification and Preliminary Response to Immune Checkpoint Blockade in Solid Tumors. *JAMA Oncol.* **4**, 1237–1244 (2018).

53. M. R. Green, S. Monti, S. J. Rodig, P. Juszczynski, T. Currie, E. O'Donnell, B. Chapuy, K. Takeyama, D. Neuberg, T. R. Golub, J. L. Kutok, M. A. Shipp, Integrative analysis reveals selective 9p24.1 amplification, increased PD-1 ligand expression, and further induction via JAK2 in nodular sclerosing Hodgkin lymphoma and primary mediastinal large B-cell lymphoma. *Blood*. **116**, 3268–3277 (2010).

54. K. Kataoka, Y. Shiraishi, Y. Takeda, S. Sakata, M. Matsumoto, S. Nagano, T. Maeda, Y. Nagata, A. Kitanaka, S. Mizuno, H. Tanaka, K. Chiba, S. Ito, Y. Watatani, N. Kakiuchi, H. Suzuki, T. Yoshizato, K. Yoshida, M. Sanada, H. Itonaga, Y. Imaizumi, Y. Totoki, W. Munakata, H. Nakamura, N. Hama, K. Shide, Y. Kubuki, T. Hidaka, T. Kameda, K. Masuda, N. Minato, K. Kashiwase, K. Izutsu, A. Takaori-Kondo, Y. Miyazaki, S. Takahashi, T. Shibata, H. Kawamoto, Y. Akatsuka, K. Shimoda, K. Takeuchi, T. Seya, S. Miyano, S. Ogawa, Aberrant PD-L1 expression through 3′-UTR disruption in multiple cancers. *Nature*. **534**, 402–406 (2016).

55. L. Chen, D. L. Gibbons, S. Goswami, M. A. Cortez, Y.-H. Ahn, L. A. Byers, X. Zhang, X. Yi, D. Dwyer, W. Lin, L. Diao, J. Wang, J. D. Roybal, M. Patel, C. Ungewiss, D. Peng, S. Antonia, M. Mediavilla-Varela, G. Robertson, S. Jones, M. Suraokar, J. W. Welsh, B. Erez, I. I. Wistuba, L. Chen, D. Peng, S. Wang, S. E. Ullrich, J. V. Heymach, J. M. Kurie, F. X.-F. Qin, Metastasis is regulated via microRNA-200/ZEB1 axis control of tumour cell PD-L1 expression and intratumoral immunosuppression. *Nat. Commun.* **5**, 5241 (2014).

56. M.-H. Lee, J. Yanagawa, L. Tran, T. C. Walser, B. Bisht, E. Fung, S. J. Park, G. Zeng, K. Krysan, W. D. Wallace, M. K. Paul, L. Girard, B. Gao, J. D. Minna, S. M. Dubinett, J. M. Lee, FRA1 contributes to MEK-ERK pathway-dependent PD-L1 upregulation by KRAS mutation in premalignant human bronchial epithelial cells. *Am. J. Transl. Res.* **12**, 409–427 (2020).

57. F. A. Mansour, A. Al-Mazrou, F. Al-Mohanna, M. Al-Alwan, H. Ghebeh, PD-L1 is overexpressed on breast cancer stem cells through notch3/mTOR axis. *Oncoimmunology*. **9**, 1729299 (2020).

58. R. Okita, A. Maeda, K. Shimizu, Y. Nojima, S. Saisho, M. Nakata, PD-L1 overexpression is partially regulated by EGFR/HER2 signaling and associated with poor prognosis in patients with non-small-cell lung cancer. *Cancer Immunol. Immunother.* **66**, 865–876 (2017).

59. M. Ruf, H. Moch, P. Schraml, PD-L1 expression is regulated by hypoxia inducible factor in clear cell renal cell carcinoma. *Int. J. Cancer*. **139**, 396–403 (2016).

60. I. Zerdes, M. Wallerius, E. G. Sifakis, T. Wallmann, S. Betts, M. Bartish, N. Tsesmetzis, N. P. Tobin, C. Coucoravas, J. Bergh, G. Z. Rassidakis, C. Rolny, T. Foukakis, STAT3 Activity Promotes Programmed-Death Ligand 1 Expression and Suppresses Immune Responses in Breast Cancer. *Cancers*. **11**, 1479 (2019).

61. S. Das, G. Suarez, E. J. Beswick, J. C. Sierra, D. Y. Graham, V. E. Reyes, Expression of B7-H1 on gastric epithelial cells: its potential role in regulating T cells during Helicobacter pylori infection. *J. Immunol. Baltim. Md 1950*. **176**, 3000–3009 (2006).

62. W. Fang, J. Zhang, S. Hong, J. Zhan, N. Chen, T. Qin, Y. Tang, Y. Zhang, S. Kang, T. Zhou, X. Wu, W. Liang, Z. Hu, Y. Ma, Y. Zhao, Y. Tian, Y. Yang, C. Xue, Y. Yan, X. Hou, P. Huang, Y. Huang, H. Zhao, L. Zhang, EBV-driven LMP1 and IFN-γ up-regulate PD-L1 in nasopharyngeal carcinoma: Implications for oncotargeted therapy. *Oncotarget*. **5**, 12189–12202 (2014).

63. J. Guillermo Espinoza-Contreras, M. Idalia Torres-Ruiz, L. Ariel Waller-González, J. De Jesús Ramírez-García, J. Torres-López, J. Ventura-Juárez, E. Verónica Moreno-Córdova, J. Ernesto López-Ramos, M. Humberto Muñoz-Ortega, M. Eugenia Vargas-Camaño, R. González-Segovia, Immunological markers and Helicobacter pylori in patients with stomach cancer: Expression and correlation. *Biomed. Rep.* **12**, 233–243 (2020).

64. B.-J. Wang, J.-J. Bao, J.-Z. Wang, Y. Wang, M. Jiang, M.-Y. Xing, W.-G. Zhang, J.-Y. Qi, M. Roggendorf, M.-J. Lu, D.-L. Yang, Immunostaining of PD-1/PD-Ls

in liver tissues of patients with hepatitis and hepatocellular carcinoma. *World J. Gastroenterol.* **17**, 3322–3329 (2011).

65. A. Franzen, T. J. Vogt, T. Müller, J. Dietrich, A. Schröck, C. Golletz, P. Brossart, F. Bootz, J. Landsberg, G. Kristiansen, D. Dietrich, PD-L1 (CD274) and PD-L2 (PDCD1LG2) promoter methylation is associated with HPV infection and transcriptional repression in head and neck squamous cell carcinomas. *Oncotarget*. **9**, 641–650 (2017).

66. S. Lyford-Pike, S. Peng, G. D. Young, J. M. Taube, W. H. Westra, B. Akpeng, T. C. Bruno, J. D. Richmon, H. Wang, J. A. Bishop, L. Chen, C. G. Drake, S. L. Topalian, D. M. Pardoll, S. I. Pai, Evidence for a role of the PD-1:PD-L1 pathway in immune resistance of HPV-associated head and neck squamous cell carcinoma. *Cancer Res.* **73**, 1733–1741 (2013).

67. P. Nagarajan, C. El-Hadad, S. K. Gruschkus, J. Ning, C. W. Hudgens, O. Sagiv, N. Gross, M. T. Tetzlaff, B. Esmaeli, PD-L1/PD1 Expression, Composition of Tumor-Associated Immune Infiltrate, and HPV Status in Conjunctival Squamous Cell Carcinoma. *Invest. Ophthalmol. Vis. Sci.* **60**, 2388–2398 (2019).

68. M. Zhang, H. Sun, S. Zhao, Y. Wang, H. Pu, Y. Wang, Q. Zhang, Expression of PD-L1 and prognosis in breast cancer: a meta-analysis. *Oncotarget*. **8**, 31347–31354 (2017).

69. L.-J. Ma, F.-L. Feng, L.-Q. Dong, Z. Zhang, M. Duan, L.-Z. Liu, J.-Y. Shi, L.-X. Yang, Z.-C. Wang, S. Zhang, Z.-B. Ding, A.-W. Ke, Y. Cao, X.-M. Zhang, J. Zhou, J. Fan, X.-Y. Wang, Q. Gao, Clinical significance of PD-1/PD-Ls gene amplification and overexpression in patients with hepatocellular carcinoma. *Theranostics*. **8**, 5690–5702 (2018).

70. J. Yang, M. Dong, Y. Shui, Y. Zhang, Z. Zhang, Y. Mi, X. Zuo, L. Jiang, K. Liu, Z. Liu, X. Gu, Y. Shi, A pooled analysis of the prognostic value of PD-L1 in melanoma: evidence from 1062 patients. *Cancer Cell Int.* **20**, 96 (2020).

71. E. F. Wheelock, Interferon-Like Virus-Inhibitor Induced in Human Leukocytes by Phytohemagglutinin. *Science*. **149**, 310–311 (1965).

72. N. Marquardt, E. Kekäläinen, P. Chen, M. Lourda, J. N. Wilson, M. Scharenberg, P. Bergman, M. Al-Ameri, J. Hård, J. E. Mold, H.-G. Ljunggren, J. Michaëlsson, Unique transcriptional and protein-expression signature in human lung tissue-resident NK cells. *Nat. Commun.* **10**, 3841 (2019).

73. S. Paul, S. Chhatar, A. Mishra, G. Lal, Natural killer T cell activation increases iNOS+CD206- M1 macrophage and controls the growth of solid tumor. *J. Immunother. Cancer*. **7**, 208 (2019).

74. G. R. Rossi, E. S. Trindade, F. Souza-Fonseca-Guimaraes, Tumor Microenvironment-Associated Extracellular Matrix Components Regulate NK Cell Function. *Front. Immunol.* **11**, 73 (2020).

75. S. Pestka, C. D. Krause, M. R. Walter, Interferons, interferon-like cytokines, and their receptors. *Immunol. Rev.* **202**, 8–32 (2004).

76. X. Zhang, Y. Zeng, Q. Qu, J. Zhu, Z. Liu, W. Ning, H. Zeng, N. Zhang, W. Du, C. Chen, J. Huang, PD-L1 induced by IFN-γ from tumor-associated macrophages via the JAK/STAT3 and PI3K/AKT signaling pathways promoted progression of lung cancer. *Int. J. Clin. Oncol.* **22**, 1026–1033 (2017).

77. J. L. Benci, L. R. Johnson, R. Choa, Y. Xu, J. Qiu, Z. Zhou, B. Xu, D. Ye, K. L. Nathanson, C. H. June, E. J. Wherry, N. R. Zhang, H. Ishwaran, M. D. Hellmann, J. D. Wolchok, T. Kambayashi, A. J. Minn, Opposing Functions of Interferon Coordinate Adaptive and Innate Immune Responses to Cancer Immune Checkpoint Blockade. *Cell*. **178**, 933-948.e14 (2019).

78. M. Y. Bhat, H. S. Solanki, J. Advani, A. A. Khan, T. S. Keshava Prasad, H. Gowda, S. Thiyagarajan, A. Chatterjee, Comprehensive network map of interferon gamma signaling. *J. Cell Commun. Signal.* **12**, 745–751 (2018).

79. M. R. Walter, W. T. Windsor, T. L. Nagabhushan, D. J. Lundell, C. A. Lunn, P. J. Zauodny, S. K. Narula, Crystal structure of a complex between interferon-gamma and its soluble high-affinity receptor. *Nature*. **376**, 230–235 (1995).

80. C. Rolvering, A. D. Zimmer, A. Ginolhac, C. Margue, M. Kirchmeyer, F. Servais, H. M. Hermanns, S. Hergovits, P. V. Nazarov, N. Nicot, S. Kreis, S. Haan, I. Behrmann, C. Haan, The PD-L1- and IL6-mediated dampening of the IL27/STAT1 anticancer responses are prevented by α-PD-L1 or α-IL6 antibodies. *J. Leukoc. Biol.* **104**, 969–985 (2018).

81. S. Zhang, K. Kohli, R. G. Black, L. Yao, S. M. Spadinger, Q. He, V. G. Pillarisetty, L. D. Cranmer, B. A. V. Tine, C. Yee, R. H. Pierce, S. R. Riddell, R. L. Jones, S. M. Pollack, Systemic Interferon-γ Increases MHC Class I Expression and T-cell Infiltration in Cold Tumors: Results of a Phase 0 Clinical Trial. *Cancer Immunol. Res.* **7**, 1237–1243 (2019).

82. G. Ding, T. Shen, C. Yan, M. Zhang, Z. Wu, L. Cao, IFN-γ down-regulates the PD-1 expression and assist nivolumab in PD-1-blockade effect on CD8+ T-lymphocytes in pancreatic cancer. *BMC Cancer*. **19**, 1053 (2019).

83. C. Baer, M. L. Squadrito, D. Laoui, D. Thompson, S. K. Hansen, A. Kiialainen, S. Hoves, C. H. Ries, C.-H. Ooi, M. De Palma, Suppression of microRNA activity amplifies IFN-γ-induced macrophage activation and promotes anti-tumour immunity. *Nat. Cell Biol.* **18**, 790–802 (2016).

84. E. Müller, M. Speth, P. F. Christopoulos, A. Lunde, A. Avdagic, I. Øynebråten, A. Corthay, Both Type I and Type II Interferons Can Activate Antitumor M1 Macrophages When Combined With TLR Stimulation. *Front. Immunol.* **9**, 2520 (2018).

85. G. Chen, A. C. Huang, W. Zhang, G. Zhang, M. Wu, W. Xu, Z. Yu, J. Yang, B. Wang, H. Sun, H. Xia, Q. Man, W. Zhong, L. F. Antelo, B. Wu, X. Xiong, X. Liu, L. Guan, T. Li, S. Liu, R. Yang, Y. Lu, L. Dong, S. McGettigan, R. Somasundaram, R. Radhakrishnan, G. Mills, Y. Lu, J. Kim, Y. H. Chen, H. Dong, Y. Zhao, G. C. Karakousis, T. C. Mitchell, L. M. Schuchter, M. Herlyn, E. J. Wherry, X. Xu, W.

Guo, Exosomal PD-L1 contributes to immunosuppression and is associated with anti-PD-1 response. *Nature*. **560**, 382–386 (2018).

86. A. Garcia-Diaz, D. S. Shin, B. H. Moreno, J. Saco, H. Escuin-Ordinas, G. A. Rodriguez, J. M. Zaretsky, L. Sun, W. Hugo, X. Wang, G. Parisi, C. P. Saus, D. Y. Torrejon, T. G. Graeber, B. Comin-Anduix, S. Hu-Lieskovan, R. Damoiseaux, R. S. Lo, A. Ribas, Interferon Receptor Signaling Pathways Regulating PD-L1 and PD-L2 Expression. *Cell Rep.* **19**, 1189–1201 (2017).

87. M. Chen, B. Pockaj, M. Andreozzi, M. T. Barrett, S. Krishna, S. Eaton, R. Niu, K. S. Anderson, JAK2 and PD-L1 Amplification Enhance the Dynamic Expression of PD-L1 in Triple-negative Breast Cancer. *Clin. Breast Cancer*. **18**, e1205–e1215 (2018).

88. S. Ghosh, A. Paul, E. Sen, Tumor Necrosis Factor Alpha-Induced Hypoxia-Inducible Factor 1α–β-Catenin Axis Regulates Major Histocompatibility Complex Class I Gene Activation through Chromatin Remodeling. *Mol. Cell. Biol.* **33**, 2718–2731 (2013).

89. K. G. Paulson, A. Tegeder, C. Willmes, J. G. Iyer, O. K. Afanasiev, D. Schrama, S. Koba, R. Thibodeau, K. Nagase, W. T. Simonson, A. Seo, D. M. Koelle, M. Madeleine, S. Bhatia, H. Nakajima, S. Sano, J. S. Hardwick, M. L. Disis, M. A. Cleary, J. C. Becker, P. Nghiem, Downregulation of MHC-I Expression Is Prevalent but Reversible in Merkel Cell Carcinoma. *Cancer Immunol. Res.* **2**, 1071–1079 (2014).

90. I. P. Wicks, T. Leizer, S. O. Wawryk, J. R. Novotny, J. Hamilton, G. Vitti, A. W. Boyd, The Effect of Cytokines on the Expression of Mhc Antigens and Icam-1 by Normal and Transformed Synoviocytes. *Autoimmunity*. **12**, 13–19 (1992).

91. G. Carbotti, G. Barisione, I. Airoldi, D. Mezzanzanica, M. Bagnoli, S. Ferrero, A. Petretto, M. Fabbi, S. Ferrini, IL-27 induces the expression of IDO and PD-L1 in human cancer cells. *Oncotarget*. **6**, 43267–43280 (2015).

92. S. Chen, G. A. Crabill, T. S. Pritchard, T. L. McMiller, P. Wei, D. M. Pardoll, F. Pan, S. L. Topalian, Mechanisms regulating PD-L1 expression on tumor and immune cells. *J. Immunother. Cancer*. **7** (2019), doi:10.1186/s40425-019-0770-2.

93. C. Kudo-Saito, H. Shirako, M. Ohike, N. Tsukamoto, Y. Kawakami, CCL2 is critical for immunosuppression to promote cancer metastasis. *Clin. Exp. Metastasis*. **30**, 393–405 (2013).

94. T.-T. Wang, Y.-L. Zhao, L.-S. Peng, N. Chen, W. Chen, Y.-P. Lv, F.-Y. Mao, J.-Y. Zhang, P. Cheng, Y.-S. Teng, X.-L. Fu, P.-W. Yu, G. Guo, P. Luo, Y. Zhuang, Q.-M. Zou, Tumour-activated neutrophils in gastric cancer foster immune suppression and disease progression through GM-CSF-PD-L1 pathway. *Gut*. **66**, 1900–1911 (2017).

95. Z. Zong, J. Zou, R. Mao, C. Ma, N. Li, J. Wang, X. Wang, H. Zhou, L. Zhang, Y. Shi, M1 Macrophages Induce PD-L1 Expression in Hepatocellular Carcinoma Cells Through IL-1β Signaling. *Front. Immunol.* **10**, 1643 (2019).

96. L.-C. Chan, C.-W. Li, W. Xia, J.-M. Hsu, H.-H. Lee, J.-H. Cha, H.-L. Wang, W.-H. Yang, E.-Y. Yen, W.-C. Chang, Z. Zha, S.-O. Lim, Y.-J. Lai, C. Liu, J. Liu, Q. Dong, Y. Yang, L. Sun, Y. Wei, L. Nie, J. L. Hsu, H. Li, Q. Ye, M. M. Hassan, H. M. Amin, A. O. Kaseb, X. Lin, S.-C. Wang, M.-C. Hung, IL-6/JAK1 pathway drives PD-L1 Y112 phosphorylation to promote cancer immune evasion. *J. Clin. Invest.* **129**, 3324–3338 (2019).

97. C.-W. Li, S.-O. Lim, W. Xia, H.-H. Lee, L.-C. Chan, C.-W. Kuo, K.-H. Khoo, S.-S. Chang, J.-H. Cha, T. Kim, J. L. Hsu, Y. Wu, J.-M. Hsu, H. Yamaguchi, Q. Ding, Y. Wang, J. Yao, C.-C. Lee, H.-J. Wu, A. A. Sahin, J. P. Allison, D. Yu, G. N. Hortobagyi, M.-C. Hung, Glycosylation and stabilization of programmed death ligand-1 suppresses T-cell activity. *Nat. Commun.* **7**, 12632 (2016).

98. S.-O. Lim, C.-W. Li, W. Xia, J.-H. Cha, L.-C. Chan, Y. Wu, S.-S. Chang, W.-C. Lin, J.-M. Hsu, Y.-H. Hsu, T. Kim, W.-C. Chang, J. L. Hsu, H. Yamaguchi, Q. Ding, Y. Wang, Y. Yang, C.-H. Chen, A. A. Sahin, D. Yu, G. N. Hortobagyi, M.-C. Hung, Deubiquitination and Stabilization of PD-L1 by CSN5. *Cancer Cell*. **30**, 925–939 (2016).

99. L. Falzone, S. Salomone, M. Libra, Evolution of Cancer Pharmacological Treatments at the Turn of the Third Millennium. *Front. Pharmacol.* **13**, 1300 (2018).

100. A. Rotte, G. D'Orazi, M. Bhandaru, Nobel committee honors tumor immunologists. *J. Exp. Clin. Cancer Res.* **37**, 262 (2018).

101. F. Cameron, G. Whiteside, C. Perry, Ipilimumab. *Drugs*. **71**, 1093–1104 (2011).

102. G. Kwok, T. C. C. Yau, J. W. Chiu, E. Tse, Y.-L. Kwong, Pembrolizumab (Keytruda). *Hum. Vaccines Immunother.* **12**, 2777–2789 (2016).

103. A. Ribas, J. D. Wolchok, Cancer immunotherapy using checkpoint blockade. *Science*. **359**, 1350–1355 (2018).

104. J. Sul, G. M. Blumenthal, X. Jiang, K. He, P. Keegan, R. Pazdur, FDA Approval Summary: Pembrolizumab for the Treatment of Patients With Metastatic Non-Small Cell Lung Cancer Whose Tumors Express Programmed Death-Ligand 1. *The Oncologist*. **21**, 643–650 (2016).

105. A. Markham, S. Duggan, Cemiplimab: First Global Approval. *Drugs*. **78**, 1841–1846 (2018).

106. A. Markham, Atezolizumab: First Global Approval. *Drugs*. **76**, 1227–1232 (2016).

107. E. Dolgin, Atezolizumab Combo Approved for PD-L1–positive TNBC. *Cancer Discov.* **9**, OF2 (2019).

108. N. J. Shah, W. J. Kelly, S. V. Liu, K. Choquette, A. Spira, Product review on the Anti-PD-L1 antibody atezolizumab. *Hum. Vaccines Immunother.* **14**, 269–276 (2017).

109. J. M. Collins, J. L. Gulley, Product review: avelumab, an anti-PD-L1 antibody. *Hum. Vaccines Immunother.* **15**, 891–908 (2018).

110. Y. Y. Syed, Durvalumab: First Global Approval. *Drugs*. **77**, 1369–1376 (2017).

111. M. L. Disis, Mechanism of action of immunotherapy. *Semin. Oncol.* **41**, S3-13 (2014).

112. R. M. Chabanon, M. Pedrero, C. Lefebvre, A. Marabelle, J.-C. Soria, S. Postel-Vinay, Mutational Landscape and Sensitivity to Immune Checkpoint Blockers. *Clin. Cancer Res. Off. J. Am. Assoc. Cancer Res.* **22**, 4309–4321 (2016).

113. D. T. Le, J. N. Durham, K. N. Smith, H. Wang, B. R. Bartlett, L. K. Aulakh, S. Lu, H. Kemberling, C. Wilt, B. S. Luber, F. Wong, N. S. Azad, A. A. Rucki, D. Laheru, R. Donehower, A. Zaheer, G. A. Fisher, T. S. Crocenzi, J. J. Lee, T. F. Greten, A. G. Duffy, K. K. Ciombor, A. D. Eyring, B. H. Lam, A. Joe, S. P. Kang, M. Holdhoff, L. Danilova, L. Cope, C. Meyer, S. Zhou, R. M. Goldberg, D. K. Armstrong, K. M. Bever, A. N. Fader, J. Taube, F. Housseau, D. Spetzler, N. Xiao, D. M. Pardoll, N. Papadopoulos, K. W. Kinzler, J. R. Eshleman, B. Vogelstein, R. A. Anders, L. A. Diaz, Mismatch repair deficiency predicts response of solid tumors to PD-1 blockade. *Science*. **357**, 409–413 (2017).

114. R. W. Jenkins, D. A. Barbie, K. T. Flaherty, Mechanisms of resistance to immune checkpoint inhibitors. *Br. J. Cancer*. **118**, 9–16 (2018).

115. G. P. Dunn, L. J. Old, R. D. Schreiber, The Three Es of Cancer Immunoediting. *Annu. Rev. Immunol.* **22**, 329–360 (2004).

116. D. Liu, R. W. Jenkins, R. J. Sullivan, Mechanisms of Resistance to Immune Checkpoint Blockade. *Am. J. Clin. Dermatol.* **20**, 41–54 (2019).

117. D. Mittal, M. M. Gubin, R. D. Schreiber, M. J. Smyth, New insights into cancer immunoediting and its three component phases — elimination, equilibrium and escape. *Curr. Opin. Immunol.* **27**, 16–25 (2014).

118. D. S. Chen, I. Mellman, Elements of cancer immunity and the cancer-immune set point. *Nature*. **541**, 321–330 (2017).

119. P. Bonaventura, T. Shekarian, V. Alcazer, J. Valladeau-Guilemond, S. Valsesia-Wittmann, S. Amigorena, C. Caux, S. Depil, Cold Tumors: A Therapeutic Challenge for Immunotherapy. *Front. Immunol.* **10** (2019), doi:10.3389/fimmu.2019.00168.

120. L. W. Pfannenstiel, C. M. Diaz-Montero, Y. F. Tian, J. Scharpf, J. S. Ko, B. R. Gastman, Immune-Checkpoint Blockade Opposes CD8+ T-cell Suppression in Human and Murine Cancer. *Cancer Immunol. Res.* **7**, 510–525 (2019).

121. S. C. Wei, N.-A. A. S. Anang, R. Sharma, M. C. Andrews, A. Reuben, J. H. Levine, A. P. Cogdill, J. J. Mancuso, J. A. Wargo, D. Pe'er, J. P. Allison, Combination anti–CTLA-4 plus anti–PD-1 checkpoint blockade utilizes cellular mechanisms partially distinct from monotherapies. *Proc. Natl. Acad. Sci. U. S. A.* **116**, 22699–22709 (2019).

122. J. M. Zaretsky, A. Garcia-Diaz, D. S. Shin, H. Escuin-Ordinas, W. Hugo, S. Hu-Lieskovan, D. Y. Torrejon, G. Abril-Rodriguez, S. Sandoval, L. Barthly, J. Saco, B. Homet Moreno, R. Mezzadra, B. Chmielowski, K. Ruchalski, I. P. Shintaku, P. J. Sanchez, C. Puig-Saus, G. Cherry, E. Seja, X. Kong, J. Pang, B. Berent-Maoz, B. Comin-Anduix, T. G. Graeber, P. C. Tumeh, T. N. Schumacher, R. S. Lo, A. Ribas, Mutations Associated with Acquired Resistance to PD-1 Blockade in Melanoma. *N. Engl. J. Med. Boston*. **375**, 819–829 (2016).

123. M. Sade-Feldman, Y. J. Jiao, J. H. Chen, M. S. Rooney, M. Barzily-Rokni, J.-P. Eliane, S. L. Bjorgaard, M. R. Hammond, H. Vitzthum, S. M. Blackmon, D. T. Frederick, M. Hazar-Rethinam, B. A. Nadres, E. E. Van Seventer, S. A. Shukla, K. Yizhak, J. P. Ray, D. Rosebrock, D. Livitz, V. Adalsteinsson, G. Getz, L. M. Duncan, B. Li, R. B. Corcoran, D. P. Lawrence, A. Stemmer-Rachamimov, G. M. Boland, D. A. Landau, K. T. Flaherty, R. J. Sullivan, N. Hacohen, Resistance to checkpoint blockade therapy through inactivation of antigen presentation. *Nat. Commun.* **8**, 1136 (2017).

124. S. J. Rodig, D. Gusenleitner, D. G. Jackson, E. Gjini, A. Giobbie-Hurder, C. Jin, H. Chang, S. B. Lovitch, C. Horak, J. S. Weber, J. L. Weirather, J. D. Wolchok, M. A. Postow, A. C. Pavlick, J. Chesney, F. S. Hodi, MHC proteins confer differential sensitivity to CTLA-4 and PD-1 blockade in untreated metastatic melanoma. *Sci. Transl. Med.* **10**, eaar3342 (2018).

125. S. Miyauchi, P. D. Sanders, K. Guram, S. S. Kim, F. Paolini, A. Venuti, E. E. W. Cohen, J. S. Gutkind, J. A. Califano, A. B. Sharabi, HPV16 E5 Mediates Resistance to PD-L1 Blockade and Can Be Targeted with Rimantadine in Head and Neck Cancer. *Cancer Res.* **80**, 732–746 (2020).

126. D. S. Shin, J. M. Zaretsky, H. Escuin-Ordinas, A. Garcia-Diaz, S. Hu-Lieskovan, A. Kalbasi, C. S. Grasso, W. Hugo, S. Sandoval, D. Y. Torrejon, N. Palaskas, G. A. Rodriguez, G. Parisi, A. Azhdam, B. Chmielowski, G. Cherry, E. Seja, B. Berent-Maoz, I. P. Shintaku, D. T. Le, D. M. Pardoll, L. A. Diaz, P. C. Tumeh, T. G. Graeber, R. S. Lo, B. Comin-Anduix, A. Ribas, Primary Resistance to PD-1 Blockade Mediated by JAK1/2 Mutations. *Cancer Discov.* **7**, 188–201 (2017).

127. M. Šmahel, PD-1/PD-L1 Blockade Therapy for Tumors with Downregulated MHC Class I Expression. *Int. J. Mol. Sci.* **18** (2017), doi:10.3390/ijms18061331.

128. L. G. Feun, Y.-Y. Li, C. Wu, M. Wangpaichitr, P. D. Jones, S. P. Richman, B. Madrazo, D. Kwon, M. Garcia-Buitrago, P. Martin, P. J. Hosein, N. Savaraj, Phase 2 study of pembrolizumab and circulating biomarkers to predict anticancer response in advanced, unresectable hepatocellular carcinoma. *Cancer*. **125**, 3603–3614 (2019).

129. R. B. Holmgaard, D. Zamarin, Y. Li, B. Gasmi, D. H. Munn, J. P. Allison, T. Merghoub, J. D. Wolchok, Tumor-expressed IDO recruits and activates MDSCs in a Treg-dependent manner. *Cell Rep.* **13**, 412–424 (2015).

130. J. Miao, X. Lu, Y. Hu, C. Piao, X. Wu, X. Liu, C. Huang, Y. Wang, D. Li, J. Liu, Prostaglandin E2 and PD-1 mediated inhibition of antitumor CTL responses in the human tumor microenvironment. *Oncotarget*. **8**, 89802–89810 (2017).

131. R. Saleh, S. M. Toor, S. Khalaf, E. Elkord, Breast Cancer Cells and PD-1/PD-L1 Blockade Upregulate the Expression of PD-1, CTLA-4, TIM-3 and LAG-3 Immune Checkpoints in CD4+ T Cells. *Vaccines*. **7**, 149 (2019).

132. C. Stecher, C. Battin, J. Leitner, M. Zettl, K. Grabmeier-Pfistershammer, C. Höller, G. J. Zlabinger, P. Steinberger, PD-1 Blockade Promotes Emerging Checkpoint Inhibitors in Enhancing T Cell Responses to Allogeneic Dendritic Cells. *Front. Immunol.* **8**, 572 (2017).

133. Y. Zhao, C. K. Lee, C.-H. Lin, R. B. Gassen, X. Xu, Z. Huang, C. Xiao, C. Bonorino, L.-F. Lu, J. D. Bui, E. Hui, PD-L1:CD80 Cis-Heterodimer Triggers the Co-stimulatory Receptor CD28 While Repressing the Inhibitory PD-1 and CTLA-4 Pathways. *Immunity*. **51**, 1059-1073.e9 (2019).

134. D. H. Kim, H. Kim, Y. J. Choi, S. Y. Kim, J.-E. Lee, K. J. Sung, Y. H. Sung, C.-G. Pack, M. Jung, B. Han, K. Kim, W. S. Kim, S. J. Nam, C.-M. Choi, M. Yun, J. C. Lee, J. K. Rho, Exosomal PD-L1 promotes tumor growth through immune escape in non-small cell lung cancer. *Exp. Mol. Med.* **51**, 94 (2019).

135. M. Poggio, T. Hu, C.-C. Pai, B. Chu, C. D. Belair, A. Chang, E. Montabana, U. E. Lang, Q. Fu, L. Fong, R. Blelloch, Suppression of Exosomal PD-L1 Induces Systemic Anti-tumor Immunity and Memory. *Cell*. **177**, 414-427.e13 (2019).

136. V. Gopalakrishnan, B. A. Helmink, C. N. Spencer, A. Reuben, J. A. Wargo, The Influence of the Gut Microbiome on Cancer, Immunity, and Cancer Immunotherapy. *Cancer Cell*. **33**, 570–580 (2018).

137. L. Derosa, B. Routy, M. Fidelle, V. Iebba, L. Alla, E. Pasolli, N. Segata, A. Desnoyer, F. Pietrantonio, G. Ferrere, J.-E. Fahrner, E. Le Chatellier, N. Pons, N. Galleron, H. Roume, C. P. M. Duong, L. Mondragón, K. Iribarren, M. Bonvalet, S. Terrisse, C. Rauber, A.-G. Goubet, R. Daillère, F. Lemaitre, A. Reni, B. Casu, M. T. Alou, C. Alves Costa Silva, D. Raoult, K. Fizazi, B. Escudier, G. Kroemer, L. Albiges, L. Zitvogel, Gut Bacteria Composition Drives Primary Resistance to Cancer Immunotherapy in Renal Cell Carcinoma Patients. *Eur. Urol.* **78**, 195–206 (2020).

138. V. Matson, J. Fessler, R. Bao, T. Chongsuwat, Y. Zha, M.-L. Alegre, J. J. Luke, T. F. Gajewski, The commensal microbiome is associated with anti–PD-1 efficacy in metastatic melanoma patients. *Science*. **359**, 104–108 (2018).

139. B. Routy, E. Le Chatelier, L. Derosa, C. P. M. Duong, M. T. Alou, R. Daillère, A. Fluckiger, M. Messaoudene, C. Rauber, M. P. Roberti, M. Fidelle, C. Flament, V. Poirier-Colame, P. Opolon, C. Klein, K. Iribarren, L. Mondragón, N. Jacquelot, B. Qu, G. Ferrere, C. Clémenson, L. Mezquita, J. R. Masip, C. Naltet, S. Brosseau, C. Kaderbhai, C. Richard, H. Rizvi, F. Levenez, N. Galleron, B. Quinquis, N. Pons, B. Ryffel, V. Minard-Colin, P. Gonin, J.-C. Soria, E. Deutsch, Y. Loriot, F. Ghiringhelli, G. Zalcman, F. Goldwasser, B. Escudier, M. D. Hellmann, A. Eggermont, D. Raoult, L. Albiges, G. Kroemer, L. Zitvogel, Gut microbiome influences efficacy of PD-1-based immunotherapy against epithelial tumors. *Science*. **359**, 91–97 (2018).

140. D. Spakowicz, R. Hoyd, M. Muniak, M. Husain, J. S. Bassett, L. Wang, G. Tinoco, S. H. Patel, J. Burkart, A. Miah, M. Li, A. Johns, M. Grogan, D. P. Carbone, C. F. Verschraegen, K. L. Kendra, G. A. Otterson, L. Li, C. J. Presley, D. H. Owen, Inferring the role of the microbiome on survival in patients treated with immune checkpoint inhibitors: causal modeling, timing, and classes of concomitant medications. *BMC Cancer*. **20**, 383 (2020).

141. V. Gopalakrishnan, C. N. Spencer, L. Nezi, A. Reuben, M. C. Andrews, T. V. et. al., Gut microbiome modulates response to anti–PD-1 immunotherapy in melanoma patients. *Science*. **359**, 97–103 (2018).

142. S. Champiat, L. Dercle, S. Ammari, C. Massard, A. Hollebecque, S. Postel-Vinay, N. Chaput, A. Eggermont, A. Marabelle, J.-C. Soria, C. Ferté, Hyperprogressive Disease Is a New Pattern of Progression in Cancer Patients Treated by Anti-PD-1/PD-L1. *Clin. Cancer Res.* **23**, 1920–1928 (2017).

143. X. Wang, F. Wang, M. Zhong, Y. Yarden, L. Fu, The biomarkers of hyperprogressive disease in PD-1/PD-L1 blockage therapy. *Mol. Cancer*. **19**, 81 (2020).

144. F. Petitprez, M. Meylan, A. de Reyniès, C. Sautès-Fridman, W. H. Fridman, The Tumor Microenvironment in the Response to Immune Checkpoint Blockade Therapies. *Front. Immunol.* **11**, 784 (2020).

145. A. A. Davis, V. G. Patel, The role of PD-L1 expression as a predictive biomarker: an analysis of all US Food and Drug Administration (FDA) approvals of immune checkpoint inhibitors. *J. Immunother. Cancer*. **7**, 278 (2019).

146. F. Bensch, E. L. van der Veen, M. N. Lub-de Hooge, A. Jorritsma-Smit, R. Boellaard, I. C. Kok, S. F. Oosting, C. P. Schröder, T. J. N. Hiltermann, A. J. van der Wekken, H. J. M. Groen, T. C. Kwee, S. G. Elias, J. A. Gietema, S. S. Bohorquez, A. de Crespigny, S.-P. Williams, C. Mancao, A. H. Brouwers, B. M. Fine, E. G. E. de Vries, 89Zr-atezolizumab imaging as a non-invasive approach to assess clinical response to PD-L1 blockade in cancer. *Nat. Med.* **24**, 1852–1858 (2018).

147. D. B. Doroshow, S. Bhalla, M. B. Beasley, L. M. Sholl, K. M. Kerr, S. Gnjatic, I. I. Wistuba, D. L. Rimm, M. S. Tsao, F. R. Hirsch, PD-L1 as a biomarker of response to immune-checkpoint inhibitors. *Nat. Rev. Clin. Oncol.*, 1–18 (2021).

148. C. Kümpers, M. Jokic, O. Haase, A. Offermann, W. Vogel, V. Grätz, E. A. Langan, S. Perner, P. Terheyden, Immune Cell Infiltration of the Primary Tumor, Not PD-L1 Status, Is Associated With Improved Response to Checkpoint Inhibition in Metastatic Melanoma. *Front. Med.* **6** (2019).

149. S. Tsukumo, K. Yasutomo, Regulation of CD8+ T Cells and Antitumor Immunity by Notch Signaling. *Front. Immunol.* **9**, 101 (2018).

150. P. C. Tumeh, C. L. Harview, J. H. Yearley, I. P. Shintaku, E. J. M. Taylor, L. Robert, B. Chmielowski, M. Spasic, G. Henry, V. Ciobanu, A. N. West, M. Carmona, C. Kivork, E. Seja, G. Cherry, A. J. Gutierrez, T. R. Grogan, C. Mateus, G. Tomasic, J. A. Glaspy, R. O. Emerson, H. Robins, R. H. Pierce, D. A. Elashoff,

C. Robert, A. Ribas, PD-1 blockade induces responses by inhibiting adaptive immune resistance. *Nature*. **515**, 568–571 (2014).

151. A. I. Daud, K. Loo, M. L. Pauli, R. Sanchez-Rodriguez, P. M. Sandoval, K. Taravati, K. Tsai, A. Nosrati, L. Nardo, M. D. Alvarado, A. P. Algazi, M. H. Pampaloni, I. V. Lobach, J. Hwang, R. H. Pierce, I. K. Gratz, M. F. Krummel, M. D. Rosenblum, Tumor immune profiling predicts response to anti–PD-1 therapy in human melanoma. *J. Clin. Invest.* **126**, 3447–3452 (2016).

152. C.-C. Balança, C.-M. Scarlata, M. Michelas, C. Devaud, V. Sarradin, C. Franchet, C. M. Gomez, C. Gomez-Roca, M. Tosolini, D. Heaugwane, F. Lauzéral-Vizcaino, L. Mir-Mesnier, V. Féliu, C. Valle, F. Pont, G. Ferron, L. Gladieff, S. Motton, Y. T. L. Gac, A. Dupret-Bories, J. Sarini, B. Vairel, C. Illac, A. Siegfried-Vergnon, E. Mery, J.-J. Fournié, S. Vergez, J.-P. Delord, P. Rochaix, A. Martinez, M. Ayyoub, Dual Relief of T-lymphocyte Proliferation and Effector Function Underlies Response to PD-1 Blockade in Epithelial Malignancies. *Cancer Immunol. Res.* **8**, 869–882 (2020).

153. S. A. Hogan, A. Courtier, P. F. Cheng, N. F. Jaberg-Bentele, S. M. Goldinger, M. Manuel, S. Perez, N. Plantier, J.-F. Mouret, T. D. L. Nguyen-Kim, M. I. G. Raaijmakers, P. Kvistborg, N. Pasqual, J. B. A. G. Haanen, R. Dummer, M. P. Levesque, Peripheral Blood TCR Repertoire Profiling May Facilitate Patient Stratification for Immunotherapy against Melanoma. *Cancer Immunol. Res.* **7**, 77–85 (2019).

154. A. M. Goodman, S. Kato, L. Bazhenova, S. P. Patel, G. M. Frampton, V. Miller, P. J. Stephens, G. A. Daniels, R. Kurzrock, Tumor Mutational Burden as an Independent Predictor of Response to Immunotherapy in Diverse Cancers. *Mol. Cancer Ther.* **16**, 2598–2608 (2017).

155. M. D. Hellmann, T.-E. Ciuleanu, A. Pluzanski, J. S. Lee, G. A. Otterson, C. Audigier-Valette, E. Minenza, H. Linardou, S. Burgers, P. Salman, H. Borghaei, S. S. Ramalingam, J. Brahmer, M. Reck, K. J. O'Byrne, W. J. Geese, G. Green, H. Chang, J. Szustakowski, P. Bhagavatheeswaran, D. Healey, Y. Fu, F. Nathan, L. Paz-Ares, Nivolumab plus Ipilimumab in Lung Cancer with a High Tumor Mutational Burden. *N. Engl. J. Med.* **378**, 2093–2104 (2018).

156. M. K. Labriola, J. Zhu, R. Gupta, S. McCall, J. Jackson, E. F. Kong, J. R. White, G. Cerqueira, K. Gerding, J. K. Simmons, D. George, T. Zhang, Characterization of tumor mutation burden, PD-L1 and DNA repair genes to assess relationship to immune checkpoint inhibitors response in metastatic renal cell carcinoma. *J. Immunother. Cancer*. **8**, e000319 (2020).

157. H. Rizvi, F. Sanchez-Vega, K. La, W. Chatila, P. Jonsson, D. Halpenny, A. Plodkowski, N. Long, J. L. Sauter, N. Rekhtman, T. Hollmann, K. A. Schalper, J. F. Gainor, R. Shen, A. Ni, K. C. Arbour, T. Merghoub, J. Wolchok, A. Snyder, J. E. Chaft, M. G. Kris, C. M. Rudin, N. D. Socci, M. F. Berger, B. S. Taylor, A. Zehir, D. B. Solit, M. E. Arcila, M. Ladanyi, G. J. Riely, N. Schultz, M. D. Hellmann, Molecular Determinants of Response to Anti-Programmed Cell Death (PD)-1 and Anti-Programmed Death-Ligand 1 (PD-L1) Blockade in Patients With

Non-Small-Cell Lung Cancer Profiled With Targeted Next-Generation Sequencing. *J. Clin. Oncol. Off. J. Am. Soc. Clin. Oncol.* **36**, 633–641 (2018).

158. A. M. Goodman, A. Castro, R. M. Pyke, R. Okamura, S. Kato, P. Riviere, G. Frampton, E. Sokol, X. Zhang, E. D. Ball, H. Carter, R. Kurzrock, MHC-I genotype and tumor mutational burden predict response to immunotherapy. *Genome Med.* **12**, 45 (2020).

159. A. Vanderwalde, D. Spetzler, N. Xiao, Z. Gatalica, J. Marshall, Microsatellite instability status determined by next-generation sequencing and compared with PD-L1 and tumor mutational burden in 11,348 patients. *Cancer Med.* **7**, 746–756 (2018).

160. T. Kikuchi, K. Mimura, H. Okayama, Y. Nakayama, K. Saito, L. Yamada, E. Endo, W. Sakamoto, S. Fujita, H. Endo, M. Saito, T. Momma, Z. Saze, S. Ohki, K. Kono, A subset of patients with MSS/MSI-low-colorectal cancer showed increased CD8(+) TILs together with up-regulated IFN-γ. *Oncol. Lett.* **18**, 5977–5985 (2019).

161. S. T. Kim, R. Cristescu, A. J. Bass, K.-M. Kim, J. I. Odegaard, K. Kim, X. Q. Liu, X. Sher, H. Jung, M. Lee, S. Lee, S. H. Park, J. O. Park, Y. S. Park, H. Y. Lim, H. Lee, M. Choi, A. Talasaz, P. S. Kang, J. Cheng, A. Loboda, J. Lee, W. K. Kang, Comprehensive molecular characterization of clinical responses to PD-1 inhibition in metastatic gastric cancer. *Nat. Med.* **24**, 1449–1458 (2018).

162. K. Hatakeyama, T. Nagashima, K. Ohshima, S. Ohnami, S. Ohnami, Y. Shimoda, M. Serizawa, K. Maruyama, A. Naruoka, Y. Akiyama, K. Urakami, M. Kusuhara, T. Mochizuki, K. Yamaguchi, Mutational burden and signatures in 4000 Japanese cancers provide insights into tumorigenesis and response to therapy. *Cancer Sci.* **110**, 2620–2628 (2019).

163. N. A. Rizvi, M. D. Hellmann, A. Snyder, P. Kvistborg, V. Makarov, J. J. Havel, W. Lee, J. Yuan, P. Wong, T. S. Ho, M. L. Miller, N. Rekhtman, A. L. Moreira, F. Ibrahim, C. Bruggeman, B. Gasmi, R. Zappasodi, Y. Maeda, C. Sander, E. B. Garon, T. Merghoub, J. D. Wolchok, T. N. Schumacher, T. A. Chan, Mutational landscape determines sensitivity to PD-1 blockade in non–small cell lung cancer. *Science*. **348**, 124–128 (2015).

164. D. Chowell, L. G. T. Morris, C. M. Grigg, J. K. Weber, R. M. Samstein, V. Makarov, F. Kuo, S. M. Kendall, D. Requena, N. Riaz, B. Greenbaum, J. Carroll, E. Garon, D. M. Hyman, A. Zehir, D. Solit, M. Berger, R. Zhou, N. A. Rizvi, T. A. Chan, Patient HLA class I genotype influences cancer response to checkpoint blockade immunotherapy. *Science*. **359**, 582–587 (2018).

165. J. Budczies, M. Bockmayr, C. Denkert, F. Klauschen, S. Gröschel, S. Darb-Esfahani, N. Pfarr, J. Leichsenring, M. L. Onozato, J. K. Lennerz, M. Dietel, S. Fröhling, P. Schirmacher, A. J. Iafrate, W. Weichert, A. Stenzinger, Pan-cancer analysis of copy number changes in programmed death-ligand 1 (PD-L1, CD274) – associations with gene expression, mutational load, and survival. *Genes. Chromosomes Cancer*. **55**, 626–639 (2016).

166. S. M. Ansell, A. M. Lesokhin, I. Borrello, A. Halwani, E. C. Scott, M. Gutierrez, S. J. Schuster, M. M. Millenson, D. Cattry, G. J. Freeman, S. J. Rodig, B. Chapuy, A. H. Ligon, L. Zhu, J. F. Grosso, S. Y. Kim, J. M. Timmerman, M. A. Shipp, P. Armand, PD-1 blockade with nivolumab in relapsed or refractory Hodgkin's lymphoma. *N. Engl. J. Med.* **372**, 311–319 (2015).

167. S. Gupta, C. M. Vanderbilt, P. Cotzia, J. A. Arias-Stella, J. C. Chang, A. Zehir, R. Benayed, K. Nafa, P. Razavi, D. M. Hyman, J. Baselga, M. F. Berger, M. Ladanyi, M. E. Arcila, D. S. Ross, Next-Generation Sequencing–Based Assessment of JAK2, PD-L1, and PD-L2 Copy Number Alterations at 9p24.1 in Breast Cancer. *J. Mol. Diagn. JMD*. **21**, 307–317 (2019).

168. A. H. Ree, V. Nygaard, H. G. Russnes, D. Heinrich, V. Nygaard, C. Johansen, I. R. Bergheim, E. Hovig, K. Beiske, A. Negård, A.-L. Børresen-Dale, K. Flatmark, G. M. Mælandsmo, Responsiveness to PD-1 Blockade in End-Stage Colon Cancer with Gene Locus 9p24.1 Copy-Number Gain. *Cancer Immunol. Res.* **7**, 701–706 (2019).

169. Y. Wang, K. Wenzl, M. K. Manske, Y. W. Asmann, V. Sarangi, P. T. Greipp, J. E. Krull, K. Hartert, R. He, A. L. Feldman, M. J. Maurer, S. L. Slager, G. S. Nowakowski, T. M. Habermann, T. E. Witzig, B. K. Link, S. M. Ansell, J. R. Cerhan, A. J. Novak, Amplification of 9p24.1 in diffuse large B-cell lymphoma identifies a unique subset of cases that resemble primary mediastinal large B-cell lymphoma. *Blood Cancer J.* **9**, 1–11 (2019).

170. A. Younes, A. Santoro, M. Shipp, P. L. Zinzani, J. M. Timmerman, S. Ansell, P. Armand, M. Fanale, V. Ratanatharathorn, J. Kuruvilla, J. B. Cohen, G. Collins, K. J. Savage, M. Trneny, K. Kato, B. Farsaci, S. M. Parker, S. Rodig, M. G. M. Roemer, A. H. Ligon, A. Engert, Nivolumab for classical Hodgkin's lymphoma after failure of both autologous stem-cell transplantation and brentuximab vedotin: a multicentre, multicohort, single-arm phase 2 trial. *Lancet Oncol.* **17**, 1283–1294 (2016).

171. L. Nayak, F. M. Iwamoto, A. LaCasce, S. Mukundan, M. G. M. Roemer, B. Chapuy, P. Armand, S. J. Rodig, M. A. Shipp, PD-1 blockade with nivolumab in relapsed/refractory primary central nervous system and testicular lymphoma. *Blood*. **129**, 3071–3073 (2017).

172. R. Chen, P. L. Zinzani, M. A. Fanale, P. Armand, N. A. Johnson, P. Brice, J. Radford, V. Ribrag, D. Molin, T. P. Vassilakopoulos, A. Tomita, B. von Tresckow, M. A. Shipp, Y. Zhang, A. D. Ricart, A. Balakumaran, C. H. Moskowitz, KEYNOTE-087, Phase II Study of the Efficacy and Safety of Pembrolizumab for Relapsed/Refractory Classic Hodgkin Lymphoma. *J. Clin. Oncol. Off. J. Am. Soc. Clin. Oncol.* **35**, 2125–2132 (2017).

173. N. J. Miller, C. D. Church, S. P. Fling, R. Kulikauskas, N. Ramchurren, M. M. Shinohara, H. M. Kluger, S. Bhatia, L. Lundgren, M. A. Cheever, S. L. Topalian, P. Nghiem, Merkel cell polyomavirus-specific immune responses in patients with Merkel cell carcinoma receiving anti-PD-1 therapy. *J. Immunother. Cancer*. **6**, 131 (2018).

174. R. L. Ferris, G. Blumenschein, J. Fayette, J. Guigay, A. D. Colevas, L. Licitra, K. J. Harrington, S. Kasper, E. E. Vokes, C. Even, F. Worden, N. F. Saba, L. C. I. Docampo, R. Haddad, T. Rordorf, N. Kiyota, M. Tahara, M. Lynch, V. Jayaprakash, L. Li, M. L. Gillison, Nivolumab vs investigator's choice in recurrent or metastatic squamous cell carcinoma of the head and neck: 2-year long-term survival update of CheckMate 141 with analyses by tumor PD-L1 expression. *Oral Oncol.* **81**, 45–51 (2018).

175. F. Petrelli, A. Iaculli, D. Signorelli, A. Ghidini, L. Dottorini, G. Perego, M. Ghidini, A. Zaniboni, S. Gori, A. Inno, Survival of Patients Treated with Antibiotics and Immunotherapy for Cancer: A Systematic Review and Meta-Analysis. *J. Clin. Med.* **9**, 1458 (2020).

176. N. Chaput, P. Lepage, C. Coutzac, E. Soularue, K. Le Roux, C. Monot, L. Boselli, E. Routier, L. Cassard, M. Collins, T. Vaysse, L. Marthey, A. Eggermont, V. Asvatourian, E. Lanoy, C. Mateus, C. Robert, F. Carbonnel, Baseline gut microbiota predicts clinical response and colitis in metastatic melanoma patients treated with ipilimumab. *Ann. Oncol. Off. J. Eur. Soc. Med. Oncol.* **28**, 1368–1379 (2017).

177. M. Janning, F. Kobus, A. Babayan, H. Wikman, J.-L. Velthaus, S. Bergmann, S. Schatz, M. Falk, L.-A. Berger, L.-M. Böttcher, S. Päsler, T. M. Gorges, L. O'Flaherty, C. Hille, S. A. Joosse, R. Simon, M. Tiemann, C. Bokemeyer, M. Reck, S. Riethdorf, K. Pantel, S. Loges, Determination of PD-L1 Expression in Circulating Tumor Cells of NSCLC Patients and Correlation with Response to PD-1/PD-L1 Inhibitors. *Cancers*. **11**, 835 (2019).

178. C. Nicolazzo, C. Raimondi, M. Mancini, S. Caponnetto, A. Gradilone, O. Gandini, M. Mastromartino, G. Del Bene, A. Prete, F. Longo, E. Cortesi, P. Gazzaniga, Monitoring PD-L1 positive circulating tumor cells in non-small cell lung cancer patients treated with the PD-1 inhibitor Nivolumab. *Sci. Rep.* **6**, 31726 (2016).

179. M. A. Papadaki, A. I. Sotiriou, C. Vasilopoulou, M. Filika, D. Aggouraki, P. G. Tsoulfas, C. A. Apostolopoulou, K. Rounis, D. Mavroudis, S. Agelaki, Optimization of the Enrichment of Circulating Tumor Cells for Downstream Phenotypic Analysis in Patients with Non-Small Cell Lung Cancer Treated with Anti-PD-1 Immunotherapy. *Cancers*. **12**, 1556 (2020).

180. S. Bergmann, A. Coym, L. Ott, A. Soave, M. Rink, M. Janning, M. Stoupiec, C. Coith, S. Peine, G. von Amsberg, K. Pantel, S. Riethdorf, Evaluation of PD-L1 expression on circulating tumor cells (CTCs) in patients with advanced urothelial carcinoma (UC). *Oncoimmunology*. **9**, 1738798 (2020).

181. L. Cabel, F. Riva, V. Servois, A. Livartowski, C. Daniel, A. Rampanou, O. Lantz, E. Romano, M. Milder, B. Buecher, S. Piperno-Neumann, V. Bernard, S. Baulande, I. Bieche, J. Y. Pierga, C. Proudhon, F.-C. Bidard, Circulating tumor DNA changes for early monitoring of anti-PD1 immunotherapy: a proof-of-concept study. *Ann. Oncol. Off. J. Eur. Soc. Med. Oncol.* **28**, 1996–2001 (2017).

182. E. J. Lipson, V. E. Velculescu, T. S. Pritchard, M. Sausen, D. M. Pardoll, S. L. Topalian, L. A. Diaz, Circulating tumor DNA analysis as a real-time method for

monitoring tumor burden in melanoma patients undergoing treatment with immune checkpoint blockade. *J. Immunother. Cancer*. **2**, 42 (2014).

183. C. Krieg, M. Nowicka, S. Guglietta, S. Schindler, F. J. Hartmann, L. M. Weber, R. Dummer, M. D. Robinson, M. P. Levesque, B. Becher, High-dimensional single-cell analysis predicts response to anti-PD-1 immunotherapy. *Nat. Med.* **24**, 144–153 (2018).

184. E. Boutsikou, K. Domvri, G. Hardavella, D. Tsiouda, K. Zarogoulidis, T. Kontakiotis, Tumour necrosis factor, interferon-gamma and interleukins as predictive markers of antiprogrammed cell-death protein-1 treatment in advanced non-small cell lung cancer: a pragmatic approach in clinical practice. *Ther. Adv. Med. Oncol.* **10**, 1758835918768238 (2018).

185. T. Kanai, H. Suzuki, H. Yoshida, A. Matsushita, H. Kawasumi, Y. Samejima, Y. Noda, S. Nasu, A. Tanaka, N. Morishita, S. Hashimoto, K. Kawahara, Y. Tamura, N. Okamoto, T. Tanaka, T. Hirashima, Significance of Quantitative Interferon-gamma Levels in Non-small-cell Lung Cancer Patients' Response to Immune Checkpoint Inhibitors. *Anticancer Res.* **40**, 2787–2793 (2020).

186. M. Ayers, J. Lunceford, M. Nebozhyn, E. Murphy, A. Loboda, D. R. Kaufman, A. Albright, J. D. Cheng, S. P. Kang, V. Shankaran, S. A. Piha-Paul, J. Yearley, T. Y. Seiwert, A. Ribas, T. K. McClanahan, IFN-γ-related mRNA profile predicts clinical response to PD-1 blockade. *J. Clin. Invest.* **127**, 2930–2940 (2017).

187. R. S. Herbst, J.-C. Soria, M. Kowanetz, G. D. Fine, O. Hamid, M. S. Gordon, J. A. Sosman, D. F. McDermott, J. D. Powderly, S. N. Gettinger, H. E. K. Kohrt, L. Horn, D. P. Lawrence, S. Rost, M. Leabman, Y. Xiao, A. Mokatrin, H. Koeppen, P. S. Hegde, I. Mellman, D. S. Chen, F. S. Hodi, Predictive correlates of response to the anti-PD-L1 antibody MPDL3280A in cancer patients. *Nature*. **515**, 563–567 (2014).

188. W. Hugo, J. M. Zaretsky, L. Sun, C. Song, B. H. Moreno, S. Hu-Lieskovan, B. Berent-Maoz, J. Pang, B. Chmielowski, G. Cherry, E. Seja, S. Lomeli, X. Kong, M. C. Kelley, J. A. Sosman, D. B. Johnson, A. Ribas, R. S. Lo, Genomic and Transcriptomic Features of Response to Anti-PD-1 Therapy in Metastatic Melanoma. *Cell*. **165**, 35–44 (2016).

189. D. Liu, B. Schilling, D. Liu, A. Sucker, E. Livingstone, L. Jerby-Amon, L. Zimmer, R. Gutzmer, I. Satzger, C. Loquai, S. Grabbe, N. Vokes, C. A. Margolis, J. Conway, M. X. He, H. Elmarakeby, F. Dietlein, D. Miao, A. Tracy, H. Gogas, S. M. Goldinger, J. Utikal, C. U. Blank, R. Rauschenberg, D. von Bubnoff, A. Krackhardt, B. Weide, S. Haferkamp, F. Kiecker, B. Izar, L. Garraway, A. Regev, K. Flaherty, A. Paschen, E. M. Van Allen, D. Schadendorf, Integrative molecular and clinical modeling of clinical outcomes to PD1 blockade in patients with metastatic melanoma. *Nat. Med.* **25**, 1916–1927 (2019).

190. S. Kato, R. Okamura, Y. Kumaki, S. Ikeda, M. Nikanjam, R. Eskander, A. Goodman, S. Lee, S. T. Glenn, D. Dressman, A. Papanicolau-Sengos, F. L. Lenzo, C. Morrison, R. Kurzrock, Expression of TIM3/VISTA checkpoints and the CD68

macrophage-associated marker correlates with anti-PD1/PDL1 resistance: implications of immunogram heterogeneity. *Oncoimmunology*. **9**, 1708065 (2020).

191. C. U. Blank, J. B. Haanen, A. Ribas, T. N. Schumacher, The "cancer immunogram." *Science*. **352**, 658–660 (2016).

192. N. van Dijk, S. A. Funt, C. U. Blank, T. Powles, J. E. Rosenberg, M. S. van der Heijden, The Cancer Immunogram as a Framework for Personalized Immunotherapy in Urothelial Cancer. *Eur. Urol.* **75**, 435–444 (2019).

193. T. Karasaki, K. Nagayama, H. Kuwano, J.-I. Nitadori, M. Sato, M. Anraku, A. Hosoi, H. Matsushita, Y. Morishita, K. Kashiwabara, M. Takazawa, O. Ohara, K. Kakimi, J. Nakajima, An Immunogram for the Cancer-Immunity Cycle: Towards Personalized Immunotherapy of Lung Cancer. *J. Thorac. Oncol. Off. Publ. Int. Assoc. Study Lung Cancer*. **12**, 791–803 (2017).

194. K.-Y. Lin, F. G. Guarnieri, K. F. Staveley-O'Carroll, H. I. Levitsky, J. T. August, D. M. Pardoll, T.-C. Wu, Treatment of Established Tumors with a Novel Vaccine That Enhances Major Histocompatibility Class II Presentation of Tumor Antigen. *Cancer Res.* **56**, 21–26 (1996).

195. M. Šmahel, P. Šıma, V. Ludvıková, I. Marinov, D. Pokorná, V. Vonka, Immunisation with modified HPV16 E7 genes against mouse oncogenic TC-1 cell sublines with downregulated expression of MHC class I molecules. *Vaccine*. **21**, 1125–1136 (2003).

196. J. Gao, L. Z. Shi, H. Zhao, J. Chen, L. Xiong, Q. He, T. Chen, J. Roszik, C. Bernatchez, S. E. Woodman, P.-L. Chen, P. Hwu, J. P. Allison, A. Futreal, J. A. Wargo, P. Sharma, Loss of IFN-γ Pathway Genes in Tumor Cells as a Mechanism of Resistance to Anti-CTLA-4 Therapy. *Cell*. **167**, 397-404.e9 (2016).

197. Y. Liang, H. Tang, J. Guo, X. Qiu, Z. Yang, Z. Ren, Z. Sun, Y. Bian, L. Xu, H. Xu, J. Shen, Y. Han, H. Dong, H. Peng, Y.-X. Fu, Targeting IFNα to tumor by anti-PD-L1 creates feedforward antitumor responses to overcome checkpoint blockade resistance. *Nat. Commun.* **9**, 4586 (2018).

198. L. Schadt, C. Sparano, N. A. Schweiger, K. Silina, V. Cecconi, G. Lucchiari, H. Yagita, E. Guggisberg, S. Saba, Z. Nascakova, W. Barchet, M. van den Broek, Cancer-Cell-Intrinsic cGAS Expression Mediates Tumor Immunogenicity. *Cell Rep.* **29**, 1236-1248.e7 (2019).

199. M. L. Ascierto, A. Makohon-Moore, E. J. Lipson, J. M. Taube, T. L. McMiller, A. E. Berger, J. Fan, G. J. Kaunitz, T. R. Cottrell, Z. A. Kohutek, A. Favorov, V. Makarov, N. Riaz, T. A. Chan, L. Cope, R. H. Hruban, D. M. Pardoll, B. S. Taylor, D. B. Solit, C. A. Iacobuzio-Donahue, S. L. Topalian, Transcriptional Mechanisms of Resistance to Anti–PD-1 Therapy. *Clin. Cancer Res.* **23**, 3168–3180 (2017).

200. J. M. Mehnert, A. Panda, H. Zhong, K. Hirshfield, S. Damare, K. Lane, L. Sokol, M. N. Stein, L. Rodriguez-Rodriquez, H. L. Kaufman, S. Ali, J. S. Ross, D. C. Pavlick, G. Bhanot, E. P. White, R. S. DiPaola, A. Lovell, J. Cheng, S. Ganesan, Immune activation and response to pembrolizumab in POLE-mutant endometrial cancer. *J. Clin. Invest.* **126**, 2334–2340 (2016).

201. N. Riaz, J. J. Havel, V. Makarov, A. Desrichard, W. J. Urba, J. S. Sims, F. S. Hodi, S. Martín-Algarra, R. Mandal, W. H. Sharfman, S. Bhatia, W.-J. Hwu, T. F. Gajewski, C. L. Slingluff, D. Chowell, S. M. Kendall, H. Chang, R. Shah, F. Kuo, L. G. T. Morris, J.-W. Sidhom, J. P. Schneck, C. E. Horak, N. Weinhold, T. A. Chan, Tumor and Microenvironment Evolution during Immunotherapy with Nivolumab. *Cell*. **171**, 934-949.e16 (2017).

202. J. Li, Y. Yang, H. Inoue, M. Mori, T. Akiyoshi, The expression of costimulatory molecules CD80 and CD86 in human carcinoma cell lines: its regulation by interferon γ and interleukin-10. *Cancer Immunol. Immunother.* **43**, 213–219 (1996).

203. M. R. Bernsen, L. Håkansson, B. Gustafsson, L. Krysander, B. Rettrup, D. Ruiter, A. Håkansson, On the biological relevance of MHC class II and B7 expression by tumour cells in melanoma metastases. *Br. J. Cancer*. **88**, 424–431 (2003).

204. I. Tirapu, E. Huarte, C. Guiducci, A. Arina, M. Zaratiegui, O. Murillo, A. Gonzalez, C. Berasain, P. Berraondo, P. Fortes, J. Prieto, M. P. Colombo, L. Chen, I. Melero, Low Surface Expression of B7-1 (CD80) Is an Immunoescape Mechanism of Colon Carcinoma. *Cancer Res.* **66**, 2442–2450 (2006).

205. X.-Y. Feng, L. Lu, K.-F. Wang, B.-Y. Zhu, X.-Z. Wen, R.-Q. Peng, Y. Ding, D.-D. Li, J.-J. Li, Y. Li, X.-S. Zhang, Low expression of CD80 predicts for poor prognosis in patients with gastric adenocarcinoma. *Future Oncol. Lond. Engl.* **15**, 473–483 (2019).

206. C. Marchiori, M. Scarpa, A. Kotsafti, S. Morgan, M. Fassan, V. Guzzardo, A. Porzionato, I. Angriman, C. Ruffolo, S. Sut, S. Dall'Acqua, R. Bardini, R. De Caro, C. Castoro, M. Scarpa, I. Castagliuolo, Epithelial CD80 promotes immune surveillance of colonic preneoplastic lesions and its expression is increased by oxidative stress through STAT3 in colon cancer cells. *J. Exp. Clin. Cancer Res.* **38**, 190 (2019).

207. P. L. Ganesan, S. I. Alexander, D. Watson, G. J. Logan, G. Y. Zhang, I. E. Alexander, Robust anti-tumor immunity and memory in Rag-1-deficient mice following adoptive transfer of cytokine-primed splenocytes and tumor CD80 expression. *Cancer Immunol. Immunother.* **56**, 1955–1965 (2007).

208. S. Spranger, H. K. Koblish, B. Horton, P. A. Scherle, R. Newton, T. F. Gajewski, Mechanism of tumor rejection with doublets of CTLA-4, PD-1/PD-L1, or IDO blockade involves restored IL-2 production and proliferation of CD8+ T cells directly within the tumor microenvironment. *J. Immunother. Cancer*. **2**, 3 (2014).

209. B. Farhood, M. Najafi, K. Mortezaee, CD8+ cytotoxic T lymphocytes in cancer immunotherapy: A review. *J. Cell. Physiol.* **234**, 8509–8521 (2019).

210. F. Bengsch, D. M. Knoblock, A. Liu, F. McAllister, G. L. Beatty, CTLA-4/CD80 pathway regulates T cell infiltration into pancreatic cancer. *Cancer Immunol. Immunother.* **66**, 1609–1617 (2017).

211. M. Scarpa, P. Brun, M. Scarpa, S. Morgan, A. Porzionato, A. Kotsafti, M. Bortolami, A. Buda, R. D'Incà, V. Macchi, G. C. Sturniolo, M. Rugge, R. Bardini,

I. Castagliuolo, I. Angriman, C. Castoro, CD80-CD28 signaling controls the progression of inflammatory colorectal carcinogenesis. *Oncotarget*. **6**, 20058–20069 (2015).

212. G. Madonna, C. Ballesteros-Merino, Z. Feng, C. Bifulco, M. Capone, D. Giannarelli, D. Mallardo, E. Simeone, A. M. Grimaldi, C. Caracò, G. Botti, B. A. Fox, P. A. Ascierto, PD-L1 expression with immune-infiltrate evaluation and outcome prediction in melanoma patients treated with ipilimumab. *OncoImmunology*. **7**, e1405206 (2018).

213. S. M. Krummey, C. R. Hartigan, D. Liu, M. L. Ford, CD28-Dependent CTLA-4 Expression Fine-Tunes the Activation of Human Th17 Cells. *iScience*. **23**, 100912 (2020).

214. T. L. Walunas, J. A. Bluestone, CTLA-4 Regulates Tolerance Induction and T Cell Differentiation In Vivo. *J. Immunol.* **160**, 3855–3860 (1998).

215. S. C. Wei, J. H. Levine, A. P. Cogdill, Y. Zhao, N.-A. A. S. Anang, M. C. Andrews, P. Sharma, J. Wang, J. A. Wargo, D. Pe'er, J. P. Allison, Distinct Cellular Mechanisms Underlie Anti-CTLA-4 and Anti-PD-1 Checkpoint Blockade. *Cell*. **170**, 1120-1133.e17 (2017).

216. W. Hansen, M. Hutzler, S. Abel, C. Alter, C. Stockmann, S. Kliche, J. Albert, T. Sparwasser, S. Sakaguchi, A. M. Westendorf, D. Schadendorf, J. Buer, I. Helfrich, Neuropilin 1 deficiency on CD4+Foxp3+ regulatory T cells impairs mouse melanoma growth. *J. Exp. Med.* **209**, 2001–2016 (2012).

217. F. Arce Vargas, A. J. S. Furness, K. Litchfield, K. Joshi, R. Rosenthal, E. Ghorani, I. Solomon, M. H. Lesko, N. Ruef, C. Roddie, J. Y. Henry, L. Spain, A. Ben Aissa, A. Georgiou, Y. N. S. Wong, M. Smith, D. Strauss, A. Hayes, D. Nicol, T. O'Brien, L. Mårtensson, et al. Effector Function Contributes to the Activity of Human Anti-CTLA-4 Antibodies. *Cancer Cell*. **33**, 649-663.e4 (2018).

218. M. Zhang, Y. Wu, D. Bastian, S. Iamsawat, J. Chang, A. Daenthanasanmak, H. D. Nguyen, S. Schutt, M. Dai, F. Chen, W.-K. Suh, X.-Z. Yu, Inducible T-Cell Co-Stimulator Impacts Chronic Graft-Versus-Host Disease by Regulating Both Pathogenic and Regulatory T Cells. *Front. Immunol.* **9**, 1461 (2018).

219. D.-Y. Li, X.-Z. Xiong, ICOS+ Tregs: A Functional Subset of Tregs in Immune Diseases. *Front. Immunol.* **11**, 2104 (2020).

220. M. L. di Ricco, E. Ronin, D. Collares, J. Divoux, S. Grégoire, H. Wajant, T. Gomes, Y. Grinberg-Bleyer, V. Baud, G. Marodon, B. L. Salomon, Tumor necrosis factor receptor family costimulation increases regulatory T-cell activation and function via NF-κB. *Eur. J. Immunol.* **50**, 972–985 (2020).

221. M. Šmahel, I. Poláková, E. Sobotková, E. Vajdová, Systemic Administration of CpG Oligodeoxynucleotide and Levamisole as Adjuvants for Gene-Gun-Delivered Antitumor DNA Vaccines. *Clin. Dev. Immunol.* **2011**, 176759 (2011).

222. C. A. Hartl, A. Bertschi, R. B. Puerto, C. Andresen, E. M. Cheney, E. A. Mittendorf, J. L. Guerriero, M. S. Goldberg, Combination therapy targeting both

innate and adaptive immunity improves survival in a pre-clinical model of ovarian cancer. *J. Immunother. Cancer*. **7**, 199 (2019).

223. K. M. Storey, S. E. Lawler, T. L. Jackson, Modeling Oncolytic Viral Therapy, Immune Checkpoint Inhibition, and the Complex Dynamics of Innate and Adaptive Immunity in Glioblastoma Treatment. *Front. Physiol.* **11**, 151 (2020).

224. A. Grzelak, I. Polakova, J. Smahelova, J. Vackova, L. Pekarcikova, R. Tachezy, M. Smahel, Experimental Combined Immunotherapy of Tumours with Major Histocompatibility Complex Class I Downregulation. *Int. J. Mol. Sci.* **19**, 3693 (2018).

225. G. M. Delgoffe, S.-R. Woo, M. E. Turnis, D. M. Gravano, C. Guy, A. E. Overacre, M. L. Bettini, P. Vogel, D. Finkelstein, J. Bonnevier, C. J. Workman, D. A. A. Vignali, Stability and function of regulatory T cells is maintained by a neuropilin-1–semaphorin-4a axis. *Nature*. **501**, 252–256 (2013).

226. N. Bercovici, A. Trautmann, Revisiting the role of T cells in tumor regression. *Oncoimmunology*. **1**, 346–350 (2012).

227. T. C. van der Sluis, M. Sluijter, S. van Duikeren, B. L. West, C. J. M. Melief, R. Arens, S. H. van der Burg, T. van Hall, Therapeutic Peptide Vaccine-Induced CD8 T Cells Strongly Modulate Intratumoral Macrophages Required for Tumor Regression. *Cancer Immunol. Res.* **3**, 1042–1051 (2015).

228. M. Thoreau, H. L. Penny, K. Tan, F. Regnier, J. M. Weiss, B. Lee, L. Johannes, E. Dransart, A. Le Bon, J.-P. Abastado, E. Tartour, A. Trautmann, N. Bercovici, Vaccine-induced tumor regression requires a dynamic cooperation between T cells and myeloid cells at the tumor site. *Oncotarget*. **6**, 27832–27846 (2015).

229. A. P. Lepique, K. R. P. Daghastanli, I. M. Cuccovia, L. L. Villa, HPV16 Tumor Associated Macrophages Suppress Antitumor T Cell Responses. *Am. Assoc. Cancer Res.* **15**, 4391–4400 (2009).

230. C. D. Mills, Anatomy of a Discovery: M1 and M2 Macrophages. *Front. Immunol.* **6**, 212 (2015).

231. A. Mantovani, S. Sozzani, M. Locati, P. Allavena, A. Sica, Macrophage polarization: tumor-associated macrophages as a paradigm for polarized M2 mononuclear phagocytes. *Trends Immunol.* **23**, 549–555 (2002).

232. M. Rath, I. Müller, P. Kropf, E. I. Closs, M. Munder, Metabolism via Arginase or Nitric Oxide Synthase: Two Competing Arginine Pathways in Macrophages. *Front. Immunol.* **5**, 532 (2014).

233. M. R. Zaidi, The Interferon-Gamma Paradox in Cancer. *J. Interferon Cytokine Res.* **39**, 30–38 (2018).

234. I. Romero, C. Garrido, I. Algarra, V. Chamorro, A. Collado, F. Garrido, A. M. Garcia-Lora, MHC Intratumoral Heterogeneity May Predict Cancer Progression and Response to Immunotherapy. *Front. Immunol.* **9**, 102 (2018).

235. F. Garrido, N. Aptsiauri, E. M. Doorduijn, A. M. Garcia Lora, T. van Hall, The urgent need to recover MHC class I in cancers for effective immunotherapy. *Curr. Opin. Immunol.* **39**, 44–51 (2016).

236. H. S. Kim, J. Garcia, M. Exley, K. W. Johnson, S. P. Balk, R. S. Blumberg, Biochemical characterization of CD1d expression in the absence of beta2-microglobulin. *J. Biol. Chem.* **274**, 9289–9295 (1999).

237. W.-C. Huang, D. Wu, Z. Xie, H. E. Zhau, T. Nomura, M. Zayzafoon, J. Pohl, C.-L. Hsieh, M. N. Weitzmann, M. C. Farach-Carson, L. W. K. Chung, beta2-microglobulin is a signaling and growth-promoting factor for human prostate cancer bone metastasis. *Cancer Res.* **66**, 9108–9116 (2006).

238. T. Nomura, W.-C. Huang, H. E. Zhau, D. Wu, Z. Xie, H. Mimata, M. Zayzafoon, A. N. Young, F. F. Marshall, M. N. Weitzmann, L. W. K. Chung, β2-Microglobulin Promotes the Growth of Human Renal Cell Carcinoma through the Activation of the Protein Kinase A, Cyclic AMP–Responsive Element-Binding Protein, and Vascular Endothelial Growth Factor Axis. *Clin. Cancer Res.* **12**, 7294–7305 (2006).

239. K. Das, D. Eisel, C. Lenkl, A. Goyal, S. Diederichs, E. Dickes, W. Osen, S. B. Eichmüller, Generation of murine tumor cell lines deficient in MHC molecule surface expression using the CRISPR/Cas9 system. *PloS One*. **12**, e0174077 (2017).

240. T. Kawano, J. Cui, Y. Koezuka, I. Toura, Y. Kaneko, K. Motoki, H. Ueno, R. Nakagawa, H. Sato, E. Kondo, H. Koseki, M. Taniguchi, CD1d-Restricted and TCR-Mediated Activation of Vα14 NKT Cells by Glycosylceramides. *Science*. **278**, 1626–1629 (1997).

7. REPRINTS OF PUBLICATIONS

International Journal of *Molecular Sciences*

MDPI

Article

Abrogation of IFN-γ Signaling May not Worsen Sensitivity to PD-1/PD-L1 Blockade

Julie Vackova [1,2], Adrianna Piatakova [1], Ingrid Polakova [1] and Michal Smahel [1,*]

[1] Department of Genetics and Microbiology, Faculty of Science, Charles University, BIOCEV, 252 50 Vestec, Czech Republic; julie.vackova@natur.cuni.cz (J.V.); grzelaka@natur.cuni.cz (A.P.); ingrid.polakova@natur.cuni.cz (I.P.)

[2] Department of Cell Biology, Faculty of Science, Charles University, BIOCEV, 252 50 Vestec, Czech Republic

* Correspondence: smahelm@natur.cuni.cz; Tel.: +420-325-873-921

Received: 21 February 2020; Accepted: 4 March 2020; Published: 6 March 2020

check for updates

Abstract: Programmed cell death protein 1 (PD-1)/PD-1 ligand 1 (PD-L1) blockade is a promising therapy for various cancer types, but most patients are still resistant. Therefore, a larger number of predictive biomarkers is necessary. In this study, we assessed whether a loss-of-function mutation of the interferon (IFN)-γ receptor 1 (IFNGR1) in tumor cells can interfere with anti-PD-L1 therapy. For this purpose, we used the mouse oncogenic TC-1 cell line expressing PD-L1 and major histocompatibility complex class I (MHC-I) molecules and its TC-1/A9 clone with reversibly downregulated PD-L1 and MHC-I expression. Using the CRISPR/Cas9 system, we generated cells with deactivated IFNGR1 (TC-1/dIfngr1 and TC-1/A9/dIfngr1). In tumors, IFNGR1 deactivation did not lead to PD-L1 or MHC-I reduction on tumor cells. From potential inducers, mainly IFN-α and IFN-β enhanced PD-L1 and MHC-I expression on TC-1/dIfngr1 and TC-1/A9/dIfngr1 cells in vitro. Neutralization of the IFN-α/IFN-β receptor confirmed the effect of these cytokines in vivo. Combined immunotherapy with PD-L1 blockade and DNA vaccination showed that IFNGR1 deactivation did not reduce tumor sensitivity to anti-PD-L1. Thus, the impairment of IFN-γ signaling may not be sufficient for PD-L1 and MHC-I reduction on tumor cells and resistance to PD-L1 blockade, and thus should not be used as a single predictive marker for anti-PD-1/PD-L1 cancer therapy.

Keywords: immune checkpoint therapy; cancer; PD-1/PD-L1; IFNGR1; IFN-α; IFN-β; MHC class I

1. Introduction

Cancer immunotherapy based on blockade of the programmed cell death protein 1 (PD-1)/PD-1 ligand 1 (PD-L1) pathway with monoclonal antibodies is increasingly applied in clinical practice [1–4]. Initially, pembrolizumab and nivolumab were approved by the Food and Drug Administration (FDA) in 2014 for the treatment of patients with advanced melanomas [4]. The number of approved antibodies for the blockade of PD-1/PD-L1 signaling has rapidly increased and improved the therapy of different malignant diseases in patients unsuccessfully treated by other methods [1]. Thus far, six antibodies (pembrolizumab, nivolumab, atezolizumab, durvalumab, avelumab, and cemiplimab) have been approved by the FDA [5,6]. Moreover, in 2015, this progress also resulted in the FDA approval of pembrolizumab as a drug for the first-line treatment of metastatic non-small cell lung cancer (NSCLC) with PD-L1 overexpression [7].

However, despite the great success of this immunotherapy, the majority of the treated patients (about 70–80%) did not respond to therapy, and secondary resistance was recorded in some patients, for instance approximately 25% of melanoma patients [8]. Therefore, reliable predictive biomarkers are required to select suitable patients for treatment to avoid unnecessary burden and reduce high

expenses. Unraveling the mechanisms of successful PD-1/PD-L1 blockade and resistance to this therapy contributes to the identification of such biomarkers [9].

Genetic analyses have suggested a relationship between treatment failure and impairment of interferon (IFN)-γ signaling in both primary [10] and secondary resistance to PD-1/PD-L1 blockade [11]. Sample analysis of four patients with melanoma who acquired resistance to the PD-1 blockade revealed mutations in genes encoding the Janus-associated kinase (JAK)-1 or JAK-2 in two patients. These mutations led to insensitivity to IFN-γ treatment, which is associated with the downregulation of major histocompatibility complex class I (MHC-I) expression. Moreover, in the third patient, a mutation in the β-2-microglobulin gene resulted in a complete loss of surface MHC-I expression [11].

Defects in responsiveness to IFN-γ stimulation were also associated with the primary resistance to blockade of another immune checkpoint, the cytotoxic T-lymphocyte-associated antigen 4 (CTLA-4) [12]. Therefore, IFN-γ signaling may be considered as a predictive biomarker for cancer immunotherapy with immune checkpoint inhibitors [13]. Somatic mutations in the *JAK1* and *JAK2* genes were identified in various types of human malignancies with a range of 6%–12% and 5%–17%, respectively. As these mutations can be responsible for the lack of acquired PD-L1 expression, they might predict patients who are unlikely to benefit from the anti-PD-1/PD-L1 therapy [10].

In our study, we derived mouse tumor cell lines unresponsive to IFN-γ stimulation and analyzed their response to treatment with PD-L1-blocking antibody. Tumors induced by these cells were sensitive to anti-PD-L1 and acquired PD-L1 expression in vivo. This finding suggests that the exclusive abrogation of IFN-γ signaling in tumor cells is not sufficient for an escape from anti-PD-L1 treatment and should not be a reason for the exclusion of patients from this therapy.

2. Results

2.1. Characterization of TC-1 or TC-1/A9 Cell Lines with IFNGR1 or PD-L1 Deactivation

In order to assess whether tumors induced by IFN-γ non-responsive tumor cells may be sensitive to PD-1/PD-L1 blockade and simultaneously enhance the efficacy of immunotherapy of tumors induced by such cells, we prepared TC-1 and TC-1/A9 clones with a deactivated IFN-γ receptor. In these cells, we determined the PD-L1 and MHC-I surface expression by flow cytometry (Figure 1A). Although TC-1 cells and TC-1 clone with a deactivated IFN-γ receptor 1 (IFNGR1; TC-1/dIfngr1) markedly expressed PD-L1 and MHC-I molecules, on TC-1/A9 cells and the respective clone with deactivated IFNGR1 (TC-1/A9/dIfngr1), PD-L1 and MHC-I expression were downregulated. After incubation with IFN-γ, PD-L1 and MHC-I expression were increased in TC-1 and TC-1/A9 cells, but TC-1/dIfngr1 and TC-1/A9/dIfngr1 clones did not respond to stimulation, which suggests successful IFNGR1 deactivation. Oncogenicity of the modified clones was similar to that of the parental cells, and TC-1/A9-induced tumors grew significantly faster than TC-1-induced tumors (Figure 1B).

To evaluate the impact of PD-L1 molecules expressed by TC-1 and TC-1/A9 cells on the protection against immune system attack, we generated cellular clones with deactivated PD-L1–TC-1/dPD-L1 and TC-1/A9/dPD-L1, respectively. As assessed by flow cytometry (Figure 1C), both clones remained PD-L1 negative after IFN-γ stimulation. The MHC-I expression was not markedly altered on unstimulated TC-1/dPD-L1 cells, but it was slightly increased on unstimulated TC-1/A9/dPD-L1 cells in comparison with the TC-1/A9 cells. This expression was further enhanced after IFN-γ treatment on both cell lines.

Oncogenicity of the TC-1/dPD-L1 and TC-1/A9/dPD-L1 cells was decreased in comparison with the parental cell lines (Figure 1D). This effect was particularly decisive for the TC-1/dPD-L1 cells that did not form tumors for the doses 3×10^4, 3×10^5, and 3×10^6 and only generated tumors after the injection of 1×10^5 cells in two out of five mice. The TC-1/A9/dPD-L1 cells formed tumors in all mice injected with both 3×10^4 and 3×10^5 cells, but their growth was significantly reduced in comparison with TC-1/A9-induced tumors. Thus, PD-L1 expressed on the TC-1 and TC-1/A9 cells plays an important role in the suppression of anti-tumor immunity. This effect is much more evident for the TC-1 cell line.

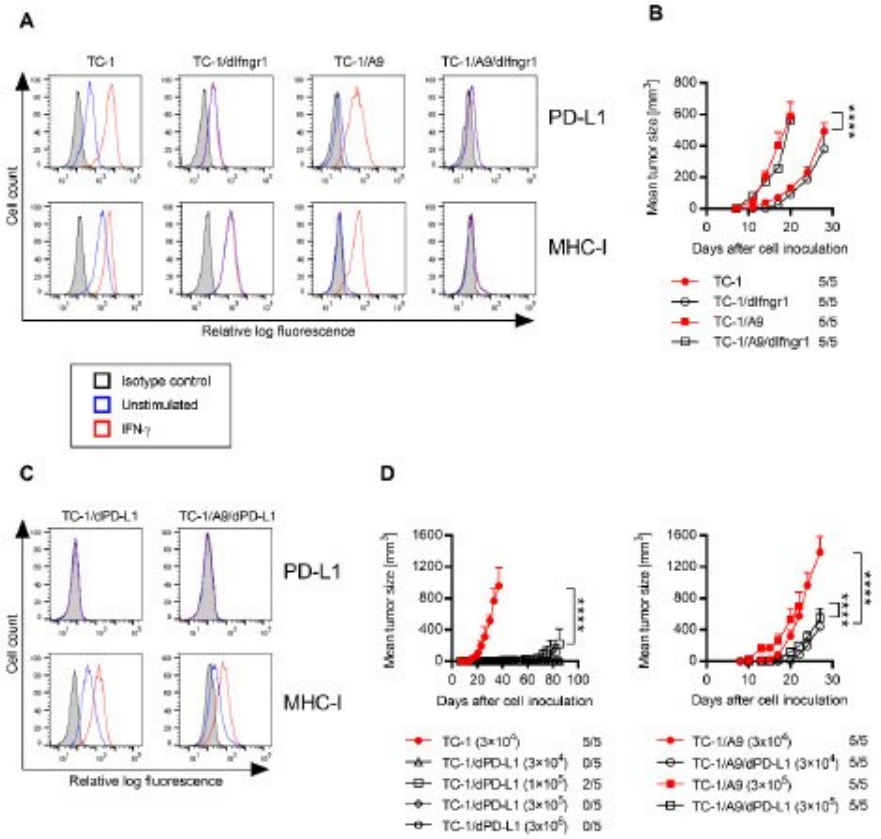

Figure 1. Characterization of the derived cell lines. Surface programmed cell death protein 1 (PD-1) ligand 1 (PD-L1) and major histocompatibility complex class I (MHC-I) expression on unstimulated and stimulated (200 IU/mL interferon (IFN)-γ for 1 day) cells were analyzed by flow cytometry in TC-1, TC-1 clone with a deactivated IFN-γ receptor 1 (IFNGR1; TC-1/dIfngr1), TC-1/A9, and TC-1/A9/dIfngr1 cell lines (**A**) and TC-1/dPD-L1 and TC-1/A9/dPD-L1 cell lines (**C**). Cells were incubated with specific antibodies or isotype control antibodies. (**B**) Oncogenicity of TC-1, TC-1/dIfngr1, TC-1/A9, and TC-1/A9/dIfngr1 cell lines was compared after subcutaneous (s.c.) administration of 3×10^4 cells to C57BL/6 mice ($n = 5$). (**D**) For the evaluation of oncogenicity of cell lines with deactivated PD-L1, various cell doses were s.c. injected. The ratio of mice with a tumor to the total number of mice in the group is shown. Bars ± SEM; **** $p < 0.0001$.

2.2. *Mechanisms Contributing to Anti-Tumor Immunity*

To analyze the effect of IFNGR1 deactivation in tumor cells on a pro-/anti-oncogenic role of immune cells, we depleted cluster of differentiation (CD)4$^+$, CD8$^+$, or natural killer (NK)1.1$^+$ cells, or macrophages in mice bearing tumors with functional or deactivated IFNGR1 (Figure 2). We also neutralized IFN-γ to evaluate its influence on the oncogenicity of tumors induced by cells non-sensitive to this cytokine. Although the depletion of CD8$^+$ or NK1.1$^+$ cells and IFN-γ neutralization enhanced TC-1-induced tumor growth, depletion of macrophages inhibited the growth of these tumors. For TC-1/dIfngr1-induced tumors, depletion of NK1.1$^+$ cells and IFN-γ neutralization had similar effects, but the impact of CD8$^+$-cell or macrophage depletion was not preserved. In mice with TC-1/A9 tumors, depletion of NK1.1$^+$ cells resulted in significant enhancement of tumor growth. On the contrary, depletion of any cell type did not have a significant influence on the growth of TC-1/A9/dIfngr1-induced tumors. However, IFN-γ neutralization significantly reduced the growth of these tumors.

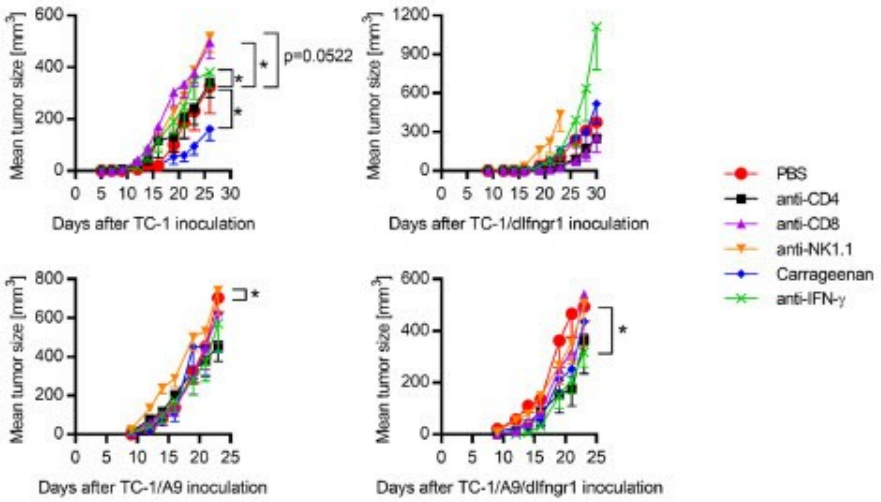

Figure 2. Mechanisms contributing to anti-tumor immunity. C57BL/6 mice ($n = 5$) were s.c. injected with 3×10^4 tumor cells and treated with anti-cluster of differentiation (CD)4, anti-CD8, anti-natural killer (NK)1.1, and anti- interferon (IFN)-γ antibodies or carrageenan. Phosphate-buffered saline (PBS) was injected as a negative control. Bars ± SEM; * $p < 0.05$.

2.3. PD-L1 and MHC-I Surface Expression on Tumor Cells

We determined the intensity of PD-L1 and MHC-I expression on tumor cells derived from the TC-1, TC-1/dIfngr1, TC-1/A9, and TC-1/A9/dIfngr1 tumors ex vivo, in order to analyze the impact of the tumor microenvironment on both molecules (Figure 3). Except for the TC-1-induced tumors, the ex vivo expression was markedly increased in comparison with in vitro cultured unstimulated cells.

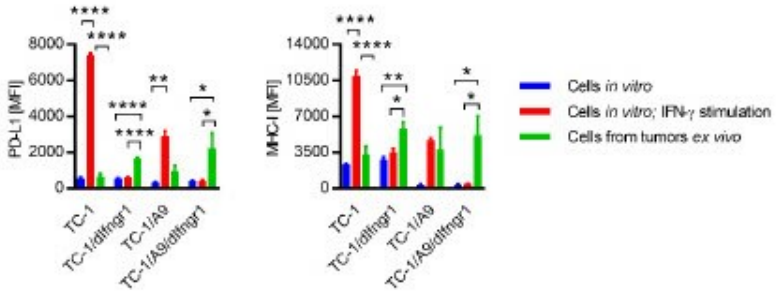

Figure 3. Ex vivo analysis of PD-L1 and MHC-I surface expression by tumor cells. Cells (3×10^4) were s.c. injected into C57BL/6 mice ($n = 3$) to form tumors. Cells harvested from tumors were stained by specific antibodies and analyzed by flow cytometry. $CD45^-$ tumor cells were compared with cell lines. In vitro cultured cell lines were untreated or stimulated for 1 day with 200 IU/mL IFN-γ. Median fluorescence intensity, MFI; columns, means of three samples; Bars, ± SEM. * $p < 0.05$, ** $p < 0.01$, **** $p < 0.0001$.

Furthermore, this expression on cells isolated from TC-1/dIfngr1 and TC-1/A9/dIfngr1 tumors was even slightly higher than on cells from TC-1 and TC-1/A9 tumors. Moreover, for TC-1/A9- and for TC-1/A9/Ifngr1-induced tumors, the expression of MHC-I in particular was comparable to that observed on TC-1/A9 cells stimulated with IFN-γ in vitro. These results showed that deactivation of the IFN-γ receptor did not reduce the level of PD-L1 and MHC-I expression in tumor cells in vivo. It suggests that other factors, besides IFN-γ, contributed to the induction of PD-L1 and MHC-I expression in tumor cells.

2.4. Cytokines Inducing PD-L1 and MHC-I Expression on Tumor Cells

Consequently, we analyzed the occurrence of presumed PD-L1 and/or MHC-I inducers (IFN-γ, IFN-α, IFN-β, interleukin (IL)-1α, IL-6, IL-27, tumor necrosis factor (TNF)-α, chemokine CCL-2, granulocyte-macrophage colony stimulating factor (GM-CSF), and epidermal growth factor (EGF)) in tumors induced by TC-1, TC-1/dIfngr1, TC-1/A9, and TC-1/A9/dIfngr1 cells and also in cell culture supernatants in vitro (Figure 4A). We found almost all these cytokines in tumors. The only exception was the absence of IFN-α in TC-1- and TC-1/dIfngr1-induced tumors. All in vitro cultured cell lines produced CCL-2 and IL-6. As the surface expression of PD-L1 and MHC-I is low on the unstimulated TC-1/A9 and TC-1/A9/dIfngr1 cells, CCL-2 and IL-6 should not induce PD-L1 and MHC-I expression. Therefore, we excluded these two cytokines from further analysis and evaluated the effect of the remaining cytokines on PD-L1 and MHC-I expression in vitro (Figure 4B). All cell lines were sensitive to type I IFNs (IFN-α and IFN-β) and cultivation of cells in the presence of these cytokines induced PD-L1 and MHC-I expression. Relative increase of PD-L1 on TC-1 cells, unlike MHC-I, was substantial after incubation with IFN-γ. Both PD-L1 and MHC-I were increased on TC-1/A9 cells after treatment with IFN-γ and type I IFNs. TC-1/A9/dIfngr1 cells were considerably more sensitive to type I IFNs than TC-1/A9. TNF-α had minor effect on all cell lines and negligibly elevated MHC-I expression only on TC-1/A9/dIfngr1 cells. None of the cell lines responded to other tested cytokines IL-1α, IL-27, GM-CSF, and EGF (data not shown).

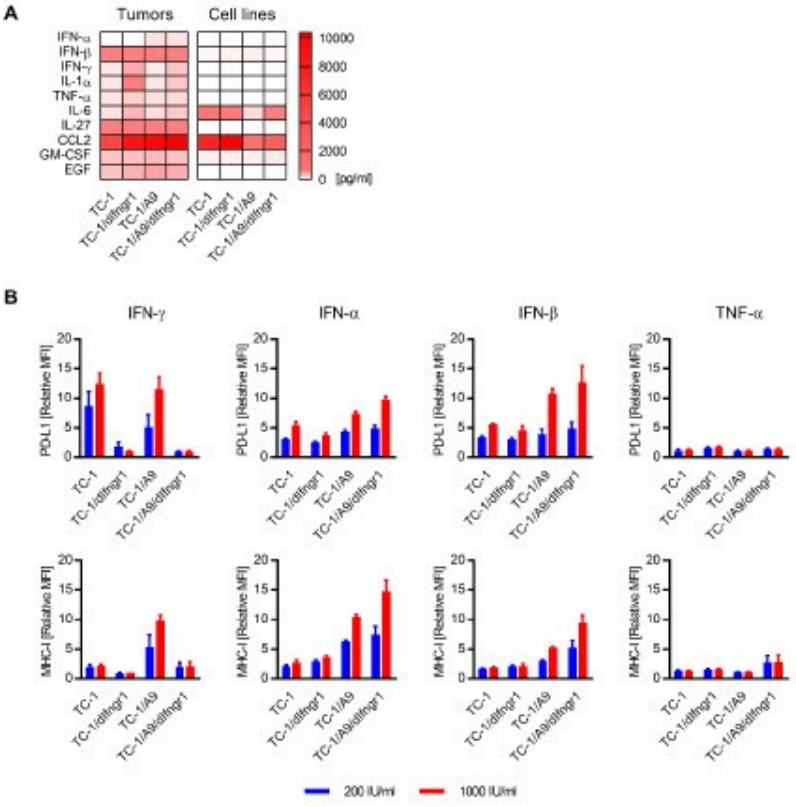

Figure 4. The effect of cytokines on PD-L1 and MHC-I surface expression. (**A**) The quantification of cytokines that can enhance PD-L1 and/or MHC-I expression in tumors and supernatants of cells cultured in vitro. (**B**) The effect of IFN-γ, IFN-α, IFN-β, or TNF-α on PD-L1 and MHC-I expression in vitro. Median fluorescence intensity, MFI. Relative MFI was calculated as $MFI_{stimulated\ cells}/MFI_{unstimulated\ cells}$. Columns, means of three samples; bars, ± SEM.

2.5. PD-L1 and MHC-I Expression ex Vivo after IFN-α and IFN-β Signaling Blockade

To elucidate the role of IFN-α and IFN-β in tumors induced by cells insensitive to IFN-γ, we applied the antibody against the receptor subunit shared by both interferons—IFN-α receptor 1 (IFNAR1)—and compared PD-L1 and MHC-I expression in tumors from mice treated with phosphate-buffered saline (PBS) or anti-IFNAR1 (Figure 5). Although the expression of these molecules was not changed on TC-1/dIfngr1 cells isolated from tumors, it was notably reduced on TC-1/A9/dIfngr1 cells after anti-IFNAR1 treatment.

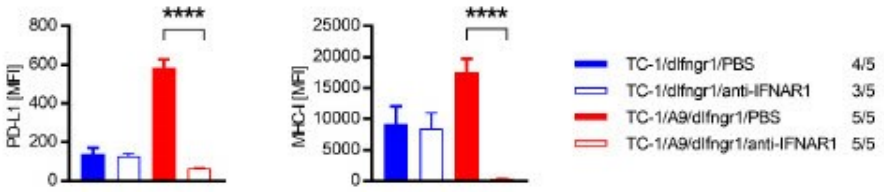

Figure 5. The role of IFN-α and IFN-β in TC-1/dIfngr1- and TC-1/A9/dIfngr1-induced tumors. Cells (3×10^4) were s.c. injected into C57BL/6 mice ($n = 5$) to form tumors. Mice were treated with anti-IFNAR1 antibody, or PBS was injected as a negative control. Cells isolated from tumors were stained by specific antibodies and analyzed by flow cytometry. The ratio of mice with tumor to the total number of mice in the group is shown. Median fluorescence intensity, MFI; columns, means of analyzed samples; bars, ± SEM; **** $p < 0.0001$.

2.6. Sensitivity to Combined Immunotherapy

As IFN-α and IFN-β induced PD-L1 and MHC-I expression on tumor cells in TC-1/A9/dIfngr1-originated tumors, we examined the sensitivity of these tumors to anti-PD-L1 therapy (Figure 6). We also included DNA vaccination against the human papillomavirus type 16 (HPV16) E7 oncoprotein to enhance the immune response against the tumor-specific antigen. In both TC-1/A9- and TC-1/A9/dIfngr1-induced tumors, the combined immunotherapy significantly reduced tumor growth and anti-PD-L1 treatment significantly supported the effect of DNA immunization.

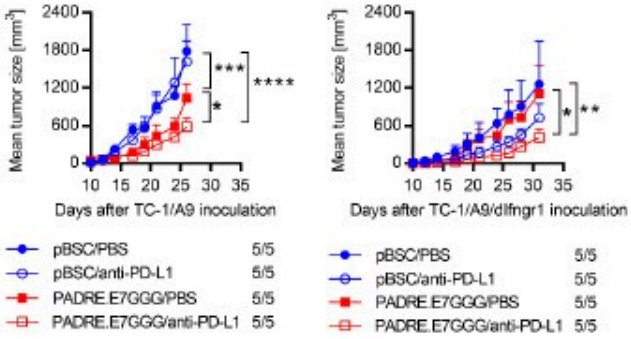

Figure 6. The sensitivity of TC-1/A9 and TC-1/A9/dIfngr1 cells to anti-PD-L1 therapy combined with DNA immunization. Cells (3×10^4) were s.c. injected to C57BL/6 mice ($n = 5$). Animals were treated with anti-PD-L1 antibody and/or the Pan DR epitope (PADRE).E7GGG DNA vaccine delivered by a gene gun. Control mice received PBS and/or pBSC. The ratio of mice with tumor to the total number of mice in the group is shown. Bars ± SEM; * $p < 0.05$, ** $p < 0.01$, *** $p < 0.001$, **** $p < 0.0001$.

3. Discussion

Although immune checkpoint blockade offers new promising possibilities in cancer treatment, the number of non-responding patients is still high. Therefore, finding predictive markers is necessary to identify potential responders. PD-L1 expression in tumors was used as the first predictive marker for

immune checkpoint blockade. Thus far, the FDA has registered four different immunohistochemical assays to assess PD-L1 expression in tumors. However, PD-L1 expression evaluated as a single biomarker appeared predictive in only 28.9% of FDA approvals of immune checkpoint inhibitors [14]. Among the many different markers currently being studied, tumor sensitivity to IFN-γ is considered advantageous for immune checkpoint therapy. In tumors of non-responders, reduced sensitivity to IFN-γ and defective MHC-I expression was found [11]. However, this work did not focus on mutations in tumors of responders to the therapy.

In this study, we tested the sensitivity of tumors induced by cells with functionally deactivated IFN-γ receptor to PD-L1 blockade. To address this question, we used TC-1 [15] and TC-1/A9 cell lines [16]. Although TC-1 cells markedly express PD-L1 and MHC-I molecules, this expression is reversibly downregulated on TC-1/A9 cells and can be induced by cytokines such as IFN-γ. To evaluate how the PD-L1 expression on TC-1 and TC-1/A9 cell lines influences oncogenicity and potential sensitivity to PD-L1 blockade, we prepared TC-1/dPD-L1 and TC-1/A9/dPD-L1 cells with deactivated PD-L1, respectively. PD-L1 on TC-1 cells strongly promoted tumor formation because, after PD-L1 deactivation, most mice did not form tumors from TC-1/dPD-L1 cells administered at different doses. The role of PD-L1 in tumor protection was lower for TC-1/A9 cells, as PD-L1 deactivation on these cells only reduced tumor growth. Because MHC-I expression on TC-1/A9/dPD-L1 cells was downregulated, these cells can be less sensitive to $CD8^+$ T cell cytotoxicity than TC-1/dPD-L1 cells, and the protective role of PD-L1 on TC-1/A9/dPD-L1 cells can thus be lower. Previous studies in various mouse tumor models showed that PD-L1 expression on both tumor and host cells can contribute to tumor escape [17–21]. The relative contribution of PD-L1 molecules expressed on tumor cells versus non-tumor cells to tumor protection was dependent on the used model.

After IFNGR1 deactivation, we evaluated the effect of this modification on tumor growth and anti-tumor immunity. Oncogenicity of the TC-1/dIfngr1 and TC-1/A9/dIfngr1 clones remained similar to that of the parental cell lines. It resembles the unchanged growth of mice tumors induced by intradermal injection of B16 cells with knockdown of the *Ifngr1* gene [12]. On the contrary, mouse ovarian cancer HM1 cell-induced tumors with *Ifngr1* knockdown grew more slowly than control tumors [22]. However, these tumors were induced in the peritoneal cavity.

The role of IFN-γ in tumor development is context-dependent [23]. On the one hand, IFN-γ promotes tumor rejection by enhancement of antigen presentation (including MHC-I upregulation) and cytotoxicity of immune cells [24], and on the other hand, a selective pressure of prolonged exposure to IFN-γ can result in downregulation of antigen presentation [25]. Moreover, IFN-γ stimulates PD-L1 and many other molecules inhibiting the anti-cancer response [26,27] and activates some immunosuppressive cells [28]. We also found different roles of IFN-γ in this study. Although in TC-1- and TC-1/dIfngr1-induced tumors, IFN-γ had an anti-tumor effect and in TC-1/A9-induced tumors, it did not markedly affect tumor growth, this cytokine supported the growth of TC-1/A9/dIfngr1-induced tumors, which was mediated by non-tumor cells sensitive to IFN-γ. IFNGR1 deactivation influenced the effect of certain immune cells on tumor development, particularly on TC-1 versus TC-1/dIfngr1 tumors, where IFNGR1 deactivation eliminated the anti-tumor effect of $CD8^+$ cells and pro-tumor effect of macrophages. Mechanisms involved in these changes are not currently clear.

As deactivation of IFNGR1 did not lead to the downregulation of the PD-L1 and MHC-I molecules on TC-1/dIfngr1 and TC-1/A9/dIfngr1 cells in vivo compared to TC-1 and TC-1/A9 cells, respectively, we hypothesized that besides IFN-γ, other cytokines induced PD-L1 and MHC-I expression. Several studies have indicated the involvement of different factors (IFN-α, IFN-β, IL-27, EGF, TNF-α, IL-6, GM-CSF, IL-1α, and CCL2 combined with lipocalin 2) in PD-L1 and MHC-I stimulation or stabilization [27,29–39]. In this study, type I IFNs (IFN-α and IFN-β) were the main inducers of PD-L1 and MHC-I expression. We found both type I IFNs in TC-1/A9/dIfngr1-induced tumors but only IFN-β in TC-1/dIfngr1-induced tumors. This observation corresponds to the expression of PD-L1 and MHC-I after IFNAR1 neutralization, which significantly downregulated this expression in TC-1/A9/dIfngr1- but not in TC-1/dIfngr1-induced tumors. It implies that from the type I IFNs, IFN-α mainly contributed to PD-L1 and MHC-I stimulation

on tumor cells in the tumor microenvironment. In general, type I IFNs are important inducers of an immune response against tumors [40]. As suggested by the experimental treatment of tumors with the IFN-α-anti-PD-L1 fusion protein, they can also enhance the efficacy of PD-L1 blockade [41].

As we found the in vivo effect of IFN-α on PD-L1 and MHC-I expression for TC-1/A9/dIfngr1-induced tumors, we tested PD-L1 blockade on these tumors. Due to poor immunogenicity of tumors with MHC-I downregulation, we combined PD-L1 blockade with DNA vaccination against the HPV16 E7 oncoprotein representing a tumor-specific antigen. After combined immunotherapy, the PD-L1 blockade significantly contributed to the inhibition of both TC-1/A9 and TC-1/A9/dIfngr1 tumor growth. Therefore, we searched whether mutations in IFN-γ signaling in human tumors occur in responders to PD-1/PD-L1 blockade. In five independent studies on different tumor types with 115 patients defined as responders to PD-1/PD-L1 blockade (i.e., patients with durable clinical benefit, complete response, or partial response according to the response evaluation criteria in solid tumors (RECIST) v1.1), seven patients (6.1%) had a missense or nonsense mutation in IFN-γ signaling: one patient in *Ifngr1* and *JAK-2*, one in *JAK-1*, and five in *JAK-2* [42–46]. Out of 250 non-responders, missense, nonsense, or splice-site mutations in IFN-γ signaling were found in only 11 patients (4.4%): three in *Ifngr1*, one in *Ifngr2*, four in *JAK-1*, and three in *JAK-2* [42,44,45,47].

The sensitivity of tumor cells to IFN-γ can play a critical role in the response to PD-1/PD-L1 blockade, which was demonstrated on lung cancer cell lines [48]. However, our data provide evidence that deactivated IFN-γ signaling may not be sufficient for PD-L1 and MHC-I reduction on tumor cells and resistance to PD-L1 blockade. We demonstrate in our TC-1/A9 tumor model that PD-L1 and MHC-I induction can be performed by other cytokines, such as IFN-α and/or IFN-β. Mutations in IFN-γ signaling in tumors of patients that responded to PD-1/PD-L1 blockade suggest that similar conditions can be found in human tumors. In cases when the resistance to PD-1/PD-L1 blockade was associated with the abrogation of IFN-γ signaling, other mutation(s) might be needed. As the tumor microenvironment is a complex system, the selection of patients suitable for PD-1/PD-L1 blockade should be conducted on the basis of a broad range of predictive markers that can include sensitivity to both IFN-γ and type I IFN signaling. The only impairment in IFN-γ pathway should not be a contraindication to anti-PD-1/PD-L1 therapy.

4. Materials and Methods

4.1. Mice

Six- to eight-week-old female C57BL/6N mice (Charles River, Sulzfeld, Germany) were used in the experiments. Animals were maintained under standard conditions and in accordance with the guidelines for the proper treatment of laboratory animals at the animal facility of the Czech Center of Phenogenomics (BIOCEV, Vestec, Czech Republic). All animal experimental procedures were carried out in compliance with Directive 2010/63/EU and animal protocols were approved by the Sectoral Expert Committee of the Czech Academy of Sciences for Approval of Projects of Experiments on Animals (reference number 46/2016, 16 May 2016).

4.2. Cell Lines and Culture Conditions

TC-1 cell line (Cellosaurus ID: CVCL_4699; provided by T.-C. Wu, John Hopkins University, Baltimore, MD, USA) was prepared by the transformation of C57BL/6 mouse primary lung cells with the HPV16 *E6/E7* oncogenes and human activated *H-ras* [15]. From a TC-1-induced tumor that developed in a mouse preimmunized against the E7 antigen, the TC-1/A9 clone was selected on the basis of a reduced surface expression of MHC-I molecules. This MHC-I downregulation is reversible and can be restored with the IFN-γ treatment [16].

To abrogate the function of the IFN-γ receptor in TC-1 and TC-1/A9 cells, the *Ifngr1* gene (NCBI reference sequence NM_010511.2) was deactivated with the CRISPR/Cas9 system. Two target sites (ATTAGAACATTCGTCGGTAC in exon 2 and CGACCGTATGTTTCGTATGT in exon 5) were designed

using the CRISPR Design Tool (http://crispr.mit.edu/) and cloned into the GeneArt CRISPR Nuclease Vector carrying the human CD4 gene (Life Technologies, Carlsbad, CA, USA). The constructed plasmids verified by sequencing were transfected by Lipofectamine 2000 (Thermo Fisher Scientific, Waltham, MA, USA) into TC-1 and TC-1/A9 cells, and three days after transfection, the successfully transfected cells were marked with magnetically labeled antibody against CD4 (Thermo Fisher Scientific), enriched by magnetic isolation, and cloned by serial dilution. The function of the IFNGR1 in clonal cell lines was tested after 40-hour incubation with 200 IU/mL IFN-γ PeproTech, Rocky Hill, NJ, USA) by flow cytometric analysis of MHC-I expression (see above). Next, the Pdcd-1L1 Double Nickase Plasmid (m) kit (sc-425636-NIC, Santa Cruz Biotechnology, Dallas, TX, USA) was used for deactivation of PD-L1 in TC-1 and TC-1/A9 cells. The transfected cells were preselected by puromycin (6 μg/mL added to the culture media 2 days after transfection) for 4 days. TC-1/dPD-L1 and TC-1/A9/dPD-L1 clone selection were performed by single-cell sorting into a 96-well plate by a FACSAria Fusion flow cytometer (BD Biosciences, Franklin Lakes, NJ, USA). Cells were stained with anti-PD-L1-PE (phycoerythrin) antibody (clone 10F.9G2; BioLegend, San Diego, CA, USA) and negatively selected.

All cells were grown in high-glucose Dulbecco's modified Eagle's medium (DMEM; Sigma-Aldrich, Merck KGaA, Darmstadt, Germany) supplemented with 10% fetal calf serum (FCS; Biosera, Nuaille, France), 100 IU/mL penicillin, and 100 μg/mL streptomycin (Biosera). Cells were passaged twice a week with 0.05% trypsin containing 0.02% ethylenediaminetetraacetic acid (EDTA; Sigma-Aldrich, Merck KGaA) in PBS (Sigma-Aldrich, Merck KGaA). In vitro cell stimulations were performed in 35 mm cell culture dishes. Cytokines IFN-γ (200 or 1000 IU/mL; PeproTech), IFN-α (200 or 1000 IU/mL; BioLegend), IFN-β (200 or 1000 IU/mL; R&D Systems, Minneapolis, MN, USA), and TNF-α (200 or 1000 IU/mL; PeproTech), IL-27 (5 IU/mL; BioLegend), IL-1α (1000 IU/mL; BioLegend), EGF (10 IU/mL; BioLegend), or GM-CSF (200 IU/mL; BioLegend) were added to 2 mL of culture media for 1 day.

4.3. Plasmids

Plasmids pBSC [49] or pBSC/Pan DR epitope (PADRE).E7GGG [50] were used for immunization. The *PADRE.E7GGG* fusion gene consists of the mutated HPV16 *E7* gene (*E7GGG*) containing three point mutations resulting in substitutions D21G, C24G, and E26G in the Rb-binding site [49] and the universal helper Pan DR epitope (PADRE) designed in silico [51].

The plasmids were transformed into the competent *E. coli* XL-1 blue strain, cultured in Luria Broth Medium (Sigma-Aldrich, Merck KGaA) with 100 μg/mL of ampicillin (Duchefa Biochemie, Haarlem, The Netherlands), and purified with the Qiagen Plasmid Maxi Kit (Qiagen, Hilden, Germany).

4.4. Preparation of Gene Gun Cartridges

Plasmid DNA was coated onto 1 μm gold particles (Bio-Rad, Hercules, CA, USA) by the procedure recommended by the producer of gold particles. Each cartridge contained 1 μg DNA coated onto 0.5 mg of gold particles.

4.5. Animal Experiments

Immunocompetent C57BL/6N mice (five per group) were challenged with tumor cells suspended in 150 μL PBS by subcutaneous (s.c.) injection into the back of animals, under anesthesia with ketamine (100 mg/kg; Bioveta, Ivanovice na Hane, Czech Republic) and xylazine (16 mg/kg; Bioveta). Tumor growth was monitored three times a week, and tumor volume was calculated using the formula (π/6) (a × b × c) where a, b, and c are the length, width, and height of the tumor, respectively.

Mice were immunized with the pBSC/PADRE.E7GGG plasmid by a gene gun (Bio-Rad, Hercules, CA, USA) on days 3, 6, and 10 after TC-1/A9 or TC-1/A9/dIfngr1 inoculation. DNA vaccination was performed at a discharge pressure of 400 psi into the shaven skin of the abdomen. Each immunization consisted of two shots delivering together 2 μg of plasmid DNA. The empty pBSC plasmid was used as a negative control.

In in vivo depletion experiments, the following doses of monoclonal antibodies (Bio X Cell, West Lebanon, NH, USA) in 200 µL PBS were intraperitoneally (i.p.) injected: 100 µg of anti-CD4 (clone GK1.5), 100 µg of anti-CD8 (clone 2.43), and 100 µg of anti-NK1.1 (clone PK136). The efficacy of depletions was verified by staining of splenocytes. To deplete macrophages, 1 mg of carrageenan IV (Sigma-Aldrich, Merck KGaA) dissolved in 200 µl PBS was inoculated i.p. neutralization of the IFNAR1 was achieved with 200 µg of anti-IFNAR1 (clone MAR1-5A3) and IFN-γ with 300 µg of anti-IFN-γ (clone P4-6A2) in 200 µL PBS per mouse. Depletions and neutralizations were performed two days before tumor-cell injection and then twice a week (or once a week in the case of anti-IFN-γ) after tumor cell inoculation.

4.6. Tumor Cell Preparation

For flow cytometry analysis, tumors with a volume of about 100 mm^3 were removed from the animals. The tumor tissue was rinsed with PBS, cut to pieces, and treated with 1 mg/mL collagenase NB 8 (SERVA, Heidelberg, Germany) and 100 µg/mL DNase I (Roche, Basel, Switzerland) in Roswell Park Memorial Institute (RPMI) 1640 medium (Sigma-Aldrich, Merck KGaK) without FCS. To achieve a single cell suspension, the treated tissue was mechanically and also enzymatically dissociated at 37 °C using predefined programs on a gentleMACS Octo Dissociator (Miltenyi Biotec, Bergisch Gladbach, Germany). The obtained cell suspension was filtered through a 70 µm cell strainer and washed with RPMI medium. Erythrocytes were removed with an ammonium-chloride-potassium (ACK) lysing buffer (0.15 M NH_4Cl, 10 mM $KHCO_3$, 1 mM EDTA, pH 7.2–7.4). Cell suspension was filtered through a 42 µm mesh.

4.7. Tumor Lysate Preparation

To measure cytokine concentration, tumors with an average weight of 700 mg were immersed in liquid nitrogen, immediately thawed, and cut into pieces. The tissue was homogenized in extraction buffer (100 mM Tris, pH 7.4, 150 mM NaCl, 1 mM ethylene glycol tetraacetic acid (EGTA), 1mM EDTA, 1% Triton X-100, 1mM phenylmethylsulfonyl fluoride, and Pierce protease inhibitor (Thermo Fisher Scientific)) at a ratio of 300 mg of the tissue to 1 mL of buffer at 4 °C. Samples were constantly agitated in a gentleMACS Octo Dissociator at 4 °C for 2 hours and then centrifuged at 10,000× g at 4 °C for 20 min. The supernatant was aliquoted and stored at −80 °C.

4.8. Flow Cytometry

Single-cell suspensions of the cell lines were incubated with Fixable Viability Dye (eFluor 455UV; eBioscience) to label dead cells. In the following step, cells were stained for surface markers with anti-mouse MHC-I-FITC (fluorescein isothiocyanate; clone 28.8.6; BD Biosciences) and anti-mouse PD-L1-PE (clone 10F.9G2; BioLegend). Isotype control antibodies for mouse IgG2a, κ (clone MOPC-173), and rat IgG2b, κ (clone RTK4530; BioLegend) were used for anti-MHC-I and anti-PD-L1 antibodies, respectively.

Cells isolated from tumors were also stained for viability as described above. Afterwards, the cells were treated with anti-mouse CD16/32 (Fc block, clone 93; BioLegend), and surface markers CD45, MHC-I, and PD-L1 were stained with the antibodies anti-CD45 (clone 30-F11, Alexa Fluor 700; BioLegend), anti-MHC-I, and anti-PD-L1, as described above. Data were analyzed with the FlowJo software, version 10.6 (BD Biosciences).

4.9. Cytokine Measurement

The presence of cytokines in tumors or in cell culture supernatants was evaluated by LEGENDplex assays (Mouse Inflammation Panel and Mouse Type 1/2 Interferon Panel; BioLegend) and the Invitrogen EGF Mouse ELISA Kit (Thermo Fisher Scientific) following the manufacturers' protocols.

4.10. Statistical Analysis

The oncogenicity and tumor growth after immunotherapy were evaluated by two-way ANOVA and Bonferroni post-test. Tumor growth after neutralization of immune cells and results obtained by flow cytometry were analyzed by one-way ANOVA and Bonferroni post-test. A difference between groups was considered significant if $p < 0.05$. The calculations were performed using the Prism software, version 7 (Graph-Pad Software, San Diego, CA, USA).

Author Contributions: J.V. and M.S. designed the experiments; J.V., M.S., I.P. and A.P. performed the animal experiments; J.V. and I.P. performed flow cytometry; J.V. performed cytokine assays; J.V. and M.S. analyzed the data; J.V., M.S., A.P. and I.P. wrote and edited the manuscript; J.V. and M.S. acquired funding. All authors have read and agreed to the published version of the manuscript.

Funding: This research was funded by the Charles University, grant number GAUK 988218; the Ministry of Education, Youth and Sports of the Czech Republic (MEYS), grant numbers LQ1604 and LM2018126; and the European Regional Development Fund and MEYS, grant numbers CZ.1.05/1.1.00/02.0109, CZ.1.05/2.1.00/19.0400, CZ.02.1.01/0.0/0.0/16_019/0000785, and CZ.1.05/2.1.00/19.0395.

Acknowledgments: The authors acknowledge Pavlina Vesela, Nela Vaclavikova, and Kristyna Penickova for technical assistance; the Imaging Methods Core Facility at BIOCEV for support with flow cytometry analysis; and the Czech Center for Phenogenomics for the mice maintenance.

Conflicts of Interest: The authors declare no conflict of interest.

References

1. Christofi, T.; Baritaki, S.; Falzone, L.; Libra, M.; Zaravinos, A. Current perspectives in cancer immunotherapy. *Cancers* **2019**, *11*, 1472. [CrossRef] [PubMed]
2. Falzone, L.; Salomone, S.; Libra, M. Evolution of cancer pharmacological treatments at the turn of the third millennium. *Front. Pharmacol.* **2018**, *9*, 1300. [CrossRef] [PubMed]
3. Liu, M.; Guo, F. Recent updates on cancer immunotherapy. *Precis. Clin. Med.* **2018**, *1*, 65–74. [CrossRef]
4. Zhang, H.; Chen, J. Current status and future directions of cancer immunotherapy. *J. Cancer* **2018**, *9*, 1773–1781. [CrossRef] [PubMed]
5. Markham, A.; Duggan, S. Cemiplimab: First global approval. *Drugs* **2018**, *78*, 1841–1846. [CrossRef] [PubMed]
6. Ribas, A.; Wolchok, J.D. Cancer immunotherapy using checkpoint blockade. *Science* **2018**, *359*, 1350–1355. [CrossRef] [PubMed]
7. Sul, J.; Blumenthal, G.M.; Jiang, X.; He, K.; Keegan, P.; Pazdur, R. FDA approval summary: Pembrolizumab for the treatment of patients with metastatic non-small cell lung cancer whose tumors express programmed death-ligand 1. *Oncologist* **2016**, *21*, 643–650. [CrossRef]
8. Ribas, A.; Hamid, O.; Daud, A.; Hodi, F.S.; Wolchok, J.D.; Kefford, R.; Joshua, A.M.; Patnaik, A.; Hwu, W.-J.; Weber, J.S.; et al. Association of pembrolizumab with tumor response and survival among patients with advanced melanoma. *JAMA* **2016**, *315*, 1600–1609. [CrossRef]
9. Buder-Bakhaya, K.; Hassel, J.C. Biomarkers for clinical benefit of immune checkpoint inhibitor treatment—A review from the melanoma perspective and beyond. *Front. Immunol.* **2018**, *9*, 1474. [CrossRef]
10. Shin, D.S.; Zaretsky, J.M.; Escuin-Ordinas, H.; Garcia-Diaz, A.; Hu-Lieskovan, S.; Kalbasi, A.; Grasso, C.S.; Hugo, W.; Sandoval, S.; Torrejon, D.Y.; et al. Primary resistance to PD-1 blockade mediated by JAK1/2 mutations. *Cancer Discov.* **2017**, *7*, 188–201. [CrossRef]
11. Zaretsky, J.M.; Garcia-Diaz, A.; Shin, D.S.; Escuin-Ordinas, H.; Hugo, W.; Hu-Lieskovan, S.; Torrejon, D.Y.; Abril-Rodriguez, G.; Sandoval, S.; Barthly, L.; et al. Mutations associated with acquired resistance to PD-1 blockade in melanoma. *N. Engl. J. Med.* **2016**, *375*, 819–829. [CrossRef] [PubMed]
12. Gao, J.; Shi, L.Z.; Zhao, H.; Chen, J.; Xiong, L.; He, Q.; Chen, T.; Roszik, J.; Bernatchez, C.; Woodman, S.E.; et al. Loss of IFN-γ pathway genes in tumor cells as a mechanism of resistance to anti-CTLA-4 therapy. *Cell* **2016**, *167*, 397–404. [CrossRef] [PubMed]
13. Lin, C.-F.; Lin, C.-M.; Lee, K.-Y.; Wu, S.-Y.; Feng, P.-H.; Chen, K.-Y.; Chuang, H.-C.; Chen, C.-L.; Wang, Y.-C.; Tseng, P.-C.; et al. Escape from IFN-γ-dependent immunosurveillance in tumorigenesis. *J. Biomed. Sci.* **2017**, *24*, 10. [CrossRef] [PubMed]

14. Davis, A.A.; Patel, V.G. The role of PD-L1 expression as a predictive biomarker: An analysis of all US Food and Drug Administration (FDA) approvals of immune checkpoint inhibitors. *J. Immunother. Cancer* **2019**, *7*, 278. [CrossRef]
15. Lin, K.-Y.; Guarnieri, F.G.; Staveley-O'Carroll, K.F.; Levitsky, H.I.; August, J.T.; Pardoll, D.M.; Wu, T.-C. Treatment of established tumors with a novel vaccine that enhances major histocompatibility class II presentation of tumor antigen. *Cancer Res.* **1996**, *56*, 21–26.
16. Smahel, M.; Sima, P.; Ludvíková, V.; Marinov, I.; Pokorná, D.; Vonka, V. Immunisation with modified HPV16 E7 genes against mouse oncogenic TC-1 cell sublines with downregulated expression of MHC class I molecules. *Vaccine* **2003**, *21*, 1125–1136. [CrossRef]
17. Juneja, V.R.; McGuire, K.A.; Manguso, R.T.; LaFleur, M.W.; Collins, N.; Haining, W.N.; Freeman, G.J.; Sharpe, A.H. PD-L1 on tumor cells is sufficient for immune evasion in immunogenic tumors and inhibits CD8 T cell cytotoxicity. *J. Exp. Med.* **2017**, *214*, 895–904. [CrossRef]
18. Kleinovink, J.W.; Marijt, K.A.; Schoonderwoerd, M.J.A.; van Hall, T.; Ossendorp, F.; Fransen, M.F. PD-L1 expression on malignant cells is no prerequisite for checkpoint therapy. *OncoImmunology* **2017**, *6*, e1294299. [CrossRef]
19. Lau, J.; Cheung, J.; Navarro, A.; Lianoglou, S.; Haley, B.; Totpal, K.; Sanders, L.; Koeppen, H.; Caplazi, P.; McBride, J.; et al. Tumour and host cell PD-L1 is required to mediate suppression of anti-tumour immunity in mice. *Nat. Commun.* **2017**, *8*, 14572. [CrossRef]
20. Noguchi, T.; Ward, J.P.; Gubin, M.M.; Arthur, C.D.; Lee, S.H.; Hundal, J.; Selby, M.J.; Graziano, R.F.; Mardis, E.R.; Korman, A.J.; et al. Temporally distinct PD-L1 expression by tumor and host cells contributes to immune escape. *Cancer Immunol. Res.* **2017**, *5*, 106–117. [CrossRef]
21. Tang, H.; Liang, Y.; Anders, R.A.; Taube, J.M.; Qiu, X.; Mulgaonkar, A.; Liu, X.; Harrington, S.M.; Guo, J.; Xin, Y.; et al. PD-L1 on host cells is essential for PD-L1 blockade-mediated tumor regression. *J. Clin. Investig.* **2018**, *128*, 580–588. [CrossRef] [PubMed]
22. Abiko, K.; Matsumura, N.; Hamanishi, J.; Horikawa, N.; Murakami, R.; Yamaguchi, K.; Yoshioka, Y.; Baba, T.; Konishi, I.; Mandai, M. IFN-γ from lymphocytes induces PD-L1 expression and promotes progression of ovarian cancer. *Br. J. Cancer* **2015**, *112*, 1501–1509. [CrossRef] [PubMed]
23. Zaidi, M.R.; Merlino, G. The two faces of interferon-γ in cancer. *Clin. Cancer Res.* **2011**, *17*, 6118–6124. [CrossRef] [PubMed]
24. Shankaran, V.; Ikeda, H.; Bruce, A.T.; White, J.M.; Swanson, P.E.; Old, L.J.; Schreiber, R.D. IFNγ and lymphocytes prevent primary tumour development and shape tumour immunogenicity. *Nature* **2001**, *410*, 1107–1111. [CrossRef] [PubMed]
25. Algarra, I.; García-Lora, A.; Cabrera, T.; Ruiz-Cabello, F.; Garrido, F. The selection of tumor variants with altered expression of classical and nonclassical MHC class I molecules: Implications for tumor immune escape. *Cancer Immunol. Immunother.* **2004**, *53*, 904–910. [CrossRef] [PubMed]
26. Benci, J.L.; Xu, B.; Qiu, Y.; Wu, T.; Dada, H.; Victor, C.T.-S.; Cucolo, L.; Lee, D.S.M.; Pauken, K.E.; Huang, A.C.; et al. Tumor interferon signaling regulates a multigenic resistance program to immune checkpoint blockade. *Cell* **2016**, *167*, 1540–1554. [CrossRef]
27. Garcia-Diaz, A.; Shin, D.S.; Moreno, B.H.; Saco, J.; Escuin-Ordinas, H.; Rodriguez, G.A.; Zaretsky, J.M.; Sun, L.; Hugo, W.; Wang, X.; et al. Interferon receptor signaling pathways regulating PD-L1 and PD-L2 expression. *Cell Rep.* **2017**, *19*, 1189–1201. [CrossRef]
28. Brody, J.R.; Costantino, C.L.; Berger, A.C.; Sato, T.; Lisanti, M.P.; Yeo, C.J.; Emmons, R.V.; Witkiewicz, A.K. Expression of indoleamine 2,3-dioxygenase in metastatic malignant melanoma recruits regulatory T cells to avoid immune detection and affects survival. *Cell Cycle* **2009**, *8*, 1930–1934. [CrossRef]
29. Chan, L.-C.; Li, C.-W.; Xia, W.; Hsu, J.-M.; Lee, H.-H.; Cha, J.-H.; Wang, H.-L.; Yang, W.-H.; Yen, E.-Y.; Chang, W.-C.; et al. IL-6/JAK1 pathway drives PD-L1 Y112 phosphorylation to promote cancer immune evasion. *J. Clin. Investig.* **2019**, *129*, 3324–3338. [CrossRef]
30. Rolvering, C.; Zimmer, A.D.; Ginolhac, A.; Margue, C.; Kirchmeyer, M.; Servais, F.; Hermanns, H.M.; Hergovits, S.; Nazarov, P.V.; Nicot, N.; et al. The PD-L1- and IL6-mediated dampening of the IL27/STAT1 anticancer responses are prevented by α-PD-L1 or α-IL6 antibodies. *J. Leukocyte Biol.* **2018**, *104*, 969–985. [CrossRef]

31. Garrido, G.; Rabasa, A.; Garrido, C.; Chao, L.; Garrido, F.; García-Lora, Á.M.; Sánchez-Ramírez, B. Upregulation of HLA Class I expression on tumor cells by the anti-EGFR antibody nimotuzumab. *Front. Pharmacol.* **2017**, *8*, 595. [CrossRef] [PubMed]
32. Wang, T.-T.; Zhao, Y.-L.; Peng, L.-S.; Chen, N.; Chen, W.; Lv, Y.-P.; Mao, F.-Y.; Zhang, J.-Y.; Cheng, P.; Teng, Y.-S.; et al. Tumour-activated neutrophils in gastric cancer foster immune suppression and disease progression through GM-CSF-PD-L1 pathway. *Gut* **2017**, *66*, 1900–1911. [CrossRef] [PubMed]
33. Li, C.-W.; Lim, S.-O.; Xia, W.; Lee, H.-H.; Chan, L.-C.; Kuo, C.-W.; Khoo, K.-H.; Chang, S.-S.; Cha, J.-H.; Kim, T.; et al. Glycosylation and stabilization of programmed death ligand-1 suppresses T-cell activity. *Nat. Commun.* **2016**, *7*, 12632. [CrossRef] [PubMed]
34. Lim, S.-O.; Li, C.-W.; Xia, W.; Cha, J.-H.; Chan, L.-C.; Wu, Y.; Chang, S.-S.; Lin, W.-C.; Hsu, J.-M.; Hsu, Y.-H.; et al. Deubiquitination and stabilization of PD-L1 by CSN5. *Cancer Cell* **2016**, *30*, 925–939. [CrossRef] [PubMed]
35. Carbotti, G.; Barisione, G.; Airoldi, I.; Mezzanzanica, D.; Bagnoli, M.; Ferrero, S.; Petretto, A.; Fabbi, M.; Ferrini, S. IL-27 induces the expression of IDO and PD-L1 in human cancer cells. *Oncotarget* **2015**, *6*, 43267–43280. [CrossRef] [PubMed]
36. Paulson, K.G.; Tegeder, A.; Willmes, C.; Iyer, J.G.; Afanasiev, O.K.; Schrama, D.; Koba, S.; Thibodeau, R.; Nagase, K.; Simonson, W.T.; et al. Downregulation of MHC-I expression is prevalent but reversible in merkel cell carcinoma. *Cancer Immunol. Res.* **2014**, *2*, 1071–1079. [CrossRef]
37. Ghosh, S.; Paul, A.; Sen, E. Tumor necrosis factor alpha-induced hypoxia-inducible factor 1α–β-catenin axis regulates major histocompatibility complex class I gene activation through chromatin remodeling. *Mol. Cell. Biol.* **2013**, *33*, 2718–2731. [CrossRef]
38. Youngnak-Piboonratanakit, P.; Tsushima, F.; Otsuki, N.; Igarashi, H.; Machida, U.; Iwai, H.; Takahashi, Y.; Omura, K.; Yokozeki, H.; Azuma, M. The expression of B7-H1 on keratinocytes in chronic inflammatory mucocutaneous disease and its regulatory role. *Immunol. Lett.* **2004**, *94*, 215–222. [CrossRef]
39. Wicks, I.P.; Leizer, T.; Wawryk, S.O.; Novotny, J.R.; Hamilton, J.; Vitti, G.; Boyd, A.W. The effect of cytokines on the expression of MHC antigens and ICAM-1 by normal and transformed synoviocytes. *Autoimmunity* **1992**, *12*, 13–19. [CrossRef]
40. Schadt, L.; Sparano, C.; Schweiger, N.A.; Silina, K.; Cecconi, V.; Lucchiari, G.; Yagita, H.; Guggisberg, E.; Saba, S.; Nascakova, Z.; et al. Cancer-cell-intrinsic cGAS expression mediates tumor immunogenicity. *Cell Rep.* **2019**, *29*, 1236–1248. [CrossRef]
41. Liang, Y.; Tang, H.; Guo, J.; Qiu, X.; Yang, Z.; Ren, Z.; Sun, Z.; Bian, Y.; Xu, L.; Xu, H.; et al. Targeting IFNα to tumor by anti-PD-L1 creates feedforward antitumor responses to overcome checkpoint blockade resistance. *Nat. Commun.* **2018**, *9*, 4586. [CrossRef] [PubMed]
42. Rizvi, H.; Sanchez-Vega, F.; La, K.; Chatila, W.; Jonsson, P.; Halpenny, D.; Plodkowski, A.; Long, N.; Sauter, J.L.; Rekhtman, N.; et al. Molecular determinants of response to anti-programmed cell death (PD)-1 and anti-programmed death-ligand 1 (PD-L1) blockade in patients with non-small-cell lung cancer profiled with targeted next-generation sequencing. *J. Clin. Oncol.* **2018**, *36*, 633–641. [CrossRef] [PubMed]
43. Ascierto, M.L.; Makohon-Moore, A.; Lipson, E.J.; Taube, J.M.; McMiller, T.L.; Berger, A.E.; Fan, J.; Kaunitz, G.J.; Cottrell, T.R.; Kohutek, Z.A.; et al. Transcriptional mechanisms of resistance to anti–PD-1 therapy. *Clin. Cancer Res.* **2017**, *23*, 3168–3180. [CrossRef] [PubMed]
44. Riaz, N.; Havel, J.J.; Makarov, V.; Desrichard, A.; Urba, W.J.; Sims, J.S.; Hodi, F.S.; Martín-Algarra, S.; Mandal, R.; Sharfman, W.H.; et al. Tumor and microenvironment evolution during immunotherapy with nivolumab. *Cell* **2017**, *171*, 934–949. [CrossRef] [PubMed]
45. Hugo, W.; Zaretsky, J.M.; Sun, L.; Song, C.; Moreno, B.H.; Hu-Lieskovan, S.; Berent-Maoz, B.; Pang, J.; Chmielowski, B.; Cherry, G.; et al. Genomic and transcriptomic features of response to anti-PD-1 therapy in metastatic melanoma. *Cell* **2016**, *165*, 35–44. [CrossRef] [PubMed]
46. Mehnert, J.M.; Panda, A.; Zhong, H.; Hirshfield, K.; Damare, S.; Lane, K.; Sokol, L.; Stein, M.N.; Rodriguez-Rodriquez, L.; Kaufman, H.L.; et al. Immune activation and response to pembrolizumab in POLE-mutant endometrial cancer. *J. Clin. Investig.* **2016**, *126*, 2334–2340. [CrossRef]
47. Sade-Feldman, M.; Jiao, Y.J.; Chen, J.H.; Rooney, M.S.; Barzily-Rokni, M.; Eliane, J.-P.; Bjorgaard, S.L.; Hammond, M.R.; Vitzthum, H.; Blackmon, S.M.; et al. Resistance to checkpoint blockade therapy through inactivation of antigen presentation. *Nat. Commun.* **2017**, *8*, 1136. [CrossRef]

48. Bullock, B.L.; Kimball, A.K.; Poczobutt, J.M.; Neuwelt, A.J.; Li, H.Y.; Johnson, A.M.; Kwak, J.W.; Kleczko, E.K.; Kaspar, R.E.; Wagner, E.K.; et al. Tumor-intrinsic response to IFNγ shapes the tumor microenvironment and anti–PD-1 response in NSCLC. *Life Sci. Alliance* **2019**, *2*, e201900328. [CrossRef]
49. Smahel, M.; Sima, P.; Ludvíkova, V.; Vonka, V. Modified HPV16 E7 genes as DNA vaccine against E7-containing oncogenic cells. *Virology* **2001**, *281*, 231–238. [CrossRef]
50. Smahel, M.; Polakova, I.; Duskova, M.; Ludvikova, V.; Kastankova, I. The effect of helper epitopes and cellular localization of an antigen on the outcome of gene gun DNA immunization. *Gene Ther.* **2014**, *21*, 225–232. [CrossRef]
51. Alexander, J.; Sidney, J.; Southwood, S.; Ruppert, J.; Oseroff, C.; Maewal, A.; Snoke, K.; Serra, H.M.; Kubo, R.T.; Sette, A.; et al. Development of high potency universal DR-restricted helper epitopes by modification of high affinity DR-blocking peptides. *Immunity* **1994**, *1*, 751–761. [CrossRef]

cancers

MDPI

Article

CD80 Expression on Tumor Cells Alters Tumor Microenvironment and Efficacy of Cancer Immunotherapy by CTLA-4 Blockade

Julie Vackova [1,2], Ingrid Polakova [1], Shweta Dilip Johari [1] and Michal Smahel [1,*]

[1] Department of Genetics and Microbiology, Faculty of Science, Charles University, BIOCEV, 252 50 Vestec, Czech Republic; julie.vackova@natur.cuni.cz (J.V.); ingrid.polakova@natur.cuni.cz (I.P.); joharis@natur.cuni.cz (S.D.J.)

[2] Department of Cell Biology, Faculty of Science, Charles University, BIOCEV, 252 50 Vestec, Czech Republic

* Correspondence: smahelm@natur.cuni.cz; Tel.: +420-325-873-921

Simple Summary: The recent discovery of immune checkpoint inhibitors constituted a breakthrough in cancer treatment, but most patients are resistant to this therapy. Although the co-stimulatory molecule cluster of differentiation (CD) 80 has been detected in several types of tumor cells, its role in the tumor microenvironment and its sensitivity to immune checkpoint blockade are unclear. We, therefore, introduced a clinically relevant mouse tumor model with deactivated CD80. The deactivation promoted a "hot" tumor microenvironment and enhanced the sensitivity to immune checkpoint blockade with antibody against the cytotoxic T-lymphocyte antigen 4 (CTLA-4). This study contributed to the research into predictive markers to select patients who are suitable for immune checkpoint blockade therapy and suggested the development of a novel cancer immunotherapy based on a tumor-cell-targeted CD80 blockade.

Abstract: Cluster of differentiation (CD) 80 is mainly expressed in immune cells but can also be found in several types of cancer cells. This molecule may either activate or inhibit immune reactions. Here, we determined the immunosuppressive role of CD80 in the tumor microenvironment by CRISPR/Cas9-mediated deactivation of the corresponding gene in the mouse oncogenic TC-1 cell line. The tumor cells with deactivated CD80 (TC-1/dCD80-1) were more immunogenic than parental cells and induced tumors that gained sensitivity to cytotoxic T-lymphocyte antigen 4 (CTLA-4) blockade, as compared with the TC-1 cells. In vivo depletion experiments showed that the deactivation of CD80 switched the pro-tumorigenic effect of macrophages observed in TC-1-induced tumors into an anti-tumorigenic effect in TC-1/dCD80-1 tumors and induced the pro-tumorigenic activity of $CD4^+$ cells. Moreover, the frequency of lymphoid and myeloid cells and the CTLA-4 expression by T helper (Th)17 cells were increased in TC-1/dCD80-1- compared with that in the TC-1-induced tumors. CTLA-4 blockade downregulated the frequencies of most immune cell types and upregulated the frequency of M2 macrophages in the TC-1 tumors, while it increased the frequency of lymphoid cells in TC-1/dCD80-1-induced tumors. Furthermore, the anti-CTLA-4 therapy enhanced the frequency of $CD8^+$ T cells as well as $CD4^+$ T cells, especially for a Th1 subset. Regulatory T cells (Treg) formed the most abundant $CD4^+$ T cell subset in untreated tumors. The anti-CTLA-4 treatment downregulated the frequency of Treg cells with limited immunosuppressive potential in the TC-1 tumors, whereas it enriched this type of Treg cells and decreased the Treg cells with high immunosuppressive potential in TC-1/dCD80-1-induced tumors. The immunosuppressive role of tumor-cell-expressed CD80 should be considered in research into biomarkers for the prediction of cancer patients' sensitivity to immune checkpoint inhibitors and for the development of a tumor-cell-specific CD80 blockade.

Keywords: CD80; CTLA-4; PD-L1; tumor-infiltrating lymphocytes; cancer; immune checkpoint blockade

Citation: Vackova, J.; Polakova, I.; Johari, S.D.; Smahel, M. CD80 Expression on Tumor Cells Alters Tumor Microenvironment and Efficacy of Cancer Immunotherapy by CTLA-4 Blockade. *Cancers* 2021, *13*, 1935. https://doi.org/10.3390/cancers13081935

Academic Editor: Peter Kern

Received: 18 March 2021
Accepted: 14 April 2021
Published: 16 April 2021

1. Introduction

The costimulatory molecule cluster of differentiation (CD) 80, which can be expressed on antigen-presenting cells (APCs) or tumor cells, interacts with both costimulatory (CD28)

and coinhibitory (cytotoxic T-lymphocyte antigen 4 (CTLA-4)) receptors and regulates the immune response [1,2]. The binding of CD28 and CTLA-4 to CD80 is competitive and regulated by several factors, such as affinity to CD80 and kinetics of CD28 and CTLA-4 expression in T cells [2]. CTLA-4 has approximately ten times higher affinity to CD80 than CD28. However, CTLA-4 is mainly expressed on activated T cells, while CD28 is expressed on T cells constitutively [3].

It has been previously reported that the expression level of CD80 may regulate the pro-/anti-oncogenic role of CD80 on tumor cells [4–6]. Low levels of CD80 expression serve as a mechanism of tumor escape from immune surveillance due to a higher affinity and, therefore, preferential binding of CTLA-4 to CD80 compared with that for CD28. On the contrary, overexpression of CD80 promotes T cell activation and tumor rejection, and a CD80 deficiency also increases the immunogenicity of tumor cells.

Furthermore, it has been shown that a soluble form of CD80 binds to programmed cell death ligand 1 (PD-L1) and inhibits the PD-1/PD-L1 axis [7]. Moreover, PD-L1 and CD80 interaction in cis, but not in trans, inhibits the immunosuppressive PD-1/PD-L1 and CTLA-4/CD80 axes [8,9]. PD-L1-blocking antibodies prevent CD80/PD-L1 interaction on tumor-associated dendritic cells (DCs) and promote the CD80-mediated anti-tumor immune response [10]. However, PD-L1 blockade may enhance CTLA-4/CD80-mediated immunosuppression in certain settings [9].

According to the dataset of The Cancer Genome Atlas (TCGA) PanCancer Atlas Studies, available at the cBioPortal (https://bit.ly/3hE21OQ, accesse on 5 March 2021; 10,953 cancer patients from 32 studies), the *CD80* gene is altered in 2% of patients, including amplifications, deletions, and mutations that may result in unfunctional CD80. A deficiency of CD28/CD80- or CD28/CD86-mediated co-stimulation induces T cell anergy or the establishment of a regulatory T cell (Treg) phenotype [11,12]. Moreover, anergic T cells can serve as precursors to the establishment of peripheral Treg cells [13,14]. Treg cells inhibit the anti-tumor immune response, enhance cancer progression, and mediate resistance to cancer therapy by several mechanisms. For instance, Treg cells secrete the immunosuppressive cytokines and cytotoxic molecules, perforin and granzymes, which target effector immune cells [15,16] and express CD39 and CD73 ectonucleotidases, which produce immunosuppressive adenosine from extracellular adenosine triphosphate (ATP), which is highly abundant in the tumor microenvironment [17,18]. In addition, some inhibitory receptors on Treg cells directly inhibit immune reactions. Surface expression of CTLA-4 is considered a key immunosuppressive mechanism of Treg cells [19]. CTLA-4 inhibits the immune response via a blockade of antigen presentation due to its higher affinity to CD80 in comparison with CD28. Treg cells also decrease the amount of CD80 on the surface of APCs by CTLA-4-mediated trans-endocytosis [20,21]. CTLA-4^{-} Treg cells had impaired immunosuppressive functions and were ineffective in the control of immune responses [22]. The direct role of the lymphocyte-activation gene 3 (Lag3) receptor in Treg immunosuppression has been reported, but this issue is still debatable [23,24].

Treg-mediated immunosuppression is tightly regulated. Inducible T cell costimulator (ICOS), glucocorticoid-induced tumor necrosis factor receptor (GITR), or neuropilin 1 (Nrp-1) induce the proliferation and effector functions of Treg cells and their tumor infiltration [25,26]. On the contrary, PD-1 signaling inhibits Treg cell effector functions. Therefore, Treg cells are activated by the blockade of the PD-1/PD-L1 axis, which may induce the hyper-progression of cancer [27,28].

Immune checkpoint inhibitors targeting the CTLA-4/CD80 or PD-1/PD-L1 axes constituted a major breakthrough in the treatment of several types of tumors, such as inoperable or metastatic melanoma and non-small-cell lung cancer (NSCLC) [29–32]. However, many patients are resistant to immune checkpoint blockade. Predictive biomarkers are, thus, necessary to distinguish patients who will benefit from this therapy [33].

Regarding the various interacting partners of CD80, with their broad range of effects on anti-tumor immune responses, the role of CD80 in the tumor microenvironment and its impact on the efficacy of cancer therapy need to be elucidated. In the present study,

we developed an experimental model of mouse tumors with functional or deactivated CD80 and compared their immunogenicity and sensitivity to immunotherapy. Tumors with CD80 deactivation were more immunogenic and prone to CTLA-4 blockade.

2. Results

2.1. CD80 Deactivation Reduced Tumor Growth

As CD80 expression on tumor cells can influence their immunogenicity, we sought to determine whether CD80 expression on TC-1 cells [34] affects tumor growth, the tumor microenvironment, and the sensitivity to immune checkpoint blockade. Therefore, we generated TC-1 cells with a deactivated CD80 molecule (TC-1/dCD80) using the CRISPR/Cas9 system. As the clones obtained after CD80 deactivation were heterogeneous in their CD80 expression, we selected three clones with apparently reduced CD80 surface expression compared with TC-1 cells (Figure 1) for an analysis of immunogenicity (Figure 2A). Deactivation of CD80 in the TC-1 cell line significantly reduced the growth of tumors induced with all three clones. While TC-1/dCD80 clone 1 (TC-1/dCD80-1) formed tumors in all inoculated mice, clones TC-1/dCD80-2 and -3 generated tumors in 80% and 60% of mice, respectively, and their growth was highly delayed. We, therefore, used the TC-1/dCD80-1 clone in our further study of the tumor microenvironment and immunotherapy response.

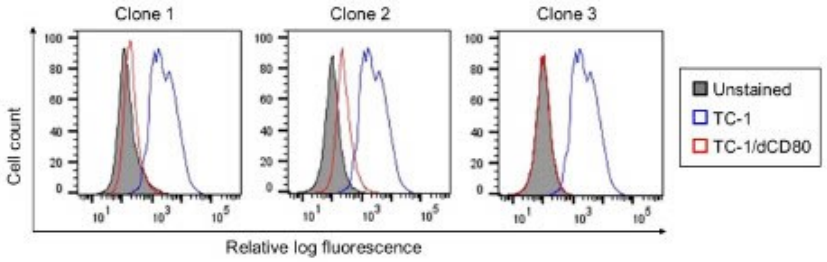

Figure 1. Flow cytometry analysis of co-stimulatory molecule cluster of differentiation (CD) 80 surface expression on the TC-1 cell line and TC-1/dCD80 clones. Unstained cells were used as the negative control.

We first tested various doses of TC-1/dCD80-1 cells to find a dose inducing tumors of a size that was comparable to the tumors induced with 3×10^4 TC-1 cells. While the growth of the TC-1/dCD80-1-induced tumors after inoculation of 3×10^4 and 1×10^5 cells was slower than that of TC-1-induced tumors, the 3×10^5 dose significantly enhanced the growth of TC-1/dCD80-1-induced tumors and provided tumors of a similar size to those induced with 3×10^4 TC-1 cells (Figure 2B).

2.2. CD80 Deactivation Altered Immune Reactions and Sensitivity to CTLA-4 Blockade

To investigate the impact of the CD80 deactivation in tumor cells on anti-tumor immune reactions, we depleted $CD4^+$, $CD8^+$, natural killer (NK) 1.1^+ cells, or macrophages in mice bearing TC-1- and TC-1/dCD80-1-induced tumors (Figure 3). The CD80 deactivation switched the pro-tumor role of macrophages observed in TC-1-induced tumors (Figure 3A) to anti-tumor abilities in TC-1/dCD80-1-induced tumors (Figure 3B). Moreover, the depletion of $CD4^+$ cells did not markedly affect the growth of TC-1-induced tumors (Figure 3A) but did reduce the growth of TC-1/dCD80-1-induced tumors (Figure 3B). $CD8^+$ cells had an anti-tumor effect regardless of CD80 expression on tumor cells. Depletion of $NK1.1^+$ cells significantly enhanced the growth of TC-1-induced tumors, whereas it did not have a significant impact on the growth of TC-1/dCD80-1-induced tumors.

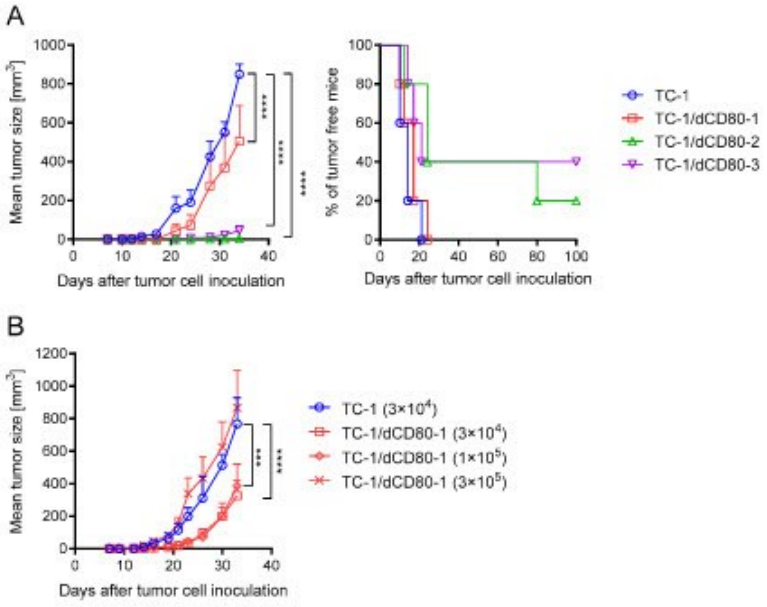

Figure 2. TC-1/dCD80 immunogenicity in comparison with TC-1 cell line. C57BL/6 mice ($n = 5$) were subcutaneously (s.c.) injected with 3×10^4 cells of three TC-1/dCD80 clones (**A**) or three different doses of the TC-1/dCD80-1 clone (**B**). In total, 3×10^4 TC-1 cells were inoculated for comparison. Tumor growth and tumor formation were evaluated. Statistical analysis indicates a comparison with TC-1 cells. Bars indicate ±standard error of mean (SEM); *** $p < 0.001$, **** $p < 0.0001$.

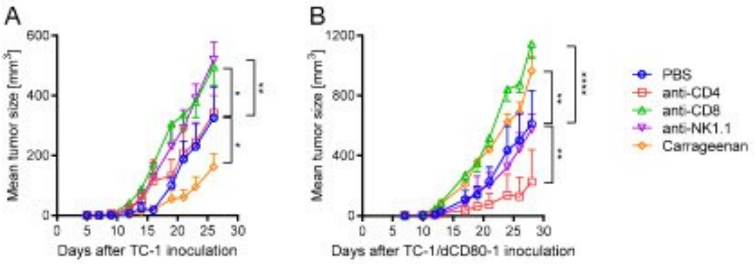

Figure 3. The role of immune cells in tumor growth. $CD4^+$, $CD8^+$, or natural killer (NK) 1.1^+ cells were depleted by monoclonal antibodies and macrophages by carrageenan in mice bearing TC-1-induced tumors (**A**) or TC-1/dCD80-1-induced tumors (**B**). Statistical analysis indicates a comparison with the phosphate-buffered saline (PBS)-treated group. Bars indicate ±SEM; * $p < 0.05$, ** $p < 0.01$, **** $p < 0.0001$.

Furthermore, we tested the efficacy of immune checkpoint blockade with anti-CTLA-4 and anti-PD-L1 antibodies in mice bearing TC-1- and TC-1/dCD80-1-induced tumors (Figure 4). Unlike the TC-1-induced tumor growth, which was negligibly reduced by anti-CTLA-4 (Figure 4A), TC-1/dCD80-1-induced tumor growth was markedly inhibited by the antibody (Figure 4B). The anti-PD-L1 antibody had no impact on either TC-1- (Figure 4A) or TC-1/dCD80-1-induced tumor growth (Figure 4B). Next, we hypothesized that the CTLA-4/CD80 axis may inhibit the effect of PD-1/PD-L1 blockade. Therefore, we simultaneously treated mice with PD-L1 and CTLA-4 blockades. However, these combined blockades did not outperform the anti-tumor effect of CTLA-4 blockade, suggesting that CTLA-4-mediated immunosuppression does not cause resistance to PD-L1 blockade.

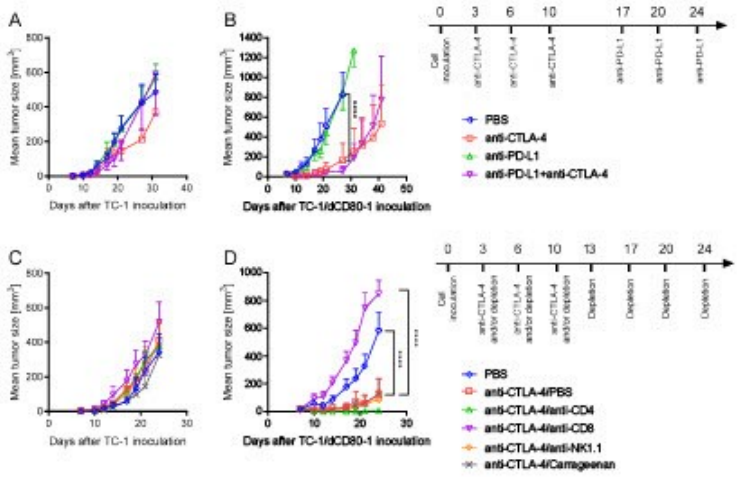

Figure 4. Immunotherapy by immune checkpoint blockade. Mice (n = 5) bearing either TC-1- (**A**) or TC-1/dCD80-1-induced tumors (**B**) were treated with anti-cytotoxic T-lymphocyte antigen 4 (CTLA-4), anti-programmed cell death ligand 1 (PD-L1), or a combination of both antibodies. The cells involved in the anti-tumor effect of CTLA-4 blockade were analyzed by depletions of $CD4^+$, $CD8^+$, $NK1.1^+$ cells, or macrophages in mice bearing TC-1-induced tumors (**C**) or TC-1/dCD80-1-induced tumors (**D**). Phosphate-buffered saline (PBS) was used as the control. Statistical analysis indicates a comparison with the anti-CTLA-4/PBS group. Bars indicate ±SEM; **** $p < 0.0001$.

To determine the immune cells involved in the therapeutic outcome of CTLA-4 blockade, we depleted $CD4^+$, $CD8^+$, $NK1.1^+$ cells, or macrophages in mice bearing TC-1- and TC-1/dCD80-1-induced tumors (Figure 4C,D). None of the depletions of immune cell subpopulations significantly influenced the growth of TC-1-induced tumors in mice treated with CTLA-4 blockade (Figure 4C). The depletion of $CD8^+$ cells abrogated the therapeutic effect of CTLA-4 blockade in TC-1/dCD80-1-induced tumors (Figure 4D). On the contrary, anti-CD4 treatment synergized with CTLA-4 blockade to reduce the growth of these tumors. The depletion of $NK1.1^+$ cells or macrophages did not influence the efficacy of CTLA-4 blockade against TC-1/dCD80-1 tumors.

2.3. CD80 Deactivation and CTLA-4 Blockade Altered Tumor Microenvironment

We next analyzed the microenvironment of TC-1- and TC-1/dCD80-1-induced tumors by flow cytometry to further characterize the immune cells that contributed to the reduced growth of tumors with deactivated CD80 and mediated the effect of immune checkpoint blockade with anti-CTLA-4 or anti-PD-L1 (Figure 5). Deactivation of CD80 in tumor cells approximately doubled the infiltration of $CD45^+$ cells, but the proportion of T lymphocytes was not substantially altered (Figure 5A). The frequency of most subpopulations of immune cells in tumors was affected by CD80 deactivation. In lymphoid cells (Figure 5B), the frequency of natural killer (NK) cells ($CD45^+$, $CD3^-$, γδ T cell receptor (TCR)$^-$, $NK1.1^+$) and natural killer T (NKT) cells ($CD45^+$, $CD3^+$, $\gamma\delta TCR^-$, $NK1.1^+$) was markedly enhanced, and the frequency of $CD4^+$ T cells ($CD45^+$, $CD3^+$, $\gamma\delta TCR^-$, $NK1.1^-$, $CD4^+$) was also increased in TC-1/dCD80-1- compared with that in TC-1-induced tumors. Similarly, the frequency of most myeloid cells was elevated in TC-1/dCD80-1- compared with that in TC-1-induced tumors (Figure 5C), such as tumor-associated macrophages (TAMs; $CD45^+$, $CD11b^+$, $Ly6G^-$, $F4/80^+$, SSC^{lo}), classical dendritic cells (cDCs; $CD45^+$, $CD11c^+$, $F4/80^-$, $Ly6C^-$, $CD317^-$), plasmacytoid dendritic cells (pDCs; $CD45^+$, $CD11c^+$, $CD11b^-$, $F4/80^-$, $Ly6C^+$, $CD317^+$), myeloid-derived suppressor cells (MDSCs; $CD45^+$, $CD11b^+$, $Ly6G^-$, $F4/80^-$, $Ly6C^{hi}$), and tumor-associated neutrophils (TANs; $CD45^+$, $CD11b^+$, $CD11c^-$, $Ly6C^{int}$, $Ly6G^+$).

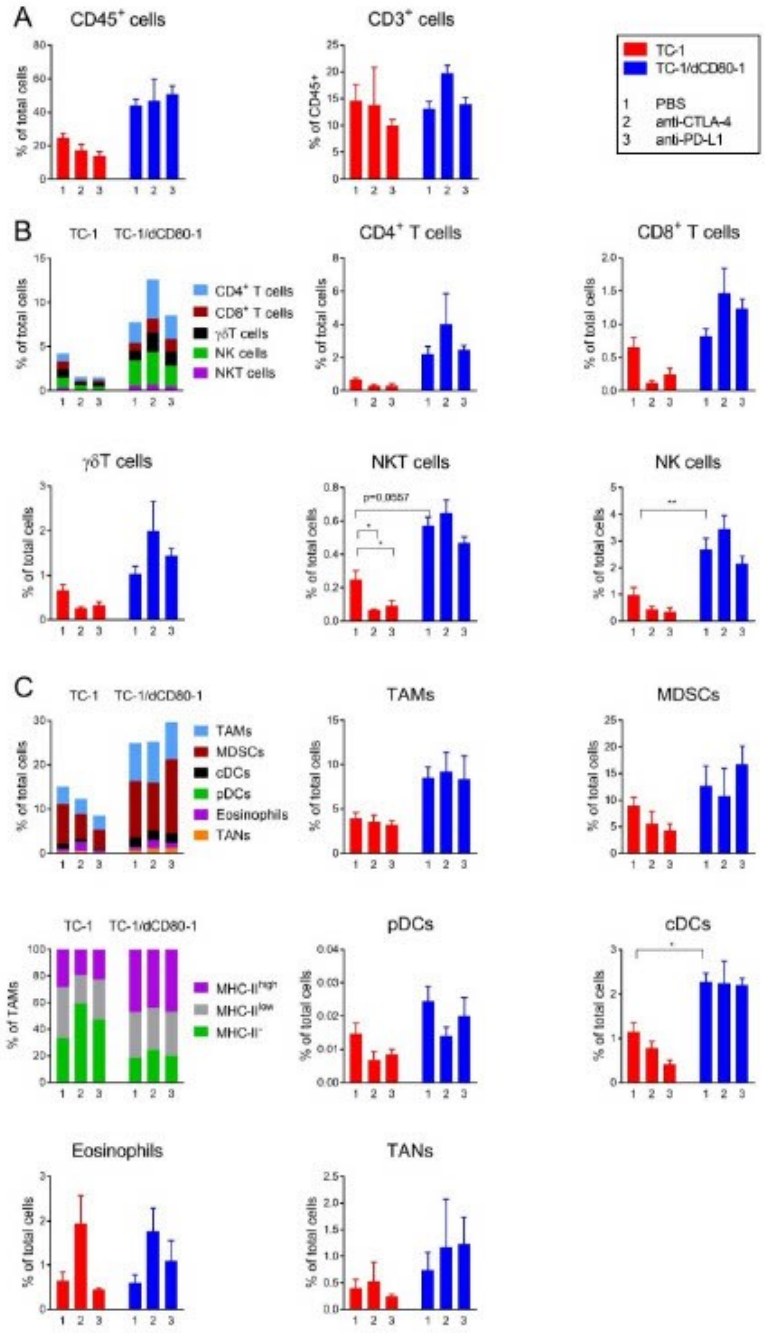

Figure 5. Flow cytometry analysis of immune cells infiltrating TC-1- and TC-1/dCD80-1-induced tumors. Mice ($n = 4$) were treated with anti-CTLA-4 or anti-PD-L1 and PBS was used as the control. The total infiltration by immune cells and the proportion of lymphocytes were determined using CD45 and CD3 markers, respectively (**A**). Cell subpopulations were stained with panels of antibodies detecting either lymphoid (**B**) or myeloid cells (**C**). Bars indicate ±SEM; * $p < 0.05$, ** $p < 0.01$.

Furthermore, CD80 deactivation affected the proportions of M1 and M2 macrophages within the TAM subpopulation, as assessed by major histocompatibility complex (MHC)-II expression (Figure 5C). The frequency of MHC-II^{hi} M1 macrophages was markedly increased, whereas the frequency of MHC-II^{-} M2 macrophages was slightly downregulated in TC-1/dCD80-1- compared with that in TC-1-induced tumors.

CTLA-4 and PD-L1 blockades considerably decreased the infiltration of most immune cells into TC-1-induced tumors, but this effect was significant only for NKT cells (Figure 5B). On the contrary, CTLA-4 blockade substantially increased the infiltration of lymphoid cells into TC-1/dCD80-1-induced tumors, such as CD4^{+} or CD8^{+} T cells, γδT cells, and NK cells, and simultaneously decreased the infiltration of pDCs. Moreover, CTLA-4 blockade enhanced the infiltration of eosinophils (CD45^{+}, CD11b^{+}, CD11c^{-}, Ly6G^{-}, SSC^{hi}) into tumors, regardless of CD80 expression on tumor cells, and increased the frequency of MHC-II^{-} M2 macrophages within the subpopulation of TAMs in TC-1-induced tumors.

PD-1 expression, a marker of immune cell activation or exhaustion, was significantly altered in some subpopulations of leucocytes after immunotherapy (Figure S1). CTLA-4 blockade enhanced PD-1 expression on γδT cells, cDCs, and eosinophils, and PD-L1 blockade achieved the same on CD4^{+} T cells in TC-1-induced tumors. Furthermore, CTLA-4 blockade significantly promoted PD-1 expression on TAMs in TC-1- as well as TC-1/dCD80-1-induced tumors. In addition, this treatment slightly downregulated PD-1 on CD8^{+} T cells in TC-1-induced tumors, whereas it had the opposite effect on TC-1/dCD80-1-induced tumors. Next, CTLA-4 blockade downregulated PD-1 on TANs, which was significant in TC-1/dCD80-1-induced tumors. PD-L1 blockade did not have a significant impact on PD-1 expression on myeloid cells.

Taken together, CD80 deactivation increased numbers of both lymphoid and myeloid cells infiltrating tumors and was associated with further enhancement of lymphoid cells after treatment with the CTLA-4 antibody.

2.4. CD80 Deactivation Resulted in Increased CTL4-4 Expression on Th17 T Cells and Enhanced Frequency of Th1 Cells in Tumors after CTLA-4 Blockade

As the above-mentioned depletion of CD4^{+} cells synergized with immunotherapy, we analyzed subsets of tumor-infiltrating CD4^{+} T cells (CD45^{+}, CD3^{+}, γδTCR^{-}, CD4^{+}; Figure 6). Treg cells (CD25^{+}, Foxp3^{+}) were the most abundant CD4^{+} T cells, while the frequency of T helper (Th)1 (IFN-γ^{+}), Th2 (IL-4^{+}), and Th17 (IL-17A^{+}) cells was relatively low in untreated tumors (Figure 6A). Therapy with anti-CTLA-4 or anti-PD-L1 downregulated all CD4^{+} T cell subsets in TC-1-induced tumors. On the contrary, immunotherapy increased the frequency of CD4^{+} T cell subsets in TC-1/dCD80-1-induced tumors, particularly CTLA-4 blockade, which markedly enhanced the frequency of Th1 cells, while the frequency of Th2, Th17, and Treg cells was slightly upregulated in these tumors. These findings indicate that the anti-tumor effect of CTLA-4 blockade in TC-1/dCD80-1-induced tumors was associated with a substantially increased frequency of Th1 cells in these tumors.

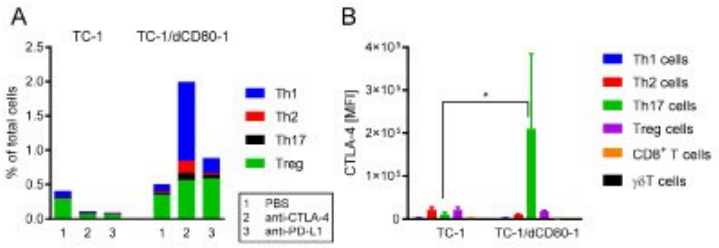

Figure 6. Flow cytometry analysis of the CD4^{+} T cell subpopulations in TC-1- and TC-1/dCD80-1-induced tumors. Tumors ($n = 4$) were treated with the anti-CTLA-4 or anti-PD-L1 antibodies and PBS was used as the control. The frequency of CD4^{+} T cell subsets (**A**) and surface expression of CTLA-4 on T cells in tumors (**B**) was evaluated. Bars indicate ± SEM; MFI—median fluorescent intensity; * $p < 0.05$.

In order to assess which T cell subsets were the main target of CTLA-4 blockade in the tumor microenvironment, we next evaluated the level of CTLA-4 expression on T cells. In non-treated tumors, CTLA-4 was mainly expressed on Th2 cells, Th17 cells, and Treg cells, whereas its expression was negligible on Th1, γδT, and $CD8^+$ T cells ($CD45^+$, $CD3^+$, $\gamma\delta TCR^-$, $CD8^+$; Figure 6B). In TC-1/dCD80-1-induced tumors, CTLA-4 expression was significantly upregulated on Th17 cells, which might be associated with the enhanced sensitivity of these tumors to CTLA-4 blockade.

2.5. CD80 Deactivation and CTLA-4 Blockade Affected Heterogeneity of Tumor-Infiltrating Treg Cells

As Treg cells were the most abundant $CD4^+$ subpopulation and their activity may critically influence the effect of immunotherapy, we analyzed the heterogeneity of Treg cells with the unsupervised clustering algorithm FlowSOM using markers of Treg cell activation and effector functions (CTLA-4, GITR, ICOS, Lag3, CD73, granzyme B (GrzB), and Nrp-1; Figure 7). We automatically generated four clusters that represent subsets of Treg cells with a distinct immunosuppressive capacity based on the intensity of expression of the respective markers—subpopulation 1 ($CTLA\text{-}4^{hi}$, $GITR^{hi}$, $ICOS^{hi}$, $Lag3^{lo}$, $CD73^-$, $GrzB^+$, $Nrp\text{-}1^{lo}$) and subpopulation 2 ($CTLA\text{-}4^{hi}$, $GITR^{hi}$, $ICOS^{hi}$, $Lag3^{lo}$, $CD73^+$, $GrzB^+$, $Nrp\text{-}1^{lo}$) with high immunosuppressive potential, and subpopulation 3 ($CTLA\text{-}4^-$, $GITR^{hi}$, $ICOS^{hi}$, $Lag3^+$, $CD73^+$, $GrzB^+$, $Nrp\text{-}1^{lo}$) and subpopulation 4 ($CTLA\text{-}4^{lo}$, $GITR^{lo}$, $ICOS^{lo}$, $Lag3^-$, $CD73^+$, $GrzB^+$, $Nrp\text{-}1^+$) with weak immunosuppressive potential—and projected the distribution of these subpopulations into t-distributed stochastic neighbor embedding (t-SNE) plots (Figure 7A). Interestingly, CD80 deactivation partially changed the distribution of Treg subpopulation 1 in the t-SNE plot, and this effect was enhanced by anti-CTLA-4 treatment. Subpopulation 2 was the most abundant phenotype within Treg cells in tumors, followed by subpopulation 3 (Figure 7B). CTLA-4 blockade significantly downregulated the frequency of Treg cells with subpopulation 3 and markedly upregulated subpopulations 2 and 4 in TC-1-induced tumors. The proportion of Treg subpopulation 3 was increased in TC-1/dCD80-1-induced tumors treated with CTLA-4 blockade, which resulted in a significant difference in this subpopulation in comparison with the TC-1-induced tumors treated with the same antibody. These data show that CD80 deactivation in tumor cells reduced the immunosuppressive potential of Treg cells after tumor treatment with CTLA-4 blockade.

Next, we evaluated the effect of CD80 deactivation in tumor cells and immune checkpoint blockade on the expression of Treg markers by the automatically generated Treg subpopulations (Figure S2). Although CD80 deactivation did not have a significant impact on the expression of most markers expressed by the Treg clusters, CD73 expression was significantly downregulated in subpopulation 2 in TC-1/dCD80-1-induced tumors compared with the same subpopulation in the TC-1-induced tumors. Immunotherapy significantly affected the expression of several markers in the Treg subsets, such as the expression of CTLA-4, GITR, CD73, and GrzB in TC-1-induced tumors and the expression of GITR in the TC-1/dCD80-1-induced tumors. These data suggest that CD80 expression in tumor cells and immune checkpoint blockade might have altered immunosuppressive potential within distinct Treg cell subsets.

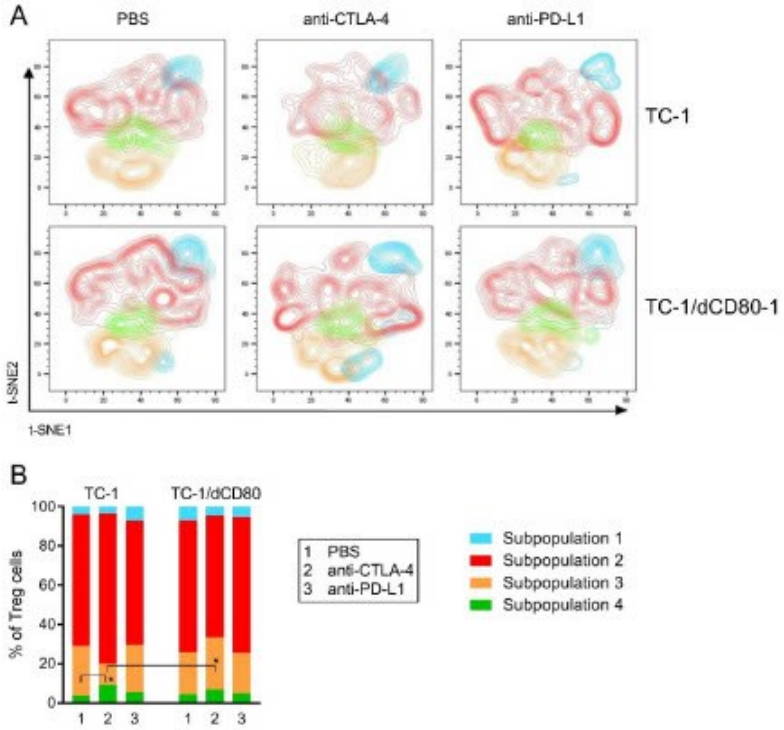

Figure 7. Diversity of Treg cells. In cells isolated from tumors (n = 4) treated with PBS, anti-CTLA-4, or anti-PD-L1, distinct Treg subpopulations were identified by the FlowSOM algorithm in the concatenate of all groups of samples and projected into t-distributed stochastic neighbor embedding (t-SNE) plots (**A**). The frequency of Treg subpopulations was statistically evaluated (**B**). * $p < 0.05$.

3. Discussion

Immune checkpoint blockade is a promising approach to cancer treatment despite its lack of efficacy in most patients. Markers for the prediction of immune checkpoint blockade efficacy are, therefore, being intensively investigated [35]. CD80 is expressed in various human tumors, such as melanoma, colon adenoma, and gastric adenocarcinoma [4,36,37], as well as in oncogenic cell lines, for instance, cell lines derived from melanoma, colorectal carcinoma, Burkitt's lymphoma, and gastrointestinal cancer [6,38]. CD80 expression has also been reported in the mouse oncogenic TC-1 cell line used in this study [34]. As CD80 may either stimulate or inhibit the immune response [1,2], we tested the role of CD80 expression on TC-1 cells in the oncogenicity and efficacy of CTLA-4 and/or PD-L1 blockades. Previously, it has been shown that CD80 silencing, as well as overexpression, in tumor cells could inhibit their oncogenicity [6]. In line with that report, CD80 deactivation in TC-1 cells reduced tumor formation and growth in our study. However, the role of CD80 may differ in various tumor types. In contrast to the aforementioned study, deactivation of CD80 expression or its neutralization by an anti-CD80 antibody has promoted the expansion of colonic neoplasia in mice and reduced T cell cytotoxicity [37].

Here, we showed that CD80 deactivation in tumor cells affected the pro-/anti-tumorigenic role of distinct immune cell populations. For instance, NK1.1$^+$ cells lost the anti-tumorigenic function in mice bearing TC-1/dCD80-1- compared with those with TC-1-induced tumors. Our data correspond to the observation of an NK cell-mediated reduction of CD80^{high} tumor growth [5]. Surprisingly, we observed that CD80 deactivation in tumor cells markedly enhanced infiltration by NK and NKT cells, although the depletion of NK1.1$^+$ cells did

not affect TC-1/dCD80-1-induced tumor growth. Next, macrophages gained an anti-tumorigenic function after CD80 deactivation in TC-1 cells, which is in agreement with the enhanced frequency of M1 macrophages in TC-1/dCD80-1-induced tumors. In line with this result, the blockade of the CTLA-4/CD80 axis with ipilimumab in melanoma patients has induced a switch in macrophage polarization from the M2 to the M1 phenotype [39]. As $CD4^+$ T cells and activated NKT cells have been reported to promote macrophage polarization into the M1 phenotype [40–42], enhanced infiltration of these cells might alter macrophage polarization in TC-1/dCD80-1-induced tumors. Furthermore, $CD4^+$ cells became pro-tumorigenic in TC-1/dCD80-1-induced tumors, while $CD8^+$ cells controlled tumor growth regardless of CD80 expression. It has been reported that $CD4^+$ T cells preferentially express CTLA-4 and, therefore, have higher immunosuppressive potential compared with that of $CD8^+$ T cells [43]. Moreover, CD80 deactivation in tumor cells promoted tumor infiltration with APCs in our model. CD28 signaling induced by APC-mediated co-stimulation has been shown to enhance CTLA-4 expression, predominantly on the Th17 cell subset [44]. In our study, the APCs in the TC-1/dCD80-1-induced tumors might enhance T cell activation and CTLA-4 expression on Th17 cells.

CTLA-4 blockade did not significantly reduce the growth of TC-1-induced tumors, while it did markedly inhibit the growth of TC-1/dCD80-1-induced tumors. Furthermore, PD-L1 blockade was ineffective as a single therapy, and it did not enhance the effect of CTLA-4 blockade in our study. However, the supportive effects of anti-CTLA-4 or anti-PD-L1 therapies on treatment with cisplatin or a synthetic fusion protein vaccine, inducing an immune response against the HPV16 E7 oncoprotein, respectively, have been previously shown in TC-1-induced tumors [45,46]. Similarly to the TC-1/dCD80-1-induced tumors, anti-CTLA-4 administered as a single therapy reduced the progression of another tumor type, i.e., mouse bladder cancer induced by the MB49 cell line with low CD80 expression [6,47].

Unlike in our study, simultaneous blockade of CTLA-4/CD80 and PD-1/PD-L1 axes has been more efficient than a single therapy in several studies [48–50]. Paradoxically, anti-PD-L1 administered as a single therapy may enhance CTLA-4/CD80-mediated immunosuppression in some patients due to the disruption of the tumor-suppressive CD80 and PD-L1 in cis interaction [9]. However, the interaction of mouse CTLA-4 with CD80 has been reported to outcompete the tumor-suppressive CD80 and PD-L1 in cis interaction [51]. This corresponds to our previous observation showing that deactivation of PD-L1 in the TC-1 cell line markedly reduced the tumorigenicity of these cells, which implies the pro-tumorigenic role of the PD-L1 molecule, rather than CD80/PD-L1-mediated tumor suppression [52]. We, therefore, assume that PD-L1 on tumor cells did not effectively control the CTLA-4/CD80 axis in TC-1- and TC-1/dCD80-1-induced tumors.

In our study, the depletion of $CD8^+$ cells abrogated the effect of CTLA-4 blockade, whereas the depletion of $CD4^+$ cells synergized with the therapy in TC-1/dCD80-1-induced tumors. This result corresponds to published data showing that the efficacy of anti-CTLA-4 treatment has been dependent on activated tumor-infiltrating $CD8^+$ T cells [53]. Moreover, distinct levels of PD-1, a marker of T cell activation, on $CD8^+$ T cells [54,55], might also support the enhanced efficacy of CTLA-4 blockade in TC-1/dCD80-1- compared with that in TC-1-induced tumors. Furthermore, we did not observe a significant impact of the depletion of $NK1.1^+$ cells or macrophages on the efficacy of CTLA-4 blockade although this treatment has been shown to induce the activation and degranulation of tumor-infiltrating NK cells [56].

CTLA-4 or PD-L1 blockade downregulated the frequency of immune cells in TC-1-induced tumors, while anti-CTLA-4 treatment upregulated the frequency of most lymphoid cells in TC-1/dCD80-1-induced tumors. Enhanced infiltration of immune cells into tumors treated with immune checkpoint inhibitors has been previously reported [57]. As the efficacy of immune checkpoint blockade is dependent on tumor-infiltrating immune cells and tumor-specific T cell responses [58], increased infiltration of TC-1/dCD80-1-induced

tumors by immune cells might contribute to the sensitivity of these tumors to anti-CTLA-4 therapy.

The $CD4^+$ T cell subsets regulate tumor growth differently [59]. Th1 cells in tumors protect the host against tumor growth, whereas Th17 and Treg cells are usually associated with progression of the disease, and Th2 cells do not correlate with clinical outcomes in many cases [59–63]. The anti-CTLA-4 treatment upregulated the frequency of Th1, Th2, Th17, and Treg cells in TC-1/dCD80-1-induced tumors. This effect was not elicited in TC-1-induced tumors. The highly increased Th1 cells probably contributed to the anti-tumor effect of CTLA-4 blockade in TC-1/dCD80-1-induced tumors. Similarly, CTLA-4 blockade has been previously reported to enrich Th1 and Th2 subsets in mouse as well as human tumors and enhance IFN-γ production by T cells [64–66].

Treg cells comprised the most abundant $CD4^+$ T cell subset in both TC-1- and TC-1/dCD80-induced tumors. Treg subpopulations 1 and 2, automatically generated by the FlowSOM software, markedly expressed CTLA-4, GITR, and ICOS molecules. High expression of CTLA-4, as well as co-stimulatory receptors GITR and ICOS, has been observed in Treg cells infiltrating mouse and human tumors [26]. CTLA-4 has been shown to be indispensable in Treg-mediated immunosuppression, as $CTLA\text{-}4^-$ Treg cells were unable to maintain self-tolerance and immune homeostasis, and Treg-specific CTLA-4 deactivation promoted anti-tumor immunity [19]. Moreover, GITR and ICOS molecules maintain Treg homeostasis, survival, and immunosuppressive functions [67–69]. Thus, we suppose that the immunosuppressive potential of subpopulations 1 and 2 was high, whereas the low CTLA-4 expression in subpopulations 3 and 4 implied limited immunosuppressive potential. Furthermore, subpopulation 4 of Treg cells was characterized by a low expression of ICOS and GITR and slightly higher Nrp-1 expression compared with that in the remaining Treg subpopulations. Similarly, Nrp-1 did not cluster with other markers in a study of the phenotypic diversity of Treg cells isolated from skin [70]. $Nrp\text{-}1^+$ Treg cells have a strong potential to infiltrate tumors in a vascular endothelial growth factor (VEGF)-dependent manner and inhibit the anti-tumor immune response [25]. As previously noted, VEGF occurs in TC-1-induced tumors [71]. However, the $ICOS^-$ Treg subset has been defined as "death prone" [67,68]. Therefore, we presume that the immunosuppressive potential of subpopulation 4 was markedly limited. Our analysis of Treg subpopulations suggests that the decreased immunosuppressive potential of Treg cells in TC-1/dCD80-1-induced tumors after CTLA-4 blockade might also contribute to the anti-tumor effect of anti-CTLA-4 therapy in these tumors.

4. Materials and Methods

4.1. Mice

Animal experiments were performed with female 6 to 8-week-old C57BL/6N mice (Charles River, Sulzfeld, Germany) that were maintained under specific pathogen-free conditions at the animal facility of the Czech Center of Phenogenomics (BIOCEV, Vestec, Czech Republic). The guidelines for the proper treatment of laboratory animals were observed.

4.2. Cells and CD80 Deactivation

The TC-1 cell line (Cellosaurus ID: CVCL_4699; provided by T.-C. Wu, John Hopkins University, Baltimore, MD, USA) was derived from C57BL/6 mouse primary lung cells by transformation with HPV16 *E6/E7* and human *H-ras* oncogenes [72].

The B7-1 Double Nickase Plasmid (m) kit (sc-419570-NIC; Santa Cruz Biotechnology, Dallas, TX, USA) was used to produce TC-1/dCD80 cell clones with deactivated CD80. The transfected cells were selected for 4 days with 6 µg/mL puromycin, which was added to the culture media 2 days after transfection. Next, cells were stained with anti-CD80-FITC (fluorescein isothiocyanate) antibody (clone 16-10A1; BD Pharmingen, San Diego, CA, USA) and single-cell clones with deactivated CD80 were selected by cell sorting into a 96-well plate using a flow cytometer FACSAria Fusion (BD Biosciences, Franklin Lakes, NJ, USA).

Deactivation of the *CD80* gene in the TC-1/dCD80-1 clone was verified by sequencing of the target site.

Cell lines were cultured in high-glucose Dulbecco's modified Eagle's medium (DMEM; Sigma-Aldrich, Merck KGaA, Darmstadt, Germany) containing 10% fetal calf serum (FCS; Biosera, Nuaille, France) and supplemented with 100 µg/mL streptomycin and 100 IU/mL penicillin (Biosera).

4.3. Animal Experiments

Tumor cells were suspended in 150 µL PBS and subcutaneously (s.c.) administered into the back of C57BL/6N mice (five per group) under anesthesia with xylazine (16 mg/kg; Bioveta, Ivanovice na Hane, Czech Republic) and ketamine (100 mg/kg; Bioveta). Tumors were measured three times a week with calipers, and tumor volume was calculated using the formula $(\pi/6)$ (a × b × c), where a, b, and c are tumor dimensions.

Animals received intraperitoneal (i.p.) treatment with anti-CTLA-4 (150 µg, clone 9D9) monoclonal antibody (Bio X Cell, West Lebanon, NH, USA) on days 3, 6, and 10 after tumor cell inoculation, or anti-PD-L1 antibody (200 µg, clone 10F.9G2) on days 17, 20, and 24 after tumor cell inoculation. For flow cytometry analysis of the tumor microenvironment, mice were treated with anti-PD-L1 on days 10, 13, and 17 after tumor cell administration.

Depletion of $CD4^+$, $CD8^+$, and $NK1.1^+$ cells in vivo was achieved by monoclonal antibodies (Bio X Cell) diluted in 200 µL PBS and injected i.p. (100 µg of anti-CD4 (clone GK1.5) with 100 µg of anti-CD8 (clone 2.43), and 100 µg of anti-NK1.1 (clone PK136)) twice a week. Macrophages were depleted by i.p. injection of 1 mg of carrageenan IV (Sigma-Aldrich, Merck KGaA) dissolved in 200 µL PBS twice a week. The initial dose of antibodies and carrageenan was administered 3 days after tumor cell inoculation. Depletion efficacy was verified by the examination of splenocytes.

4.4. Stimulation of Cells Isolated from Tumors

Single-cell suspensions were prepared from tumors as previously described [52] and stimulated prior to staining with panels of antibodies for flow cytometry analysis of the T cells. In total, 2.5×10^6 cells were cultivated for 3 hours in 2 mL of Roswell Park Memorial Institute (RPMI) 1640 medium (Sigma-Aldrich, Merck KGaA) supplemented with 10% FCS (Biosera), 100 IU/mL penicillin, 100 µg/mL streptomycin (Biosera), and 50 µM 2-mercaptoethanol and containing 81 nM phorbol 12-myristate 13-acetate, 1.34 µM ionomycin, 2 µM monensin, and 10.6 µM brefeldin A (Abcam, Cambridge, UK).

4.5. Flow Cytometry

Cells obtained from tumors were incubated with Fixable Viability Dye eFluor 455UV (eBioscience) to stain dead cells. Then, the cells were treated with anti-mouse CD16/32 (Fc block, clone 93; BioLegend) and subsequently with antibodies binding surface markers (Table 1). The washed cells were fixed and permeabilized with the Fixation/Permeabilization working solution (eBioscience, Thermo Fisher Scientific, Waltham, MA, USA). Furthermore, a working solution of the Permeabilization Buffer (eBioscience) was used to stain intracellular and nuclear markers with respective antibodies. Measurement of the stained samples was performed on LSRFortessa (BD Biosciences, San Diego, CA, USA) and CytoFLEX LX (Beckman Coulter, Indianapolis, IN, USA) flow cytometers. FlowJo™ software version 10.7 (BD Biosciences), FlowSOM version 2.6 [73], and R version 4.0.2 were used for data analysis. Gating strategies are depicted in Figures S3 and S4. The values of the parameters were as follows for the calculation of t-SNE: iterations—1000, perplexity—30, learning rate (Eta)—478, gradient algorithm—Barnes–Hut; and, for FlowSOM, number of meta clusters: 4; set seed: 3.

Table 1. Antibodies for flow cytometry.

Antigen	Conjugate	Clone	Source	Staining	Panels			
CD11b	BV421	M1/70	BioLegend	Surface		1		
CD11c	APC-Cy7	N418	BioLegend	Surface		1		
CD25	APC	PC61.5	eBiosciences	Surface	1		1	1
CD3	APC-Cy7	145-2C11	BioLegend	Surface	1		1	1
CD317	APC	927	BioLegend	Surface		1		
CD4	BV510[1]/PerCP-Cy5.5[2]	RM4-5	BioLegend	Surface	1		2	2
CD45	Alexa Fluor 700	30-F11	BioLegend	Surface	1	1	1	1
CD73	BV605	TY/11.8	BioLegend	Surface				1
CD8	FITC	53-6.7	BD Biosciences	Surface	1		1	
CTLA-4	PE/Dazzle594	UC10-4B9	BioLegend	Surface			1	1
F4/80	BV510	BM8	BioLegend	Surface		1		
Foxp3	PE	FJK-16s	eBiosciences	Nuclear	1		1	1
GITR	FITC	DTA-1	BioLegend	Surface				1
Granzyme B	PE/Cy7	NGZB	BioLegend	Intracellular			1	1
ICOS	BV650	7E.17G9	BioLegend	Surface				1
IFN-γ	BV421	XMG1.2	BioLegend	Intracellular			1	
IL-17A	BV650	TC11-18H10.1	BioLegend	Intracellular			1	
IL-4	BV786	11B11	BD Biosciences	Intracellular			1	
Lag3	BV785	C9B7W	BioLegend	Surface				1
Ly6C	BV786	HK1.4	BioLegend	Surface		1		
Ly6G	FITC	1A8	BioLegend	Surface		1		
MHC-II	PE-Cy7	114.15.2	BioLegend	Surface		1		
NK1.1	BV650	PK136	BioLegend	Surface	1			
Nrp-1	BV 421	3E12	BioLegend	Surface				1
PD-1	PE-Cy7[1]/PE[2]	29F.1A12	BioLegend	Surface	1	2		
PD-L1	PE-DAZZLE 594[1]/BV650[2]	10F.9G2	BioLegend	Surface	1	2		
TCR γ/δ	BV605	GL3	BioLegend	Surface	1		1	

[1,2]—antibody present in a panel.

4.6. Statistical Analysis

Flow cytometry analysis and animal experiments were evaluated by two-way analysis of variance and Bonferroni's post-test using Prism software, version 7 (GraphPad Software, San Diego, CA, USA). A difference of results was considered significant if $p < 0.05$.

5. Conclusions

CD80 expression on TC-1 tumor cells affected the tumor microenvironment and sensitivity to immunotherapy. CD80 deactivation in these cells was associated with a "hotter" microenvironment, decreased tumor growth, and enhanced sensitivity to CTLA-4 blockade. The impact of CD80 expression on tumor cells on the efficacy of CTLA-4 blockade has not been sufficiently investigated yet. Our study implies that CD80 expression on tumor cells should be evaluated further as a possible predictive marker that may assist clinicians in the selection of cancer patients who may be suitable for CTLA-4 blockade cancer therapy. Finally, the development of the tumor-cell-targeted CD80 blockade should be assessed as a novel immunotherapeutic approach.

Supplementary Materials: The following are available online at https://www.mdpi.com/article/10.3390/cancers13081935/s1, Figure S1: Surface expression of PD-1 by leucocytes infiltrating TC-1- and TC-1/dCD80-induced tumors. Figure S2: Expression of Treg markers on the FlowSOM-identified subpopulations 1–4. Figure S3: Gating strategy for lymphoid subpopulations. Figure S4: Gating strategy for myeloid subpopulations.

Author Contributions: Conceptualization, J.V. and M.S.; data analysis, J.V.; animal experiments, J.V., M.S., I.P., and S.D.J.; flow cytometry J.V. and I.P., writing—original draft preparation, J.V. and M.S.; writing—review and editing, M.S., I.P., S.D.J., and J.V.; supervision, M.S.; funding acquisition, M.S. and J.V. All authors have read and agreed to the published version of the manuscript.

Funding: This research was funded by Charles University, grant numbers GAUK 988218 and SVV 260568; the Czech Science Foundation, grant number GA19-00816S; the Ministry of Education, Youth and Sports of the Czech Republic (MEYS), grant number LM2018126; and the European

Regional Development Fund and MEYS, grant numbers CZ.02.1.01/0.0/0.0/16_019/0000785, and CZ.1.05/2.1.00/19.0395.

Institutional Review Board Statement: All animal experiments were conducted in compliance with Directive 2010/63/EU, and animal protocols were approved by the Sectoral Expert Committee of the Czech Academy of Sciences for Approval of Projects of Experiments on Animals (reference number 11/2019, 16 January 2019).

Informed Consent Statement: Not applicable.

Data Availability Statement: Data is contained within the article or Supplementary Material.

Acknowledgments: The authors would like to thank technicians Pavlina Vesela and Nela Vaclavikova for their technical assistance, the Imaging Methods Core Facility at BIOCEV for flow cytometry services, and the Czech Center for Phenogenomics for maintaining the mice.

Conflicts of Interest: The authors declare no conflict of interest.

References

1. Lenschow, D.J.; Su, G.H.; Zuckerman, L.A.; Nabavi, N.; Jellis, C.L.; Gray, G.S.; Miller, J.; Bluestone, J.A. Expression and Functional Significance of an Additional Ligand for CTLA-4. *Proc. Natl. Acad. Sci. USA* **1993**, *90*, 11054–11058. [CrossRef] [PubMed]
2. Sansom, D.M. CD28, CTLA-4 and their ligands: Who does what and to whom? *Immunology* **2000**, *101*, 169–177. [CrossRef] [PubMed]
3. Lindsten, T.; Lee, K.P.; Harris, E.S.; Petryniak, B.; Craighead, N.; Reynolds, P.J.; Lombard, D.B.; Freeman, G.J.; Nadler, L.M.; Gray, G.S. Characterization of CTLA-4 structure and expression on human T cells. *J. Immunol.* **1993**, *151*, 3489–3499.
4. Feng, X.-Y.; Lu, L.; Wang, K.-F.; Zhu, B.-Y.; Wen, X.-Z.; Peng, R.-Q.; Ding, Y.; Li, D.-D.; Li, J.-J.; Li, Y.; et al. Low expression of CD80 predicts for poor prognosis in patients with gastric adenocarcinoma. *Future Oncol. Lond. Engl.* **2019**, *15*, 473–483. [CrossRef]
5. Ganesan, P.L.; Alexander, S.I.; Watson, D.; Logan, G.J.; Zhang, G.Y.; Alexander, I.E. Robust anti-tumor immunity and memory in rag-1-deficient mice following adoptive transfer of cytokine-primed splenocytes and tumor CD80 expression. *Cancer Immunol. Immunother.* **2007**, *56*, 1955–1965. [CrossRef]
6. Tirapu, I.; Huarte, E.; Guiducci, C.; Arina, A.; Zaratiegui, M.; Murillo, O.; Gonzalez, A.; Berasain, C.; Berraondo, P.; Fortes, P.; et al. Low surface expression of B7-1 (CD80) is an immunoescape mechanism of colon carcinoma. *Cancer Res.* **2006**, *66*, 2442–2450. [CrossRef]
7. Ostrand-Rosenberg, S.; Horn, L.A.; Alvarez, J.A. Novel strategies for inhibiting PD-1 pathway-mediated immune suppression while simultaneously delivering activating signals to tumor-reactive T cells. *Cancer Immunol. Immunother.* **2015**, *64*, 1287–1293. [CrossRef]
8. Chaudhri, A.; Xiao, Y.; Klee, A.N.; Wang, X.; Zhu, B.; Freeman, G.J. PD-L1 binds to B7-1 only in cis on the same cell surface. *Cancer Immunol. Res.* **2018**, *6*, 921–929. [CrossRef]
9. Zhao, Y.; Lee, C.K.; Lin, C.-H.; Gassen, R.B.; Xu, X.; Huang, Z.; Xiao, C.; Bonorino, C.; Lu, L.-F.; Bui, J.D.; et al. PD-L1:CD80 cis-heterodimer triggers the co-stimulatory receptor CD28 while repressing the inhibitory PD-1 and CTLA-4 pathways. *Immunity* **2019**, *51*, 1059–1073.e9. [CrossRef]
10. Mayoux, M.; Roller, A.; Pulko, V.; Sammicheli, S.; Chen, S.; Sum, E.; Jost, C.; Fransen, M.F.; Buser, R.B.; Kowanetz, M.; et al. Dendritic cells dictate responses to PD-L1 blockade cancer immunotherapy. *Sci. Transl. Med.* **2020**, *12*. [CrossRef]
11. Liu, A.; Hu, P.; Khawli, L.A.; Epstein, A.L. B7.1/NHS76: A new costimulator fusion protein for the immunotherapy of solid tumors. *J. Immunother.* **2006**, *29*, 425–435. [CrossRef]
12. Mikami, N.; Kawakami, R.; Chen, K.Y.; Sugimoto, A.; Ohkura, N.; Sakaguchi, S. Epigenetic conversion of conventional T Cells into regulatory T cells by CD28 signal deprivation. *Proc. Natl. Acad. Sci. USA* **2020**, *117*, 12258–12268. [CrossRef] [PubMed]
13. Kalekar, L.A.; Schmiel, S.E.; Nandiwada, S.L.; Lam, W.Y.; Barsness, L.O.; Zhang, N.; Stritesky, G.L.; Malhotra, D.; Pauken, K.E.; Linehan, J.L.; et al. CD4+ T cell anergy prevents autoimmunity and generates regulatory T cell precursors. *Nat. Immunol.* **2016**, *17*, 304–314. [CrossRef] [PubMed]
14. Pletinckx, K.; Vaeth, M.; Schneider, T.; Beyersdorf, N.; Hünig, T.; Berberich-Siebelt, F.; Lutz, M.B. Immature dendritic cells convert anergic nonregulatory T Cells into Foxp3−IL-10+ regulatory T cells by engaging CD28 and CTLA-4. *Eur. J. Immunol.* **2015**, *45*, 480–491. [CrossRef]
15. Ronchetti, S.; Ricci, E.; Petrillo, M.G.; Cari, L.; Migliorati, G.; Nocentini, G.; Riccardi, C. Glucocorticoid-induced tumour necrosis factor receptor-related protein: A key marker of functional regulatory T cells. *J. Immunol. Res.* **2015**, *2015*, 171520. [CrossRef]
16. Sun, B.; Liu, M.; Cui, M.; Li, T. Granzyme b-expressing treg cells are enriched in colorectal cancer and present the potential to eliminate autologous t conventional cells. *Immunol. Lett.* **2020**, *217*, 7–14. [CrossRef]
17. Di Virgilio, F.; Sarti, A.C.; Falzoni, S.; De Marchi, E.; Adinolfi, E. Extracellular ATP and P2 purinergic signalling in the tumour microenvironment. *Nat. Rev. Cancer* **2018**, *18*, 601–618. [CrossRef] [PubMed]
18. de Leve, S.; Wirsdörfer, F.; Jendrossek, V. Targeting the immunomodulatory CD73/adenosine system to improve the therapeutic gain of radiotherapy. *Front. Immunol.* **2019**, *10*, 698. [CrossRef]

19. Wing, K.; Onishi, Y.; Prieto-Martin, P.; Yamaguchi, T.; Miyara, M.; Fehervari, Z.; Nomura, T.; Sakaguchi, S. CTLA-4 control over Foxp3+ regulatory T cell function. *Science* **2008**, *322*, 271–275. [CrossRef]
20. Hou, T.Z.; Qureshi, O.S.; Wang, C.J.; Baker, J.; Young, S.P.; Walker, L.S.K.; Sansom, D.M. A transendocytosis model of CTLA-4 function predicts its suppressive behavior on regulatory T Cells. *J. Immunol. Baltim. Md 1950* **2015**, *194*, 2148–2159. [CrossRef]
21. Sugár, I.P.; Das, J.; Jayaprakash, C.; Sealfon, S.C. Multiscale modeling of complex formation and CD80 depletion during immune synapse development. *Biophys. J.* **2017**, *112*, 997–1009. [CrossRef] [PubMed]
22. Rudd, C.E. CTLA-4 co-receptor impacts on the function of treg and CD8+ T-cell subsets. *Eur. J. Immunol.* **2009**, *39*, 687–690. [CrossRef] [PubMed]
23. Huang, C.-T.; Workman, C.J.; Flies, D.; Pan, X.; Marson, A.L.; Zhou, G.; Hipkiss, E.L.; Ravi, S.; Kowalski, J.; Levitsky, H.I.; et al. Role of LAG-3 in regulatory T cells. *Immunity* **2004**, *21*, 503–513. [CrossRef] [PubMed]
24. Maruhashi, T.; Sugiura, D.; Okazaki, I.; Okazaki, T. LAG-3: From molecular functions to clinical applications. *J. Immunother. Cancer* **2020**, *8*, e001014. [CrossRef]
25. Hansen, W.; Hutzler, M.; Abel, S.; Alter, C.; Stockmann, C.; Kliche, S.; Albert, J.; Sparwasser, T.; Sakaguchi, S.; Westendorf, A.M.; et al. Neuropilin 1 deficiency on CD4+Foxp3+ regulatory t cells impairs mouse melanoma growth. *J. Exp. Med.* **2012**, *209*, 2001–2016. [CrossRef] [PubMed]
26. Arce Vargas, F.; Furness, A.J.S.; Litchfield, K.; Joshi, K.; Rosenthal, R.; Ghorani, E.; Solomon, I.; Lesko, M.H.; Ruef, N.; Roddie, C.; et al. Fc effector function contributes to the activity of human anti-CTLA-4 antibodies. *Cancer Cell* **2018**, *33*, 649–663.e4. [CrossRef] [PubMed]
27. Kamada, T.; Togashi, Y.; Tay, C.; Ha, D.; Sasaki, A.; Nakamura, Y.; Sato, E.; Fukuoka, S.; Tada, Y.; Tanaka, A.; et al. PD-1+ regulatory t cells amplified by PD-1 blockade promote hyperprogression of cancer. *Proc. Natl. Acad. Sci. USA* **2019**, *116*, 9999–10008. [CrossRef]
28. Tan, C.L.; Kuchroo, J.R.; Sage, P.T.; Liang, D.; Francisco, L.M.; Buck, J.; Thaker, Y.R.; Zhang, Q.; McArdel, S.L.; Juneja, V.R.; et al. PD-1 restraint of regulatory T cell suppressive activity is critical for immune tolerance. *J. Exp. Med.* **2021**, *218*, e20182232. [CrossRef]
29. Cameron, F.; Whiteside, G.; Perry, C. Ipilimumab. *Drugs* **2011**, *71*, 1093–1104. [CrossRef]
30. Kwok, G.; Yau, T.C.C.; Chiu, J.W.; Tse, E.; Kwong, Y.-L. Pembrolizumab (Keytruda). *Hum. Vaccines Immunother.* **2016**, *12*, 2777–2789. [CrossRef]
31. Ribas, A.; Wolchok, J.D. Cancer immunotherapy using checkpoint blockade. *Science* **2018**, *359*, 1350–1355. [CrossRef]
32. Sul, J.; Blumenthal, G.M.; Jiang, X.; He, K.; Keegan, P.; Pazdur, R. FDA approval summary: Pembrolizumab for the treatment of patients with metastatic non-small cell lung cancer whose tumors express programmed death-ligand 1. *Oncologist* **2016**, *21*, 643–650. [CrossRef]
33. Barrueto, L.; Caminero, F.; Cash, L.; Makris, C.; Lamichhane, P.; Deshmukh, R.R. Resistance to checkpoint inhibition in cancer immunotherapy. *Transl. Oncol.* **2020**, *13*, 100738. [CrossRef]
34. Janousková, O.; Síma, P.; Kunke, D. Combined suicide gene and immunostimulatory gene therapy using AAV-mediated gene transfer to HPV-16 transformed mouse cell: Decrease of oncogenicity and induction of protection. *Int. J. Oncol.* **2003**, *22*, 569–577. [CrossRef]
35. Bodor, J.N.; Boumber, Y.; Borghaei, H. Biomarkers for immune checkpoint inhibition in non-small cell lung cancer (NSCLC). *Cancer* **2020**, *126*, 260–270. [CrossRef]
36. Bernsen, M.R.; Håkansson, L.; Gustafsson, B.; Krysander, L.; Rettrup, B.; Ruiter, D.; Håkansson, A. On the biological relevance of MHC Class II and B7 expression by tumour cells in melanoma metastases. *Br. J. Cancer* **2003**, *88*, 424–431. [CrossRef]
37. Marchiori, C.; Scarpa, M.; Kotsafti, A.; Morgan, S.; Fassan, M.; Guzzardo, V.; Porzionato, A.; Angriman, I.; Ruffolo, C.; Sut, S.; et al. Epithelial CD80 promotes immune surveillance of colonic preneoplastic lesions and its expression is increased by oxidative stress through STAT3 in colon cancer cells. *J. Exp. Clin. Cancer Res.* **2019**, *38*, 190. [CrossRef] [PubMed]
38. Li, J.; Yang, Y.; Inoue, H.; Mori, M.; Akiyoshi, T. The expression of costimulatory molecules CD80 and CD86 in human carcinoma cell lines: Its regulation by interferon γ and interleukin-10. *Cancer Immunol. Immunother.* **1996**, *43*, 213–219. [CrossRef]
39. Madonna, G.; Ballesteros-Merino, C.; Feng, Z.; Bifulco, C.; Capone, M.; Giannarelli, D.; Mallardo, D.; Simeone, E.; Grimaldi, A.M.; Caracò, C.; et al. PD-L1 Expression with immune-infiltrate evaluation and outcome prediction in melanoma patients treated with ipilimumab. *OncoImmunology* **2018**, *7*, e1405206. [CrossRef]
40. Bogen, B.; Fauskanger, M.; Haabeth, O.A.; Tveita, A. CD4+ T Cells indirectly kill tumor cells via induction of cytotoxic macrophages in mouse models. *Cancer Immunol. Immunother.* **2019**, *68*, 1865–1873. [CrossRef]
41. Eisel, D.; Das, K.; Dickes, E.; König, R.; Osen, W.; Eichmüller, S.B. Cognate interaction with CD4+ T cells instructs tumor-associated macrophages to acquire m1-like phenotype. *Front. Immunol.* **2019**, *10*, 219. [CrossRef] [PubMed]
42. Paul, S.; Chhatar, S.; Mishra, A.; Lal, G. Natural killer T cell activation increases INOS+CD206- M1 macrophage and controls the growth of solid tumor. *J. Immunother. Cancer* **2019**, *7*, 208. [CrossRef] [PubMed]
43. Chan, D.V.; Gibson, H.M.; Aufiero, B.M.; Wilson, A.J.; Hafner, M.S.; Mi, Q.-S.; Wong, H.K. Differential CTLA-4 expression in human CD4+ versus CD8+ T cells is associated with increased NFAT1 and inhibition of CD4+ proliferation. *Genes Immun.* **2014**, *15*, 25–32. [CrossRef] [PubMed]
44. Krummey, S.M.; Hartigan, C.R.; Liu, D.; Ford, M.L. CD28-dependent CTLA-4 expression fine-tunes the activation of human Th17 cells. *iScience* **2020**, *23*, 100912. [CrossRef]

45. Beyranvand Nejad, E.; van der Sluis, T.C.; van Duikeren, S.; Yagita, H.; Janssen, G.M.; van Veelen, P.A.; Melief, C.J.M.; van der Burg, S.H.; Arens, R. Tumor eradication by cisplatin is sustained by CD80/86-mediated costimulation of CD8+ T cells. *Cancer Res.* **2016**, *76*, 6017–6029. [CrossRef]
46. Liu, Z.; Zhou, H.; Wang, W.; Fu, Y.-X.; Zhu, M. A Novel dendritic cell targeting HPV16 E7 synthetic vaccine in combination with PD-L1 blockade elicits therapeutic antitumor immunity in mice. *Oncoimmunology* **2016**, *5*, e1147641. [CrossRef]
47. van Hooren, L.; Sandin, L.C.; Moskalev, I.; Ellmark, P.; Dimberg, A.; Black, P.; Tötterman, T.H.; Mangsbo, S.M. Local checkpoint inhibition of CTLA-4 as a monotherapy or in combination with anti-PD1 prevents the growth of murine bladder cancer. *Eur. J. Immunol.* **2017**, *47*, 385–393. [CrossRef]
48. Fiegle, E.; Doleschel, D.; Koletnik, S.; Rix, A.; Weiskirchen, R.; Borkham-Kamphorst, E.; Kiessling, F.; Lederle, W. Dual CTLA-4 and PD-L1 blockade inhibits tumor growth and liver metastasis in a highly aggressive orthotopic mouse model of colon cancer. *Neoplasia* **2019**, *21*, 932–944. [CrossRef]
49. Baweja, A.; Mar, N. Metastatic penile squamous cell carcinoma with dramatic response to combined checkpoint blockade with ipilimumab and nivolumab. *J. Oncol. Pharm. Pract.* **2021**, *27*, 212–215. [CrossRef]
50. Parikh, N.D.; Marshall, A.; Betts, K.A.; Song, J.; Zhao, J.; Yuan, M.; Wu, A.; Huff, K.D.; Kim, R. Network meta-analysis of nivolumab plus ipilimumab in the second-line setting for advanced hepatocellular carcinoma. *J. Comp. Eff. Res.* **2021**. [CrossRef]
51. Garrett-Thomson, S.C.; Massimi, A.; Fedorov, E.V.; Bonanno, J.B.; Scandiuzzi, L.; Hillerich, B.; Iii, R.D.S.; Love, J.D.; Garforth, S.J.; Guha, C.; et al. Mechanistic dissection of the PD-L1:B7-1 co-inhibitory immune complex. *PLoS ONE* **2020**, *15*, e0233578. [CrossRef]
52. Vackova, J.; Piatakova, A.; Polakova, I.; Smahel, M. Abrogation of IFN-γ signaling may not worsen sensitivity to PD-1/PD-L1 blockade. *Int. J. Mol. Sci.* **2020**, *21*, 1806. [CrossRef]
53. Spranger, S.; Koblish, H.K.; Horton, B.; Scherle, P.A.; Newton, R.; Gajewski, T.F. Mechanism of tumor rejection with doublets of CTLA-4, PD-1/PD-L1, or IDO blockade involves restored IL-2 production and proliferation of CD8+ T cells directly within the tumor microenvironment. *J. Immunother. Cancer* **2014**, *2*, 3. [CrossRef]
54. Ahn, E.; Araki, K.; Hashimoto, M.; Li, W.; Riley, J.L.; Cheung, J.; Sharpe, A.H.; Freeman, G.J.; Irving, B.A.; Ahmed, R. Role of PD-1 during effector CD8 T cell differentiation. *Proc. Natl. Acad. Sci. USA* **2018**, *115*, 4749–4754. [CrossRef]
55. Siddiqui, I.; Schaeuble, K.; Chennupati, V.; Fuertes Marraco, S.A.; Calderon-Copete, S.; Pais Ferreira, D.; Carmona, S.J.; Scarpellino, L.; Gfeller, D.; Pradervand, S.; et al. Intratumoral Tcf1+PD-1+CD8+ T cells with stem-like properties promote tumor control in response to vaccination and checkpoint blockade immunotherapy. *Immunity* **2019**, *50*, 195–211.e10. [CrossRef]
56. Sanseviero, E.; O'Brien, E.M.; Karras, J.R.; Shabaneh, T.B.; Aksoy, B.A.; Xu, W.; Zheng, C.; Yin, X.; Xu, X.; Karakousis, G.C.; et al. Anti-CTLA-4 activates intratumoral NK cells and combined with IL15/IL15Rα complexes enhances tumor control. *Cancer Immunol. Res.* **2019**, *7*, 1371–1380. [CrossRef] [PubMed]
57. Liu, X.; Hogg, G.D.; DeNardo, D.G. Rethinking Immune checkpoint blockade: Beyond the T cell. *J. Immunother. Cancer* **2021**, *9*, e001460. [CrossRef]
58. Galon, J.; Bruni, D. Approaches to treat immune hot, altered and cold tumours with combination immunotherapies. *Nat. Rev. Drug Discov.* **2019**, *18*, 197–218. [CrossRef]
59. Tosolini, M.; Kirilovsky, A.; Mlecnik, B.; Fredriksen, T.; Mauger, S.; Bindea, G.; Berger, A.; Bruneval, P.; Fridman, W.-H.; Pagès, F.; et al. Clinical impact of different classes of infiltrating t cytotoxic and helper cells (Th1, Th2, Treg, Th17) in patients with colorectal cancer. *Cancer Res.* **2011**, *71*, 1263–1271. [CrossRef]
60. De Simone, V.; Franzè, E.; Ronchetti, G.; Colantoni, A.; Fantini, M.C.; Di Fusco, D.; Sica, G.S.; Sileri, P.; MacDonald, T.T.; Pallone, F.; et al. Th17-type cytokines, IL-6 and TNF-α synergistically activate STAT3 and NF-KB to promote colorectal cancer cell growth. *Oncogene* **2015**, *34*, 3493–3503. [CrossRef]
61. Kaewkangsadan, V.; Verma, C.; Eremin, J.M.; Cowley, G.; Ilyas, M.; Eremin, O. Crucial contributions by t lymphocytes (effector, regulatory, and checkpoint inhibitor) and cytokines (TH1, TH2, and TH17) to a pathological complete response induced by neoadjuvant chemotherapy in women with breast cancer. *J. Immunol. Res.* **2016**, *2016*, 4757405. [CrossRef]
62. Ohue, Y.; Nishikawa, H. Regulatory T (Treg) cells in cancer: Can treg cells be a new therapeutic target? *Cancer Sci.* **2019**, *110*, 2080–2089. [CrossRef]
63. Liu, D.; Xing, S.; Wang, W.; Huang, X.; Lin, H.; Chen, Y.; Lan, K.; Chen, L.; Luo, F.; Qin, S.; et al. Prognostic value of serum soluble interleukin-23 receptor and related T-helper 17 cell cytokines in non-small cell lung carcinoma. *Cancer Sci.* **2020**, *111*, 1093–1102. [CrossRef]
64. Walunas, T.L.; Bluestone, J.A. CTLA-4 Regulates tolerance induction and t cell differentiation in vivo. *J. Immunol.* **1998**, *160*, 3855–3860. [PubMed]
65. Gao, J.; Shi, L.Z.; Zhao, H.; Chen, J.; Xiong, L.; He, Q.; Chen, T.; Roszik, J.; Bernatchez, C.; Woodman, S.E.; et al. Loss of IFN-γ pathway genes in tumor cells as a mechanism of resistance to anti-CTLA-4 therapy. *Cell* **2016**, *167*, 397–404.e9. [CrossRef]
66. Wei, S.C.; Levine, J.H.; Cogdill, A.P.; Zhao, Y.; Anang, N.-A.A.S.; Andrews, M.C.; Sharma, P.; Wang, J.; Wargo, J.A.; Pe'er, D.; et al. Distinct cellular mechanisms underlie anti-CTLA-4 and anti-PD-1 checkpoint blockade. *Cell* **2017**, *170*, 1120–1133.e17. [CrossRef]
67. Zhang, M.; Wu, Y.; Bastian, D.; Iamsawat, S.; Chang, J.; Daenthanasanmak, A.; Nguyen, H.D.; Schutt, S.; Dai, M.; Chen, F.; et al. Inducible T-cell co-stimulator impacts chronic graft-versus-host disease by regulating both pathogenic and regulatory t cells. *Front. Immunol.* **2018**, *9*, 1461. [CrossRef]

68. Li, D.-Y.; Xiong, X.-Z. ICOS+ tregs: A functional subset of tregs in immune diseases. *Front. Immunol.* **2020**, *11*, 2104. [CrossRef] [PubMed]
69. Ricco, M.L.; Ronin, E.; Collares, D.; Divoux, J.; Grégoire, S.; Wajant, H.; Gomes, T.; Grinberg-Bleyer, Y.; Baud, V.; Marodon, G.; et al. Tumor necrosis factor receptor family costimulation increases regulatory T-cell activation and function via NF-KB. *Eur. J. Immunol.* **2020**, *50*, 972–985. [CrossRef]
70. Ikebuchi, R.; Fujimoto, M.; Nakanishi, Y.; Okuyama, H.; Moriya, T.; Kusumoto, Y.; Tomura, M. Functional phenotypic diversity of regulatory T cells remaining in inflamed skin. *Front. Immunol.* **2019**, *10*, 1098. [CrossRef]
71. Predina, J.; Eruslanov, E.; Judy, B.; Kapoor, V.; Cheng, G.; Wang, L.-C.; Sun, J.; Moon, E.K.; Fridlender, Z.G.; Albelda, S.; et al. Changes in the local tumor microenvironment in recurrent cancers may explain the failure of vaccines after surgery. *Proc. Natl. Acad. Sci. USA* **2013**, *110*, E415–E424. [CrossRef]
72. Lin, K.-Y.; Guarnieri, F.G.; Staveley-O'Carroll, K.F.; Levitsky, H.I.; August, J.T.; Pardoll, D.M.; Wu, T.-C. Treatment of established tumors with a novel vaccine that enhances major histocompatibility class II presentation of tumor antigen. *Cancer Res.* **1996**, *56*, 21–26. [PubMed]
73. Van Gassen, S.; Callebaut, B.; Van Helden, M.J.; Lambrecht, B.N.; Demeester, P.; Dhaene, T.; Saeys, Y. FlowSOM: Using self-organizing maps for visualization and interpretation of cytometry data. *Cytol. J. Int. Soc. Anal. Cytol.* **2015**, *87*, 636–645. [CrossRef] [PubMed]

International Journal of
Molecular Sciences

MDPI

Article

Experimental Combined Immunotherapy of Tumours with Major Histocompatibility Complex Class I Downregulation

Adrianna Grzelak, Ingrid Polakova, Jana Smahelova, Julie Vackova, Lucie Pekarcikova, Ruth Tachezy and Michal Smahel *

Department of Genetics and Microbiology, Faculty of Science, Charles University, BIOCEV, 25250 Vestec, Czech Republic; grzelaka@natur.cuni.cz (A.G.); ingrid.polakova@natur.cuni.cz (I.P.); smahelovaj@natur.cuni.cz (J.S.); julie.vackova@natur.cuni.cz (J.V.); lucie.pekarcikova@natur.cuni.cz (L.P.); tachezr@natur.cuni.cz (R.T.)

* Correspondence: smahelm@natur.cuni.cz; Tel.: +420-325 873 921

Received: 12 October 2018; Accepted: 17 November 2018; Published: 21 November 2018

Abstract: Combined immunotherapy constitutes a novel, advanced strategy in cancer treatment. In this study, we investigated immunotherapy in the mouse TC-1/A9 model of human papillomavirus type 16 (HPV16)-associated tumors characterized by major histocompatibility complex class I (MHC-I) downregulation. We found that the induction of a significant anti-tumor response required a combination of DNA vaccination with the administration of an adjuvant, either the synthetic oligodeoxynucleotide ODN1826, carrying immunostimulatory CpG motifs, or α-galactosylceramide (α-GalCer). The most profound anti-tumor effect was achieved when these adjuvants were applied in a mix with a one-week delay relative to DNA immunization. Combined immunotherapy induced tumor infiltration with various subsets of immune cells contributing to tumor regression, of which cluster of differentiation (CD) 8^+ T cells were the predominant subpopulation. In contrast, the numbers of tumor-associated macrophages (TAMs) were not markedly increased after immunotherapy but in vivo and in vitro results showed that they could be repolarized to an anti-tumor M1 phenotype. A blockade of T cell immunoglobulin and mucin-domain containing-3 (Tim-3) immune checkpoint had a negligible effect on anti-tumor immunity and TAMs repolarization. Our results demonstrate a benefit of combined immunotherapy comprising the activation of both adaptive and innate immunity in the treatment of tumors with reduced MHC-I expression.

Keywords: MHC-I; cancer immunotherapy; DNA immunization; CpG ODN; α-galactosylceramide; tumor-associated macrophages

1. Introduction

With the advent of immunotherapy, new prospects have been opened up for successful cancer treatment. Increasing evidence shows that the efficacy of immunotherapeutic drugs can be enhanced by combined applications, which are believed to support the anti-tumor response at multiple sites [1,2]. Further advances include optimization of immunotherapy timing as well as deeper investigation and better understanding of tumor microenvironment biology [2].

It is well established that cluster of differentiation (CD) 8^+ cytotoxic T lymphocytes (CTLs) are the main anti-tumor effectors that are able to kill cancer cells in terms of their binding with the major histocompatibility complex class I (MHC-I) molecules presenting antigenic peptides on a tumor-cell surface. As MHC-I downregulation is a mechanism widely used by tumor cells to avoid the recognition by T cells and finally escape the immune surveillance [3], upregulation of MHC-I cell-surface expression has recently been proclaimed the critical step to improve response to cancer immunotherapy [4].

DNA vaccines constitute an attractive immunotherapeutic tool since they are stable, safe and reproducible; they also involve low-cost production and easy modification of an antigen. Although low immunogenicity is the major obstacle that limits large-scale application of DNA immunization [5], the potency of these vaccines can be enhanced by adjuvants, for example, ligands for Toll-like receptors (TLRs) [6]. Synthetic oligodeoxynucleotides (ODNs) carrying unmethylated immunostimulatory CpG motifs and levamisole (LMS) can activate TLR-9 and TLR-2, respectively, which leads to the enhancement of T helper 1 (Th1) immune response and stimulation of antigen presenting cells (APC) [7,8]. Another compound with strong adjuvant activity is α-galactosylceramide (α-GalCer) binding specifically to the CD1d protein present on APCs. These cells subsequently activate invariant natural killer T (iNKT) cells [9]. Through the production of vast amounts of cytokines of both Th1 pro-inflammatory (e.g., interferon γ; IFN-γ, or tumor necrosis factor α; TNF-α) and Th2 anti-inflammatory (e.g., interleukins (IL), such as IL-4, IL-10 and IL-13) responses followed by downstream activation of natural killer (NK) cells, B cells, dendritic cells (DCs) and conventional T cells, iNKT cells bridge the innate and adaptive immunity and affect both MHC-I positive and negative tumor cells, which are the targets for CTL and NK cell lysis, respectively. This is an especially attractive approach for elimination of heterogeneous tumor cells with respect to the MHC-I variability [10].

T cell immunoglobulin and mucin-domain containing-3 (Tim-3) was initially identified as a molecule expressed on the differentiated Th1 cells [11]. The results on preclinical cancer models have revealed that Tim-3 acts as an immune checkpoint receptor whose expression on dysfunctional $CD8^+$ T cells and regulatory T lymphocytes (Tregs) attenuates the Th1 response [12]. Moreover, dysregulation of Tim-3 expression is not limited to T cells, as ample evidence shows that it affects functionality of innate immunity cells, including NK cells, DCs, mast cells and macrophages (MΦs) [13], thus making Tim-3 a suitable candidate for cancer immunotherapy [12].

MΦs are the most abundant tumor infiltrating cells that can represent up to 50% of tumor cell mass and their presence at the tumor site is associated with poor prognosis in the major types of solid tumors [14]. Regarding the anti-tumor immunity, classically activated MΦs (M1) are considered advantageous due to their ability to eliminate tumor cells. This type of MΦs produce pro-inflammatory cytokines, such as IL-12 and TNF-α and the free radical NO, a product of inducible nitric oxide synthase (iNOS) [15]. As the tumor progresses, M1-like MΦs may change their functional phenotype to the alternatively activated tumor-promoting M2 profile associated with the increased Tim-3 expression [16]. Furthermore, expression of high levels of arginase 1 is the hallmark of M2 MΦs [15]. This enzyme competes with iNOS for the common substrate-arginine-and directs metabolism of this amino acid to the production of ornithine, a precursor of collagen [17]. Tumor-associated macrophages (TAMs) mostly resemble the M2 phenotype in already established tumors [18] and promote tumor growth and metastasis [19]. Therefore, an increasing attention is paid to the strategies that affect TAMs in order to increase the efficacy of anti-tumor therapies, for example, by inhibition of MΦ infiltration and their survival in the tumor microenvironment or by blocking pro-tumorigenic activity of TAMs [20]. Moreover, repolarization of M2-like TAMs to the tumoricidal M1 phenotype by modulating the tumor microenvironment has recently attracted much interest [19] because MΦs utilize different mechanisms of tumor-cell killing than T cells and can act when CTL-mediated killing is not evoked or tumor cells are resistant to the CTL activity [21,22]. Indeed, it has been demonstrated in various murine tumor models that upon proper stimulation, MΦs can perform tumoristatic activities both in vitro and in vivo [23–27].

Based on these findings, we investigated a combined immunotherapy that stimulated both adaptive immunity (via DNA immunization) and innate immunity (by administration of TLRs agonists or α-GalCer) in the murine TC-1/A9 tumor model characterized by downregulated MHC-I expression. We also aimed to inhibit immunosuppression by blocking the Tim-3 receptor. Combined immunotherapy reduced the growth of tumors resistant to single therapeutics. In this effect, $CD8^+$ T cells, $NK1.1^+$ cells and MΦs were involved but the contribution of Tim-3 blockade was marginal.

2. Results

2.1. ODN1826 and α-GalCer Are Effective Vaccine Adjuvants for DNA Immunization against Tumors with Reduced Expression of MHC Class I Molecules

In initial experiments, mice were immunized with the pBSC/PADRE.E7GGG plasmid by a gene gun 3, 6 and 10 days after inoculation of TC-1/A9 cells. Systemic activation of innate immunity with ODN1585, LMS, ODN1826, or α-GalCer as well as inhibition of immunosuppression by antibody against Tim-3 were performed on the same days as DNA immunization. In accordance with the previous study, DNA vaccination against the E7 oncoprotein did not affect the growth of TC-1/A9-induced tumors. Moreover, the efficacy of DNA immunization was not improved after administration of Tim-3 blockade. A significant tumor growth retardation in immunized mice was found when either ODN1826 or α-GalCer were administered (Figure S1). Blockade of Tim-3 resulted in enhanced anti-tumor response only in mice treated with immunization and α-GalCer ($p < 0.05$, 31 days after inoculation of tumor cells). Additionally, in two immunized mice treated with either ODN1826 or α-GalCer, the tumor did not develop or completely regressed.

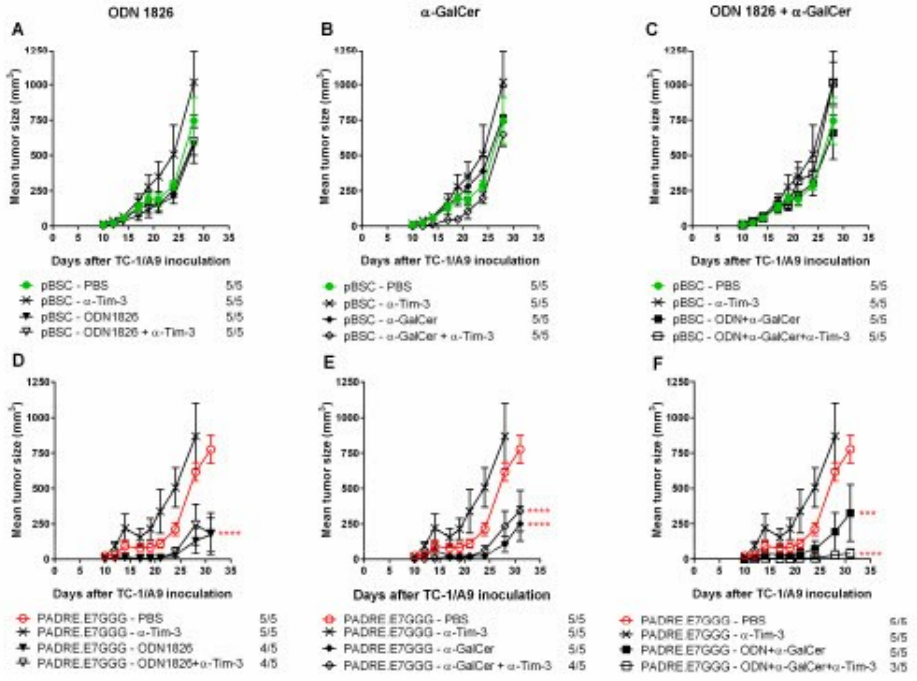

Figure 1. Comparison of the anti-tumor effects induced after the administration of CpG ODN1826 and α-GalCer either alone or in a mix in the non-immunized and immunized mice. Animals ($n = 5$) were injected s.c. with TC-1/A9 cells and immunized 3 times by a gene gun with either the empty pBSC plasmid (referred to as non-immunized mice, **A–C**) or pBSC/PADRE.E7GGG (immunized mice, **D–F**). Vaccine adjuvants ODN1826 (**A**,**D**), α-GalCer (**B**,**E**), or a mix of ODN1826 and α-GalCer (**C**,**F**) were administered on the same days as DNA vaccines. Some groups received a monoclonal antibody against Tim-3. No. of mice with a tumor/no. of mice in the group is indicated. Bars: ±SEM; *** $p < 0.001$, **** $p < 0.0001$. Statistical significance refers to the comparison with the group immunized with the *PADRE.E7GGG* gene. The experiment was repeated with similar results.

As we demonstrated the significant adjuvant effect only for ODN1826 and α-GalCer, we focused on these two compounds in subsequent experiments. At first, we asked whether these two immunostimulators can exert an anti-tumor response in non-immunized mice (Figure 1A–C).

Simultaneously, we evaluated the combination of ODN1826 and α-GalCer (Figure 1C,F). This experiment confirmed the adjuvant efficacy of ODN1826 (Figure 1D) and α-GalCer (Figure 1E) in immunized mice but the combination of these two adjuvants did not further enhance the suppression of tumor growth. Moreover, co-administration of antibody against Tim-3 significantly supported the anti-tumor effect solely in ODN1826 and α-GalCer mixture, resulting in inhibition of tumor growth in 2 out of 5 mice in the group. In non-immunized mice, ODN1826, α-GalCer and anti-Tim-3, neither alone nor in any combination, induced the inhibition of tumor growth.

These data showed that DNA immunization against the E7 oncoprotein was indispensable for combined immunotherapy of tumors with downregulated expression of MHC-I molecules and that combination of two adjuvants, ODN1826 and α-GalCer, did not induce stronger anti-tumor response than single adjuvants.

2.2. Delayed Administration of ODN1826 and α-GalCer in Combination Promoted Inhibition of Tumor Growth

In spite of the substantial efficacy of combined immunotherapy against TC-1/A9 cells, most mice still developed a tumor. Therefore, we also tested modifications in the number and timing of doses. To this end, we compared previously used injection of the ODN1826 plus α-GalCer mixture (supplemented with anti-Tim-3 in some groups) on days of immunization (i.e., 3 doses delivered 3, 6 and 10 days after inoculation of tumor cells, Figure 2A) with injection of 5 doses on days 3, 6, 10, 13 and 17 (Figure 2B) and 3 doses on days 10, 13 and 17 (Figure 2C). Application of two additional doses enhanced the anti-tumor response in comparison to three doses on days of DNA immunization but even higher improvement was achieved with three doses delayed by one week in comparison with the original schedule. After postponing the administration of immunostimulatory compounds, a portion of initially developed tumors partially regressed until day 24 but they subsequently progressed in all mice. Co-administration of anti-Tim-3 did not improve the anti-tumor effect in any group. In summary, the highest efficacy of the adjuvants was achieved when administered one week after DNA immunization.

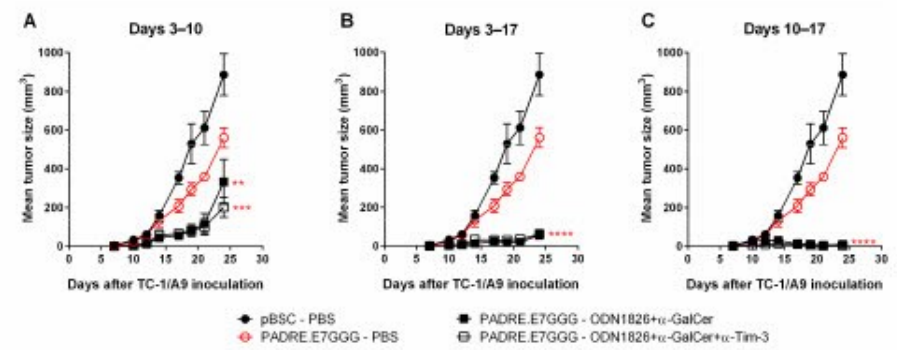

Figure 2. The effects of different dosage and timing protocols. Mice ($n = 5$) were injected with TC-1/A9 cells and immunized by a gene gun. Mice received combinations of ODN1826, α-GalCer and α-Tim-3 3 times on the days of immunization (**A**), 5 times with two additional doses on days 13 and 17 (**B**) and 3 times with a one-week delay following DNA immunization (i.e., on days 10, 13 and 17) (**C**). Bars: ±SEM; ** $p < 0.01$, *** $p < 0.001$, **** $p < 0.0001$. Statistical significance refers to the comparison with the group immunized with the *PADRE.E7GGG* gene. The experiment was repeated with similar results.

2.3. Immunotherapy Induced Infiltration of Tumors with Various Immune Cells that Differently Affected Tumor Growth

To find cells with anti-tumor activity, we first studied infiltration of tumors with immune cells by flow cytometry using two panels of antibodies identifying the main subpopulations of lymphoid and myeloid cells. We isolated cells from the tumors of the treated mice 14–18 days after inoculation of

TC-1/A9 cells, because in this period tumor growth was slowed down and tumors partially regressed in some mice. In the tumors of non-treated mice analyzed 12 days after tumor-cell inoculation, $CD45^+$ cells constituted about 5% of total live cells (Figure 3A). After DNA immunization, the numbers of these cells approximately doubled and further increase was recorded when ODN1826 or α-GalCer were administered on days of DNA immunization. A mix of ODN1826 and α-GalCer did not outperform the effect of single adjuvants. $CD3^+$ cells constituted about 20% of $CD45^+$ cells in non-treated mice, almost 40% in DNA-immunized mice and approximately 60% in mice receiving combined immunotherapy (Figure 3A). Antibody against Tim-3 influenced neither infiltration of $CD45^+$ cells nor a proportion of $CD3^+$ cells.

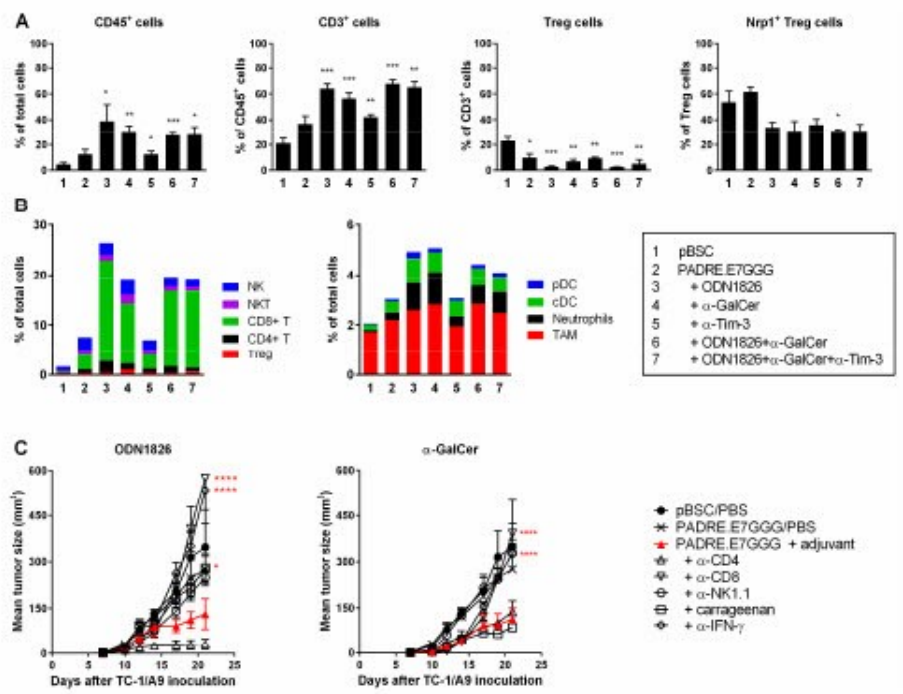

Figure 3. Tumor-infiltrating immune cells and their role in tumor growth. Analysis of tumor-infiltrating cells was performed by flow cytometry (**A**,**B**). Mice (n = 4) were injected with tumor cells and immunized by a gene gun. Vaccine adjuvants and anti-Tim-3 were administered on the same days as the DNA vaccines. Tumor cells were isolated on day 12 from non-treated tumors and on days 14–18 from treated tumors and stained with fluorochrome-labeled antibodies. (**A**) Frequencies of $CD45^+$ and $CD3^+$ cells, Treg ($CD4^+CD25^+Foxp3^+$) and $Nrp1^+$ Treg cells. Statistical significance refers to the comparison with the non-treated (pBSC) group. (**B**) Overview of the mean percentages of the major subpopulations of tumor-infiltrating cells in total cells. (**C**) The effect of in vivo depletion of immune cells and neutralization of IFN-γ on the anti-tumor response induced by immunotherapies with ODN1826 or α-GalCer in the immunized mice (n = 5). Vaccine adjuvants were injected on the days of immunization. Statistical significance refers to the comparison with the group that was immunized with the *PADRE.E7GGG* gene and received an adjuvant. Bars: ±SEM; * $p < 0.05$, ** $p < 0.01$, *** $p < 0.001$, **** $p < 0.0001$.

In non-treated tumors, the population of $CD45^+$ cells comprised particularly TAMs (defined as $CD11b^+F4/80^+Gr1^{-/low}$) and NK cells ($CD3^-NK1.1^+$) (Figure 3B). After DNA immunization, all of the detected subpopulations were increased and this increase was enhanced after co-administration of ODN1826 or α-GalCer. $CD8^+$ T cells were the predominant subpopulation of infiltrating cells in treated tumors, especially after combined immunotherapy. Of the myeloid cells ($CD3^-$), TAMs

were the most abundant but the highest increase was found for neutrophils ($CD11b^+F4/80^-Gr1^{high}$) and classical DCs (cDC; $CD11c^+F4/80^-Gr1^-MHC\text{-}II^+$). Increase in plasmacytoid DCs (pDC; $CD11c^+Gr1^{-/low}F4/80^-CD11b^-CD317^+$) was observed as well.

Intratumoral regulatory T cells (Treg; $CD4^+CD25^+Foxp3^+$) were also increased after immunotherapy (Figure 3B) but the proportion of Tregs in $CD3^+$ cells was reduced from approximately 20% in non-treated tumors up to 3% in tumors treated with DNA immunization and ODN1826 (Figure 3A). As neuropilin 1 (Nrp1) has been identified as a critical factor for the stability of Treg cells and their suppression of anti-tumor immunity [28] we tested Nrp1 expression on Tregs. While in tumors of non-treated and DNA-immunized mice, about 60% of Tregs expressed Nrp1, after combined immunotherapy, Nrp1 expression was decreased to about 40% (Figure 3A).

To further investigate the mechanisms underlying the anti-tumor efficacy of ODN1826 or α-GalCer in the immunized mice that were injected with TC-1/A9 tumor cells, we depleted in vivo $CD4^+$, $CD8^+$, or $NK1.1^+$ cells with monoclonal antibodies and MΦs by administration of carrageenan. Furthermore, we performed IFN-γ neutralization with monoclonal antibody. After administration of ODN1826, depletion of $CD8^+$ cells and neutralization of IFN-γ completely abolished the anti-tumor effect of combined immunotherapy and inoculation of carrageenan and anti-NK1.1 partially restored tumor growth. On the contrary, antibody depletion of $CD4^+$ cells increased the anti-tumor response. In mice treated with DNA immunization and α-GalCer, antibodies against CD8, NK1.1 and IFN-γ induced tumor growth but carrageenan and anti-CD4 did not have a marked effect (Figure 3C).

In summary, after combined immunotherapy, TC-1/A9-induced tumors were increasingly infiltrated with various immune cells. $CD8^+$ cells, $NK1.1^+$ cells and IFN-γ contributed to the anti-tumor effect of both ODN1826 and α-GalCer but MΦs reduced tumor growth only after administration of ODN1826 and this adjuvant stimulated also immunosuppressive $CD4^+$ cells.

2.4. Combined Immunotherapy Did Not Substantially Enhance Either Systemic or Intratumoral Activation of $CD8^+$ Cells

As $CD8^+$ T lymphocytes were the predominant cells that infiltrated tumors after combined immunotherapy, we tested their systemic activation by an ELISPOT assay detecting the IFN-γ production in mononuclear cells isolated from spleens of non-tumor-bearing mice. For this testing, we applied the immunization schedules used in our previous immunotherapeutic experiments. Mononuclear splenocytes were activated with either the $E7_{49-57}$ peptide carrying the immunodominant $H\text{-}2D^b$-restricted epitope that activates $CD8^+$ T cells specific for the human papillomavirus type 16 (HPV16) E7 oncoprotein or the PADRE peptide representing a universal helper epitope activating $CD4^+$ T cells (Figure 4A). Immunization of mice with the empty pBSC plasmid served as a negative control and restimulation of mononuclear splenocytes from these mice with either peptide did not result in their activation to produce IFN-γ. A significant induction of both E7-and PADRE-specific reactions was observed when mice received the PADRE.E7GGG DNA vaccine. Administration of ODN1826 on days of DNA immunization augmented the PADRE-specific immunity about three times but this strong activation resulted in only slight stimulation of the response of $CD8^+$ T cells. α-GalCer did not promote activation of either $CD4^+$ or $CD8^+$ T cells (it rather slightly reduced stimulation of the E7-specific response). Activation of $CD8^+$ cells induced by DNA immunization was not also enhanced by combined immunotherapy that included antibody against Tim-3 and/or a mix of ODN1826 and α-GalCer or by one-week-delayed administration of adjuvants.

Next, we evaluated the functional state of $CD8^+$ T cells in tumors by flow cytometry determining the production of IFN-γ and TNF-α cytokines and the expression of PD-1 and Tim-3 immune checkpoints. While in non-treated mice, the expression of IFN-γ and TNF-α in $CD8^+$ T cells was negligible, both cytokines were increased after immunotherapy (reaching at least 3% and 1% positive cells, respectively; Figure 4B) but this increase was relatively low. The mean expression of PD-1 and Tim-3 in non-treated mice was about 35% and 8%, respectively and it was significantly increased up to

about 80% and 60% after immunotherapy, respectively (Figure 4B). Tim-3 blockade slightly reduced upregulation of these checkpoints.

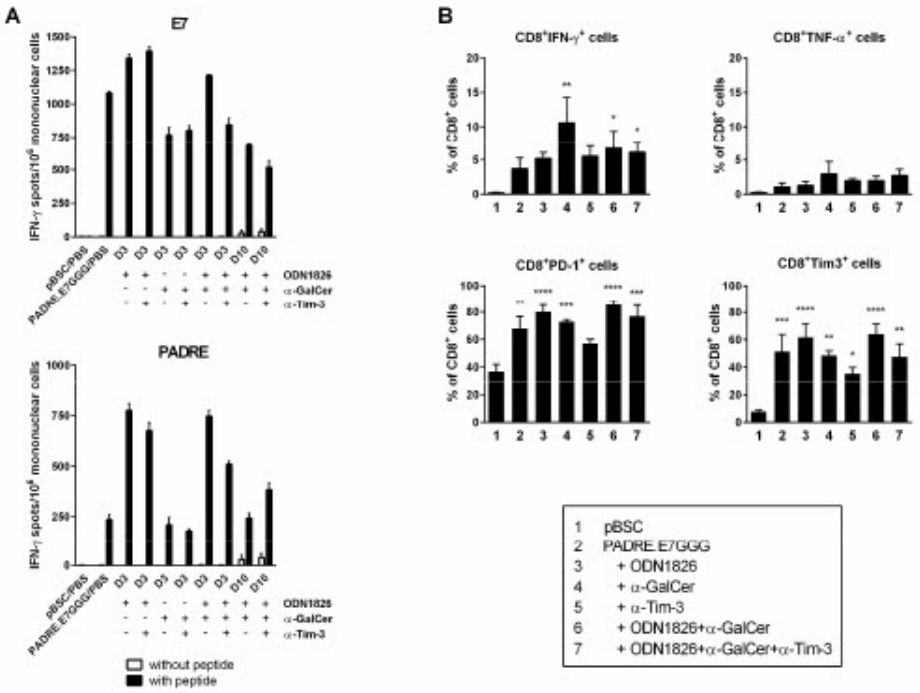

Figure 4. Activation of CD8+ T cells by combined immunotherapy and characterization of tumor-infiltrating CD8+ T cells. (**A**) Analysis of activated CD8+ cells by an ELISPOT assay. Mice ($n = 3$) were immunized by a gene gun on days 3, 6 and 10 and inoculated with ODN1826, α-GalCer and anti-Tim-3 on the days of immunization (D3) or with a one-week delay following DNA immunization (D10). Eight days after the last immunization, mononuclear cells were prepared from pooled splenocytes, restimulated with peptides and IFN-γ-producing-cells were detected. Columns, mean of triplicate samples; bars, ± SEM. The experiment was repeated with similar results. (**B**) Analysis of intratumoral CD8+ T cells by flow cytometry. The experiment was performed as in Figure 3. Columns, mean of four samples; bars, ± SEM; * $p < 0.05$, ** $p < 0.01$, *** $p < 0.001$, **** $p < 0.001$. Statistical significance refers to the comparison with the non-treated (pBSC) group.

These data also show that activation of specific CD8+ T cells induced by DNA immunization was not further significantly enhanced by adjuvants. High expression of immune checkpoints on intratumoral CD8+ lymphocytes after immunotherapy could be responsible for their relatively low expression of IFN-γ and TNF-α.

2.5. Immunotherapy Induced Polarization of TAMs into M1 MΦs

We monitored polarization of TAMs by staining of MHC-II molecules that are used as a marker of M1 MΦs. In flow cytometry analysis of TAMs, we distinguished cells with low and high MHC-II expression (Figure 5A). In tumors of non-treated mice, the proportion of M2 MΦs was more than 60% (Figure 5B). After DNA immunization, we found about 20% of M2 MΦs and their proportion further decreased after the addition of ODN1826 and/or α-GalCer. iNOS and TNF-α are other markers of M1 MΦs [29]. However, iNOS expression was significantly increased only in the group with the strongest M1 polarization, that is, after DNA immunization accompanied by ODN1826 administration (Figure 5C) and TNF-α expression was not enhanced after immunotherapy. TNF-α was produced by

about 40–50% of TAMs but in tumors treated with DNA immunization and ODN1826 or anti-Tim-3, its expression was significantly reduced to 30–35% (Figure 5C). Tim-3 blockade did not markedly promote M1 polarization, although the Tim-3 receptor was expressed on about 30% of TAMs in non-treated tumors and this expression was significantly augmented to 60–85% after administration of ODN1826 and/or α-GalCer.

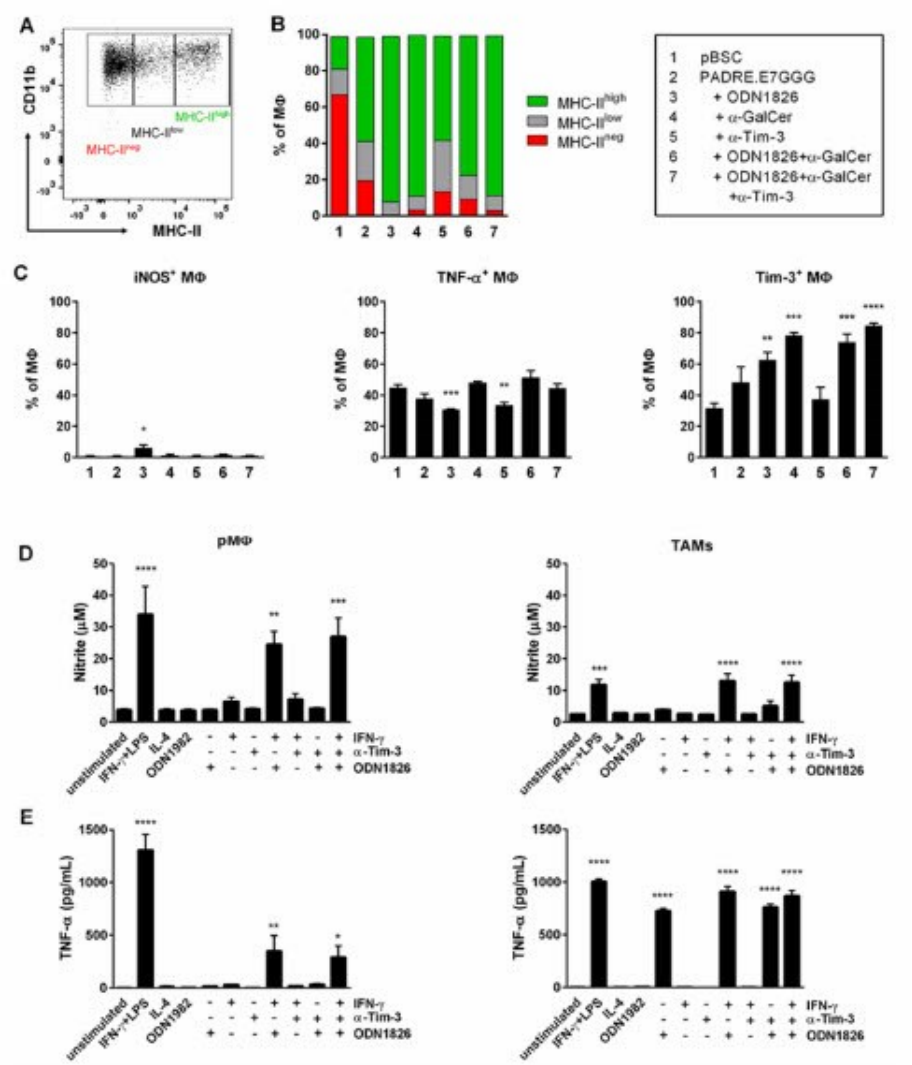

Figure 5. Characterization of TAMs. After immunotherapy, TAMs were isolated from tumors and analyzed by flow cytometry. The experiment was performed as in Figure 3. (**A**) Gating of an MHC-II marker. (**B**) Overview of mean percentages of TAM subpopulations distinguished by MHC-II expression. (**C**) Frequencies of iNOS$^+$, TNF-α$^+$ and Tim-3$^+$ MΦs; columns, mean of four samples. TAMs were also isolated from non-treated tumors and stimulated in vitro. The nitrite (**D**) and TNF-α (**E**) concentrations were measured in the supernatants by Griess reagent and ELISA test, respectively. pMΦs were used for comparison. Columns, mean of 3 independent experiments. Bars, ± SEM; * $p < 0.05$, ** $p < 0.01$, *** $p < 0.001$, **** $p < 0.0001$. Statistical significance refers to the comparison with the non-treated (pBSC)/unstimulated group.

To study the effect of ODN1826 on MΦs, in vitro stimulations of TAMs and peritoneal MΦs (pMΦs) were performed. pMΦs are one of the best-studied MΦ populations. They are characterized by plasticity that allows them to acquire specific phenotypes upon stimulation with different cytokines. The isolated pMΦs and TAMs were stimulated in vitro with ODN1982, ODN1826, IFN-γ and anti-Tim-3 to investigate polarization to the anti-tumor M1 phenotype. We hoped to elucidate the function of Tim-3 in this polarization as Tim-3 was shown to be expressed on the surface of elicited pMΦs from C56BL/6 mice [30]. For analysis of MΦ stimulation, we used enzymatic activity of iNOS and TNF-α production. Incubation with IFN-γ together with lipopolysaccharide (LPS; a positive control for M1 polarization) and with IFN-γ+ODN1826 led to the induction of iNOS expression (Figure 5D) and secretion of TNF-α (Figure 5E) in both TAMs and pMΦs. ODN1826 alone induced production of TNF-α and slight activation of iNOS but only in TAMs. Blockade of Tim-3, stimulation with IL-4 (used as a positive control for M2 polarization), or incubation with the control ODN1982 did not influence activation of any M1 marker.

To summarize, these data show that TAMs were polarized in vivo into M1 MΦs after combined immunotherapy. Both TAMs and pMΦs from naïve mice were polarized to the M1 phenotype upon in vitro stimulation with the combination of ODN1826 and IFN-γ but ODN1826 alone significantly induced only TNF-α production in TAMs. Tim-3 blockade did not influence M1 polarization.

2.6. Co-Culture of TAMs with TC-1/A9 Tumor Cells Enhanced iNOS and Arginase Activity

Expression of iNOS and arginase are hallmarks of M1 and M2 phenotypes, respectively [29]. In fact, little is known about the modulation of activity of both enzymes with respect to the interaction of TAMs with tumor cells. To address this question, we performed co-culture experiments, where TAMs isolated from TC-1/A9-induced tumors were cultured in vitro with TC-1/A9 cells in stimulation variants comprising IFN-γ, a TLR agonist (LPS or ODN1826) and anti-Tim-3, followed by measurement of nitrite and urea concentrations (Figure 6), which are the reaction products of iNOS and arginase, respectively. Stimulation of co-cultures with IFN-γ+LPS and IFN-γ+ODN1826 resulted in further enhancement of nitrite production in comparison to the production of this iNOS metabolite in TAMs alone (Figure 6A). Moreover, co-culture of tumor cells with TAMs stimulated with either IFN-γ or ODN1826 significantly induced iNOS activity, while slight increase of nitrite production was detected in TAMs stimulated alone. Blockade of Tim-3 in the co-cultures, either alone or in combination with ODN1826 or IFN-γ, did not affect iNOS activity. Nitrite concentration in co-cultures upon stimulation with IL-4 or control ODN1982 remained unchanged with respect to TAMs alone. These results indicate that TC-1/A9 cells promoted the iNOS induction in TAMs activated by IFN-γ or ODN1826.

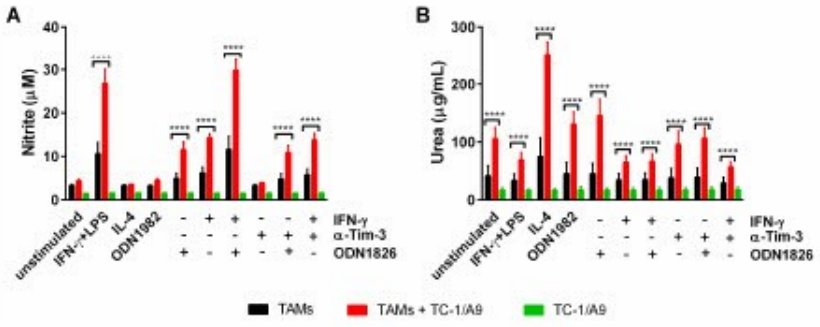

Figure 6. In vitro modulation of iNOS and arginase activity in the co-culture of TAMs with TC-1/A9 cells. Co-cultures as well as control cells, i.e., TAMs and TC-1/A9 cells alone, were stimulated for 44 h. The nitrite concentration was determined by Griess reagent (**A**) and urea was quantified by the microplate method (**B**). Columns, mean of three independent experiments; bars ± SEM; **** $p < 0.0001$. Statistical significance refers to the comparison of co-cultures with TAMs alone.

In TAMs isolated from the TC-1/A9-induced tumors, urea production was only augmented after stimulation with IL-4 (Figure 6B, $p < 0.05$), a classical activator of the M2 phenotype. This effect was markedly enhanced by co-culture of TAMs with TC-1/A9 tumor cells (Figure 6B). The co-culture alone significantly enhanced urea production in TAMs and after stimulation of co-cultures with ODN1826, further enhancement was recorded. IFN-γ inhibited the stimulatory activity of co-culture. Blockade of Tim-3 did not affect the arginase activity in co-cultures. The urea background in TC-1/A9 cells was lower than in TAMs and was not influenced by any stimulation. In summary, co-culture alone stimulated arginase in TAMs. While IL-4 promoted this effect, IFN-γ reduced arginase activity.

2.7. Enhancement of IFN–γ Expression in Tumors Correlated with Induction of Ido1 Expression

Next, we analyzed immune reactions in the tumor microenvironment by RT-qPCR. As we induced only temporary inhibition of tumor growth by combined immunotherapy, we supposed that immunosuppressive mechanisms outperformed antitumor immunity during tumor development. Therefore, we focused this analysis on the expression of some genes that could be associated with immunosuppression, namely *Tgfb1* and *Il10* producing cytokines TGF-β1 and IL-10, respectively, *Foxp3* that is activated in Treg cells, *Ido1* and *Arg1* encoding enzymes indoleamine 2,3-dioxygenase 1 (IDO1) and arginase 1, respectively and *Ncf1* coding for the p47(phox) subunit of the inducible NADPH oxidase type 2 (NOX2) produced in myeloid derived suppressor cells (MDSC) and Treg cells. The expression of *Ifng* encoding IFN-γ was also tested. The highest induction of expression after immunotherapy was found for *Ido1* and *Ifng* (Figure 7). Despite high variability, the expression of these two genes significantly correlated (Figure 7). The expression was also increased for *Il10* and *Foxp3* but when compared with the pBSC-treated group by multiple comparisons, no significant difference was observed. These data suggest that IFN-γ induced by immunotherapy initiated not only activation of anti-tumor reactions but also immunosuppression that was mediated particularly by IDO1 in the tumor microenvironment.

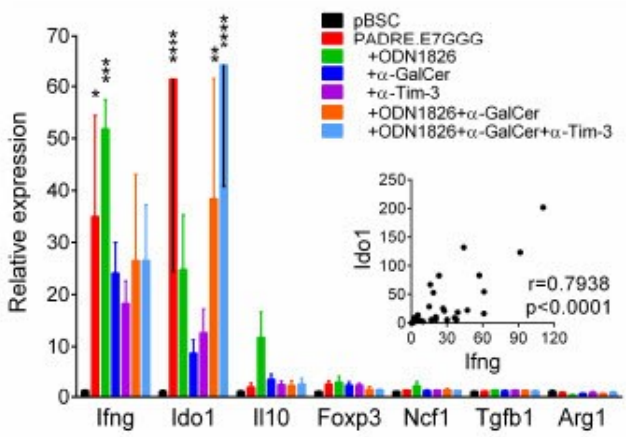

Figure 7. Analysis of gene expression in tumors by RT-qPCR. The experiment was performed as in Figure 3. Columns, mean of 4–6 samples; bars, ± SEM; * $p < 0.05$, ** $p < 0.01$, *** $p < 0.001$, **** $p < 0.0001$. Relative expression and statistical significance refer to the comparisons with the non-treated (pBSC) group. The inserted graph shows the correlation between *Ifng* and *Ido1* expression.

3. Discussion

It is increasingly evident that highly efficient cancer immunotherapy must include activation of both adaptive and innate immunity accompanied by the inhibition of immunosuppressive mechanisms [31–33]. In this study, combined immunotherapy was designed to target tumors induced by subcutaneous (s.c.) injection of mouse oncogenic TC-1/A9 cells, characterized by reversible

downregulation of MHC-I molecules. Since, in our previous studies, we had demonstrated that TC-1/A9- induced tumors were poorly sensitive to DNA vaccination against the E7 oncoprotein [34] and in tumors developed from parental TC-1 tumor cells, the effect of DNA immunization was markedly enhanced by systemic delivery of ODN1826 or LMS [35], we tested these immunostimulatory drugs against MHC-I-deficient TC-1/A9 cells in this study. Moreover, as we identified a substantial proportion of NK and NKT cells in immune cells infiltrating TC-1-induced tumors [36], we also evaluated the effect of ODN1585 used for the activation of NK cells and α-GalCer inducing NKT cells.

After the initial screening of four immunostimulatory drugs combined with DNA immunization, we performed our next experiments with the two most efficient compounds, ODN1826 and α-GalCer. As their primary target cells are different—TLR-9-expressing cells, mainly MΦs, DCs and NK cells for ODN1826 and iNKT cells for α-GalCer—we hoped for their possible synergistic or additive effect. We found that both ODN1826 and α-GalCer had to be combined with DNA immunization for the induction of anti-tumor effect. Reinis et al. demonstrated the anti-tumor effect of monotherapy with immunostimulatory drugs against TC-1/A9 cells but they applied ODN1826 or ODN1585 intratumorally [37] or administered β-GalCer intraperitoneally (i.p.) in different dosage and timing protocols [38]. A mix of ODN1826 and α-GalCer did not promote DNA immunization more efficiently than single adjuvants. Only when the number of adjuvant doses was increased from three to five or when three adjuvant doses were administered with a one-week delay after DNA immunization, tumor growth was further inhibited but this reduction was transient. The delayed delivery of adjuvants probably enables activation of adaptive immunity induced by DNA vaccination that subsequently cooperates with innate immunity stimulated by adjuvants [38]. This enhancement is similar to the impact of delayed PD-1/PD-L1 blockade [36,39].

Given that most cells infiltrating TC-1 tumors are M2-polarized MΦs [40] that produce the Tim-3 receptor (our unpublished result), we included the Tim-3 blockade into our combined immunotherapy in order to support the activity of adjuvants in M1 polarization of TAMs. As this polarization into the anti-tumorigenic phenotype could substantially contribute to the anti-tumor effect irrespective of MHC-I expression on tumor cells, this study focused on repolarization of TAMs and their involvement in anti-tumor immunity in this study. However, we found only weak and inconsistent effect of anti-Tim-3 treatment on anti-tumor response. Moreover, flow cytometric and functional in vitro analysis of TAMs did not show any benefit of Tim-3 blockade for M1 polarization and anti-tumor stimulation of TAMs.

In an attempt to detect cells and mechanisms contributing to temporary tumor regression, we analyzed the tumor microenvironment during this period. In comparison with non-treated mice, all detected populations of lymphoid and myeloid cells were increased after DNA immunization. Following the addition of ODN1826 and/or α-GalCer, $CD8^+$ T cells in particular were further increased. When we tested the systemic activation of E7-specific $CD8^+$ T cells by DNA immunization, we found a weak enhancement induced by ODN1826 but α-GalCer rather reduced this response, which corresponded to results obtained after the combination of α-GalCer administration with DNA vaccination against *Trypanosoma cruzi* trans-sialidase surface antigen [41]. Repeated administration of α-GalCer could be responsible for the impairment of immunity induced by a DNA vaccine [42].

In vivo depletion and neutralization showed an involvement of $CD8^+$ T cells, $NK1.1^+$ cells and IFN-γ in anti-tumor immunity induced by both ODN1826 and α-GalCer. However, TAMs were only necessary for the anti-tumor effect elicited by ODN1826 stimulation. Which cells directly killed tumor cells is doubtful. Despite MHC-I downregulation in oncogenic TC-1/A9 cells, these cells could be a target for $CD8^+$ T cells because MHC-I expression has been upregulated in vivo [34]. However, Bercovici and Trautmann challenged the idea that the main function of $CD8^+$ T cells in tumor regression is direct tumor cell killing [43]. Instead, they proposed a role of MΦs and neutrophils in this process and supported their suggestion experimentally in the TC-1 tumor model [27]. In that study, they showed a dynamic cooperation between $CD8^+$ T cells and myeloid cells in the microenvironment of regressing tumors and demonstrated killing of tumor cells by TAMs via TNF-α production and

phagocytosis. Similar results showing cooperation between $CD8^+$ T cells and TAMs and a critical role of TAMs in elimination of TC-1-induced tumors were also observed in another study after vaccination with peptides [44].

Further flow cytometric analysis of $CD8^+$ T cells from regressing tumors showed increased production of IFN-γ and TNF-α after immunotherapy but only in a small portion of cells and no difference was found between DNA immunization and combined immunotherapy. Increased PD-1 expression suggests that most cells were activated by immunotherapy but as the majority of these cells also expressed Tim-3, they were probably exhausted [45]. Additionally, other immunosuppression mechanisms may have outweighed the induced anti-tumor reactions, such as PD-L1 and IDO1 expression (found by RT-qPCR analysis) that may have been induced by IFN-γ elicited by immunotherapy.

In parallel to the in vivo experiments, we tested the in vitro activation of MΦs by ODN1826, anti-Tim-3 and IFN-γ that were supposed to mimic the in vivo immunotherapies. Besides TAMs isolated from TC-1/A9-induced tumors, pMΦs were examined in these experiments as the reference cells. We observed that neither IFN-γ nor ODN1826 could significantly induce iNOS in both types of MΦs but their combination resulted in high NO production. This result corresponds to the concept of 'priming' by IFN-γ and 'triggering' by various TLR agonists, indicating that MΦ activation requires two signals for inducing iNOS activity [46,47].

TNF-α is a pro-inflammatory cytokine, which can negatively regulate the expression of M2 MΦ genes, both in vivo and in vitro [48]. In contrast to the high amounts of TNF-α produced by TAMs and pMΦs upon stimulation with IFN-γ plus the TLR ligand, ODN1826 differently affected these MΦ populations in our in vitro experiments. We observed low amounts of TNF-α secreted by ODN1826-activated pMΦs, while ODN1826-activated TAMs produced bulk of this cytokine. This result suggests that different mechanisms govern the production of TNF-α in both types of MΦs, which may be ascribed to the functional heterogeneity of these cells or presence of mechanisms that neutralize TNF-α in a long-term culture of ODN1826-activated pMΦs [49].

Despite the growing evidence of NO contribution to MΦ-mediated tumor cell killing [24,25], the role of this molecule in cancer remains controversial, as its pro- or anti-tumor activities depend strongly on concentration [50]. To delineate how tumor cells can affect NO production by MΦs, we set up co-culture experiments of TAMs with TC-1/A9 cells. Additionally, we tested arginase activity as this enzyme competes with iNOS for arginine but performs antagonistic activity [17] or may work as the iNOS modulator to overcome the exacerbating NO production [51,52]. In culture with tumor cells, TAMs produced significantly more NO than in mono-culture, provided that they were simultaneously challenged with IFN-γ plus TLR agonists. Tumor cells also induced iNOS activity in IFN-γ- or ODN1826-stimulated TAMs. However, whether such activated TAMs are tumoricidal remains questionable. As previously reported, tumor cells can provide a co-stimulatory signal for increased NO production by activated pMΦs but this NO enhancement did not correlate with cytotoxicity exerted on tumor cells in vitro [53]. Furthermore, while in in vivo immunotherapies against TC-1-induced tumors, NO did not affect the tumor regression [27], NO produced by in vitro activated pMΦs can act as one of the cytotoxic mediators against tumor cells [24,25]. On the other hand, tumor cells may also suppress NO production by pMΦs [22].

In our study, arginase activity in TAMs seemed to be upregulated more easily than iNOS. While NO production in co-culture with TC-1/A9 cells was limited to the simultaneous stimulation with IFN-γ, the TLR ligand, or their combination, arginase activity in TAMs was upregulated by co-culture with tumor cells regardless of further stimulation. We hypothesize that such arginase upregulation may be either due to more efficient arginine utilization by M2 MΦs [17] or influenced by the presence of other cell types, which were detected in the adherent population of $CD45^+$ cells. A recent study has described a $CD11b^+Gr1^+F4/80^-$ cell subpopulation that adheres strongly to the plastic surface but is unable to differentiate into TAMs and additionally resembles more MDSCs than MΦs [54]. Although

the authors do not report on whether this cell subpopulation expresses either of the enzymes studied in our experiments, it is well established that MDSCs can upregulate arginase but also iNOS [55].

MΦs are gaining increasing interest as they are numerous in tumors and possess potential for adaptation to perform anti-tumor activities. In this study, we showed that TAMs isolated from TC-1/A9-induced tumors are plastic cells that can be polarized to the M1 phenotype by combined immunotherapy that is efficient against tumor cells with reduced MHC-I expression. Thus, TAMs should not be neglected when designing the immunotherapy against tumors with downregulated MHC-I molecules.

4. Materials and Methods

4.1. Preparation of Reagents and Media

The TLR-9 agonists ODN1826 (class B; TCCATGACGTTCCTGACGTT) and ODN1585 (class A; GGGGTCAACGTTGAGGGGG) carrying immunostimulatory CpG motifs and a negative control, ODN1982 (TCCAGGACTTCTCTCAGGTT) without CpG motifs, were synthetized with a phosphorothioate-modified backbone (Generi Biotech, Hradec Kralove, Czech Republic) and dissolved in phosphate-buffered saline (PBS; ODN1826 and ODN1982) or deionized water (ODN1585). α-GalCer (Abcam, Cambridge, UK, ab144262) was solubilized in dimethyl sulfoxide (DMSO; Sigma-Aldrich, St. Louis, MO, USA) by heating at 80 °C for 20 min and sonication in an ultrasonic bath until complete dissolution.

TC-1/A9 cells were grown in high glucose Dulbecco's Modified Eagle's Medium (DMEM; Sigma-Aldrich, St. Louis, MO, USA, D6429) supplemented with 10% fetal bovine serum (FBS; Biosera, Nuaille, France, FB-1090) and 100 U/mL penicillin and 100 µg/mL streptomycin (DMEM-K). MΦs were maintained in DMEM F12 medium (Biosera, Nuaille, France LM-D1222) with 10% FBS and antibiotics as mentioned above (DMEM F12/10).

4.2. Mice

Seven- to eight-week-old female C57BL/6NCrl mice (Charles River, Sulzfeld, Germany) were used in the immunization experiments. Animals were maintained under standard conditions and in accordance with the guidelines for the proper treatment of laboratory animals at the Animal Facility of the Czech Center of Phenogenomics (BIOCEV, Vestec, Czech Republic). All animal experimental procedures were carried out in compliance with Directive 2010/63/EU and animal protocols were approved by the Sectoral Expert Committee of the Czech Academy of Sciences for Approval of Projects of Experiments on Animals (reference number 46/2016, 16th May 2016).

4.3. Tumor Cell Line

Tumor development in mice was induced with the TC-1/A9 clone [34] that was derived from mouse TC-1 cell line. TC-1 cells were generated by transformation of primary C57BL/6 mouse lung cells with the HPV16 *E6/E7* oncogenes and activated *H-ras* [56]. From a TC-1-induced tumor that developed in a mouse preimmunized against the E7 antigen, the TC-1/A9 clone was selected based on a reduced surface expression of MHC-I molecules. This MHC-I downregulation is reversible and can be restored with the IFN-γ treatment [34].

4.4. Plasmids

The pBSC [57] and pBSC/PADRE.E7GGG [58] plasmids were used for immunization of mice. The *PADRE.E7GGG* fusion gene consists of the mutated HPV16 *E7* gene (*E7GGG*) containing three-point mutations resulting in substitutions D21G, C24G and E26G in the Rb-binding site of the E7 oncoprotein [57] and the sequence encoding the Pan DR helper epitope (PADRE) designed in silico [59]. The plasmids were transformed into competent *E. coli* XL-1 blue strain, cultured in

Luria Broth Medium with 100 µg/mL of ampicillin and purified with the NucleoBond Xtra Maxi Kit (Macherey-Nagel, Duren, Germany, 740414).

4.5. Combined Immunotherapy Experiments

C57BL/6NCrl mice (five per group) were challenged with 3×10^4 TC-1/A9 tumor cells suspended in 0.15 mL PBS by s.c. injection into the back under anesthesia (day 0). Mice were immunized with the pBSC/PADRE.E7GGG plasmid by a gene gun (Bio-Rad, Hercules, CA, USA) on days 3, 6 and 10 after tumor-cell inoculation. DNA vaccination was applied at a discharge pressure of 400 psi into the shaven skin of the abdomen. Each immunization consisted of two shots delivering together 2 µg of plasmid DNA. The empty pBSC plasmid was used as a negative control.

The immunized mice were injected i.p. with four different vaccine adjuvants dissolved in 200 µL PBS. ODN1826 and ODN1585 were administered at a dose of 50 µg, LMS (Sigma-Aldrich, St. Louis, MO, USA, L9756) at a dose of 20 µg and α-GalCer at a dose of 2 µg. Some groups of mice were injected i.p. with 200 µg/200 µl PBS of anti-Tim-3 monoclonal antibody (clone RMT 3-23; Bio X Cell, West Lebanon, NH, USA). Control mice received PBS. The immunostimulatory compounds ODN1826 and α-GalCer were also administered in a mix. Different schedules and numbers of doses in combined immunotherapy were tested as specified for each experiment.

In the depletion experiments, the following doses of monoclonal antibodies (Exbio, Prague, Czech Republic) were injected i.p.: 100 µL of anti-CD4 (clone GK1.5), 100 µL of anti-CD8 (clone 2.43) and 400 µL of anti-NK1.1 (clone PK136). To deplete MΦs, 1 mg of carrageenan IV (Sigma-Aldrich, St. Louis, MO, USA, 22049) dissolved in 200 µL PBS was inoculated i.p. [60]. Neutralization of IFN-γ was achieved with 300 µg of monoclonal antibody per mouse (clone P4-6A2, Bio X Cell, West Lebanon, NH, USA). Depletions and neutralizations were performed on days 4, 7, 11, 14, 18 and 21 after tumor-cell inoculation.

Tumor growth was monitored three times a week and tumor volume was calculated using the formula $(\pi/6)$ $(a \times b \times c)$, where a, b, c are length, width and height of the tumor.

4.6. Isolation of TAMs

For in vitro experiments on TAMs, C57BL/6NCrl mice were injected s.c. with 3×10^5 TC-1/A9 cells. Non-necrotic tumors were excised as soon as they reached 10 mm in diameter (i.e., on days 13–14). To obtain single-cell suspension, removed tumors were washed in PBS, cut into <3 mm pieces and disaggregated with 1 mg/mL collagenase NB 8 (SERVA, Heidelberg, Germany, 17456) and 100 µg/mL DNase I (SERVA, Heidelberg, Germany, 18535) in RPMI-1640 medium (without FBS) at 37 °C using a gentleMACS Octo Dissociator (Miltenyi Biotec, Bergisch Gladbach, Germany). The obtained cell suspension was filtered through a 70-µm mesh (Miltenyi Biotec, Bergisch Gladbach, Germany). Red blood cells were lysed with the ACK buffer (0.15 M NH_4Cl, 10 mM $KHCO_3$, 0.5 M EDTA, pH 7.2–7.4), which was followed by positive selection of $CD45^+$ cells using anti-CD45 antibody-conjugated magnetic beads (Miltenyi Biotec, Bergisch Gladbach, Germany, 130-097-153) and an autoMACS Pro Separator device (Miltenyi Biotec, Bergisch Gladbach, Germany) according to the manufacturer's instruction. The selected $CD45^+$ cells were plated on a 10-cm dish at a concentration of 1.5×10^6 cells/mL adjusted with the complete DMEM F12/10 medium and allowed to adhere to the plastic at 37 °C and 5% CO_2 for 3–4 h. Then, the non-adherent cells were removed by extensive washing with warm PBS. The adherent cells were collected by gentle scraping in cold 10 mM EDTA/PBS and 5×10^5 cells per well were plated into a 24-well plate in complete DMEM F12/10 medium. The cells were incubated at 37 °C and 5% CO_2 overnight for the subsequent in vitro experiments.

4.7. Isolation of pMΦs

Peritoneal cells were collected by peritoneal cavity lavage. C57BL/6NCrl mice were injected i.p. with 1 mL of 3% Brewer thioglycolate broth (Sigma-Aldrich, St. Louis, MO, USA, 70157) 96 h prior collection. pMΦs were enriched by adhesion to plastic for 3 h by plating 5×10^5 cells per well into a

24-well plate containing 750 µL of DMEM F12/10. Non-adherent cells were removed by washing with warm PBS and adherent cells were incubated in a fresh medium at 37 °C and 5% CO_2 overnight.

4.8. In Vitro Stimulations of TAMs and pMΦs

For in vitro stimulations, cells were cultured in a final volume of 1 mL of DMEM-K in a 24-well plate. Different variants of cell activation were tested with the following concentrations of reagents: 5 µg/mL of ODNs, 10 µg/mL of LMS, 10 µg/mL of anti-Tim-3, 10 ng/mL of LPS (Sigma-Aldrich, St. Louis, MO, USA, L4391) and 200 U/mL IFN-γ (PeproTech, Rocky Hill, NJ, USA, 315-05). Stimulation with LPS+IFN-γ served as a positive control for M1 MΦs and activation of MΦs to M2 type was achieved by incubation with 25 ng/mL IL-4 (PeproTech, Rosky Hill, NJ, USA, 214-14). Unstimulated cells served as a negative control. pMΦs were stimulated for 72 h and TAMs for 48 h. Supernatants were collected, centrifuged for 5 min at 350× *g* and used in aliquots for NO and TNF-α assays.

4.9. NO Measurement

NO was determined by measurement of its stable metabolite NO_2^- in supernatants by Griess reagent composed of 0.2% naphthylethylenediamine dihydrochloride (Sigma-Aldrich, St. Louis, MO, USA, 222488) and 2% sulphanilamide (Sigma-Aldrich, St. Louis, MO, USA, S9251) in 5% phosphoric acid. Equal volumes of the supernatant from in vitro cell stimulations and Griess reagent were mixed and incubated in the dark at room temperature (RT) for 10 min. The absorbance was measured at 540 nm using a microplate reader (Tecan, Männedorf, Switzerland). The nitrite concentration was determined by using the standard curve of sodium nitrite (0–100 µM; Sigma-Aldrich, St. Louis, MO, USA, 31443).

4.10. TNF-α Enzyme-Linked Immunosorbent Assay (ELISA)

TNF-α concentration was determined in the supernatants from in vitro cell stimulations using sandwich ELISA (eBioscience, San Diego, CA, USA, 88-7324-22) according to the manufacturer's protocol.

4.11. IFN-γ Enzyme-Linked Immunospot (ELISPOT) Assay

An IFN-γ ELISPOT assay was performed on mononuclear cells isolated from pools of splenocytes (3 mice per group) according to the protocol described previously [36]. Cells were incubated with either 0.1 µg/mL of the $E7_{49–57}$ peptide (RAHYNIVTF, > 96% pure; Clonestar Biotech, Brno, Czech Republic) derived from the HPV16 E7 oncoprotein or 1 µg/mL of the PADRE peptide (AKFVAAWTLKAAA, >81% pure; GenScript, Piscataway, NJ, USA) at 37 °C in 5% CO2 for 24 h.

4.12. Co-Culture of TC-1/A9 Tumor Cells with TAMs

TAMs from TC-1/A9-induced tumors were isolated according to the protocol decribed above. The concentration of the collected adherent cells was adjusted to 1×10^6 cells/mL with DMEM F12/10 and 100 µL of this cell suspension was distributed into the 96-well plate and incubated at 37 °C in 5% CO_2 for the subsequent co-culture experiments. On the next day, the adherent cells were washed with warm PBS and some of them were overlaid with 1×10^4 TC-1/A9 tumor cells in 100 µL of DMEM-K. Control cells, that is, TAMs without tumor cells and TC-1/A9 cells alone, were incubated in DMEM-K as well. After the adhesion of TC-1/A9 cells, the cells (i.e., TC-1/A9, MΦs and their co-culture) were washed with PBS and subsequently 100 µL of stimulatory compounds with the concentrations described above were applied for the next 44 h. Afterwards, the supernatants were collected for the measurement of nitrite by the Griess reagent and the cells were washed with PBS for the arginase microplate assay. Incubation of DMEM-K with stimulatory compounds without cells followed by measurement with the Griess reagent was performed in order to eliminate the interference with this reagent.

4.13. Arginase Microplate Assay

Arginase activity was measured in terms of urea quantification using the microplate method [61] on 1×10^5 of TAMs, 1×10^4 of TC-1/A9 cells, or their co-culture after 44-h stimulation. The absorbance was measured at 540 nm using a microplate reader and the urea concentration was calculated using the calibration curve ranging from 0 to 320 µg/mL.

4.14. Flow Cytometry

The preparation of a single cell suspension from a tumor tissue was performed as described previously [36] (see also isolation of TAMs). Four panels of fluorescent-labeled antibodies were used to identify the main cell populations infiltrating the tumor (Table 1). Staining was performed in 96-well plates. Prior to surface staining, the cells were stained for viability with Fixable Viability dye eFluor 455UV (eBioscience, San Diego, CA, USA, 65-0868-14) in PBS. Staining of surface markers was followed by a fixation and permeabilization step if needed. To detect the nuclear Foxp3 transcription factor, the cells were treated with the Fixation/Permeabilization Concentrate (eBioscience, San Diego, CA, USA, 00-5123-43) diluted 1:3 with the Fixation/Permeabilization Diluent (eBioscience, San Diego, CA, USA, 00-5223-56). Cytokine and iNOS production were observed after incubation with the IC Fixation buffer (eBioscience, San Diego, CA, USA, 00-8222-49). In both cases, a washing step with the Permeabilization buffer (eBioscience, San Diego, CA, USA, 00-8333-56) followed the fixation and permeabilization. Subsequently, the cells were measured on an LSRFortessa (BD Biosciences, San Diego, CA, USA) flow cytometer and the results were analyzed with FlowJo v10.4.2 software (BD Biosciences, San Diego, CA, USA).

Table 1. List of antibodies used for flow cytometry.

Antigen	Conjugate	Clone	Source	Staining	Panels			
CD11b	BV421	M1/70	BioLegend, 101251	Surface		●		●
CD11c	BV650	N418	BioLegend, 117339	Surface		●		
CD25	APC	PC61.5	eBiosciences, 17-0251-81	Surface	●			
CD3	APC-Cy7	145-2C11	BioLegend, 100330	Surface	●	●	●	●
CD317	APC	927	BioLegend, 127015	Surface				
CD4	BV510	RM4-5	BioLegend, 100559	Surface	●		●	
CD45	Alexa Fluor 700	30-F11	BioLegend, 103128	Surface	●	●	●	●
CD8	FITC	53-6.7	BD Biosciences, 553031	Surface	●	●	●	
F4/80	BV510	BM8	BioLegend, 123135	Surface		●		
Foxp3	PE	FJK-16s	eBiosciences, 12-5773-82	Nuclear	●			
Gr-1	PE/BV786 ♦	RB6-8C5	BioLegend, 108407/BD Biosciences, 740850 ♦	Surface		●		♦
IFN-γ	BV421	XMG1.2	BD Biosciences, 563376	Intracellular			●	
MHC-II	PerCP-Cy5.5/PE-Cy7 ♦	M5/114.15.2	BioLegend, 107625/BioLegend 107629 ♦	Surface		●		♦
NK1.1	BV650	PK136	BioLegend, 108736	Surface	●		●	
iNOS	Alexa Fluor 488	CXNFT	eBiosciences, 53-5920-80	Intracellular				●
Nrp1	BV421	3E12	BioLegend, 145209	Surface	●			
PD-1	PE-Cy7	29F1A12	BioLegend, 135215	Surface			●	
Tim-3	APC	RMT3-23	BioLegend, 119706	Surface			●	●
TNF-α	PE-DAZZLE594	MP6-XT22	BioLegend, 506346	Intracellular			●	●

● ♦, antibody present in a panel.

4.15. Quantification of mRNA Expression by RT-qPCR

Specific primers for the detection of target genes (Table 2) were designed and evaluated with SYBR green chemistry by the Gene Core-qPCR and dPCR Core Facility (BIOCEV, Vestec, Czech Republic), which also performed all qPCR reactions. As reference genes for normalization, *Tbp* (TATAA-box binding protein), *Ywhas* (Tyrosine 3-tryptophan 5-monooxygenase activation protein) and *Rplp* (Ribosomal protein P0, large) were selected from the Reference Gene Panel (Mouse) (TATAA Biocenter, Goteborg, Sweden, A102). For the selection of these genes with the most stable expression, 36 tumors induced by TC-1 or TC-/A9 cells were utilized. To ensure variability of the tumor microenvironment with respect to immunotherapy, some mice were treated with DNA immunization, LMS, ODN1826,

ODN1585, carrageenan, or antibody against IFN-γ as described above. After the excision of tumors from mice, a representative part of samples was immediately placed into the RNAlater Solution (Thermo Fisher Scientific, Waltham, MA, USA, AM7021) and stored at 4 °C for a maximum of 14 days prior to RNA isolation. Then, samples were disrupted by a rotor-stator homogenizer (Omni TH, Kennesaw, GA, USA) in a lysis buffer from the NucleoSpin RNA kit (Macherey-Nagel, Duren, Germany, 740955) and total RNA was isolated. One microgram of RNA was reverse transcribed in a 20-µL reaction using the TATAA GrandScript cDNA Synthesis kit (TATAA Biocenter, Goteborg, Sweden, A103b) according to the manufacturer's instructions. The amplifications of cDNA of the target genes and three reference genes were done simultaneously in duplicates in a 384-well microplate format of the LightCycler 480 Real-Time PCR System (Roche Diagnostics, Basel, Switzerland). Ten microliters of the reaction solution contained 1× TATAA SYBR Grandmaster mix (TATAA Biocenter, Goteborg, Sweden), 400 nM of each of primer and 2 µL cDNA (diluted 10×). The standard program was used (95 °C for 30 s followed by 40 cycles of 95 °C for 5 s, 60 °C for 15 s, 72 °C for 10 s and melting curve). For the control of the genomic DNA background, the ValidPrime assay (TATAA Biocenter, Goteborg, Sweden) was done. The data processing and relative quantification of mRNA expression were performed using the GenEx v6 software (TATAA Biocenter, Goteborg, Sweden).

Table 2. List of target genes and primer sequences for qPCR assays.

Target Gene	Reference Sequence (NCBI ID)	Forward Primer 5′ → 3′	Reverse Primer 5′ → 3′	Amplicon (bp)
Ifng	NM_008337.4	TTCCTCATGGCTGTTTCTGG	CACCATCCTTTTGCCAGTTC	148
Ido1	NM_001293690.1	GTCTGGAGAAAGCCAAGGAA	ATATGCGGAGAACGTGGAAA	81
Il10	NM_010548.2	GGTGAGAAGCTGAAGACCC	ATGGCCTTGTAGACACCTTG	137
Foxp3	NM_001199347.1	ACCTGGCTGGGAAGATG	TCCCGAGGAGCAGACC	124
Ncf1	NM_010876.4	TGTTCCTGGTTAAGTGGCAG	GGTGTGGGATGACTCTGTTC	144
Tgfb1	NM_011577.2	TCAGACATTCGGGAAGCAG	AAGGTAACGCCAGGAATTGT	135
Arg1	NM_007482.3	ATGGAAGAGTCAGTGTGGTG	GGGAGTGTTGATGTCAGTGT	128

NCBI, National Center for Biotechnology Information; *Ifng*, interferon gamma; *Ido1*, indoleamine 2,3-dioxygenase 1; *Il10*, interleukin 10; *Foxp3*, forkhead box P3; *Ncf1*, neutrophil cytosolic factor 1; *Tgfb1*, transforming growth factor beta 1; *Arg1*, arginase, liver.

4.16. Statistical Analysis

Tumor growth was analyzed by two-way analysis of variance (ANOVA) and Sidak multiple comparisons. Intergroup comparisons from flow cytometry and in vitro stimulations of peritoneal cells and $CD45^+$ adherent cells were made by one-way ANOVA and Dunnett multiple comparisons. Co-culture and RT-qPCR experiments were analyzed by two-way ANOVA and Dunnett multiple comparisons. The Spearman coefficient was calculated for the analysis of the correlation between *Ifng* and *Ido1* expression. Results were considered significantly different if $p < 0.05$. Calculations were performed using the GraphPad Prism 6 software (GraphPad Software, San Diego, CA, USA).

5. Conclusions

This study demonstrates that for immunotherapy of tumors with MHC-I downregulation, the combined activation of both adaptive and innate immunity is needed. Despite negligible sensitivity of these tumor cells to DNA immunization, $CD8^+$ T cells activated by immunization played an important role in the anti-tumor response elicited by combined immunotherapy. In addition, $NK1.1^+$ cells and MΦs repolarized to the M1 phenotype were involved in the inhibition of tumor growth. However, Tim-3 blockade did not significantly contribute to the anti-tumor effect. As tumor growth was reduced only transiently, further efforts should enhance the combined immunotherapy to handle immunosuppression that probably prevailed in progressing tumors.

Supplementary Materials: Supplementary materials can be found at http://www.mdpi.com/1422-0067/19/11/3693/s1.

Author Contributions: M.S., A.G. and I.P. conceived and designed the experiments; A.G., I.P., M.S., J.S., J.V., L.P. and R.T. performed the experiments and analyzed the data; A.G., M.S., I.P. and J.S. wrote the paper.

Funding: This research was funded by the Czech Science Foundation, grant number GA16-04477S, the Ministry of Education, Youth and Sports of the Czech Republic (MEYS), grant numbers LQ1604 and LM2015040, and the European Regional Development Fund and MEYS, grant numbers CZ.1.05/1.1.00/02.0109, CZ.1.05/2.1.00/19.0400 and CZ.1.05/2.1.00/19.0395.

Acknowledgments: The authors would like to thank Pavlina Vesela and Kristyna Klecakova for technical assistance and Jan Musil for his helpful advice during the optimization of the flow cytometry method. We also acknowledge the Imaging Methods Core Facility at BIOCEV for their support with obtaining flow cytometry data presented in this paper.

Conflicts of Interest: The authors declare no conflict of interest.

References

1. Morrissey, K.; Yuraszeck, T.; Li, C.; Zhang, Y.; Kasichayanula, S. Immunotherapy and novel combinations in oncology: Current landscape, challenges and opportunities. *Clin. Transl. Sci.* **2016**, *9*, 89–104. [CrossRef] [PubMed]
2. Beyranvand Nejad, E.; Welters, M.J.P.; Arens, R.; van der Burg, S.H. The importance of correctly timing cancer immunotherapy. *Expert. Opin. Biol. Ther.* **2017**, *17*, 87–103. [CrossRef] [PubMed]
3. Garcia-Lora, A.; Algarra, I.; Garrido, F. MHC class I antigens, immune surveillance and tumor immune escape. *J. Cell. Physiol.* **2003**, *195*, 346–355. [CrossRef] [PubMed]
4. Garrido, F.; Aptsiauri, N.; Doorduijn, E.M.; Garcia Lora, A.M.; van Hall, T. The urgent need to recover MHC class I in cancers for effective immunotherapy. *Curr. Opin. Immunol.* **2016**, *39*, 44–51. [CrossRef] [PubMed]
5. Yang, B.; Jeang, J.; Yang, A.; Wu, T.C.; Hung, C.-F. DNA vaccine for cancer immunotherapy. *Hum. Vaccin. Immunother.* **2014**, *10*, 3153–3164. [CrossRef] [PubMed]
6. Vacchelli, E.; Eggermont, A.; Sautès-Fridman, C.; Galon, J.; Zitvogel, L.; Kroemer, G.; Galluzzi, L. Trial Watch: Toll-like receptor agonists for cancer therapy. *Oncoimmunology* **2013**, *2*, e25238. [CrossRef] [PubMed]
7. Klinman, D.M. Immunotherapeutic uses of CpG oligodeoxynucleotides. *Nat. Rev. Immunol.* **2004**, *4*, 249–258. [CrossRef] [PubMed]
8. Chen, L.-Y.; Lin, Y.-L.; Chiang, B.-L. Levamisole enhances immune response by affecting the activation and maturation of human monocyte-derived dendritic cells. *Clin. Exp. Immunol.* **2008**, *151*, 174–181. [CrossRef] [PubMed]
9. Brennan, P.J.; Brigl, M.; Brenner, M.B. Invariant natural killer T cells: An innate activation scheme linked to diverse effector functions. *Nat. Rev. Immunol.* **2013**, *13*, 101–117. [CrossRef] [PubMed]
10. Robertson, F.C.; Berzofsky, J.A.; Terabe, M. NKT cell networks in the regulation of tumor immunity. *Front. Immunol.* **2014**, *5*, 543. [CrossRef] [PubMed]
11. Monney, L.; Sabatos, C.A.; Gaglia, J.L.; Ryu, A.; Waldner, H.; Chernova, T.; Manning, S.; Greenfield, E.A.; Coyle, A.J.; Sobel, R.A.; et al. Th1-specific cell surface protein Tim-3 regulates macrophage activation and severity of an autoimmune disease. *Nature* **2002**, *415*, 536–541. [CrossRef] [PubMed]
12. Anderson, A.C. Tim-3: An emerging target in the cancer immunotherapy landscape. *Cancer Immunol. Res.* **2014**, *2*, 393–398. [CrossRef] [PubMed]
13. Han, G.; Chen, G.; Shen, B.; Li, Y. Tim-3: An activation marker and activation limiter of innate immune cells. *Front. Immunol.* **2013**, *4*, 449. [CrossRef] [PubMed]
14. Bingle, L.; Brown, N.J.; Lewis, C.E. The role of tumour-associated macrophages in tumour progression: Implications for new anticancer therapies. *J. Pathol.* **2002**, *196*, 254–265. [CrossRef] [PubMed]
15. Mills, C.D.; Ley, K. M1 and M2 macrophages: The chicken and the egg of immunity. *J. Innate Immun.* **2014**, *6*, 716–726. [CrossRef] [PubMed]
16. Ocana-Guzman, R.; Torre-Bouscoulet, L.; Sada-Ovalle, I. TIM-3 regulates distinct functions in macrophages. *Front. Immunol.* **2016**, *7*, 229. [CrossRef] [PubMed]
17. Rath, M.; Muller, I.; Kropf, P.; Closs, E.I.; Munder, M. Metabolism via arginase or nitric oxide synthase: Two competing arginine pathways in macrophages. *Front. Immunol.* **2014**, *5*, 532. [CrossRef] [PubMed]
18. Biswas, S.K.; Sica, A.; Lewis, C.E. Plasticity of macrophage function during tumor progression: Regulation by distinct molecular mechanisms. *J. Immunol.* **2008**, *180*, 2011–2017. [CrossRef] [PubMed]

19. Zheng, X.; Turkowski, K.; Mora, J.; Brune, B.; Seeger, W.; Weigert, A.; Savai, R. Redirecting tumor-associated macrophages to become tumoricidal effectors as a novel strategy for cancer therapy. *Oncotarget* **2017**, *8*, 48436–48452. [CrossRef] [PubMed]
20. Tang, X.; Mo, C.; Wang, Y.; Wei, D.; Xiao, H. Anti-tumour strategies aiming to target tumour-associated macrophages. *Immunology* **2013**, *138*, 93–104. [CrossRef] [PubMed]
21. Buhtoiarov, I.N.; Sondel, P.M.; Wigginton, J.M.; Buhtoiarova, T.N.; Yanke, E.M.; Mahvi, D.A.; Rakhmilevich, A.L. Anti-tumour synergy of cytotoxic chemotherapy and anti-CD40 plus CpG-ODN immunotherapy through repolarization of tumour-associated macrophages. *Immunology* **2011**, *132*, 226–239. [CrossRef] [PubMed]
22. Rakhmilevich, A.L.; Baldeshwiler, M.J.; Van De Voort, T.J.; Felder, M.A.R.; Yang, R.K.; Kalogriopoulos, N.A.; Koslov, D.S.; Van Rooijen, N.; Sondel, P.M. Tumor-associated myeloid cells can be activated in vitro and in vivo to mediate antitumor effects. *Cancer Immunol. Immunother.* **2012**, *61*, 1683–1697. [CrossRef] [PubMed]
23. Buhtoiarov, I.N.; Lum, H.; Berke, G.; Paulnock, D.M.; Sondel, P.M.; Rakhmilevich, A.L. CD40 ligation activates murine macrophages via an IFN-gamma-dependent mechanism resulting in tumor cell destruction in vitro. *J. Immunol.* **2005**, *174*, 6013–6022. [CrossRef] [PubMed]
24. Buhtoiarov, I.N.; Sondel, P.M.; Eickhoff, J.C.; Rakhmilevich, A.L. Macrophages are essential for antitumour effects against weakly immunogenic murine tumours induced by class B CpG-oligodeoxynucleotides. *Immunology* **2007**, *120*, 412–423. [CrossRef] [PubMed]
25. Lum, H.D.; Buhtoiarov, I.N.; Schmidt, B.E.; Berke, G.; Paulnock, D.M.; Sondel, P.M.; Rakhmilevich, A.L. Tumoristatic effects of anti-CD40 mAb-activated macrophages involve nitric oxide and tumour necrosis factor-alpha. *Immunology* **2006**, *118*, 261–270. [CrossRef] [PubMed]
26. Jensen, J.L.; Rakhmilevich, A.; Heninger, E.; Broman, A.T.; Hope, C.; Phan, F.; Miyamoto, S.; Maroulakou, I.; Callander, N.; Hematti, P.; et al. Tumoricidal effects of macrophage-activating immunotherapy in a murine model of relapsed/refractory multiple myeloma. *Cancer Immunol. Res.* **2015**, *3*, 881–890. [CrossRef] [PubMed]
27. Thoreau, M.; Penny, H.L.; Tan, K.; Regnier, F.; Weiss, J.M.; Lee, B.; Johannes, L.; Dransart, E.; Le Bon, A.; Abastado, J.-P.; et al. Vaccine-induced tumor regression requires a dynamic cooperation between T cells and myeloid cells at the tumor site. *Oncotarget* **2015**, *6*, 27832–27846. [CrossRef] [PubMed]
28. Delgoffe, G.M.; Woo, S.-R.; Turnis, M.E.; Gravano, D.M.; Guy, C.; Overacre, A.E.; Bettini, M.L.; Vogel, P.; Finkelstein, D.; Bonnevier, J.; et al. Stability and function of regulatory T cells is maintained by a neuropilin-1–semaphorin-4a axis. *Nature* **2013**, *501*, 252–256. [CrossRef] [PubMed]
29. Mills, C.D. Anatomy of a discovery: M1 and M2 macrophages. *Front. Immunol.* **2015**, *6*, 212. [CrossRef] [PubMed]
30. Nakayama, M.; Akiba, H.; Takeda, K.; Kojima, Y.; Hashiguchi, M.; Azuma, M.; Yagita, H.; Okumura, K. Tim-3 mediates phagocytosis of apoptotic cells and cross-presentation. *Blood* **2009**, *113*, 3821–3830. [CrossRef] [PubMed]
31. Smyth, M.J.; Ngiow, S.F.; Ribas, A.; Teng, M.W.L. Combination cancer immunotherapies tailored to the tumour microenvironment. *Nat. Rev. Clin. Oncol.* **2015**, *13*, 143–158. [CrossRef] [PubMed]
32. Moynihan, K.D.; Opel, C.F.; Szeto, G.L.; Tzeng, A.; Zhu, E.F.; Engreitz, J.M.; Williams, R.T.; Rakhra, K.; Zhang, M.H.; Rothschilds, A.M.; et al. Eradication of large established tumors in mice by combination immunotherapy that engages innate and adaptive immune responses. *Nat. Med.* **2016**, *22*, 1402–1410. [CrossRef] [PubMed]
33. Aris, M.; Mordoh, J.; Barrio, M.M. Immunomodulatory monoclonal antibodies in combined immunotherapy trials for cutaneous melanoma. *Front. Immunol.* **2017**, *8*, 1024. [CrossRef] [PubMed]
34. Smahel, M.; Sima, P.; Ludvikova, V.; Marinov, I.; Pokorna, D.; Vonka, V. Immunisation with modified HPV16 E7 genes against mouse oncogenic TC-1 cell sublines with downregulated expression of MHC class I molecules. *Vaccine* **2003**, *21*, 1125–1136. [CrossRef]
35. Smahel, M.; Polakova, I.; Sobotkova, E.; Vajdova, E. Systemic administration of CpG oligodeoxynucleotide and levamisole as adjuvants for gene-gun-delivered antitumor DNA vaccines. *Clin. Dev. Immunol.* **2011**, *2011*, 176759. [CrossRef] [PubMed]
36. Kastankova, I.; Polakova, I.; Duskova, M.; Smahel, M. Combined cancer immunotherapy against aurora kinase A. *J. Immunother.* **2016**, *39*, 160–170. [CrossRef] [PubMed]
37. Reinis, M.; Simova, J.; Bubenik, J. Inhibitory effects of unmethylated CpG oligodeoxynucleotides on MHC class I-deficient and -proficient HPV16-associated tumours. *Int. J. Cancer* **2006**, *118*, 1836–1842. [CrossRef] [PubMed]

38. Simova, J.; Indrova, M.; Bieblova, J.; Mikyskova, R.; Bubenik, J.; Reinis, M. Therapy for minimal residual tumor disease: β-galactosylceramide inhibits the growth of recurrent HPV16-associated neoplasms after surgery and chemotherapy. *Int. J. Cancer* **2010**, *126*, 2997–3004. [CrossRef] [PubMed]
39. Duraiswamy, J.; Freeman, G.J.; Coukos, G. Therapeutic PD-1 pathway blockade augments with other modalities of immunotherapy T-cell function to prevent immune decline in ovarian cancer. *Cancer Res.* **2013**, *73*, 6900–6912. [CrossRef] [PubMed]
40. Lepique, A.P.; Daghastanli, K.R.P.; Cuccovia, I.M.; Villa, L.L. HPV16 tumor associated macrophages suppress antitumor T cell responses. *Clin. Cancer Res.* **2009**, *15*, 4391–4400. [CrossRef] [PubMed]
41. Miyahira, Y.; Katae, M.; Takeda, K.; Yagita, H.; Okumura, K.; Kobayashi, S.; Takeuchi, T.; Kamiyama, T.; Fukuchi, Y.; Aoki, T. Activation of natural killer T cells by α-galactosylceramide impairs DNA vaccine-induced protective immunity against Trypanosoma cruzi. *Infect. Immun.* **2003**, *71*, 1234–1241. [CrossRef] [PubMed]
42. Kim, D.; Hung, C.-F.; Wu, T.-C.; Park, Y.-M. DNA vaccine with α-galactosylceramide at prime phase enhances anti-tumor immunity after boosting with antigen-expressing dendritic cells. *Vaccine* **2010**, *28*, 7297–7305. [CrossRef] [PubMed]
43. Bercovici, N.; Trautmann, A. Revisiting the role of T cells in tumor regression. *Oncoimmunology* **2012**, *1*, 346–350. [CrossRef] [PubMed]
44. Van der Sluis, T.C.; Sluijter, M.; van Duikeren, S.; West, B.L.; Melief, C.J.M.; Arens, R.; van der Burg, S.H.; van Hall, T. Therapeutic peptide vaccine-induced CD8 T cells strongly modulate intratumoral macrophages required for tumor regression. *Cancer. Immunol. Res.* **2015**, *3*, 1042–1051. [CrossRef] [PubMed]
45. Jiang, Y.; Li, Y.; Zhu, B. T-cell exhaustion in the tumor microenvironment. *Cell Death Dis.* **2015**, *6*, e1792. [CrossRef] [PubMed]
46. Jones, B.W.; Heldwein, K.A.; Means, T.K.; Saukkonen, J.J.; Fenton, M.J. Differential roles of Toll-like receptors in the elicitation of proinflammatory responses by macrophages. *Ann. Rheum. Dis.* **2001**, *60* (Suppl. S3), iii6–iii12. [CrossRef] [PubMed]
47. Muller, E.; Christopoulos, P.F.; Halder, S.; Lunde, A.; Beraki, K.; Speth, M.; Øynebråten, I.; Corthay, A. Toll-like receptor ligands and interferon-γ synergize for induction of antitumor M1 macrophages. *Front. Immunol.* **2017**, *8*, 1383. [CrossRef] [PubMed]
48. Kratochvill, F.; Neale, G.; Haverkamp, J.M.; de Velde, L.-A.V.; Smith, A.M.; Kawauchi, D.; McEvoy, J.; Roussel, M.F.; Dyer, M.A.; Qualls, J.E.; et al. TNF counterbalances the emergence of M2 tumor macrophages. *Cell Rep.* **2015**, *12*, 1902–1914. [CrossRef] [PubMed]
49. Jin, L.; Raymond, D.P.; Crabtree, T.D.; Pelletier, S.J.; Houlgrave, C.W.; Pruett, T.L.; Sawyer, R.G. Enhanced murine macrophage TNF receptor shedding by cytosine-guanine sequences in oligodeoxynucleotides. *J. Immunol.* **2000**, *165*, 5153–5160. [CrossRef] [PubMed]
50. Vannini, F.; Kashfi, K.; Nath, N. The dual role of iNOS in cancer. *Redox Biol.* **2015**, *6*, 334–343. [CrossRef] [PubMed]
51. Chang, C.I.; Liao, J.C.; Kuo, L. Arginase modulates nitric oxide production in activated macrophages. *Am. J. Physiol.* **1998**, *274*, H342–H348. [CrossRef] [PubMed]
52. Liscovsky, M.V.; Ranocchia, R.P.; Gorlino, C.V.; Alignani, D.O.; Morón, G.; Maletto, B.A.; Pistoresi-Palencia, M.C. Interferon-γ priming is involved in the activation of arginase by oligodeoxinucleotides containing CpG motifs in murine macrophages. *Immunology* **2009**, *128*, e159–e169. [CrossRef] [PubMed]
53. Calorini, L.; Bianchini, F.; Mannini, A.; Mugnai, G.; Ruggieri, S. Enhancement of nitric oxide release in mouse inflammatory macrophages co-cultivated with tumor cells of a different origin. *Clin. Exp. Metastasis* **2005**, *22*, 413–419. [CrossRef] [PubMed]
54. Tsubaki, T.; Kadonosono, T.; Sakurai, S.; Shiozawa, T.; Goto, T.; Sakai, S.; Kuchimaru, T.; Sakamoto, T.; Watanabe, H.; Kondoh, G.; et al. Novel adherent CD11b+ Gr-1+ tumor-infiltrating cells initiate an immunosuppressive tumor microenvironment. *Oncotarget* **2018**, *9*, 11209–11226. [CrossRef] [PubMed]
55. Gabrilovich, D.I.; Nagaraj, S. Myeloid-derived-suppressor cells as regulators of the immune system. *Nat. Rev. Immunol.* **2009**, *9*, 162–174. [CrossRef] [PubMed]
56. Lin, K.Y.; Guarnieri, F.G.; Staveley-O'Carroll, K.F.; Levitsky, H.I.; August, J.T.; Pardoll, D.M.; Wu, T.C. Treatment of established tumors with a novel vaccine that enhances major histocompatibility class II presentation of tumor antigen. *Cancer Res.* **1996**, *56*, 21–26. [PubMed]

57. Smahel, M.; Sima, P.; Ludvikova, V.; Vonka, V. Modified HPV16 E7 genes as DNA vaccine against E7-containing oncogenic cells. *Virology* **2001**, *281*, 231–238. [CrossRef] [PubMed]
58. Smahel, M.; Polakova, I.; Duskova, M.; Ludvikova, V.; Kastankova, I. The effect of helper epitopes and cellular localization of an antigen on the outcome of gene gun DNA immunization. *Gene Ther.* **2014**, *21*, 225–232. [CrossRef] [PubMed]
59. Alexander, J.; Sidney, J.; Southwood, S.; Ruppert, J.; Oseroff, C.; Maewal, A.; Snoke, K.; Serra, H.M.; Kubo, R.T.; Sette, A. Development of high potency universal DR-restricted helper epitopes by modification of high affinity DR-blocking peptides. *Immunity* **1994**, *1*, 751–761. [CrossRef]
60. Ishizaka, S.; Kuriyama, S.; Tsujii, T. In vivo depletion of macrophages by desulfated iota-carrageenan in mice. *J. Immunol. Methods* **1989**, *124*, 17–24. [CrossRef]
61. Corraliza, I.M.; Campo, M.L.; Soler, G.; Modolell, M. Determination of arginase activity in macrophages: A micromethod. *J. Immunol. Methods* **1994**, *174*, 231–235. [CrossRef]

Establishment and characterization of a mouse tumor cell line with irreversible downregulation of MHC class I molecules

KAROLINA LHOTAKOVA[1,2], ADRIANNA GRZELAK[2], INGRID POLAKOVA[2], JULIE VACKOVA[1,2] and MICHAL SMAHEL[2]

Departments of [1]Cell Biology and [2]Genetics and Microbiology, Faculty of Science, Charles University, BIOCEV, 252 50 Vestec, Czech Republic

Received March 29, 2019; Accepted August 23, 2019

DOI: 10.3892/or.2019.7356

Abstract. In the majority of human tumors, downregulation of major histocompatibility complex class I (MHC-I) expression contributes to the escape from the host immune system and resistance to immunotherapy. Relevant animal models are therefore needed to enhance the efficacy of cancer immunotherapy. As loss of β-2 microglobulin expression results in irreversible downregulation of surface MHC-I molecules in various human tumors, the β-2 microglobulin gene (*B2m*) was deactivated in a mouse oncogenic TC-1 cell line and a TC-1/dB2m cell line that was negative for surface MHC-I expression was derived. Following stimulation with interferon γ, MHC-I heavy chains, particularly the H-2D^b molecules, were found to be expressed at low levels on the cell surface, but without β-2 microglobulin. *B2m* deactivation in TC-1/dB2m cells led to reduced proliferation and tumor growth. These cells were insensitive to DNA vaccination and only weakly responsive to combined immunotherapy with a DNA vaccine and the ODN1826 adjuvant. *In vivo* depletion demonstrated that NK1.1$^+$ cells were involved in both reduced tumor growth and an antitumor effect of immunotherapy. The number of immune cells infiltrating TC-1/dB2m-induced tumors was comparable with that in tumors developing from TC-1/A9 cells characterized by reversible MHC-I downregulation. However, the composition of the cell infiltrate was different and, most importantly, infiltration with immune cells was not increased in TC-1/dB2m tumors after immunotherapy. Therefore, the TC-1/dB2m cell line represents a clinically relevant tumor model that may be used for enhancement of cancer immunotherapy.

Correspondence to: Dr Michal Smahel, Department of Genetics and Microbiology, Faculty of Science, Charles University, BIOCEV, Prumyslova 595, 252 50 Vestec, Czech Republic
E-mail: smahelm@natur.cuni.cz

Key words: major histocompatibility complex class I, cancer immunotherapy, β-2 microglobulin, tumor microenvironment, DNA vaccination, CpG ODN

Introduction

During tumor development, oncogenic cells are under the surveillance of the host immune system. This leads to the selection of cells with adaptations that confer a survival advantage (1). The reduced expression of surface major histocompatibility complex class I (MHC-I) molecules is one of the most frequent mechanisms of evasion from immune reactions in different human tumors, ranging from 15% in renal carcinoma to 93% in lung cancer and >75% in most types of epithelial-derived tumors (2). The majority of MHC-I aberrations are reversible and are often associated with defects in the antigen-processing machinery (APM). In that case, reduced MHC-I expression is usually caused by epigenetic silencing of the genes coding for MHC-I heavy chains or APM components (3) and may be restored by cytokines [e.g., interferon (IFN)-γ or tumor-necrosis factor (TNF)-α]. Mutations or chromosomal aberrations that affect genes encoding MHC-I heavy chains, β-2 microglobulin, proteins regulating MHC-I expression, or APM components, are responsible for the irreversible changes in surface MHC-I expression detected in approximately one-third of human tumors (4). An analysis of genomic datasets generated from thousands of solid tumors including samples of 18 tumor types revealed an association of immune cytolytic activity based on granzyme A and perforin expression with mutations in the invariant MHC-I chain (β-2 microglobulin) and MHC-I (HLA) loci (5), further confirming that reduced production of MHC-I molecules is an important mechanism of tumor immune evasion. However, despite the frequency and clinical importance of MHC-I downregulation, overcoming this escape mechanism by cancer immunotherapy has not been sufficiently investigated.

The efficacy of cancer immunotherapy may be enhanced by a combination of different immunotherapeutic approaches that include activation of both adaptive and innate immunity and inhibition of immunosuppressive mechanisms (6,7). Such combinations have achieved a notable antitumor effect in preclinical models (8,9). However, although some mechanisms contributing to the antitumor effect are MHC-I-independent, the association of MHC-I expression on tumor cells with treatment efficacy has not been investigated. In our previous study, we examined combined immunotherapy of tumors induced in mice by the TC-1/A9 cells characterized by reversible MHC-I

downregulation (10), and found that the combination of DNA immunization with either α-galactosylceramide (GalCer) or the synthetic oligodeoxynucleotide ODN1826, carrying immunostimulatory CpG motifs, induced temporary tumor regression. $CD8^+$ T cells, IFN-γ, and $NK1.1^+$ cells were involved in this response. For ODN1826, antitumor activity of M1-polarized macrophages was also suggested.

In the present study, TC-1/dB2m cells with a deactivated β-2 microglobulin gene (*B2m*) were developed as a model of tumor cells with irreversible MHC-I downregulation in order to examine tumor growth, immune cell infiltration and sensitivity to immunotherapy by DNA vaccination combined with ODN1826 injection.

Materials and methods

Animals. A total of 250 female C57BL/6NCrl mice (7-8-weeks-old and weighing 17-22 g) were obtained from Charles River Laboratories to be used in animal experiments after at least 2 weeks of acclimatization. The mice were housed (n=5 per cage) and maintained under specific pathogen-free conditions and a 12/12-h light/dark cycle in a temperature-controlled room (20-24˚C) with a relative humidity of 50-60%. The animals had access to food and water *ad libitum*. All animal handling procedures complied to the guidelines for the proper treatment of laboratory animals at the Czech Center for Phenogenomics (BIOCEV).

Cell lines. TC-1 tumor cells (Cellosaurus ID: CVCL_4699; kindly provided by T.-C. Wu, Johns Hopkins University) were prepared by transformation of C57BL/6 mouse primary lung cells with human papillomavirus (HPV) 16 *E6*/*E7* oncogenes and activated *H-ras* (11). TC-1/A9 cells with reversibly downregulated MHC-I expression were derived from TC-1 cells as described previously (12). The cells were grown in high-glucose Dulbecco's modified Eagle's medium (DMEM; Sigma-Aldrich; Merck KGaA) supplemented with 10% fetal bovine serum (Biosera), 2 mM L-glutamine, 100 U/ml penicillin and 100 µg/ml streptomycin.

Plasmids. The pBSC (13) and pBSC/PADRE.E7GGG (14) plasmids were used in immunization experiments. The pBSC/PADRE.E7GGG plasmid contains the HPV16 *E7* oncogene with three point mutations in the pRb-binding site (E7GGG) (13) and the helper Pan HLA-DR reactive epitope (PADRE) designed *in silico* (15).

Deactivation of B2m with the CRISPR/Cas9 system. The deactivation of the *B2m* gene was performed with the GeneArt CRISPR Nuclease Vector Kit (Thermo Fisher Scientific, Inc.). The target site 5'-CCGAGCCCAAGACCGTCTAC-3' located in exon 2 was designed using an online software (http://crispr.mit.edu/) and cloned into the CRISPR nuclease vector as the corresponding annealed oligonucleotides synthetized by Integrated DNA Technologies. The resultant plasmid was multiplied in *Escherichia coli* XL-1 Blue cells, isolated by the NucleoSpin Plasmid Kit (Macherey-Nagel), and verified by sequencing with the BigDye Terminator v3.1 Cycle Sequencing Kit (Applied Biosystems; Thermo Fisher Scientific, Inc.). This plasmid was transfected into TC-1 cells by Lipofectamine 2000 (Invitrogen; Thermo Fisher Scientific, Inc.). The cells carrying the transfected vector were selected by magnetic beads (Dynabeads FlowComp Human CD4; Thermo Fisher Scientific, Inc.) based on the human *CD4* reporter gene encoded by the vector. Clones were prepared from isolated cells and analyzed by flow cytometry for MHC-I and β-2 microglobulin surface expression. The resultant clone with the deactivated *B2m* gene was designated as TC-1/dB2m.

Treatment with IFN-γ. Cells were stimulated with 200 U/ml mouse recombinant IFN-γ (PeproTech, Inc.) for 48 h.

Flow cytometry. Cells grown in tissue culture were harvested with trypsin, washed with PBS, and stained with the following monoclonal antibodies diluted in FACS buffer (2% fetal bovine serum and 0.03% sodium azide in PBS) at 4˚C for 30 min: FITC-labeled mouse anti-B2m (clone S19.8; 1:100 dilution; Santa Cruz Biotechnology, Inc.), FITC-labeled mouse anti-mouse $H\text{-}2K^b$ (clone CTKb; 1:200 dilution; BD Pharmingen; BD Biosciences), FITC-labeled mouse anti-mouse $H\text{-}2D^b$ (clone 28-14-8; 1:400 dilution; BD Pharmingen; BD Biosciences), or PE-labeled rat anti-mouse CD1d (clone 1B1; 1:100 dilution; BD Pharmingen; BD Biosciences). Subsequently, the cells were washed twice and measured on an LSRFortessa flow cytometer (BD Biosciences). The results were analyzed using FlowJo software v10.5.3 (BD Biosciences).

For analysis of tumor-infiltrating cells, single-cell suspensions were prepared from tumors with a longest diameter of 5-10 mm by using the gentleMACS Octo Dissociator (Miltenyi Biotec, GmbH), as described previously (16). The obtained cells were stained with two panels of fluorescence-labeled antibodies (Table I) to identify several subpopulations of lymphoid and myeloid cells (gating strategy in Figs. S1 and S2, respectively). Viability staining was performed with Fixable Viability Dye eFluor 455UV (eBioscience; Thermo Fisher Scientific, Inc.) in PBS, prior to surface staining. To detect the nuclear Foxp3 transcription factor, the cells were treated with Fixation/Permeabilization Concentrate (eBioscience; Thermo Fisher Scientific, Inc.) diluted 1:3 with Fixation/Permeabilization Diluent (eBioscience; Thermo Fisher Scientific, Inc.). Fixation and permeabilization were followed by a washing step with permeabilization buffer (eBioscience; Thermo Fisher Scientific, Inc.) and Foxp3 staining.

In vitro cell proliferation assay. Approximately half a million live cells were seeded into three 10-cm dishes. The cells were counted after 24, 48 or 72 h (one dish at each interval) using a hemocytometer. Proliferation was evaluated by non-linear regression for exponential growth. Calculations were performed using Prism 8 software (GraphPad Software, Inc.).

Preparation of gene gun cartridges. Plasmid DNA was coated onto 1-µm gold particles (Bio-Rad Laboratories. Inc.) according to the manufacturer's recommendations. Each cartridge contained 1 µg DNA coated onto 0.5 mg of gold particles (13).

Oncogenicity of TC-1/dB2m cells. Counts of $3x10^4$, $1x10^5$ or $3x10^5$ TC-1/dB2m cells suspended in 0.15 ml PBS were subcutaneously (s.c.) inoculated into the backs of mice (n=5 per

Table I. Antibodies used for flow cytometry.

Antigen	Conjugate	Clone	Source	Staining	Panels	
CD11b	BV421	M1/70	BioLegend	Surface		[a]
CD11c	APC-Cy7	N418	BioLegend	Surface		[a]
CD25	APC	PC61.5	eBiosciences	Surface	[a]	
CD3	APC-Cy7	145-2C11	BioLegend	Surface	[a]	
CD317	APC	927	BioLegend	Surface		[a]
CD4	BV510	RM4-5	BioLegend	Surface	[a]	
CD45	Alexa Fluor 700	30-F11	BioLegend	Surface	[a]	[a]
CD8	FITC	53-6.7	BD Pharmingen	Surface	[a]	
F4/80	BV510	BM8	BioLegend	Surface		[a]
Foxp3	PE	FJK-16s	eBiosciences	Nuclear	[a]	
Ly6C	BV786	HK1.4	BioLegend	Surface		[a]
Ly6G	FITC	1A8	BioLegend	Surface		[a]
MHC-II	PE-Cy7	114.15.2	BioLegend	Surface		[a]
NK1.1	BV650	PK136	BioLegend	Surface	[a]	
PD-1	PE-Cy7/PE[b]	29F.1A12	BioLegend	Surface	[a]	[b]
PD-L1	BV650	10F.9G2	BioLegend	Surface		[a]
TCR γ/δ	BV605	GL3	BioLegend	Surface	[a]	

[a,b], Antibody present in a panel.

group) under anesthesia with ketamine (100 mg/kg) and xylazine (16 mg/kg). Tumor growth was measured three times per week, and tumor size was calculated using the formula (height x length x width) π/6. To determine the effect of *B2m* deactivation on the metastatic capacity of the TC-1-derived cells, the mice were s.c. injected with $3x10^5$ TC-1/dB2m cells. When the size of the tumors reached 2 cm in any of the measured dimensions, the mice were sacrificed by cervical dislocation and dissected. The lungs were inspected for macrometastases, stained with hematoxylin and eosin, and examined under a light microscope in the Czech Center for Phenogenomics to detect micrometastases.

Immunization experiments. The mice were immunized using a gene gun (Bio-Rad Laboratories, Inc.) three times with two shots each delivering 1 μg of plasmid DNA. The DNA was applied into the shaven skin of the abdomen at a discharge pressure of 400 psi. In preventive immunization experiments, mice (n=5 per group) were first immunized with the pBSC/PADRE.E7GGG plasmid at 1-week interval. The pBSC plasmid was used as a negative control. One week after the last immunization, $3x10^5$ TC-1 or TC-1/dB2m cells or $3x10^4$ TC-1/A9 cells were s.c. inoculated into the backs of the mice. In the combined immunotherapy experiments, $3x10^5$ TC-1/dB2m cells were s.c. injected and DNA immunization was performed after 3, 6 and 10 days. DNA vaccination was combined with an intraperitoneal (i.p.) injection of 50 μg ODN1826 (Generi Biotech) or 2 μg GalCer (Abcam) diluted in 200 μl PBS. These immunostimulants were injected in three or five doses, as indicated in Fig. 3. Control mice received PBS.

In vivo depletion experiments. Different subpopulations of immune cells were depleted with the following antibodies (Bio X Cell) injected i.p. in a volume of 200 μl of PBS: 100 μg anti-CD4 (clone GK1.5), 100 μg anti-CD8 (clone 2.43), or 100 μg anti-NK1.1 (clone PK136). These antibodies were applied 2 days before and after inoculation of tumor cells ($3x10^4$ TC-1 cells or $3x10^5$ TC-1/dB2m cells), and then at 3-4-day intervals for 5 weeks. Moreover, 1 mg carrageenan IV (Sigma-Aldrich; Merck KGaA) dissolved in 200 μl PBS was inoculated on the same days to deplete macrophages. For neutralization of IFN-γ, 300 μg anti-IFN-γ (clone P4-6A2; Bio X Cell) was injected 2 days prior and 5, 12, 19 and 26 days after tumor cell inoculation.

In immunotherapeutic experiments, antibodies and carrageenan were administered from the 7th day onwards after inoculation of tumor cells.

Statistical analysis. Cell proliferation and tumor growth were evaluated by two-way analysis of variance (ANOVA) and the Sidak multiple comparisons test. Intergroup comparisons of flow cytometry data were made by one-way ANOVA and Dunnett's multiple comparisons test. Calculations were performed using GraphPad Prism 8 (GraphPad Software, Inc.), and the results were considered statistically significant at $P<0.05$.

Results

In vitro characterization of the TC-1 clone with B2m gene deactivation. To abrogate MHC-I expression on TC-1 tumor cells, the *B2m* gene was deactivated by the CRISPR/Cas9 system and the TC-1/dB2m cell line was derived. These cells did not express β-2 microglobulin or MHC-I heavy chains on their surface (Fig. 1A). Following stimulation with IFN-γ, β-2 microglobulin was still absent on TC-1/dB2m cells, but weak MHC-I expression was induced, particularly for H-$2D^b$ molecules.

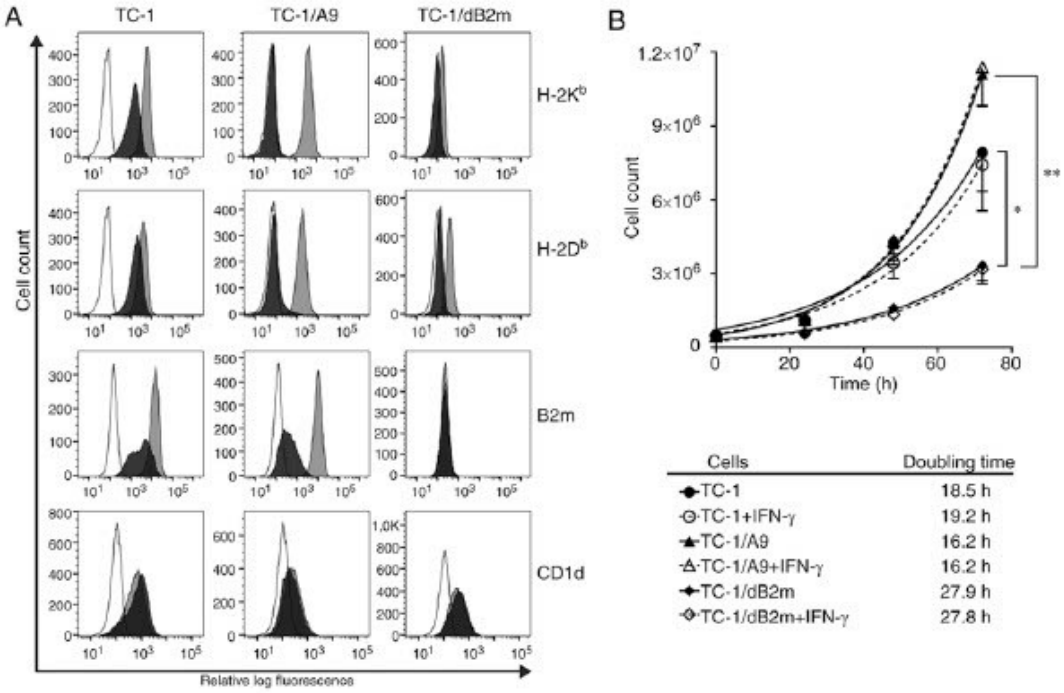

Figure 1. *In vitro* characterization of TC-1/dB2m cells. (A) Surface expression of H-2K^b, H-2D^b, β-2 microglobulin (B2m) and CD1d molecules on TC-1, TC-1/A9 and TC-1/dB2m cells was analyzed by flow cytometry. Cells untreated (black histograms) or treated (grey histograms) with 200 U/ml of interferon (IFN)-γ for 48 h were stained with specific monoclonal antibodies or isotype control antibodies (open histograms). (B) *In vitro* proliferation of TC-1, TC-1/A9 and TC-1/dB2m cells was determined at 24, 48 and 72 h after seeding on dishes with or without IFN-γ. The results represent the mean values of three independent experiments. Bars, ± standard error of the mean; $^*P<0.05$, $^{**}P<0.01$.

As β-2 microglobulin also forms a complex with the CD1d molecules expressed on the cell surface and CD1d expression has been demonstrated on TC-1 and TC-1/A9 cells (17), CD1d expression was detected on TC-1/dB2m cells. *B2m* deactivation did not prevent surface expression of the CD1d molecules (Fig. 1A).

Next, the proliferation rates of TC-1/dB2m, TC-1 and TC-1/A9 cells were compared. The doubling time of TC-1/dB2m cells was significantly increased by ~9 and 11 h in comparison with TC-1 and TC-1/A9 cells, respectively (Fig. 1B). Incubation with IFN-γ slightly reduced TC-1 cell proliferation, but did not affect TC-1/A9 and TC-1/dB2m cells.

In summary, deactivation of the *B2m* gene in the TC-1/dB2m cell line resulted in abrogation of β-2 microglobulin production and downregulation of surface MHC-I expression, which was associated with reduced proliferation rate.

Deactivation of the B2m gene alters oncogenicity/immunogenicity of tumor cells. To induce tumor formation, mice were inoculated s.c. with $3x10^4$ TC-1 or TC-1/A9 cells. As a pilot experiment demonstrated delayed growth of tumors induced by this number of TC-1/dB2m cells, we also tested inoculation using higher numbers: $1x10^5$ and $3x10^5$ TC-1/dB2m cells (Fig. 2A). However, even for the highest TC-1/dB2m cell number ($3x10^5$), tumor growth was delayed by ~20 days compared with tumors induced by $3x10^4$ TC-1 cells. Moreover, tumors developing from TC-1/dB2m cells were more elongated in comparison with TC-1-induced tumors, particularly at the early growth phase. Spontaneous lung metastasis formation was not observed after s.c. induced tumors.

To identify the immune cells that could inhibit the growth of TC-1/dB2m-induced tumors, some subpopulations were depleted *in vivo* by monoclonal antibodies (Fig. 2B). For TC-1-induced tumors, CD8$^+$ and NK1.1$^+$ cells were found to contribute to the reduction of tumor growth, and macrophages supported this growth. NK1.1$^+$ cells also inhibited TC-1/A9 and TC-1/dB2m tumors, but there was no involvement of CD8$^+$ cells or macrophages. In all types of tumors, the depletion of CD4$^+$ cells or neutralization of IFN-γ did not significantly affect tumor growth (the antitumor effect of IFN-γ was only apparent during the initial phase of the growth of TC-1 tumors).

Next, the sensitivity of TC-1/dB2m-induced tumors to adaptive immunity activated against the HPV16 E7 oncoprotein was evaluated. While TC-1 tumors are highly sensitive to therapeutic DNA immunization by the PADRE.E7GGG vaccine (14), the sensitivity of TC-1/A9 tumors to DNA vaccination is low (10). After more efficient preventive immunization with the PADRE.E7GGG gene, the growth of TC-1/A9-induced tumors was significantly reduced, but the TC-1/dB2m tumors were resistant to DNA vaccination (Fig. 2C). The development of control TC-1 tumors was inhibited in all mice.

Collectively, these findings indicate that deactivation of the *B2m* gene resulted in delayed tumor growth and resistance to adaptive immunity.

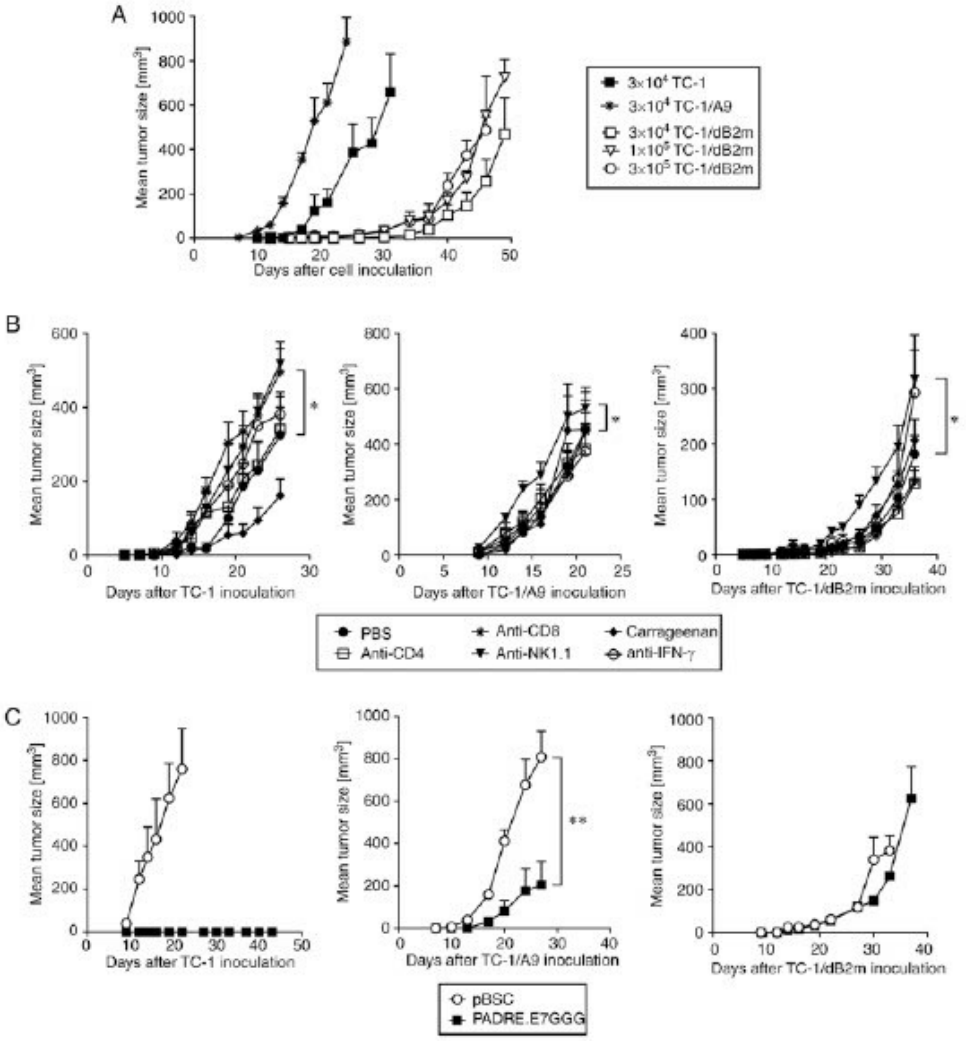

Figure 2. *In vivo* characterization of TC-1/dB2m cells. (A) Tumor growth in mice (n=5) was evaluated after s.c. inoculation. (B) Immune cells involved in inhibition of tumor growth were analyzed by *in vivo* depletion with anti-CD4, anti-CD8 and anti-NK1.1 antibodies and carrageenan IV. The effect of interferon (IFN)-γ was examined by neutralization with anti-IFN-γ. PBS was used as control. (C) Sensitivity to DNA immunization was tested in mice preimmunized three times with the PADRE.E7GGG vaccine. Empty pBSC plasmid and parental TC-1 cells were used as controls. Tumor growth was measured three times per week. Bars, ± standard error of the mean; *P<0.05, **P<0.01.

TC-1/dB2m cells are slightly sensitive to combined immunotherapy. As combinations of DNA vaccination with i.p. injection of ODN1826 or GalCer reduced tumor growth of TC-1/A9 cells (10), these immunotherapies were also examined against TC-1/dB2m cells. However, only a weak antitumor effect was observed (Fig. 3A). Due to the delayed growth of TC-1/dB2m tumor, and in an attempt to enhance antitumor immunity, the interval between the injections of immunostimulatory drugs was prolonged and the number of ODN1826 doses was increased from three to five. Although these modifications only exerted a weak effect, a significant reduction of tumor growth was achieved by ODN1826 combined with DNA immunization (Fig. 3B). This experiment also demonstrated that a combination of DNA vaccination with ODN1826 or GalCer was necessary for the antitumor response, as either therapy alone did not result in tumor reduction. Thus, repeated experiments suggested a weak inhibition of tumor development following combined immunotherapy, and this effect was more obvious for ODN1826.

NK1.1⁺ cells mainly contribute to the antitumor effect of combined immunotherapy. In order to identify the immune cells involved in the antitumor response to combined therapy against TC-1/dB2m tumors, tumor-infiltrating cells were first analyzed by flow cytometry using two panels of monoclonal antibodies. In this experiment, tumor-infiltrating cells in TC-1- and TC-1/A9-induced tumors were also compared. The numbers of CD45⁺ cells in the tumors were comparable for

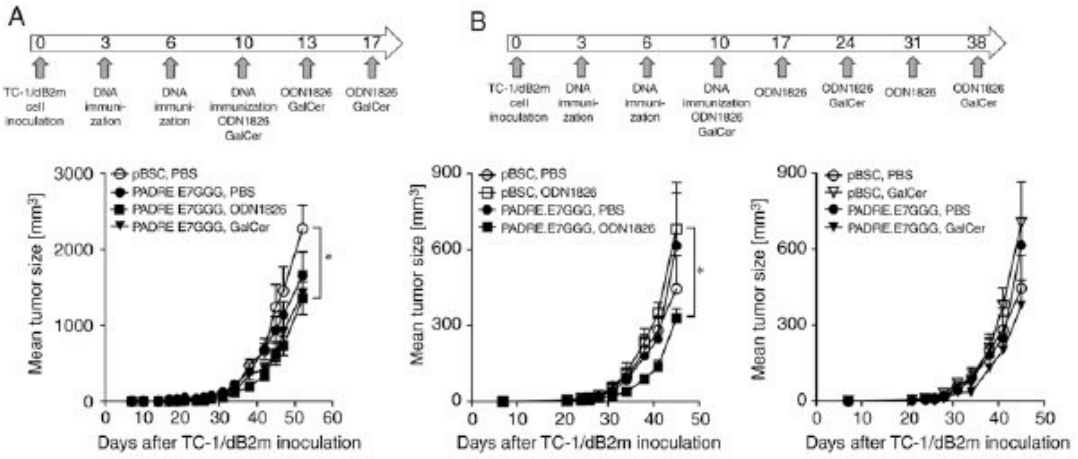

Figure 3. Antitumor effect of DNA vaccination combined with either ODN1826 or GalCer. Adjuvants were administered 10-17 days (A) or 10-38 days (B) after inoculation of tumor cells. pBSC and PBS were used as controls. Tumor growth was measured three times a week. Bars, ± standard error of the mean; *P<0.05.

all three cell lines examined, and did not change after therapy of TC-1/dB2m-induced tumors. In tumors that developed from TC-1/dB2m cells, $CD3^+$ cells comprised a significantly higher proportion of $CD45^+$ cells (~11%) that was not altered following immunotherapy (Fig. 4A).

Among lymphoid cells (Fig. 4B), NK cells ($CD3^-NK1.1^+$) were predominant in all types of tumors, but their proportion was significantly lower in TC-1/dB2m compared with that in TC-1/A9 tumors (accounting for 13 and 30% of $CD45^+$ cells, respectively). On the contrary, the proportion of $CD4^+$ T cells and γδ T cells was significantly higher in TC-1/dB2m tumors compared with those in TC-1/A9 and TC-1 tumors. Regulatory T cells (Treg; $CD4^+CD25^+Foxp3^+$) were partially responsible for the increase in $CD4^+$ T cells. The numbers of NKT cells ($CD3^+TCR\gamma/\delta^-NK1.1^+$) were also higher in TC-1/dB2m tumors, but this difference was not significant. After immunotherapy of TC-1/dB2m tumors, the proportion of any lymphoid subpopulation was not significantly altered. Significantly enhanced PD-1 expression was only observed on NK and NKT cells.

Tumor-associated macrophages (TAMs; $CD11b^+Ly6G^-Ly6C^-F4/80^+$) comprised a major subpopulation of myeloid cells in all types of tumors (Fig. 4C). In TC-1/dB2m tumors, their numbers were significantly lower compared with those in TC-1 and TC-1/A9 tumors, but they expressed a higher level of MHC-II molecules that are considered a marker of M1-polarized macrophages (18,19). Following immunotherapy of TC-1/dB2m tumors, the numbers of macrophages and their PD-1 expression were slightly enhanced. In TC-1/dB2m tumors generated in non-treated mice, the populations of dendritic cells, both conventional (cDC; $CD11c^+Ly6G^-Ly6C^-F4/80^-MHC\text{-}II^+$) and plasmacytoid (pDC; $CD11c^+CD11b^-Ly6G^-Ly6C^+F4/80^-MHC\text{-}II^+CD317^+$), were significantly higher compared with those in TC-1 and TC-1/A9 tumors and were not altered after immunotherapy. The numbers of myeloid-derived suppressor cells ($CD11c^+CD11b^+Ly6G^-Ly6C^{high}$) and tumor-associated neutrophils ($CD11b^+Ly6G^{high}Ly6C^{low}$) were comparable in all types of tumors.

Next, we examined cells involved in antitumor immunity by *in vivo* depletion. In mice treated with immunotherapy (DNA vaccination plus injection of ODN1826), tumor growth was significantly enhanced only after elimination of $NK1.1^+$ cells (Fig. 4D). Neutralization of IFN-γ suggested that this cytokine played a crucial role in the antitumor effect. After depletion of $CD8^+$ cells, tumor growth was comparable to that in mice treated with anti-$NK1.1^+$ until day 27 after inoculation of tumor cells. Subsequently, the growth of tumors was similarly reduced in animals with depleted $CD8^+$ cells and administered immunotherapy alone.

In summary, combined immunotherapy of TC-1/dB2m-induced tumors did not result in significantly increased immune cell infiltration. $NK1.1^+$ cells and IFN-γ contributed to the weak antitumor effect. Enhanced expression of the PD-1 receptor on NK and NKT cells suggests that both types of cells may be involved in this effect.

Discussion

The production of β-2 microglobulin is often abrogated by genetic alterations in human tumors (20). As these modifications lead to irreversible downregulation of surface MHC-I expression that is associated with resistance to $CD8^+$ cytotoxic T lymphocytes (CTLs), they enable evasion of adaptive immune responses generated during tumor development or induced by immunotherapy. Such resistance has also been demonstrated for a blockade of the PD-1 immune checkpoint by a monoclonal antibody (21). Therefore, the development of relevant tumor models is necessary for studies of experimental cancer immunotherapy that may result in enhancement of clinical trial efficacy.

The CRISPR/Cas9 system has been recently used for the deactivation of the *B2m* gene in two mouse tumor cell lines, namely melanoma B16F10 and breast cancer EO-771 cells (22). In the present study, the *B2m* gene was deactivated in the mouse TC-1 cell line, which is often used to examine various cancer therapies. *B2m* deactivation in TC-1/dB2m

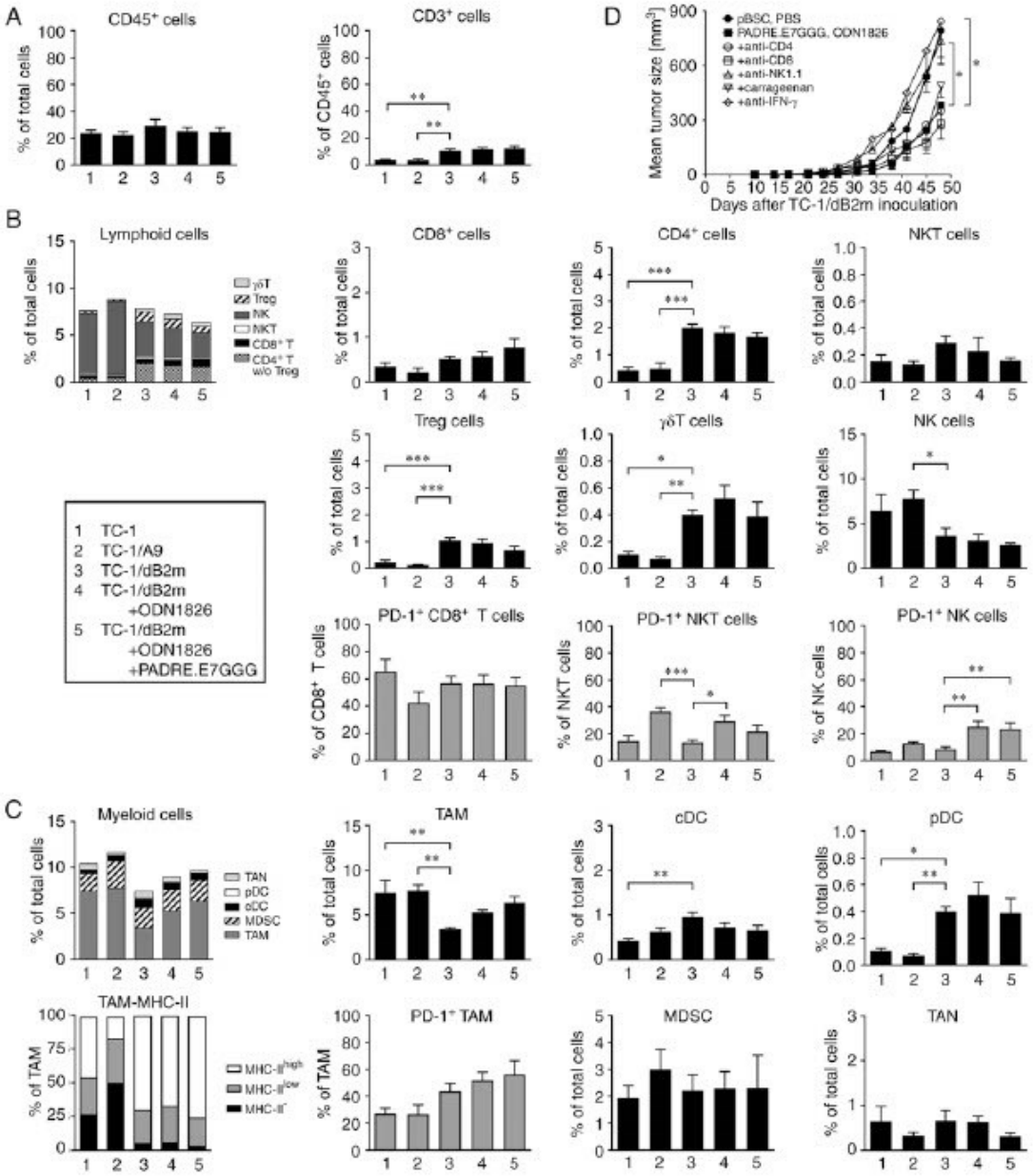

Figure 4. Immune cells contributing to the antitumor effect. (A-C) The cells infiltrating tumors induced by TC-1, TC-1/A9, or TC-1/dB2m cells were analyzed by flow cytometry. For TC-1/dB2m cells, tumors after immunotherapy with ODN1826 and DNA vaccination with PADRE.E7GGG were also examined. Using two panels of monoclonal antibodies, (B) lymphoid and (C) myeloid subpopulations were identified. (D) Infiltrating immune cells contributing to the reduction of tumor growth after combined immunotherapy with ODN1826 and PADRE.E7GGG were identified by *in vivo* depletion. Interferon (IFN)-γ was also neutralized. Bars, ± standard error of the mean; *P<0.05, **P<0.01, ***P<0.001.

cells was associated with loss of surface MHC-I expression, but when inducibility by IFN-γ was tested, a slight restoration of MHC-I expression on the cell surface, particularly of molecules from the D locus, was observed. As β-2 microglobulin expression remained negative, it was hypothesized that β-2 microglobulin-free MHC-I heavy chains were displayed on the cells. Such molecules, particularly H-2D^{b}, have been reported for both β-2 microglobulin-negative and -positive mouse cells (23-25); however, the role of IFN-γ stimulation was not described in these studies. In a human neuroblastoma cell line producing β-2 microglobulin, the expression of β-2 microglobulin-free MHC-I molecules was enhanced upon differentiation with either retinoic acid or serum starvation. Incubation with IFN-γ increased the surface expression of

MHC-I heterodimers, but not of β-2 microglobulin-free MHC-I molecules (26). In concordance with the published results (27), the present study demonstrated that *B2m* deactivation did not prevent CD1d surface expression.

Deactivation of the *B2m* gene significantly reduced the proliferation of TC-1/dB2m cells and the growth of TC-1/dB2m-induced tumors. These results correspond to the findings that β-2 microglobulin promotes cell proliferation, migration, and invasion in different tumor types (28,29). A key role in this β-2 microglobulin-mediated signaling was attributed to its binding with hemochromatosis (HFE) protein, a non-classical MHC-I molecule that regulates iron concentration in cells. Following formation of the β-2 microglobulin/HFE complex, iron influx is inhibited and numerous intracellular pathways are affected (30).

A reduced proliferation rate may contribute to the delay in tumor growth, but does not appear to be a crucial factor responsible for the substantially decreased oncogenicity of TC-1/dB2m cells. As *in vivo* depletion was associated with partial restoration of tumor growth after application of NK1.1-specific antibody, enhanced sensitivity to elimination by NK cells may be more important. Das *et al* (22) observed a similar reduction of oncogenicity following *B2m* deactivation in two mouse tumor cell lines and also suggested a role of NK cells in this phenomenon.

The effect of MHC-I downregulation after *B2m* deactivation was also manifested by the loss of sensitivity to depletion of $CD8^+$ cells and to adaptive immunity induced by DNA immunization and mediated by CTLs. As similar effects were observed for TC-1/A9 cells, where a combination of DNA immunization and an adjuvant (ODN1826 or GalCer) significantly reduced tumor growth (10), the efficacy of this combined immunotherapy was also examined against TC-1/dB2m tumors. However, only the combination of DNA vaccination and ODN1826 injection significantly inhibited tumor growth, and this effect was less notable compared with that against TC-1/A9-induced tumors.

Flow cytometric analysis of tumor-infiltrating immune cells and *in vivo* depletion after immunotherapy revealed several marked differences between TC-1/dB2m and TC-1/A9 tumors: i) TC-1/dB2m tumors contained more pDCs, $CD4^+$ T, Treg, and γδ T cells, but fewer TAMs and NK cells. However, this observation should be interpreted with caution, as infiltration of tumors with immune cells is a dynamic process with specific kinetics of individual subpopulations (8,31-33), which hampers a direct comparison among tumors induced by different cells. Although we strived to analyze tumors of similar size, the composition of the cell infiltrate may be affected by the markedly different growth of TC-1-, TC-1/A9- and TC-1/dB2m-induced tumors. ii) Following combined immunotherapy, none of the examined subpopulations of infiltrating immune cells was increased in the TC-1/dB2m tumors, while in the TC-1/A9 tumors, most subpopulations were increased, particularly $CD8^+$ T cells (10). iii) MHC-II^{high} TAMs were predominant in TC-1/dB2m tumors, even without immunotherapy (while in the TC-1/A9 tumors, they were predominant only after immunotherapy). Reduced numbers of M2 TAMs were mainly responsible for this effect. Movahedi *et al* reported similar results for the 4T1 cell line (18). Progressing tumors induced by these cells accumulated MHC-II^{high} TAMs, in contrast to tumors induced by 3LL or TS/A cells, and these TAMs remained M1 polarized. Therefore, it was concluded that the proportions of TAM subsets were tumor-dependent. iv) For TC-1/A9 tumors, $NK1.1^+$ cells, $CD8^+$ cells and TAMs cooperated in the antitumor response, but only $NK1.1^+$ cells were significantly implicated in the delay of TC-1/dB2m tumor growth. Enhanced PD-1 expression on both NK and NKT cells after immunotherapy suggested activation of both cell types by treatment and their possible involvement in antitumor immunity.

By using *in vivo* depletion of $CD8^+$, $CD4^+$ and $NK1.1^+$ cells, studies comparing immunotherapy against TC-1 cells and TC-1 clones with reversible MHC-I downregulation demonstrated that only $CD8^+$ T cells were necessary for the antitumor effect against TC-1 cells, and that both $CD8^+$ and $NK1.1^+$ cells may be involved in the inhibition of tumors induced by cells with reversibly downregulated MHC-I expression (34,35), which was confirmed in our previous study with TC-1/A9 cells (10). This study extended these observations for the TC-1 clone with irreversible MHC-I downregulation, demonstrating that $NK1.1^+$ cells were the most important for the antitumor effect stimulated by immunotherapy against TC-1/dB2m cells. For TC-1-induced tumors, two other studies demonstrated the cooperation of $CD8^+$ T cells with other immune cells in the antitumor response after immunotherapy, but suggested that $CD8^+$ T cells were not the main cytotoxic cells eliminating MHC-I-proficient TC-1 cells (8,36). Our study with TC-1/A9 cells, which are deficient in MHC-I expression, also demonstrated a role of $CD8^+$ T cells activated by DNA vaccination in the antitumor response (10). However, in the present study, despite the fact that DNA vaccination was necessary for the induction of the antitumor effect by combined immunotherapy, the level of $CD8^+$ T cells in the tumors was not increased by treatment, and the function of $CD8^+$ T cells was not proven by *in vivo* depletion. The only observation suggesting the involvement of $CD8^+$ T cells was derived from the *in vivo* depletion experiment, where augmented tumor growth was recorded at the initial phase of tumor development (up to day 27) following application of anti-CD8. As tumor infiltration by immune cells is a dynamic process (8), this fact should be confirmed by further studies investigating a more efficient immunotherapy against TC-1/dB2m cells, which may also help elucidate the role of $CD8^+$ T cells and other immune cells in this tumor model.

As combined immunotherapy only weakly inhibited the growth of TC-1/dB2m tumors and did not affect infiltration of these tumors by immune cells, immunosuppressive mechanisms most likely prevail in the microenvironment of early-stage tumors. This condition resembles human MHC-I-negative tumors that are often devoid of immune cells in the tumor parenchyma and contain unfunctional immune cells in the tumor stroma (37,38). Therefore, for successful immunotherapy of such tumors, activation of adaptive and innate immunity should be accompanied by appropriate inhibition of immunosuppression and recovery of MHC-I expression (4,39,40).

The mechanisms of immune reactions against TC-1/dB2m-induced tumors were not completely elucidated in the present study, and will be the subject of further analyses. The present results suggest that, following immunotherapy, $NK1.1^+$ cells were the major cell type exhibiting

antitumor activity against TC-1/dB2m tumors. The possible involvement of both NK and NKT cells was indicated by enhanced PD-1 expression, which suggested the activation and subsequent inactivation of these cells. The antitumor effect of NKT cells, which constitute a minor subpopulation of NK1.1$^+$ cells, was also suggested by immunotherapy with GalCer, as this adjuvant activates NKT cells. However, NK cells are likely the main effector cells, as they can eliminate tumor cells with downregulated MHC-I expression. Unfortunately, they can also contribute to tumor immune evasion (41). The antitumor effect of ODN1826 may not be dependent on adaptive immunity (42); however, DNA immunization was necessary for the reduced growth of TC-1/dB2m tumors. The role of CD8$^+$ T cells in antitumor reactions was not clearly confirmed by *in vivo* depletion, but this experiment indicated the effect of these cells during early tumor growth. At a later stage of tumor development, CD8$^+$ T cells are likely inactivated by the immunosuppressive tumor microenvironment (43).

In conclusion, deactivation of the *B2m* gene led to the creation of the TC-1/dB2m cell line, which is characterized by irreversible MHC-I downregulation, and a reduced proliferation rate and tumor growth. These cells displayed loss of sensitivity to DNA immunization and, in comparison to the TC-1/A9 cells with reversible MHC-I downregulation, they responded more weakly to combined immunotherapy consisting of DNA vaccination and either ODN1826 or GalCer injection. Moreover, infiltration of TC-1/dB2m tumors with immune cells was not enhanced after immunotherapy, and only NK1.1$^+$ cells were confirmed to contribute to the antitumor effect. In a set with TC-1 and TC-1/A9 cells, the TC-1/dB2m cell line may be utilized for enhancement of cancer immunotherapy with a potentially high clinical benefit, as human tumors are heterogeneous in terms of MHC-I expression, which enables evasion of the immune response and confers resistance to therapy.

Acknowledgements

The authors would like to thank Pavlina Vesela, Kristyna Klecakova and Nela Vaclavikova for technical assistance. We also acknowledge the Imaging Methods Core Facility at BIOCEV for their support with obtaining the flow cytometry data presented in this article.

Funding

The present study was funded by the Czech Science Foundation (grant nos. GA16-04477S and GA19-00816S); the European Regional Development Fund (grant nos. CZ.02.1.01/0.0/0.0/16_019/0000785, CZ.1.05/1.1.00/02.0109, CZ.1.05/2.1.00/19.0400 and CZ.1.05/2.1.00/19.0395); the Ministry of Education, Youth and Sports of the Czech Republic (grant nos. LQ1604 and LM2015040); and Charles University (grant no. SVV-2017-260426).

Availability of data and materials

All data generated or analyzed during the present study are included in this published article.

Authors' contributions

MS conceived and designed the study. KL, AG, IP, JV and MS performed the experiments. MS, IP, KL and JV analyzed and interpreted the data. KL, MS and IP wrote the manuscript. All authors have read and approved the final version of this manuscript for publication.

Ethics approval and consent to participate

All animal experimental procedures were performed in compliance with Directive 2010/63/EU, and animal protocols were approved by the Sectoral Expert Committee of the Czech Academy of Sciences for Approval of Projects of Experiments on Animals (reference no. 46/2016, 16 May 2016).

Patient consent for publication

Not applicable.

Competing interests

The authors declare that they have no competing interests.

References

1. Khong HT and Restifo NP: Natural selection of tumor variants in the generation of 'tumor escape' phenotypes. Nat Immunol 3: 999-1005, 2002.
2. Garrido F, Ruiz-Cabello F and Aptsiauri N: Rejection versus escape: The tumor MHC dilemma. Cancer Immunol Immunother 66: 259-271, 2017.
3. Reinis M: Immunotherapy of MHC class I-deficient tumors. Future Oncol 6: 1577-1589, 2010.
4. Garrido F, Aptsiauri N, Doorduijn EM, Garcia Lora AM and van Hall T: The urgent need to recover MHC class I in cancers for effective immunotherapy. Curr Opin Immunol 39: 44-51, 2016.
5. Rooney MS, Shukla SA, Wu CJ, Getz G and Hacohen N: Molecular and genetic properties of tumors associated with local immune cytolytic activity. Cell 160: 48-61, 2015.
6. Smyth MJ, Ngiow SF, Ribas A and Teng MW: Combination cancer immunotherapies tailored to the tumour microenvironment. Nat Rev Clin Oncol 13: 143-158, 2016.
7. Zappasodi R, Merghoub T and Wolchok JD: Emerging concepts for immune checkpoint blockade-based combination therapies. Cancer Cell 33: 581-598, 2018.
8. Thoreau M, Penny HL, Tan K, Regnier F, Weiss JM, Lee B, Johannes L, Dransart E, Le Bon A, Abastado JP, *et al*: Vaccine-induced tumor regression requires a dynamic cooperation between T cells and myeloid cells at the tumor site. Oncotarget 6: 27832-27846, 2015.
9. Moynihan KD, Opel CF, Szeto GL, Tzeng A, Zhu EF, Engreitz JM, Williams RT, Rakhra K, Zhang MH, Rothschilds AM, *et al*: Eradication of large established tumors in mice by combination immunotherapy that engages innate and adaptive immune responses. Nat Med 22: 1402-1410, 2016.
10. Grzelak A, Polakova I, Smahelova J, Vackova J, Pekarcikova L, Tachezy R and Smahel M: Experimental combined immunotherapy of tumours with major histocompatibility complex class I downregulation. Int J Mol Sci 19: E3693, 2018.
11. Lin KY, Guarnieri FG, Staveley-O'Carroll KF, Levitsky HI, August JT, Pardoll DM and Wu TC: Treatment of established tumors with a novel vaccine that enhances major histocompatibility class II presentation of tumor antigen. Cancer Res 56: 21-26, 1996.
12. Smahel M, Sima P, Ludvikova V, Marinov I, Pokorna D and Vonka V: Immunisation with modified HPV16 E7 genes against mouse oncogenic TC-1 cell sublines with downregulated expression of MHC class I molecules. Vaccine 21: 1125-1136, 2003.
13. Smahel M, Sima P, Ludvikova V and Vonka V: Modified HPV16 E7 genes as DNA vaccine against E7-containing oncogenic cells. Virology 281: 231-238, 2001.

14. Smahel M, Polakova I, Duskova M, Ludvikova V and Kastankova I: The effect of helper epitopes and cellular localization of an antigen on the outcome of gene gun DNA immunization. Gene Ther 21: 225-232, 2014.
15. Alexander J, Sidney J, Southwood S, Ruppert J, Oseroff C, Maewal A, Snoke K, Serra HM, Kubo RT and Sette A: Development of high potency universal DR-restricted helper epitopes by modification of high affinity DR-blocking peptides. Immunity 1: 751-761, 1994.
16. Kaštánková I, Poláková I, Dušková M and Šmahel M: Combined cancer immunotherapy against aurora kinase A. J Immunother 39: 160-170, 2016.
17. Simova J, Indrova M, Bieblová J, Mikyskova R, Bubeník J and Reinis M: Therapy for minimal residual tumor disease: β-galactosylceramide inhibits the growth of recurrent HPV16-associated neoplasms after surgery and chemotherapy. Int J Cancer 126: 2997-3004, 2010.
18. Movahedi K, Laoui D, Gysemans C, Baeten M, Stange G, Van den Bossche J, Mack M, Pipeleers D, In't Veld P, De Baetselier P and Van Ginderachter JA: Different tumor microenvironments contain functionally distinct subsets of macrophages derived from Ly6C(high) monocytes. Cancer Res 70: 5728-5739, 2010.
19. Mills CD and Ley K: M1 and M2 macrophages: The chicken and the egg of immunity. J Innate Immun 6: 716-726, 2014.
20. Bernal M, Ruiz-Cabello F, Concha A, Paschen A and Garrido F: Implication of the β2-microglobulin gene in the generation of tumor escape phenotypes. Cancer Immunol Immunother 61: 1359-1371, 2012.
21. Zaretsky JM, Garcia-Diaz A, Shin DS, Escuin-Ordinas H, Hugo W, Hu-Lieskovan S, Torrejon DY, Abril-Rodriguez G, Sandoval S, Barthly L, *et al*: Mutations associated with acquired resistance to PD-1 blockade in melanoma. N Engl J Med 375: 819-829, 2016.
22. Das K, Eisel D, Lenkl C, Goyal A, Diederichs S, Dickes E, Osen W and Eichmüller SB: Generation of murine tumor cell lines deficient in MHC molecule surface expression using the CRISPR/Cas9 system. PLoS One 12: e0174077, 2017.
23. Potter TA, Boyer C, Verhulst AM, Golstein P and Rajan TV: Expression of H-2Db on the cell surface in the absence of detectable beta 2 microglobulin. J Exp Med 160: 317-322, 1984.
24. Allen H, Fraser J, Flyer D, Calvin S and Flavell R: Beta 2-microglobulin is not required for cell surface expression of the murine class I histocompatibility antigen H-2Db or of a truncated H-2Db. Proc Natl Acad Sci USA 83: 7447-7451, 1986.
25. Bix M and Raulet D: Functionally conformed free class I heavy chains exist on the surface of beta 2 microglobulin negative cells. J Exp Med 176: 829-834, 1992.
26. Marozzi A, Meneveri R, Bunone G, De Santis C, Lopalco L, Beretta A, Agresti A, Siccardi AG, Della Valle G and Ginelli E: Expression of β2m-free HLA class I heavy chains in neuroblastoma cell lines. Scand J Immunol 37: 661-667, 1993.
27. Kim HS, Garcia J, Exley M, Johnson KW, Balk SP and Blumberg RS: Biochemical characterization of CD1d expression in the absence of beta2-microglobulin. J Biol Chem 274: 9289-9295, 1999.
28. Huang WC, Wu D, Xie Z, Zhau HE, Nomura T, Zayzafoon M, Pohl J, Hsieh CL, Weitzmann MN, Farach-Carson MC and Chung LW: Beta2-Microglobulin is a signaling and growth-promoting factor for human prostate cancer bone metastasis. Cancer Res 66: 9108-9116, 2006.
29. Nomura T, Huang WC, Zhau HE, Wu D, Xie Z, Mimata H, Zayzafoon M, Young AN, Marshall FF, Weitzmann MN and Chung LW: Beta2-microglobulin promotes the growth of human renal cell carcinoma through the activation of the protein cinase A, Cyclic AMP–responsive element-binding protein, and vascular endothelial growth factor axis. Clin Cancer Res 12: 7294-7305, 2006.
30. Nomura T, Huang WC, Zhau HE, Josson S, Mimata H and Chung LW: β2-Microglobulin-mediated signaling as a target for cancer therapy. Anticancer Agents Med Chem 14: 343-352, 2014.
31. Sneed RA, Stevenson AP and Stewart CC: Quantitation of the host cell infiltration kinetics of the nonimmunogenic colon 26 tumor by multiparameter flow cytometry. J Leukoc Biol 46: 547-555, 1989.
32. Kennedy BC, Maier LM, D'Amico R, Mandigo CE, Fontana EJ, Waziri A, Assanah MC, Canoll P, Anderson RC, Anderson DE and Bruce JN: Dynamics of central and peripheral immunomodulation in a murine glioma model. BMC Immunol 10: 11, 2009.
33. Bindea G, Mlecnik B, Tosolini M, Kirilovsky A, Waldner M, Obenauf AC, Angell H, Fredriksen T, Lafontaine L, Berger A, *et al*: Spatiotemporal dynamics of intratumoral immune cells reveal the immune landscape in human cancer. Immunity 39: 782-795, 2013.
34. Cheng WF, Hung CF, Lin KY, Ling M, Juang J, He L, Lin CT and Wu TC: CD8 + T cells, NK cells and IFN-gamma are important for control of tumor with downregulated MHC class I expression by DNA vaccination. Gene Ther 10: 1311-1320, 2003.
35. Indrová M, Símová J, Bieblová J, Bubeník J and Reinis M: NK1.1+ cells are important for the development of protective immunity against MHC I-deficient, HPV16-associated tumours. Oncol Rep 25: 281-288, 2011.
36. van der Sluis TC, Sluijter M, van Duikeren S, West BL, Melief CJ, Arens R, van der Burg SH and van Hall T: Therapeutic peptide vaccine-induced CD8 T cells strongly modulate intratumoral macrophages required for tumor regression. Cancer Immunol Res 3: 1042-1051, 2015.
37. Perea F, Bernal M, Sánchez-Palencia A, Carretero J, Torres C, Bayarri C, Gómez-Morales M, Garrido F and Ruiz-Cabello F: The absence of HLA class I expression in non-small cell lung cancer correlates with the tumor tissue structure and the pattern of T cell infiltration. Int J Cancer 140: 888-899, 2017.
38. Aptsiauri N, Ruiz-Cabello F and Garrido F: The transition from HLA-I positive to HLA-I negative primary tumors: The road to escape from T-cell responses. Curr Opin Immunol 51: 123-132, 2018.
39. Ugurel S, Spassova I, Wohlfarth J, Drusio C, Cherouny A, Melior A, Sucker A, Zimmer L, Ritter C, Schadendorf D and Becker JC: MHC class-I downregulation in PD-1/PD-L1 inhibitor refractory Merkel cell carcinoma and its potential reversal by histone deacetylase inhibition: A case series. Cancer Immunol Immunother 68: 983-990, 2019.
40. Zhang S, Kohli K, Black RG, Yao L, Spadinger SM, He Q, Pillarisetty VG, Cranmer LD, Van Tine BA, Yee C, *et al*: Systemic interferon-γ increases MHC class I expression and T-cell infiltration in cold tumors: Results of a phase 0 clinical trial. Cancer Immunol Res 7: 1237-1243, 2019.
41. Di Vito C, Mikulak J, Zaghi E, Pesce S, Marcenaro E and Mavilio D: NK cells to cure cancer. Semin Immunol 41: 101272, 2019.
42. Wright SE, Rewers-Felkins KA, Chowdhury NI, Ahmed J and Srivastava SK: Prevention of human adenocarcinoma with CpG-ODN in a mouse model. Oncol Lett 4: 1061-1063, 2012.
43. Maimela NR, Liu S and Zhang Y: Fates of CD8+ T cells in tumor microenvironment. Comput Struct Biotechnol J 17: 1-13, 2018.